

Biochemical Characterisation Of The Catalytic Domain Of Neuropathy Target Esterase

**Thesis submitted for the degree of
Doctor of Philosophy
at Leicester University**

by

**Jane Atkins
Department of Biochemistry
University of Leicester**

Submitted August 2000

UMI Number: U532870

All rights reserved

INFORMATION TO ALL USERS

The quality of this reproduction is dependent upon the quality of the copy submitted.

In the unlikely event that the author did not send a complete manuscript and there are missing pages, these will be noted. Also, if material had to be removed, a note will indicate the deletion.



UMI U532870

Published by ProQuest LLC 2013. Copyright in the Dissertation held by the Author.
Microform Edition © ProQuest LLC.

All rights reserved. This work is protected against
unauthorized copying under Title 17, United States Code.



ProQuest LLC
789 East Eisenhower Parkway
P.O. Box 1346
Ann Arbor, MI 48106-1346

ACKNOWLEDGEMENTS

I am deeply grateful to Dr. Paul Glynn for his excellent supervision, constructive advice and endless enthusiasm during the course of this project.

I would like to thank Professor Bill Brammar and Dr. Lu-Yun Lian for their useful advice and support as members of my PhD committee. My thanks also to Kath Lilley and the Protein and Nucleic Acid Chemistry Laboratory (Leicester University) for oligonucleotide synthesis, protein and DNA sequencing.

Finally I am indebted to Matthew Squires for his constant support during the preparation of this thesis, and to my parents for their encouragement and financial support over the last three years.

Biochemical Characterisation Of The Catalytic Domain Of Neuropathy Target Esterase

Jane Atkins

ABSTRACT

Neuropathy target esterase (NTE) is an integral membrane protein found predominantly in neurones. Covalent modification of NTE's active site serine, by certain organophosphates (OPs), results in a neurodegenerative syndrome. NTE's physiological substrate is unknown and its catalytic activity does not seem to be vital in the adult animal.

The enzyme domain of human NTE (residues 727-1216), called NEST, was expressed in *E. coli* and reacted with a carboxyl ester substrate and OP inhibitors the same as native NTE. During purification catalytic activity was lost, but was restored by reconstitution into liposomes. Site-directed mutagenesis revealed that S966, D960 and D1086 were critical for catalysis. Mutation of two histidines, H860 and H885, also resulted in a loss of activity. Reacting NEST with [³H]diisopropylfluorophosphate, confirmed S966 as the active site serine and showed that an isopropyl group is transferred to an aspartate residue.

Standard hydropathy analysis predicts no membrane-spanning helices in NEST; however, biochemical evidence indicated that NEST is an integral membrane protein. TMpred analysis, on the other hand, predicts three transmembrane helices (TM2-4), with S966 at the centre of TM4. For S966 to be located within the membrane, TM4 would need to line the lumen of an aqueous pore to allow access of water for catalysis. Patch clamp studies on NEST-containing giant liposomes indicated that NEST forms a pore *in vitro*, while other experiments demonstrated that NEST monomers are catalytically active: this raises the possibility that NEST forms a β -barrel structure in the membrane.

NEST, fatty acid amide hydrolase and calcium-independent phospholipase A2 displayed different rank order to inhibition by a series of serine hydrolase inhibitors. Methylarachidonylfluorophosphonate, which reacts with arachidonyl-binding sites, was the most potent inhibitor of NEST tested. Lyso-platelet activating factor inhibited NEST but lysophosphatidylcholine (lysoPC) did not, suggesting that lysoPC is hydrolysed by NEST. However, of the potential substrates tested, only 2-arachidonyl glycerol was hydrolysed by NEST, indicating NEST has a monoacylglycerol lipase activity.

CONTENTS

	Page Number
TITLE PAGE	I
ACKNOWLEDGEMENTS	II
ABSTRACT	III
CONTENTS	IV
ABBREVIATIONS	X
FIGURES	XVI
TABLES	XIX
CHAPTER 1: INTRODUCTION.....	1
1.1 Serine Hydrolases.....	1
1.2 Reaction of Organophosphorus Compounds with Serine Hydrolases.....	6
1.3 Toxic Effects of Organophosphates.....	7
<i>1.3.1 Acute cholinergic syndrome.....</i>	<i>7</i>
<i>1.3.2 Intermediate syndrome.....</i>	<i>8</i>
<i>1.3.3 Organophosphate induced delayed neuropathy (OPIDN).....</i>	<i>9</i>
1.4 The Role of NTE in OPIDN.....	10
1.5 Neuropathy Target Esterase (NTE): Molecular Aspects and Related Proteins	12
1.6 Aims of Project	15

**CHAPTER 2: CHARACTERISATION OF THE RECOMBINANT ESTERASE
DOMAIN OF NTE, NEST.27**

2.1 Introduction27

2.2 Results and Discussion27

2.2.1 Validation of the D16 cDNA clone.....27

2.2.2 Expression of shorter constructs of NTE in Escherichia coli29

2.2.3 Solubilisation, purification and reconstitution of NEST31

2.2.3.1 Solubilisation of NEST 31

2.2.3.2 Purification of NEST using nickel affinity and gel filtration chromatography 33

2.2.3.3 Reconstitution of NEST into synthetic phospholipid liposomes 34

*2.2.4 Comparison of NEST in bacterial membranes and DOPC liposomes with native
NTE in chicken brain microsomes36*

2.2.4.1 Catalytic Centre Activity of NEST and NTE..... 37

2.2.4.2 Covalent inhibitors of NEST and NTE 37

2.2.4.3 Aging of NEST and NTE..... 38

2.2.5 Determination of residues critical to catalysis and aging of NTE.....39

2.2.5.1 Identification of the active site serine and possible candidates for site Z 39

2.2.5.2 Identification of residues critical for catalysis by site-directed mutagenesis 41

2.3 General Discussion43

**CHAPTER 3: INVESTIGATION OF THE MOLECULAR ORGANISATION OF
NEST IN DOPC LIPOSOMES.....70**

3.1 Introduction70

3.2 Results and Discussion71

3.2.1 Membrane association of NEST..... 71

3.2.2 Does NEST form a transmembrane pore? 73

3.2.3 Are monomers of NEST catalytically active?..... 76

3.3 General Discussion	81
CHAPTER 4: PRELIMINARY INVESTIGATIONS INTO IDENTIFYING A POSSIBLE SUBSTRATE FOR NTE.....	102
4.1 Introduction	102
4.2 Results and Discussion	103
<i>4.2.1 Effect of phospholipids on NEST phenyl valerate hydrolase activity</i>	<i>103</i>
<i>4.2.2 Inhibitors of serine hydrolases: effects on NEST phenyl valerate hydrolase activity</i>	<i>105</i>
4.2.2.1 p-Bromophenacyl bromide (BPAB)	105
4.2.2.2 Bromoenol lactone (BEL).....	106
4.2.2.3 Methyl arachidonyl fluorophosphonate (MAFP).....	107
4.2.2.4 Trifluoromethyl ketone analogues of arachidonic and palmitic acid (AACOCF3 and PACOCF3)	108
4.2.2.5 N-Arachidonyl-5-hydroxytryptamine (AA-5HT)	109
4.2.2.6 Phenylmethanesulfonyl fluoride (PMSF)	109
<i>4.2.3 Potential endogenous substrates for neuropathy target esterase (NTE)</i>	<i>110</i>
4.2.3.1 Phospholipid substrates.....	110
4.2.3.2 Phosphatidic acid, tri-, di- and mono-acyl glycerols.....	113
4.2.3.3 Fatty acid amides	114
4.3 General Discussion	115
CHAPTER 5: DISCUSSION	131
5.1 Delineation of the Recombinant NTE Esterase Domain (NEST) and Comparison with Native NTE.....	131
5.2 Residues Involved in Catalysis and the Reaction of NTE with Organophosphates.....	132
5.3 Membrane-Association of the Catalytic Domain of Human NTE.....	133

5.4 What is the Physiological Role of NTE?	135
CHAPTER 6: MATERIALS AND METHODS.....	140
6.1 Materials	140
6.1.1 <i>General chemicals and materials.....</i>	140
6.1.2 <i>Organophosphates</i>	140
6.1.3 <i>Radiochemicals</i>	140
6.1.4 <i>Antibodies.....</i>	140
6.1.5 <i>Kits</i>	140
6.1.6 <i>Plasmids</i>	141
6.1.7 <i>Bacterial strains and growth media.....</i>	141
6.1.8 <i>Eukaryotic cells.....</i>	141
6.1.9 <i>Cell culture media and supplements</i>	142
6.1.10 <i>Serine hydrolase inhibitors</i>	142
6.1.11 <i>Potential endogenous substrates.....</i>	142
6.2 Growth and Maintenance of Cell Culture	143
6.2.1 <i>Resuscitation of cells from frozen storage</i>	143
6.2.2 <i>Subculturing of cell lines.....</i>	143
6.2.3 <i>Storage of cells.....</i>	143
6.3 Protein-Related Methods.....	144
6.3.1 <i>Protein concentration determination (Bradford method).....</i>	144
6.3.2 <i>One-dimensional SDS-polyacrylamide gel electrophoresis (SDS-PAGE)</i>	144
6.3.2.1 <i>SDS-PAGE (Laemlli)</i>	144
6.3.2.1 <i>Tricine-SDS-PAGE</i>	146
6.3.3 <i>Western blot analysis</i>	147
6.3.3.1 <i>Solutions</i>	147
6.3.3.2 <i>Transfer of SDS-PAGE gel onto nitro-cellulose or Immobilon membranes</i>	147
6.3.3.3 <i>Visualisation of Proteins using an alkaline phosphatase conjugate</i>	148
6.4 Isolation and Purification of Nucleic Acids	148
6.4.1 <i>Small scale preparation of plasmid DNA.....</i>	148

6.4.1.1	Buffers supplied with QIAprep spin miniprep kit	148
6.4.1.2	Protocol.....	149
6.4.2	<i>Medium scale preparation of plasmid DNA</i>	149
6.4.2.1	Composition of buffers required for QIAGEN midiprep kit.....	149
6.4.2.2	Protocol.....	150
6.4.3	<i>QIAquick PCR Purification Kit</i>	150
6.4.3.1	Buffers provided with QIAquick kit	150
6.4.3.2	Protocol.....	150
6.4.4	<i>QIAquick Gel Extraction Kit</i>	151
6.4.4.1	Buffers	151
6.4.4.2	Protocol.....	151
6.4.5	<i>Precipitation of Oligodeoxynucleotide Primers</i>	151
6.4.6	<i>Quantification of nucleic acid concentration by spectrophotometry</i>	152
6.4.6.1	Double-stranded DNA	152
6.4.6.2	Oligodeoxynucleotide primers.....	152
6.5	<i>Enzymic Manipulation of DNA</i>	152
6.5.1	<i>Restriction enzyme digestion</i>	152
6.5.2	<i>Polymerase chain reaction (PCR)</i>	153
6.5.3	<i>Dephosphorylation of linearised plasmid DNA</i>	153
6.5.4	<i>Ligation protocol</i>	154
6.5.5	<i>Transformation protocol</i>	154
6.5.6	<i>Sequencing reactions</i>	155
6.5.7	<i>Mutagenesis of NEST</i>	156
6.5.7.1	Mutagenesis primers.....	157
6.5.7.2	Mutagenesis reactions.....	159
6.6	<i>Escherichia Coli Expression</i>	161
6.6.1	<i>E. coli expression constructs</i>	161
6.6.2	<i>Oligonucleotide design</i>	162
6.6.2.1	NEST forward primers.....	162
6.6.2.2	NEST reverse primers.....	164
6.6.3	<i>Protein expression and purification</i>	164
6.6.3.1	Small-scale expression cultures	164
6.6.3.2	Large-scale expression cultures	165
6.6.3.3	Solubilisation of NEST constructs.....	165

6.6.3.4 Purification on nickel resin	166
6.6.3.5 Gel filtration chromatography.....	166
6.6.3.6 Functional reconstitution of recombinant NEST	167
6.7 Mammalian Expression	168
6.7.1 Mammalian expression constructs.....	168
6.7.2 Large scale transfections using Perfect™ lipids (Invitrogen).....	169
6.8 Enzyme-Related Methods.....	169
6.8.1 Phenyl valerate hydrolase assay (Johnson, 1977).....	169
6.8.2 Inhibition of NEST and NTE phenyl valerate hydrolase activity.....	171
6.8.2.1 Preparation of NEST-containing bacterial particulate fraction.....	171
6.8.2.2 Chicken brain microsomes (CBM)	171
6.8.2.3 Reaction with covalent inhibitors of NTE	171
6.8.2.4 Reaction of NEST-containing DOPC liposomes with serine hydrolase inhibitors.....	174
6.8.2.5 Reaction of NEST-containing DOPC liposomes with phospholipids.....	175
6.8.2.6 Radiation inactivation experiments.....	175
6.8.3 Oxime reactivation	176
6.8.4 [³ H]DFP-labelling experiments.....	176
6.8.4.1 Volatilisable counts assay (Williams, 1983).....	177
6.8.4.2 Catalytic centre activity	177
6.8.5 Endoproteinase Glu-C digestion.....	178
6.8.6 Proteinase K treatment	179
6.8.7 Phase partitioning.....	180
6.8.8 Potential substrates.....	180
6.9 Electrophysiology	183
6.9.1 Preparation of DOPC liposomes containing NEST and of giant liposomes	183
6.9.2 Patch-clamp recording experiments	183
6.10 Electron Microscopy	185

ABBREVIATIONS

β -Gal	β -galactosidase
[¹⁴ C]AA-PI	1-stearoyl-[2- ¹⁴ C]arachidonyl-phosphatidylinositol
[³ H]	tritiated
1(3)-AG	1(3)-arachidonyl glycerol
2-AG	2-arachidonyl glycerol
Å	angstrom(s)
A ₍₆₀₀₎	absorbance at (600)
AA	arachidonic acid
AA-5HT	arachidonylserotonin
AACOCF ₃	arachidonyl trifluoromethylketone
AAP	4-amino antipyrine
AA-PA	2-arachidonyl phosphatidic acid
AA-PAF	arachidonyl-platelet activating factor
AA-PC	1-stearoyl-2-arachidonyl-phosphatidylcholine
ACh	acetylcholine
AChE	acetylcholinesterase
AE	anandamide
AEG	arachidonyl ethylene glycol
AMP	ampicillin
APS	ammonium persulphate
AQ	aqueous phase
Arg (R)	arginine
Asn (N)	asparagine
Asp (D)	aspartate
ATP	adenosine triphosphate
BCIP	5-bromo-4-chloro-3-indolyl phosphate
BEL	bromo-enol lactone
bp	base pairs
BPAB	bromophenacylbromide
BSA	bovine serum albumin

<i>C. elegans</i>	<i>Caenorhabditis elegans</i>
Ca ²⁺	calcium
CaCl ₂	calcium chloride
CB1	cannabinoid receptor 1
CB2	cannabinoid receptor 2
CBM	chicken brain microsomes
cDNA	complementary DNA
cfu	colony forming unit
Ch	choline
CHAPS	3-[(3-cholamidopropyl)dimethylammonio]-1-propane-sulfonate
CHO	Chinese hamster ovary
CIAP	calf intestinal alkaline phosphatase
CMC	critical micellar concentration
CMV	cytomegalovirus
CNS	central nervous system
cPLA2	cytosolic calcium-dependent phospholipase A2
C-termin(al) or (us)	carboxy terminal or terminus
Cu ²⁺	copper
Cyt c	cytochrome c
DAG	diacylglycerol
DEPC	diethyl pyrocarbonate
DET	detergent phase
DFP	diisopropylfluorophosphate
DMEM	Dulbecco's modified Eagle medium
DMF	dimethylformamide
DMSO	dimethylsulfoxide
dNTP	mixture of the four deoxynucleotide triphosphates
DOC	sodium deoxycholate
DOPC	L- α -phosphatidylcholine, dioleoyl
DPM	disintegrations per minute
DTT	dithiothreitol

<i>E. coli</i>	<i>Escherichia coli</i>
EDTA	ethylenediaminetetra-acetic acid
EGS	ethylene glycolbis(succinimidylsuccinate)
EPN	ethylphenylphosphonic acid
EtOH	ethanol
FAAH	fatty acid amide hydrolase
FCS	foetal calf serum
FTIR	Fourier transform infrared
g	relative centrifugal force
G6PDH	glucose-6-phosphate dehydrogenase
GFP	green fluorescent protein
Gln (Q)	glutamine
Glu (E)	glutamate
Gly (G)	glycine
HCl	hydrochloric acid
HELSS	haloenol lactone suicide substrate
His (H)	histidine
His ₆ tag	hexahistidine tag
HPLC	high performance liquid chromatography
IC50	concentration of inhibitor which gives 50% inhibition
IgG	immunoglobulin G
INAP	isonitrosoacetophenone
iPLA2	calcium-independent phospholipase A2
IPTG	isopropyl-β-D-thiogalactopyranoside
K ⁺	potassium
kb	kilobases
KCl	potassium chloride
kDa	kiloDalton
KF	potassium fluoride
LB	Luria-Berani
Lys (K)	lysine
lysoPA	lysophosphatidic acid
lysoPAF	lyso-platelet activating factor

lysoPC	lysophosphatidylcholine
M.E.	mutagenesis efficiency
MAFP	methyl arachidonyl fluorophosphonate
MAG	monoacylglycerol
Mg ²⁺	magnesium
min	minutes
MIP	mipaflox
MNTFK	3-(9'-mercaptiononylthio)-1.1.1-trifluoroketone
MOPS	3-[N-Morpholino]propanesulfonic acid
MscL	large mechanosensitive ion channel
MW	molecular weight
MWCO	molecular weight cut-off
n/d	not done
Na ⁺	sodium
nAChR	nicotinic acetylcholine receptor
NaCl	sodium chloride
NaOH	sodium hydroxide
NaP	sodium phosphate buffer
NBT	nitro blue tetrazolium
NEST	NTE esterase domain
NHS-esters	N-hydroxysuccimide esters
Ni-NTA	nickel-nitrilotriacetic acid
NTE	neuropathy target esterase
N-termin(al) or (us)	amino terminal or terminus
OA	oleic acid
OD	optical density
OE	oleamide
OEP	outer envelope protein
OMPLA	outer membrane phospholipase A
OP(s)	organophosphate(s)
OPIDN	organophosphate induced delayed neuropathy
OTFP	3-octylthio-1,1,1-trifluoropropan-2-one
<i>P. aeruginosa</i>	<i>Psuedomonas aeruginosa</i>
PA	phosphatidic acid

PACOCF3	palmitoyl trifluoromethylketone
PAF	platelet activating factor (1- <i>O</i> -hexadecyl-2-acetyl-phosphatidylcholine)
PAF-AH	platelet activating factor acetylhydrolase
PAP-1	magnesium-dependent phosphatidate phosphohydrolase
PBS	phosphate buffered saline
PC	phosphatidylcholine
PC12	pheochromocytoma cells
PCR	polymerase chain reaction
PDPP	phenyl dipentylphosphinate
PE	phosphatidylethanolamine
PI	phosphatidylinositol
PK	proteinase K
PKA	protein kinase A
PKC	protein kinase C
PLA1	phospholipase A1
PLA2	phospholipase A2
PMSF	phenyl methylsulfonylfluoride
PNACL	protein and nucleic acid chemistry laboratory
P _o	open probability
PPA	phenyl phenyl acetate
PS	phosphatidylserine
pS	picoSiemens
PSP	phenyl saligenin phosphate
PV	phenyl valerate
PVDF	polyvinylidene difluoride
PVP40	polyvinylpyrrolidone
PXN	paraoxon
RP-HPLC	reverse-phase high performance liquid chromatography
RyR	ryanodine receptor
<i>S. cerevisiae</i>	<i>Saccharomyces cerevisiae</i>
SDS	sodium dodecyl sulfate

SDS-PAGE	sodium dodecylsulfate polyacrylamide gel electrophoresis
Ser (S)	serine
sPLA2	secretory phospholipase A2
Sulfo-EGS	ethylene glycolbis(sulfosuccinimidylsuccinate)
SV40	simian virus 40
SWS	Swiss cheese protein
<i>sws</i>	Swiss cheese gene
$T_{1/2}$	half life
TAG	triacylglycerol
TBST	Tris buffered saline with Tween
TE	Tris/EDTA
TEMED	N,N,N',N'-Tetramethylethylenediamine
TEPP	tetraethyl pyrophosphate
TFMK	trifluoromethylketone
TLC	thin layer chromatography
TM	transmembrane segment
TOCP	tri-ortho-cresyl phosphate
Tris	2-amino-2-(hydroxymethyl)-1,3-propanediol
TX-100	TRITON X-100
TX-114	TRITON X-114
U	Units
V	Volts
v/v	volume for volume
V_0	void volume
VDAC	voltage-dependent anion channel
V_e	elution volume
V_h	holding potential
W.T.	wild-type
w/w	weight for weight
X-Gal	5-bromo-4-chloro-3-indolyl β -D-galactopyranoside
Zn^{2+}	zinc

FIGURES

	Page Number
1.1 Catalytic mechanism of α -chymotrypsin.	20
1.2 Steps in the interaction of a serine hydrolase with an organophosphate inhibitor.	21
1.3 Neurotoxic and non-neurotoxic organophosphorus esters.	22
1.4 Secondary structure predictions for NTE using standard hydropathy analysis and the TMpred programme.	23
1.5 NTE is a member of a novel family of proteins.	24
1.6 Multiple sequence alignment of the conserved C-terminal domain of proteins shown in Fig. 1.5.	25
1.7 Region of homology between NTE and a calcium-dependent Phospholipase A2.	26
2.1 Transient transfection of D16 cDNA in COS7 cells.	53
2.2 Western blot of untransfected and D16 transfected COS7 cells.	54
2.3 NEST constructs expressed in the <i>E. coli</i> expression system.	55
2.4 Western blot of NEST constructs solubilised in non-denaturing and denaturing detergent.	56
2.5 Constructs designed to investigate the C-terminal boundary of NEST.	57
2.6 Western blot of NEST (55 kDa) solubilised in Triton X-100, CHAPS and deoxycholate.	58
2.7 (a) Coomassie stained gels and (b) Western blot of NEST purification.	59
2.8 Gel filtration profile of NEST.	60
2.9 Time course of NEST phenyl valerate hydrolase activity.	61
2.10 Influence of pH on NEST phenyl valerate hydrolase activity.	62
2.11 Proteolytic digest of tritiated DFP-labelled NEST.	63
2.12 Partial peptide map of NEST.	64
2.13 Localisation of [³ H]DFP-derived label in NEST fragments Bands 6 and 8.	65
2.14 Alignment of sequences of NTE homologues over the 200 residue conserved region.	66
2.15 Mutagenesis of conserved residues within NEST.	67

2.16	Western blot to demonstrate expression levels of nine NEST mutants compared to wild-type (W.T.) NEST.	68
2.17	(a) Phenyl valerate hydrolase activity and (b) [³ H]DFP binding of NEST mutants expressed as a percentage of wild-type NEST PV-hydrolase activity.	69
3.1	Phase partitioning of TX-114-solubilised NEST.	86
3.2	SDS-PAGE of (a) Untreated and DFP-inhibited NEST solubilised in TX-114 or CHAPS. (b) Untreated, PSP-inhibited, DFP-inhibited, PDPP-inhibited and PMSF-inhibited NEST solubilised in TX-114.	87
3.3	Proteinase K treatment of NEST-containing liposomes.	88
3.4	T7 and His ₆ blots of proteinase K digestion of NEST in DOPC liposomes.	89
3.5	Long and short dwell-time pores in NEST-containing excised liposome patches.	90
3.6	Wild-type and S966A mutant NEST-containing excised liposomes patches: electrophysiological comparison.	91
3.7	Effect on pore properties of covalent chemical modification of serine 966 in NEST-containing excised liposome patches.	93
3.8	Gel filtration profile of standard proteins.	95
3.9	Plot of the log molecular weight versus V_e/V_0 .	96
3.10	Gel filtration profile of NEST-containing liposomes solubilised in limiting detergent.	97
3.11	SDS-PAGE of NEST-containing liposomes cross-linked with glutaraldehyde, Sulfo-EGS and EGS.	98
3.12	Effects of varying cross-linker concentration on NEST phenyl valerate activity.	99
3.13	Effect of varying the concentration of (a) glutaraldehyde and (b) valeraldehyde on NEST phenyl valerate hydrolase activity.	100
3.14	SDS-PAGE of NEST-containing liposomes cross-linked with increasing concentrations of glutaraldehyde.	101
4.1	Effect of phosphatidylcholine, phosphatidylethanolamine, phosphatidylinositol and phosphatidylserine on NEST PV-hydrolase activity.	121
4.2	Inhibition of NEST PV-hydrolase activity by PAF, lysoPAF, AA-PAF and lysoPC.	122

4.3	Time-course of NEST inactivation with PAF.	123
4.4	Time-course of NEST inactivation with MAFP.	124
4.5	Inhibition of NEST PV-hydrolase activity by the trifluoromethylketone analogues of arachidonic and palmitic acid.	125
4.6	TLC plates (AA-PC, AA-PI, DOPC, AA-PAF)	126
4.7	TLC plates (lysoPC, lysoPA)	127
4.8	Metabolism of diacylglycerol (DAG)	128
4.9	TLC plates (AA-PA, 2-AG, AEG)	129
4.10	TLC plates (AE, OE)	130
6.1	Effect of solvents on NEST PV-hydrolase activity	173

TABLES

	Page Numbers
1.1 Members of the serine hydrolase superfamily grouped according to function.	17
1.2 Proteins homologous to AChE, chymotrypsin, FAAH, NTE and OMPLA.	18
1.3 Organic derivatives of phosphoric acid, which show anticholinesterase activity.	19
2.1 Endogenous NTE phenyl valerate hydrolase activity of five cell lines	47
2.2 Effect of detergents on NEST activity in the soluble and particulate fractions.	48
2.3 Catalytic centre activities for NEST in E. coli lysates, NEST in DOPC liposomes and NTE from chicken brain microsomes.	48
2.4 IC ₅₀ values (μM) for covalent inhibitors of NTE and NEST.	49
2.5 Aging of native NTE and NEST.	50
2.6 Reactivation of NTE and NEST with the oxime isonitrosoacetphenone (INAP).	51
2.7 Specific radioactivity, percentage volatile counts and N-terminal sequence (not done for all 12 bands) of the twelve distinct polypeptide bands.	52
4.1 Phenyl valerate hydrolase activity of NEST reconstituted into DOPC, PC, PE + DOPC, PI and PS liposomes.	118
4.2 IC ₅₀ values (μM) for the action of inhibitors on NEST phenyl valerate hydrolase activity.	119
4.3 Hydrolysis of 1-stearoyl-[2- ¹⁴ C]arachidonyl-phosphatidylinositol.	120
6.1 Serine hydrolase inhibitors.	174
6.2 Lipid molecules tested as substrates for NEST.	182

CHAPTER 1: INTRODUCTION

In man and some other vertebrates, diisopropylfluorophosphate (DFP) and certain other organophosphates (OPs) cause degeneration of long axons in the peripheral nerves and spinal cord. The primary target for these OPs is neuropathy target esterase (NTE), an integral membrane protein found in vertebrate neurones. The covalent reaction of NTE with DFP identified this protein as a member of the serine hydrolase superfamily (Johnson 1969a,b). However, molecular cloning and sequencing have revealed that NTE is unrelated to known serine hydrolases and belongs to a novel protein family represented in species from bacteria to man (Lush et al., 1998).

1.1 SERINE HYDROLASES

Serine hydrolases are a superfamily of proteins, which includes serine esterases, proteases, lipases and amidases (Table 1.1). These enzymes are characterised by an active site serine, which participates covalently in catalysis. The catalytic serine of all serine hydrolases is generally found in the motif Gly-X-Ser-X-Gly. Serine hydrolases can be grouped in terms of function, as depicted in Table 1.1, or with respect to their primary sequences (Table 1.2). Database searches for proteins with primary sequence homology to chymotrypsin, acetylcholinesterase, fatty acid amide hydrolase, neuropathy target esterase and outer membrane phospholipase A reveal that these enzymes belong to separate protein families and demonstrate the diversity of serine hydrolases (Table 1.2). Even among the serine proteases, while chymotrypsin and subtilisin have similar active sites and employ the same type of mechanisms, the primary sequence of these enzymes are clearly unrelated and represent a striking example at the molecular level of apparent evolutionary convergence (Creighton, 1984).

Most serine hydrolases use a charge relay system or “catalytic triad” for catalysis, consisting of a serine, a histidine and an acidic residue (either aspartate or glutamate). This triad, first observed in serine proteases, exists in a variety of forms and evolved a number of times independently. At the active site the serine is within hydrogen-bonding distance of a ring nitrogen of histidine ($N^{\epsilon 2}$) and the other ring nitrogen ($N^{\delta 1}$) is hydrogen-bonded to

the carboxylate group of aspartate or glutamate (Blow, 1990). The three residues within the catalytic triad have a specific role in generating the nucleophilic potential at the seryl oxygen (O_γ). The acidic residue, which is hydrogen-bonded to the adjacent imidazole group, orients this group in the catalytic triad and increases the group's pKa. This is an advantage because a histidine residue, when buried by the substrate during the reaction, would otherwise have a reduced pKa and be more reluctant to accept a proton (Dodson & Wlodawer, 1998).

The first serine hydrolase catalytic triad, revealed by Matthews et al. (1967) over thirty years ago using X-ray crystallography, was that of α -chymotrypsin. The catalytic mechanism of chymotrypsin is shown in Fig. 1.1 (Bugg, 1997). It is a classic example of covalent catalysis, in which the active site serine (Ser195) attacks the amide carbonyl of peptide substrates. The substrate binds in the specificity pocket of the enzyme and the hydroxyl group of Ser195 makes a nucleophilic attack on the carbonyl bond of the substrate to form a tetrahedral oxyanion intermediate. The imidazole group of His57 ($N^{\epsilon 2}$) accepts the seryl O_γ proton, becomes positively charged and forms a salt bridge with Asp102. Stabilisation of the oxyanion intermediate takes place via formation of two hydrogen bonds between the tetrahedral oxyanion and the backbone amide bonds of Ser195 and Gly193. As the bond between the serine and the carbonyl bond is formed, the C=O bond lengthens to become a single bond. The tetrahedral intermediate collapses and protonation of the leaving group by His57 ($N^{\epsilon 2}$) leads to the formation of the acylenzyme intermediate. His57 ($N^{\epsilon 2}$) then acts as a base to deprotonate water attacking the acylenzyme intermediate, leading to a second tetrahedral oxyanion intermediate, which is once again stabilised by hydrogen bond formation. Protonation of the departing serine oxygen (O_γ) by the histidine ($N^{\epsilon 2}$) leads to the release of the carboxylic acid product and completion of the catalytic cycle (Bugg, 1997).

Crystal structures have been solved for several members of the serine hydrolase superfamily. The serine proteases are the most extensively studied enzymes. This class of proteases contains two major evolutionary families that have very similar mechanisms of action even though not otherwise detectably related. One family is represented by the bacterial subtilisins and the other is the trypsin family, which includes chymotrypsin, trypsin and elastase from mammals as well as many other bacterial proteases. The trypsin

family also includes thrombin, plasmin, kallikrein, acrosin and others, which are involved in a diverse range of cellular functions, including blood clotting, complement activation, hormone production and fertilisation (Creighton, 1984).

Chymotrypsin cleaves peptides on the carbonyl side of aromatic residues, such as phenylalanine and tyrosine. The three-dimensional structure for chymotrypsin, trypsin and elastase are very similar. Chymotrypsin contains an α -helix at the C-terminal end and two homologous domains, containing six-stranded β -barrels, with the active site between these domains (Matthews et al., 1967). Most of the aromatic and hydrophobic residues are buried in the interior of the protein, and most of the charged or hydrophilic residues are on the surface. Three polar residues, His57, Asp102 and Ser195, form the catalytic triad of chymotrypsin as discussed previously (Blow, 1996). These residues are conserved in trypsin (Stroud et al., 1971) and elastase as well (Watson et al., 1970).

Acetylcholinesterase (AChE), a serine esterase, has been well characterised both biochemically and structurally. The principal biological role of AChE is the termination of impulse transmission at cholinergic synapses by rapid hydrolysis of the neurotransmitter, acetylcholine (ACh) (Garrett & Grisham, 1995). In accordance with this role, AChE is characterised by a high turnover number, functioning at a rate close to the limits of diffusion. The active site of AChE is located at the bottom of a deep gorge, which is lined with rings of aromatic residues (Sussman et al., 1991; Axelsen et al., 1994). AChE is a member of the α/β hydrolase-fold family of enzymes (Ollis et al., 1992; Cygler et al., 1993) and the enzyme monomer consists of a 12-stranded mixed β -sheet surrounded by 14 α -helices (Sussman et al., 1991). The predominant form of AChE in the central nervous system is the amphiphilic tetramer anchored to the membrane by a hydrophobic non-catalytic subunit. The active site of AChE is unusual because it contains a glutamate residue, not an aspartate, in the Ser-His-acid catalytic triad and this triad is of the opposite “handedness” to that of chymotrypsin (Sussman et al., 1991). A number of proteins have been shown to be homologous to the catalytic domain of cholinesterases (Krejci et al., 1991). These include carboxylesterases, pancreatic lysophospholipase and a lipase from *Geotrichum candidum*. In addition, this family includes several non-catalytic proteins: thyroglobulin, neurotactin and glutactin.

Outer membrane phospholipase A (OMPLA) is an integral membrane protein, which has a catalytic triad containing a serine (Ser144), histidine (His142) and a neutral asparagine (Asn156) instead of an aspartate residue (Snijder et al., 1999). The active serine, Ser144, is part of the sequence HDSNG, which differs slightly from the usual GX SXG motif of other serine hydrolases. Although OMPLA is a serine lipase, database searches showed no similarity to any other members of the lipase family (Table 1.2). OMPLA hydrolyses the acyl ester bonds of (phospho)lipids in the outer membrane of Gram negative bacteria. In normally growing cells, OMPLA displays no enzyme activity, however, activity is induced by various processes which perturb the membrane (de Geus et al., 1983; Luirink et al., 1986). Dekker et al. (1997) demonstrated that, under conditions in which the enzyme displayed full activity, OMPLA was dimeric. The structure of OMPLA consists of a 12-stranded antiparallel β -barrel (Snijder et al., 1999). The N- and C-termini and three extracellular loops cover the barrel's interior and obstruct pore function of this protein.

Cytosolic phospholipase A2 (cPLA2) is a member of a diverse superfamily of phospholipase A2 enzymes (Dennis, 1997), but is also a serine hydrolase, as it utilises serine as its active site nucleophile. Site-directed mutagenesis demonstrated that Ser228 and Asp549 were essential for catalysis, but none of the 19 histidines were enzymatically relevant (Pickard et al., 1996). Interestingly mutation of Arg200 also resulted in loss of catalytic activity suggesting a novel catalytic mechanism in which arginine replaced histidine in the catalytic triad (Pickard et al., 1996). The elucidation of the crystal structure of human cPLA2 (Dessen et al., 1999), however, revealed that instead of the expected triad, cPLA2 utilises a non-conventional catalytic mechanism. Cytosolic PLA2 uses a catalytic dyad in which the O γ atom of the serine is only 2.9Å from O δ 2 of Asp549, whereas the guanidinium group of Arg200 is 9Å away from the seryl oxygen and all the histidines are outside of a 10 Å radius. The cPLA2 monomer is a two domain structure, an N-terminal C2 domain and a catalytic domain. The N-terminal domain consists of eight antiparallel β -strands interconnected by six loops, folding into a β -sandwich. The catalytic domain of cPLA2 is composed of 14 β -strands and 13 α -helices. Detailed comparison of the structure of cPLA2 and the classic α/β hydrolase fold clearly argues that cPLA2 contains a novel topology (Dessen et al., 1999).

Platelet-activating factor (PAF) is a potent pro-inflammatory phospholipid and its production is tightly regulated both at the synthetic and degradative levels. PAF is inactivated when the sn-2 ester bond is hydrolysed by platelet-activating factor acetylhydrolase (PAF-AH) to yield the biologically inactive lysoPAF (Stafforini et al., 1997). The catalytic triad of PAF-AH was investigated using site-directed mutagenesis and Ser273, Asp296 and His351 were identified as critical residues (Tjoelker et al., 1995). The order in which the triad occurs (Ser-Asp-His) is consistent with the well-known α/β hydrolase fold (Ollis et al., 1992), which is found in almost all esterases and neutral lipases that have been structurally characterised to date. The most abundant brain PAF-acetylhydrolase is a heterotrimeric protein complex, PAF-AH(Ib), which contains two homologous catalytic domains, α_1 and α_2 (63% amino acid sequence identity), and a 45 kDa β -subunit. The crystal structure of the α_1 homodimer has been solved (Ho et al., 1997). Each monomer contains a single α/β domain with a central, parallel, 6-stranded β -sheet. The two active sites are in close proximity at the bottom of a gorge formed between the two monomers. There is not enough space to accommodate two PAF molecules, which suggests that only one site can be active at any time. The structure of the β -subunit of PAF-AH(Ib) has not been solved but the primary sequence contains seven WD-repeats, characteristic of a large family, whose best known members are the β -subunits of trimeric G-proteins. The seven WD repeats of the β -subunits of G-proteins form a seven-blade propeller structure, with each blade made up of four antiparallel β -strands (Sondek et al., 1996).

Fatty acid amide hydrolase is also a serine hydrolase and is a relatively recent addition to the serine hydrolase superfamily (Cravatt et al., 1996). FAAH is responsible for the hydrolysis of fatty acid amides and 2-arachidonyl glycerol (Maurelli et al., 1995; Goparaju et al., 1998). Among the amidase signature enzymes, FAAH is of particular interest due to the intriguing biological activities of its fatty acid amide substrates and the fact that FAAH is an integral membrane protein (Patricelli et al., 1998). The crystal structure has not been solved, but the residues involved in catalysis have been identified using site-directed mutagenesis (Patricelli et al., 1999; Patricelli & Cravatt, 1999). The catalytic properties of FAAH have identified the enzyme as a non-conventional amidase that utilises a serine nucleophile (Ser241) and nonhistidine catalytic base (Patricelli et al., 1999). Further studies identified lysine 142 (Lys142) as the basic residue involved in catalysis (Patricelli

& Cravatt, 1999) and also suggested that this residue may function as the general acid catalyst involved in leaving group protonation. Therefore, unlike many of the other members of the serine hydrolase family, FAAH and cytosolic phospholipase A2 can function catalytically without using a histidine residue (Patricelli et al., 1999; Dessen et al., 1999).

1.2 REACTION OF ORGANOPHOSPHORUS COMPOUNDS WITH SERINE HYDROLASES

Organophosphorus compounds, such as phosphonates and phosphates inhibit serine hydrolases by reacting with the active site serine. The tetravalent phosphonate and phosphate adducts formed with the active site serine of these enzymes have been considered “transition state analogues” (Lienhardt, 1973) since they resemble the tetrahedral Michaelis complex formed by the reaction of the enzyme with its substrate. In addition, transition state analogues bind more tightly than the substrate and as such they have become probes of the structural features of enzyme active sites in the course of catalysis (Kossiakoff & Spencer, 1981; Gnatt et al., 1994; Marcel et al., 2000). Kossiakoff and Spencer (1981) used neutron diffraction (a technique that can readily position hydrogen atoms) of trypsin modified by diisopropylfluorophosphate (DFP), to show that the proton which is abstracted from the serine is retained by the histidine residue and not the aspartate.

Organophosphorus esters (OPs) have been widely used as inhibitors in biochemical studies of serine esterases and proteases (Aldridge & Reiner, 1972; Powers & Harper, 1986). Anticholinesterase OPs have been used in human medicine, for example, ecothiopate for glaucoma and malathion for headlouse infestation, and on a much larger scale, are used as pesticides.

1.3 TOXIC EFFECTS OF ORGANOPHOSPHATES

Acute toxicity of organophosphates (OPs) is predicated on their action on acetylcholinesterase (AChE) (Johnson, 1980). AChE is not, however, the only target for organophosphates. OPs inhibit numerous serine hydrolases in the brain (Richards et al, 1999), but very few have been as well characterised as AChE. Neuropathy target esterase (NTE), however, has been extensively studied over the last thirty years, and modification of this enzyme is known to result in organophosphate-induced delayed neuropathy (Johnson, 1990).

1.3.1 Acute cholinergic syndrome

Acetylcholinesterase is an important part of the central nervous system, as it inactivates the neurotransmitter acetylcholine in the synapses of the brain and neuromuscular junction (Garrett & Grisham, 1995). Anticholinesterase OPs are derivatives of phosphonic or phosphoric acid or their sulphur containing analogues; they usually have two alkyl substituents and a third substituent, the leaving group, which is often an aryl group or heterocycle, or in the case of most nerve agents, fluorine (Table 1.3). The leaving group is more labile to hydrolysis than the two alkyl groups (Marrs, 1996).

The reaction of OPs with AChE is analogous to that of acetylcholine (ACh), whereby the phosphorus atom becomes attached to the enzyme via the serine residue at the active site. The leaving group is lost and a dialkylphosphoryl enzyme complex is formed (Fig. 1.2). The difference between this complex and the normal substrate-enzyme complex is that the phosphorus-enzyme bond is fairly stable and dephosphorylation occurs much more slowly than deacetylation.

Inhibition of acetylcholinesterase (AChE) results in acute cholinergic overstimulation at nicotinic and muscarinic synapses of the peripheral, autonomic and central nervous system (Abou-Donia & Lapadula, 1990; Marrs, 1993). The onset of poisoning depends on the inhibition and reactivation rates. Reactivation with dimethyl OPs is more rapid than with diethyl OPs (Mason et al., 1993). After inhibition by certain OP nerve agents reactivation

is almost non-existent, because of a further reaction known as aging, which involves monodealkylation of the dialkylphosphonyl enzyme (Fig. 1.2).

Clinical signs and symptoms of OP poisoning are generally attributable to acetylcholine accumulation and onset occurs less than 12-24 hours after exposure to OP. Bronchoconstriction and increased bronchial secretions are characteristic signs of OP poisoning. In the cardiovascular system, bradycardia and tachycardia can occur, depending on the predominance of muscarinic or nicotinic effects. Where death occurs, it is commonly due to centrally or peripherally mediated respiratory paralysis (Chang et al., 1990). If the patient survives the acute toxicity, the effects of the OP insecticides are largely reversible, because of spontaneous reactivation of the enzyme. This is true even of soman and DFP poisoning, although with these compounds recovery is slow, as it depends upon the resynthesis of AChE.

There are a number of other syndromes that may occur after the acute cholinergic syndrome, which include the “intermediate syndrome” and organophosphate induced delayed neuropathy (OPIDN).

1.3.2 Intermediate Syndrome

Compared to acute cholinergic toxicity or organophosphate induced delayed neuropathy (OPIDN) the intermediate syndrome is a recently observed toxic effect of OPs (Senanayake & Karallidde, 1987). This syndrome may follow treatment and resolution of the cholinergic signs of OP poisoning. The exact mechanism of this syndrome is not understood and it may or may not be related to cholinergic effects. The manifestations of the syndrome are proximal flaccid limb paralysis, weakness of the neck flexor muscles and cranial nerve involvement appearing 24-96 hours after poisoning. These symptoms are not influenced by atropine or oximes, which are used to treat the acute cholinergic syndrome. In addition, the respiratory muscles may be affected and the patient may require respiratory support. This new clinical entity was interpreted as neuromuscular junction dysfunction, and it might be related to muscular necrosis, known to occur in rats after severe cholinergic toxicity (Wecker et al., 1978).

1.3.3 Organophosphate induced delayed neuropathy (OPIDN)

Organophosphate induced delayed neuropathy (OPIDN) is distinct from acute cholinergic toxicity and is initiated by the phosphorylation and covalent modification of a protein called neuropathy target esterase (NTE) (Johnson, 1969a,b; Johnson, 1974).

Prior to 1930 neuropathy was known to occur occasionally in tuberculosis patients being treated with phosphocresote, a mixture of esters derived from phosphoric acid and coal-tar phenols (Johnson, 1982). However, the neurotoxicity of this medicine was not realised until 1930 when a massive outbreak of poisoning, involving more than 10,000 people, occurred in the USA (Smith et al., 1930). The epidemic was a result of ingestion of contaminated liquor ("Ginger Jake"), which resulted in a delayed neuropathy, subsequently known as organophosphate-induced delayed neuropathy (OPIDN). Tri-*o*-cresyl phosphate (TOCP) was identified as the main aetiological agent, using the adult hen as an experimental model (Smith et al., 1930). In the 1950s a clinically similar poisoning episode occurred during pilot plant synthesis of a new candidate pesticide, mipafox (Bidstrup et al., 1953).

To date OPIDN has been tested mainly by *in vivo* methods in hens and by examination of inhibition of NTE in neuronal tissue (Johnson, 1975a; Bouldin & Cavanagh, 1979a,b; Lotti et al, 1984). The adult hen has been used for studies because OPIDN can be recognised by obvious clinical signs, as well as by histological changes (Dudek & Richardson, 1982). Hen brain also constitutes one of the most abundant sources of NTE (Tormo et al., 1993). Inhibition and aging of hen brain NTE has been used to assess the neurotoxic potential of many OP esters.

A delay of 8-14 days between administration of active compounds and the appearance of clinical signs was found for both hens and humans. Even if daily doses are given, signs are not seen until the eighth day (Johnson, 1975). Over the past thirty years many more species have been shown to be susceptible to OPIDN after a single dose. The list now includes cat, dog, horse, cow, sheep, pig and monkey. Other, usually smaller, species appear resistant to varying degrees and immature animals are always less susceptible. In all susceptible species the clinical conditions and the distribution of the histopathological lesions in the central nervous system were similar (Johnson, 1992).

Clinical onset of OPIDN develops 1-3 weeks after the initial exposure to OP, unlike the effects on acetylcholinesterase where the onset of clinical symptoms is immediate. OPIDN is characterised by initial sensory disorders (cramps, tingling), followed by weakness and ataxia which progresses to a flaccid paralysis of the limbs (Lotti et al., 1984). Histological examination of hens, cats, dogs and calves paralysed by doses of TOCP led to the mistaken conclusion that the lesions were due to the loss of the myelin sheath surrounding long nerve axons (Smith & Lillie, 1931). However, later studies revealed that the nerve axon itself was initially affected and damage to the myelin sheath was a secondary event.

In a study by Bouldin and Cavanagh (1979a), histology sections of the central and peripheral nervous systems of DFP-treated cats, 21 days after dosing, revealed a characteristic distribution of “dying-back” neuropathy (Bouldin & Cavanagh, 1979a). The latter is characterised by the selective degeneration of the distal ends of long, large diameter axons. Degenerating nerve fibres were frequently present in the plantar nerve, less frequent in the posterior tibial nerve, and rarely present in the sciatic nerve. Within the central nervous system, occasional degenerating fibres were found in the white matter of the cerebellum; however, there was no evidence of neuronal cell death. Degeneration of nerve fibres was most prominent in the spinal cord within the fasciculus gracilis and within the lateral funiculus (Bouldin & Cavanagh, 1979a).

1.4 THE ROLE OF NTE IN OPIDN

The reaction of NTE with organophosphorus esters is similar to that of AChE (Fig. 1.2). Carbamates (Johnson & Lauwerys, 1969), phosphinates and sulphonyl fluorides (Johnson, 1974) react covalently at the active site of NTE and inhibit NTE (reaction 2), but do not produce a neuropathy. This is because aging cannot occur when these compounds inhibit NTE. After inhibition with phenyl dipentylphosphinate (PDPP), NTE can be reactivated (reaction 3) using fluoride salts (Clothier & Johnson, 1980) or nucleophilic oximes (Johnson et al., 1988, Meredith & Johnson, 1988). Neuropathic OPs, such as, phosphates, phosphonates and phosphoramidates (Fig. 1.3) can inhibit NTE and also undergo the aging reaction (reaction 4). Once reaction (4) occurs, reactivation in the manner of reaction (3) is no longer feasible.

Studies of OPIDN and NTE in the adult chicken have revealed that two molecular events are essential for the initiation of this syndrome (Johnson, 1982): firstly, NTE must be inhibited by greater than 70% and secondly, aging of phosphorylated NTE must occur leaving a negatively-charged group still attached to the active site serine (cf. Fig. 1.2).

Unambiguous chemical proof of aging has only been provided for a few OP compounds (Aldridge, 1995) and among them is DFP (Clothier & Johnson, 1979). Aging of DFP-inhibited NTE occurs rapidly *in vitro* and differs from aging of DFP-inhibited acetylcholinesterase (AChE) in that the fate of the isopropyl group is different, i.e. an intramolecular transfer of the isopropyl group occurs in NTE, whereas in AChE the group is lost from the molecule. Aging of NTE can be measured in two ways; either as a loss of reactivity (Clothier & Johnson, 1979) or as the radiochemical change from a di-isopropyl phosphoryl to mono-isopropyl phosphoryl residue attached to the protein (Williams, 1983).

Several lines of evidence exist to support the concept that neuropathy target esterase is the target for initiation of OPIDN. M.K. Johnson first proposed NTE (previously known as neurotoxic esterase) as the target for OPIDN in 1969 (Johnson 1969a,b). Using radiolabelled DFP, Johnson (1969a) demonstrated the labelling of several phosphorylation sites in hen brain. Twenty percent of these sites were resistant to inhibition by the anticholinesterases, tetraethyl pyrophosphate (TEPP) and paraoxon (PXN), and of these sites approximately one fifth (i.e. 4%) were inhibited by the neuropathic agents, mipafox (MIP) and phenyl saligenin phosphate (PSP) (Johnson 1969a, 1970). The correlation between these sites and the target for OPIDN was supported by the ability of 15 test compounds to block the target site (assayed *ex-vivo* 24hr after dosing) with OPIDN effects (positive or negative) seen 14 days after dosing (Johnson, 1969a, 1970).

On the basis of general knowledge of antiesterase activity of OPs it was proposed that the target site was an esterase and that a mixture of an appropriate esterase substrate with radiolabelled DFP in assays *in vitro* would displace DFP and diminish the rate and extent of progressive covalent binding. Out of more than 30 substrates tested only phenyl phenyl acetate (PPA) was effective at displacing DFP (Johnson, 1969b). All of the PPA esterases of the hen brain were dissected and one minor activity (NTE) was characterised as having the same inhibitor responses as the OPIDN target (Johnson, 1969b, 1970).

Proof has also been provided that aging is essential for initiation of OPIDN. Reaction of NTE with carbamates, phosphinates, sulphonates or sulfonyl fluorides results in phosphorylation of the enzyme, but does not result in neuropathy as NTE cannot age (Fig. 1.3; Johnson, 1973). Interestingly, blockade of the phosphorylation site by these compounds prevents the two-step initiation and hens become resistant to subsequent challenge doses of neurotoxic OPs, such as phosphates, phosphonates and phosphoramidates (Fig. 1.3). This prophylaxis is specific for neuropathic effects and has no influence on cholinergic effects (Johnson, 1992). Another particularly convincing proof of the necessity for the second step in the initiation of OPIDN comes from the observed effects of the enantiomers of ethylphenylphosphonic acid oxon (EPN oxon). Both isomers inhibit NTE *in vitro*, but the aging characteristics of the two are totally different. *In vivo* the L(-)-isomer produces inhibited NTE which ages rapidly, whereas the D(+)-isomer produces an inhibited NTE which cannot age. The L(-)-isomer induces OPIDN and the D(+)-isomer is actually prophylactic rather than neuropathic (Johnson & Read, 1987).

Although the hen model has provided a system in which to study OPIDN, it is essential that the effects seen in hen are also replicated in humans if extrapolations are to be made between the two species. Lotti and Johnson (1978) demonstrated that the IC₅₀ values for 22 compounds, with a wide range of structures, were similar between hen brain and human brain. A wide distribution of NTE in regions of human brain has been reported and rapid aging of DFP-inhibited human NTE has been demonstrated (Moretto & Lotti, 1988; Lotti & Johnson, 1980). In addition, the clinical symptoms reported for cases of human poisoning (Bidstrup et al., 1953; Hierons & Johnson, 1978) are similar to those observed in the hen model.

1.5 NEUROPATHY TARGET ESTERASE (NTE): MOLECULAR ASPECTS AND RELATED PROTEINS

NTE was originally detected in hen brain homogenates by selective assays involving either binding of radiolabelled OP (DFP) or the hydrolysis of an ester (phenyl phenyl acetate or phenyl valerate) (Johnson, 1969a,b). Using these assays it was shown that, in brain, NTE is associated with microsomal membranes (Richardson et al., 1979) and has a subunit size of 155 kDa (Williams & Johnson, 1981; Carrington & Abou-Donia, 1985; Thomas et al.,

1989); this is twice the subunit mass of better characterised esterases such as AChE and liver carboxyesterases. NTE is also present in non-neural tissues of the hen, including ileum, spleen, thymus and heart (Johnson, 1982).

NTE is present throughout the hen nervous system and appears to be confined to neurones and absent from glia. Immunolocalisation revealed that NTE is intracellular rather than on the cell surface and is absent from the nucleus, suggesting that it resides in the endoplasmic reticulum and/or Golgi apparatus of neurones (Glynn et al., 1998).

Efforts to characterise NTE and to determine the mechanism of its involvement in OPIDN have been hampered, until recently, by the lack of a suitable method for its purification. Isolation of native NTE proved difficult due to its low abundance (0.03% of brain microsomal protein; Williams & Johnson, 1981), membrane-bound nature, loss of activity upon solubilisation and inactivation during purification. Detergent is required for solubilisation of NTE and the enzyme's phenyl valerate hydrolase activity is inhibited by even low concentrations of detergent (Johnson, 1982). Thomas et al. (1990) demonstrated that the loss of catalytic activity upon solubilisation could be restored by the inclusion of phospholipid (asolectin) during solubilisation. Pope and Padilla (1989b) also demonstrated that certain phospholipids could stimulate the catalytic activity of partially purified NTE. These results clearly indicate a requirement of lipid for the catalytic function of NTE.

Various approaches have been used to try and purify NTE, such as gel filtration chromatography, ion-exchange chromatography, sucrose density centrifugation and preparative isoelectric focusing with limited success (Pope & Padilla, 1989a; Chemnitius et al., 1984; Ruffer-Turner et al, 1992; Thomas et al., 1989; Thomas et al., 1990; Ishikawa et al., 1983). Therefore, it became necessary to use active-site-directed reagents to isolate NTE.

The first successful attempt to affinity purify NTE was accomplished by Thomas et al. (1993) using 3-(9'-mercaptononylthio)-1.1.1-trifluoroketone (MNTFK) bound to Sepharose. In 1994, Glynn et al. isolated a 155 kDa polypeptide using a biotinylated saligenin phosphate analogue as an active-site ligand. Neither of these methods resulted in an active purified enzyme. However, the latter method produced enough purified biotinylated-NTE to carry out limited digestion using endoproteinase Glu-C. N-terminal

sequencing of 7 NTE peptide fragments (one similar to human EST clone 204484) allowed screening of a lambda Zap foetal human brain cDNA library. From this screening four clones (3.2, 4.2, 4.5 and 4.7kb) were isolated. The sequence of the 4.5kb clone, termed D16, predicts a 1327 amino acid protein (Lush et al., 1998). Standard hydropathy analysis predicts one transmembrane segment, TM1, close to the N-terminus of NTE (Fig. 1.4). TMpred analysis (Hofmann & Stofel, 1993), however, predicts four putative transmembrane segments, TM1-4 (Fig. 1.4).

Database searches (BLASTp) revealed that NTE was similar to conceptual proteins from nematode, yeast and bacteria and also the recently cloned Swiss cheese (SWS) protein of *Drosophila* (Kretzschmar et al., 1997). Six representative members of this group of proteins are shown in Fig. 1.5. These proteins all contain a conserved C-terminal domain of around 200 residues, which includes the motif glycine-X-serine-X-glycine, characteristic of serine hydrolases (Fig. 1.6). In addition, there are also several other conserved residues, such as His945 and D960, which might form a catalytic triad (Lush et al., 1998). Upstream of this common C-terminal domain, the predicted proteins show increasingly extended similarity to NTE with evolutionary progression. In addition, the eukaryotic members of the family have a domain, which resembles the regulatory subunit of cyclic AMP-dependent protein kinase A (Lush et al., 1998).

The Swiss cheese protein and human NTE are 41% identical over almost their full-lengths (Kretzschmar et al., 1997). Swiss cheese mutant flies develop normally during larval life, but show an age-dependent neurodegeneration in the pupa and adult. In late pupae, glial processes form abnormal, multilayered wrappings around neurones and axons. Degeneration first becomes evident in young flies as apoptosis in single scattered cells in the CNS, however it later becomes more severe and widespread. In the adult the number of glial wrappings increases with age. The phenotype of Swiss cheese suggests an involvement of the protein in mechanisms regulating proper ensheathment, either by signalling glia that the correct amount of wrapping has been achieved or by switching off a signal that promotes wrapping. If this fails, glial cells continue to wrap neurones, as seen in the mutant flies, which would finally lead to apoptosis and breakdown of the entire nervous system (Kretzschmar et al., 1997). The high sequence homology between NTE and Swiss cheese, suggests that NTE may have a similar role in neural development.

In addition to the family of homologous proteins, database searches revealed a low homology between the catalytic domain of NTE and a calcium-independent phospholipase A2 (iPLA2) (Fig. 1.7). Phospholipase A2s are a family of proteins, which hydrolyse the sn-2 bond of phospholipids, releasing a fatty acid and generating a lysophospholipid. In terms of a possible role for NTE in a signalling pathway between cells in the developing nervous system, it is interesting that lysophospholipids have been described as second messengers in a number of systems (Wang & Dennis, 1999).

1.6 AIMS OF PROJECT

The overall aim of the project was to characterise the catalytic domain of human neuropathy target esterase (NTE), to gain insight into the physiological role of NTE in neurones and the mechanism of initiation of OPIDN.

Several questions regarding the characteristics of the catalytic domain of human NTE were addressed in this PhD project:

1. What is the minimum NTE amino acid sequence required for expression of a protein with NTE's catalytic activity? (Is the conserved C-terminal domain of 200 amino acids sufficient for catalysis?)
2. Is NTE a conventional serine hydrolase?
3. Does NTE use a catalytic triad for catalysis and what are the residues involved?
4. What are the residues involved in aging of OP-inhibited NTE?
5. Is the catalytic domain of NTE membrane-associated? (Do the putative transmembrane segments, TM2-4, exist?)
6. What is the physiological substrate of NTE?

These questions were investigated and the results are discussed in Chapter 2 (Questions 1-4), Chapter 3 (Question 5) and Chapter 4 (Question 6). Each results chapter contains a combined results and discussion section followed by a general discussion to summarise and draw together the findings of the chapter. Chapter 5 provides an overall discussion of the findings of the PhD project and suggests possible avenues of further investigation. A detailed description of materials and methods is given in Chapter 6.

SERINE HYDROLASES			
AMIDASES	ESTERASES	LIPASES	PROTEASES
Fatty acid amide hydrolase (anandamide, oleamide)	Neuropathy target esterase (unknown)	Outer membrane phospholipase A (phospholipids)	Chymotrypsin (cleaves peptides after aromatic residues)
Acetamidase (acetamide)	Acetylcholinesterase (acetylcholine)	Hormone sensitive lipase (triacylglycerol)	Trypsin (cleaves peptides after basic residues)
Indolacetamidase (indolacetamide)	Butyrylcholinesterase (unknown)	Lipoprotein lipase (triacylglycerol)	Elastase (cleaves peptides after small non-polar residues)
Propionamidase (propionamide)	Carboxylesterase (unknown)	Platelet-activating factor acetyl hydrolase (PAF)	Subtilisin (cleaves peptides after neutral/ acidic residues)
	Juvenile hormone esterase (insect juvenile hormone)	Cytosolic phospholipase A2 (phospholipids)	Proteinase K (cleaves peptides before aromatic/ hydrophobic residues)

Table 1.1: Members of the serine hydrolase superfamily grouped according to function. Examples of serine amidases, esterases, lipases and proteases are shown along with their physiological substrates in brackets.

Acetyl-cholinesterase	Chymotrypsin	Fatty acid amide hydrolase	Neuropathy target esterase	Outer membrane phospholipase A
Cholinesterase	Plasminogen	Vitamin D3 hydroxylase-associated protein	Swiss cheese protein (<i>Drosophila</i>)	NADH-ubiquinone oxidoreductase chain 1
Carboxylesterase	Trypsin	Acetamidase	YOL4 hypothetical protein (<i>C. elegans</i>)	Alpha-amylase 2B (human)
Butyrylcholinesterase	Elastase	Putative amidase (<i>S. cerevisiae</i>)	YMF9 hypothetical protein (<i>S. cerevisiae</i>)	Pancreatic alpha-amylase (human)
Esterase 6	Enteropeptidase	Putative amidase (<i>M. tuberculosis</i>)	YP65 hypothetical protein (<i>M. tuberculosis</i>)	Salivary alpha-amylase (human)
Esterase P	Kallikrein	Indolacetamidase	YCHK hypothetical protein (<i>E. coli</i>)	
Juvenile hormone esterase	Acrosin	Urea amidolyase	cAMP-dependent protein kinase regulatory chain	
Thyroglobulin	Neuropsin		cGMP-dependent protein kinase	
Neurotactin	Vitamin K dependent protein C		Cyclic nucleotide gated channel	
Glutactin	Prothrombin		Glycoprotein I	
TAG lipase	Complement factor I		Anaerobic regulatory protein	

Table 1.2: Proteins homologous to acetylcholinesterase, chymotrypsin, fatty acid amide hydrolase, neuropathy target esterase and outer membrane phospholipase A. BLASTp searches were carried out on AChE, chymotrypsin, FAAH, NTE and OMPLA. Several proteins found to be homologous to these serine hydrolases are shown above.

TYPE OF OP	STRUCTURE	EXAMPLE
Phosphates	$\begin{array}{c} \text{O} \\ \parallel \\ \text{RO}-\text{P}-\text{OR} \\ \\ \text{OR} \end{array}$	Dichlorvos
Phosphonates	$\begin{array}{c} \text{O} \\ \parallel \\ \text{RO}-\text{P}-\text{R} \\ \\ \text{OR} \end{array}$	Trichlorfon
Phosphorothioates	$\begin{array}{c} \text{S} \\ \parallel \\ \text{RO}-\text{P}-\text{OR} \\ \\ \text{OR} \end{array}$	Diazinon
Phosphonothioates	$\begin{array}{c} \text{S} \\ \parallel \\ \text{RO}-\text{P}-\text{R} \\ \\ \text{OR} \end{array}$	Leptophos
Phosphorodithioates	$\begin{array}{c} \text{S} \\ \parallel \\ \text{RS}-\text{P}-\text{OR} \\ \\ \text{OR} \end{array}$	Malathion
Phosphoramidates	$\begin{array}{c} \text{O} \quad \text{R} \\ \parallel \quad \diagup \\ \text{RO}-\text{P}-\text{N} \\ \quad \diagdown \\ \text{OR} \quad \text{R} \end{array}$	Fenamiphos
Phosphorofluoridates	$\begin{array}{c} \text{O} \\ \parallel \\ \text{RO}-\text{P}-\text{F} \\ \\ \text{OR} \end{array}$	DFP
Phosphonofluoridates	$\begin{array}{c} \text{O} \\ \parallel \\ \text{RO}-\text{P}-\text{F} \\ \\ \text{R} \end{array}$	Soman

Table 1.3: Organic derivatives of phosphoric acid, which show anticholinesterase activity. DFP and soman were developed as nerve gases for military use, the remainder are used as pesticides. Thioates are converted by oxidation in vivo to the active P=O form.

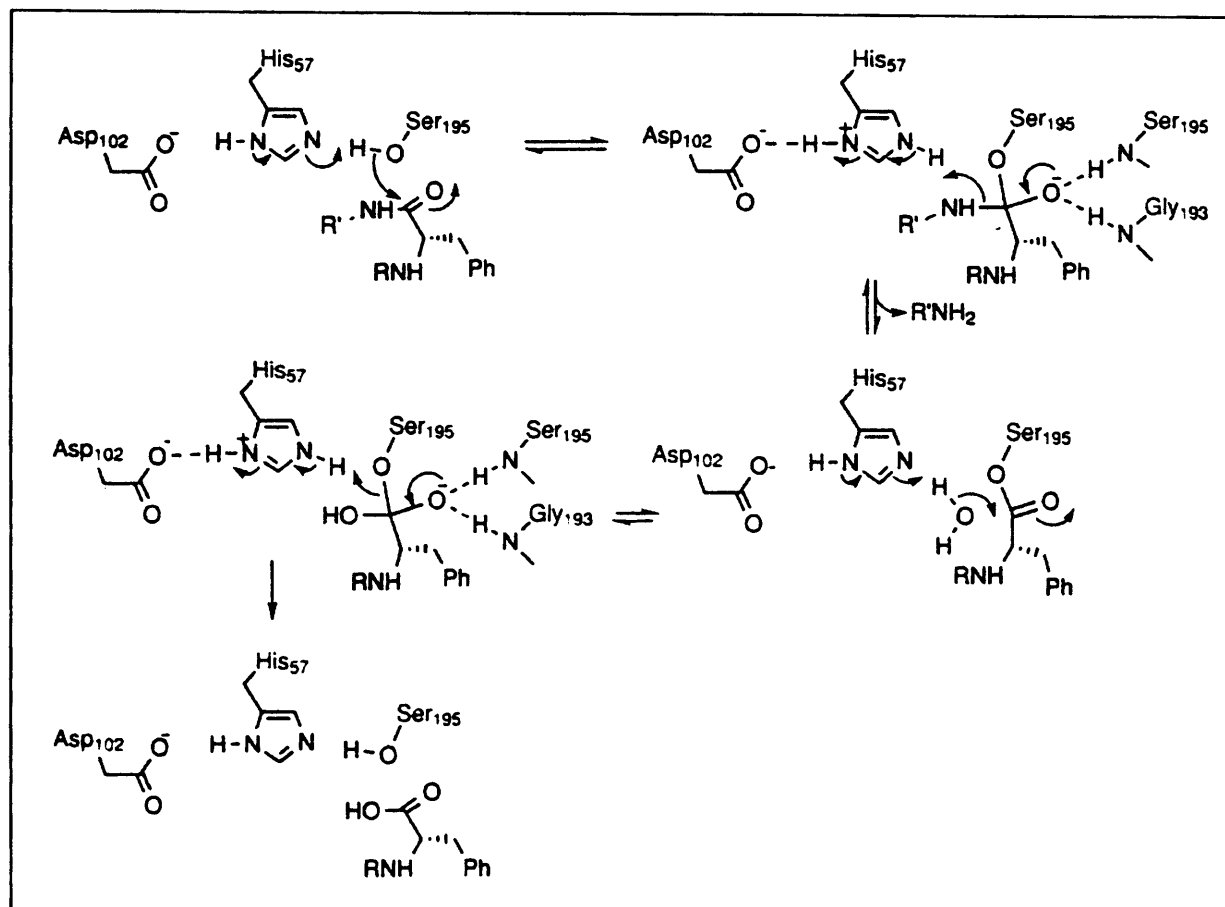


Fig. 1.1: Catalytic mechanism of α -Chymotrypsin (Bugg, 1997).

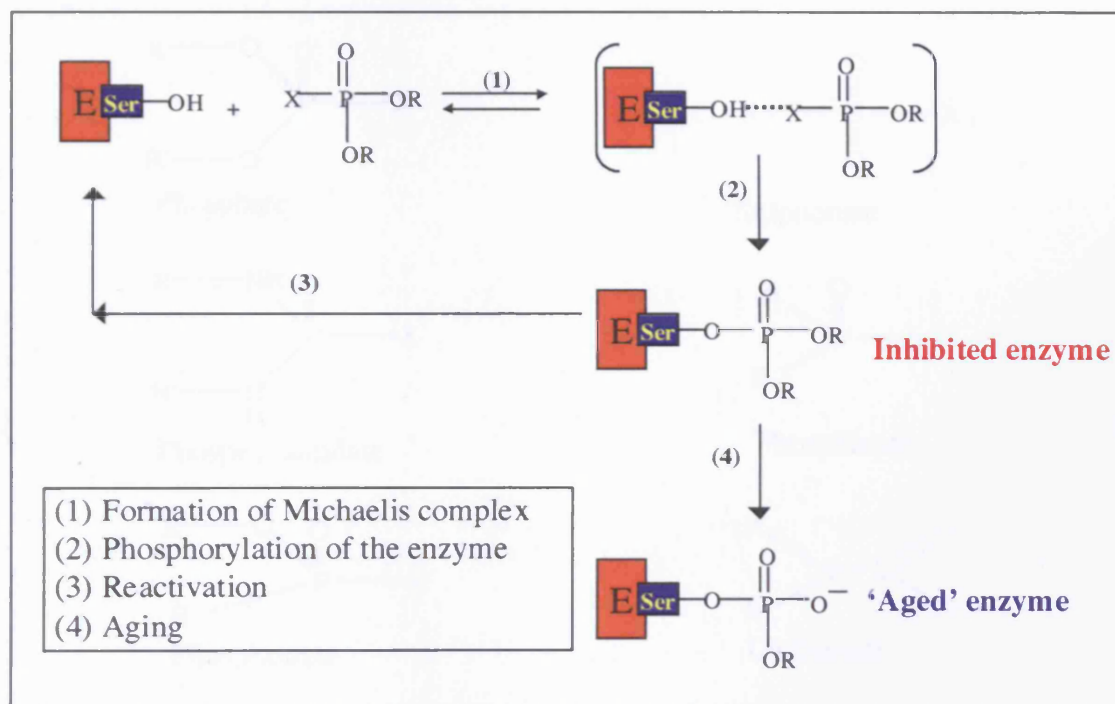


Fig. 1.2: Steps in the interaction of a serine hydrolase with an organophosphate inhibitor. (1) Formation of tetrahedral Michaelis complex; (2) Organophosphorylation of the enzyme; (3) Reactivation (spontaneous or forced by oximes or KF); (4) Aging. Aging is detected as a time-dependent loss of responsiveness to reactivating agents and is proposed to involve loss of an R group leaving a negatively-charged group attached to the serine residue.

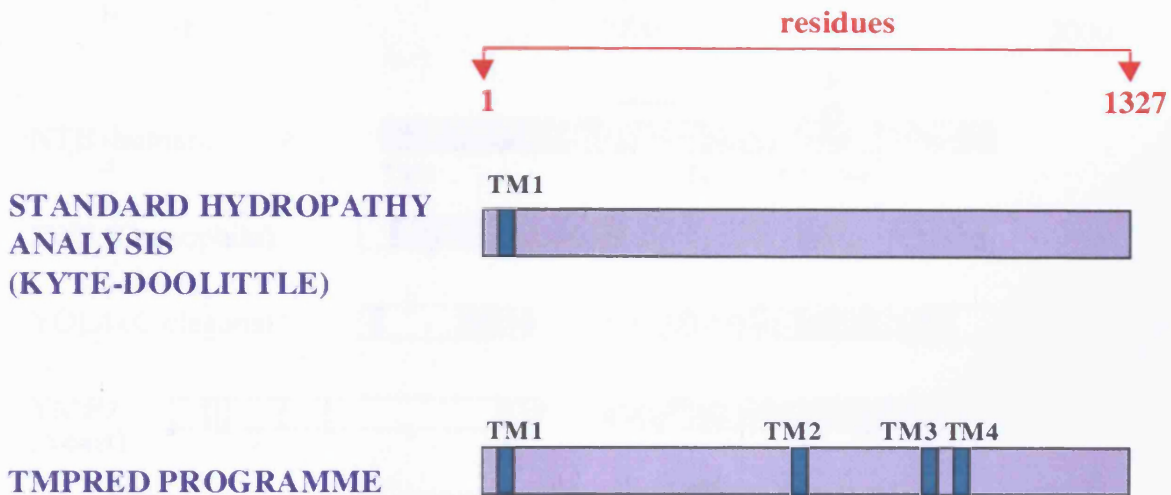


Fig. 1.4: Secondary structure predictions for NTE using standard hydropathy analysis and the TMpred programme. Standard hydropathy analysis predicts one transmembrane segment, TM1 (residues 11-32), whereas the TMpred programme predicts four transmembrane segments, TM1 (residues 11-32), TM2 (residues 734-753), TM3 (residues 925-943) and TM4 (residues 956-976).

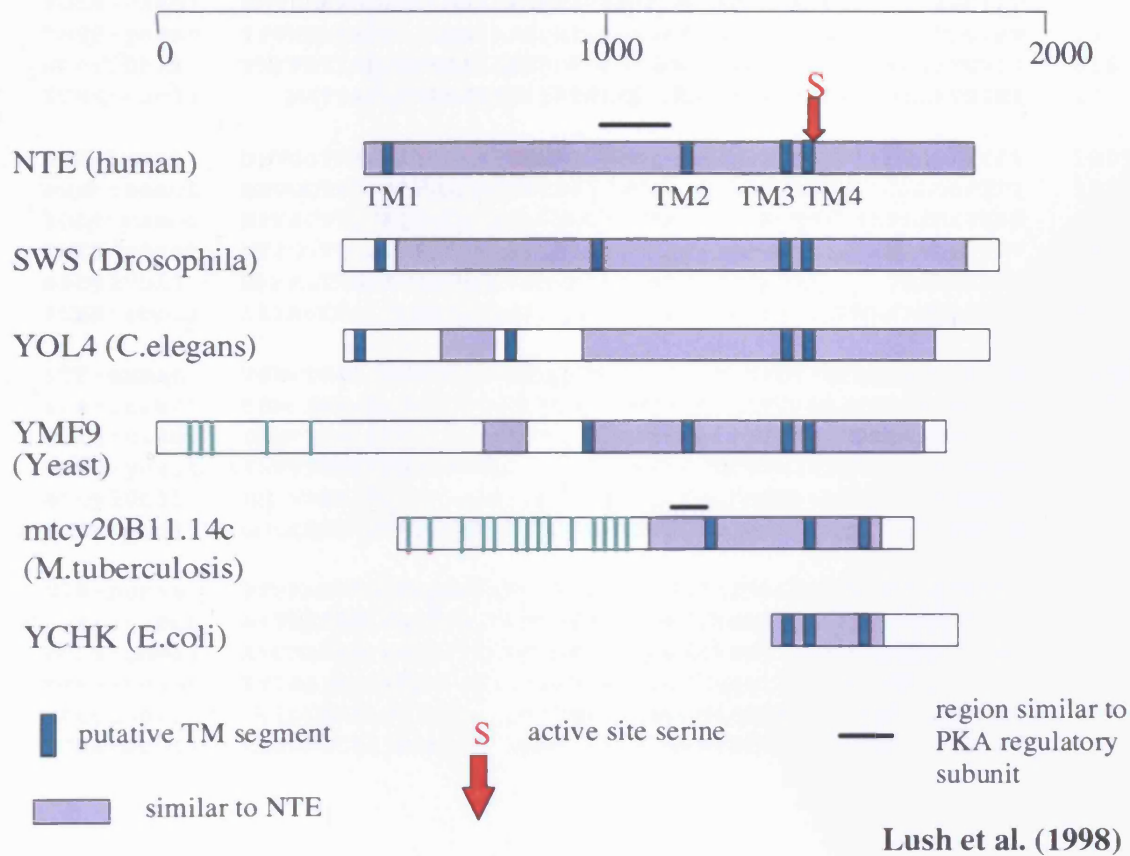


Fig. 1.5: NTE is a member of a novel family of proteins. Representative conceptual proteins homologous to NTE are shown. Database accession numbers are: NTE (AJ004832), SWS (Z97187), YOL4 (Q02331), YMF9 (Q04958), mtcy20b11.14c (Z95121) and YCHK (P37063). The region of sequence homologous to NTE (blue area) and the putative transmembrane segments predicted by TMpred programme (green bars) are shown. The active site serine of NTE, to which organophosphates bind, is highlighted in red.

NTE-human	SRRADRHSDFSRL L ARVLTGNTIALVLGGGG A RGC S HIGVLKALEEAGVPV	959
sws-insect	LSEPNMHSDFSRL L ARWLTGNSIGLVLGGGG A RGA A HIGMLKAIQEAGIPV	978
YOL4-caeel	FWTPDRRSDFSRL L ARILTGNAIGLVLGGGG A RGA A HVGVLRALREEGIPV	966
YMF9-yeast	TPVHRHKNDFLRL L ARILSGQAIGLVLGGGG A RGI S H L GV I Q A IEEQGIPV	1399
mtcy20b11	VHYRRILENVRPL L AARIAGRSIGLVLGGGG A R F AHLGVLDELERVGVTI	816
YCHK-ecoli	...MATIAFQGN L AGIMRKIKIGLALGSG A ARG W SHIGVINALKKVGIEI	47
NTE-human	DLVGG T S IGSFIGALYAEERSASRTKQ R AREWAKSMTSVLEPVLDLTYPV	1009
sws-insect	DMVGG V S IGALMGALWCSE R NITVTQKAREWSKKMTKWFLQLLDLTYPI	1028
YOL4-caeel	DIVGG T S IGSLIGGLYAETPDDVVVETRAASWFNGMSSLWRKLLDLTYAH	1016
YMF9-yeast	DVIG G T S IGSFVGGGLYAKDYDLVPIYGRVKKFAGRISSIW R MLTDLTWPV	1449
mtcy20b11	DRFAG T S MGAVIAVFGACGMDAATADAYAYEYFIRHN...PLSDYAFPV	862
YCHK-ecoli	DIVAG C S IGSLVGAAYACD.RLSALEDWVTSFSYW...DVLRLMDLSWQR	93
NTE-human	TSMFTGS A FNRSIHRVFQDKQ I EDLWLPYFNVTDDITASAMRVHKDGS L W	1059
sws-insect	TSMFSGREFNKT I HDTFGDVS I EDLWIPYFTLTTDITASCHR I HTNGSLW	1078
YOL4-caeel	SAMFTGAQFNFSIKDLFEER L IEDLWISYFCISTDISTSEM R VHRSGPLW	1066
YMF9-yeast	TSYTTGHEFN R GIWKT F GD T RIEDFWIQYYC N STNITDSVQ E IHSFGYAW	1499
mtcy20b11	RGLVRGRR T LTLEAAFGDRL V EELPK E FR C VSVDLLARRPVVHRR R LV	912
YCHK-ecoli	GGLLRGERVFNQYREIMP E TE I ENCSRRFAAVATNLSTGRELW F TEGD L H	143
NTE-human	RYVRASMTLSGYLPPLCDPKDG H LLMDGGYINNLPADIAR S MGAKTVIA I	1109
sws-insect	RYVRSSMSLSGYMPPLCDPKDG H LLLDGGYVNNLPADVMHNLGA A HI I AI	1128
YOL4-caeel	AYCRASMSLAGYLPPLCDPQDG H LLLDGGYVNNVPADVMRNLGAR C VI A C	1116
YMF9-yeast	RYIRASMSLAGLLPPL..EENG S MLLDGGYVDNLPV T EMRARG C Q T IFAV	1547
mtcy20b11	DVIGCSLRLPGIYPP..QVYNGRL H VDGGVLDNLPVS.TRASPDG P LI A V	959
YCHK-ecoli	LAI R ASCSIPGLMAPV..AHNGYWLVDGAVVN P IPISL T RALGADIV I AV	191

Fig. 1.6: Multiple sequence alignment of the conserved C-terminal domain of proteins shown in Fig. 1.5. Sequences of NTE (human), Swiss cheese (*Drosophila*), YOL4 (*C. elegans*), YMF9 (*S. cerevisiae*), mtcy20b11 (*M. tuberculosis*) and YCHK (*E. coli*) are shown. Residues identical in all six proteins are shown in bold. The serine hydrolase consensus sequence (red), histidine 945 (blue) and several conserved aspartates (D960, D1004, D1086) (blue) are also highlighted.

CHAPTER 1: CHARACTERIZATION OF THE RECOMBINANT ESTERASE GXSXG FROM *S. aureus*

Identities = 49/191 (25%), Positives = 69/191 (35%), Gaps = 36/191 (18%)

1.1 INTRODUCTION

```

NTE : 965  LVLGGGGARGCSHIGVLKALEEA-GVPV----DLVGGTSIGSFIGALYAEERS----- 1012
          L L GGG +G  I +L A+E+A GV      D V GTS G  +      +S
IPLA2: 481  LCLDGGGVKGLIIIQLLIAIEKASGVATKDLFDWVAGTSTGGILALAILHSKSMAYMRGM 540

NTE : 1013  -----ASRTKQRARFTEWAKSMTSVLEPVLDLTYPVTSMTGSAFNR---SIHRV 1059
          SR  +      E+ K      + D+ P  M TG+  +R  +H
IPLA2: 541  YFRMKDEVFRGSRPYESGPLEEFLKREFGEHTKMTDVRKPKV-MLTGTLSDRQPAELHLF 599

NTE : 1060  FQDKQIEDLWLPYFNVTDDITASFTAMRVHKDGLWRYVRASMTLSGYLPPLCDPKDGHL 1119
          E + P FN  ++      D +WR R+S  Y P  +G
IPLA2: 600  RNYDAPETVREPRFNQNVNLRPPAQP----SDQLVWRAARSSGAAPTYFRP-----NGRF 650

NTE : 1120  LMDGGYINNLP 1130
          L DGG + N P
IPLA2: 651  L-DGGLLANNP 660

```

1.2 RESULTS

Fig. 1.7: Region of homology between NTE and a calcium-independent phospholipase A2 (iPLA2) (BLASTp). NTE and iPLA2 (SwissProt sp060733) show 25% sequence identity and 35% sequence similarity. Identical and similar residues are highlighted in red and the consensus sequence GXSXG is highlighted in blue.

CHAPTER 2: CHARACTERISATION OF THE RECOMBINANT ESTERASE DOMAIN OF NTE, NEST.

2.1 INTRODUCTION

The isolation of the cDNA clone, D16, which putatively encodes human NTE was described in Chapter 1. The initial aim of this study was to validate the D16 cDNA clone as human NTE. This was achieved by over-expression of the cDNA in a mammalian cell line. Having determined that the D16 cDNA encoded full-length human NTE, several shorter constructs were expressed in *Escherichia coli* in order to find the minimal protein sequence required for catalytic activity. The catalytic domain of NTE was expressed and was termed NEST for NTE esterase domain. Expression and purification of NEST enabled a detailed biochemical characterisation to be carried out, which could be compared to full-length chicken brain NTE. In addition, several conserved residues within NEST were mutated to establish their involvement in catalysis and reaction with organophosphates (OPs).

2.2 RESULTS & DISCUSSION

2.2.1 Validation of the D16 cDNA clone

Previous studies on NTE have used cultured cell lines as an alternative to *in vivo* methods for studying the morphological and biochemical damage caused by neurotoxic OP compounds. Several cell types have been tested for their NTE phenyl valerate (PV) hydrolase activity. Amongst these are rat adrenal pheochromocytoma (PC12) cells and rat brain glial tumour (C6) cells (Li & Casida, 1998), human-derived neuroblastoma (SH-SY5Y) cells (Nostrandt & Ehrich, 1992) and bovine chromaffin cells (Sogorb et al., 1996).

In order to find a cell line with a low endogenous level of NTE suitable for transfection of the D16 cDNA clone, five cell lines were tested for their NTE phenyl valerate hydrolase activity. These were Swiss 3T3 (mouse embryo fibroblasts), CHO (Chinese hamster ovary), COS-7 (monkey kidney), HEK293 (hamster embryonic kidney) and L35 (pig lymphocyte) cells. Out of the five cell lines tested, 3T3 fibroblasts had the lowest

endogenous NTE PV-hydrolase activity, followed by CHO, HEK293, COS-7 and the L35 cell line with the highest activity (Table 2.1). All of the cell lines tested were found to have lower NTE PV-hydrolase activity than the previously studied bovine adrenal chromaffin cells, which have a NTE PV-hydrolase activity of $9.3 \text{ nmol}/10^6 \text{ cells}/\text{min}$ (Sogorb et al., 1996).

Due to their low level of endogenous NTE, 3T3 fibroblasts were chosen for stable transfection of D16 cDNA. The D16 cDNA clone (4.5kb) was sub-cloned into the pTarget™ mammalian expression vector, which was transfected into the 3T3 cells using a lipid transfection method. After 4 weeks of selection with the antibiotic G418, no clones were found with NTE PV-hydrolase activity above background levels. As no stable cell line expressing D16 could be established, a second approach was taken. This involved a transient transfection of the same pTarget™/D16 construct into the COS-7 cell line. COS-7 cells have been used successfully for the high level expression of membrane proteins, such as the Shaker K⁺ channel (Sue et al., 1994).

COS-7 cells were transiently transfected with the pTarget™ vector containing the D16 clone. As a control, the pTarget™ vector alone was also transfected into COS-7 cells to show whether the vector had any effect on NTE levels. Untransfected cells were also assayed to give a background level of endogenous NTE PV-hydrolase activity. Several transfections and subsequent NTE PV-hydrolase assays were carried out. In two of the transient transfections a vector containing the green fluorescent protein (GFP) was also included, to try and establish the transfection efficiency. Twenty-four hours after transfection the cells were visualised under a fluorescence microscope. Although the total number of GFP-containing and GFP-lacking cells were not counted, in a random field approximately 10% of the cells were found to fluoresce. As shown in Fig. 2.1, the NTE PV-hydrolase activity in COS-7 cells transiently transfected with D16 was 3-6 fold greater than the activity found in untransfected cells. Cells transfected with the vector alone showed no significant increase in activity compared to control untransfected cells (data not shown).

Having established that transfection of the D16 cDNA clone produced a catalytically active recombinant protein; it was necessary to determine whether D16 produced full-length

NTE. NTE has been previously shown to be a 155 kDa protein (Williams & Johnson, 1981). Control COS-7 cells and cells transfected with the pTarget™/D16 construct were harvested, run on SDS-PAGE and blotted onto nitrocellulose membrane. Western blot analysis allowed detection of NTE using an antibody to the C-terminus of NTE. Untransfected COS-7 cells showed no detectable band, but cells transfected with D16 showed a band at approximately 155 kDa (Fig. 2.2).

The results from the NTE PV-hydrolase assay and the Western blot analysis demonstrate that D16 encodes a 155 kDa protein with NTE phenyl valerate hydrolase activity. Therefore, the D16 cDNA encodes human NTE and can be used as a template to generate shorter constructs of NTE to determine the minimum protein sequence required for catalytic activity.

2.2.2 Expression of shorter constructs of NTE in *Escherichia coli*

Although several mammalian cell lines are available in which NTE could be expressed, the quantities of protein produced would be small. Over-expression of shorter constructs of NTE in a system, such as *Escherichia coli* or baculovirus, could provide milligram quantities of protein. Due to the large molecular size of NTE it was not possible to over-express the full-length protein in *E. coli*. In this lab, full-length NTE has been cloned in the pET-21b vector and expressed in *E. coli*, but the recombinant protein was extensively degraded and could only be solubilised under denaturing conditions (Y. Li, unpublished). Taking into account the homology within the NTE protein family and the position of the predicted transmembrane segments (TM), constructs were designed to establish the minimum protein sequence required for catalytic activity (Fig. 2.3).

PCR products were sub-cloned into the pET-21b vector using BamHI and SalI restriction sites. The pET-21b vector contains a T7 tag of 11 aminoacids at the N-terminus, which allows detection of recombinant proteins by Western blot analysis. At the C-terminus, is a hexahistidine (His₆) tag, which allows detection by Western blot and purification on nickel resin. Constructs were transformed into XL-10 Gold cells and transformants checked for

the correct insert by diagnostic PCR. Having identified positive transformants these were transformed into the expression strain BL21(DE3)pLysS.

Expression of recombinant proteins was demonstrated by running Western blots and probing with the T7 tag antibody. NEST F-11F/3R all expressed in the BL21(DE3)pLysS strain at different protein levels (data not shown). NEST 9F/3R expressed at very low levels compared to NEST 2F/3R, NEST 4F/3R and NEST 11F/3R, which expressed at very high levels. *E. coli* lysates of all eight constructs were solubilised with either 1% CHAPS or 1% CHAPS plus 8M urea. Only NEST 2F/3R and NEST 4F/3R could be extracted in CHAPS alone, and all the other constructs required denaturing conditions for extraction. A blot of NEST 2F/3R, 4F/3R, 4F/7R and 11F/3R solubilised in CHAPS or CHAPS plus urea is shown in Fig. 2.4.

In addition, phenyl valerate hydrolase assays were carried out on *E. coli* lysates of all eight constructs (Fig. 2.3). Interestingly, only NEST 2F/3R and NEST 4F/3R showed any PV-hydrolase activity, 19,000 and 12,500 nmol/min/mg total protein respectively. Taken together with the extraction data, this suggests that only these two polypeptides are folded correctly when expressed in the BL21(DE3)pLysS strain. All of the other polypeptides were inactive (Fig. 2.3) and insoluble, suggesting that they may be present in insoluble aggregates, known as inclusion bodies.

Of the eight constructs expressed only NEST 2F/3R (residues 727-1216) and NEST 4F/3R (734-1216) had catalytic activity. NEST 2F/3R was found to express at slightly higher levels than NEST 4F/3R and was therefore chosen for use in all subsequent experiments. The N-terminal limit of the NEST constructs was also suggested by previous observations (Lush et al., 1998) that endoproteinase Glu-C cleavage of NTE generated a number of peptides initiated by L727. This suggested that L727 might lie in the area of a protein domain boundary. In addition, TM2, the second of NTE's four putative transmembrane segments begins at L734, which is the initial residue in the NEST 4F/3R construct. In contrast, the other six constructs, which contained only part or none of TM2 were not catalytically active. Therefore, residue 734 appears to be the N-terminal boundary for expression of a catalytically active recombinant protein.

The C-terminal boundary of NEST was not investigated in detail. However, two PCR products were designed, NEST 4F/6R and NEST 4F/7R (Fig. 2.5). Unfortunately, cloning of the NEST 4F/6R product into the pET-21b vector was unsuccessful. However, NEST 4F/7R was cloned into the pET vector and expressed in the *E. coli* strain, BL21(DE3)pLysS. Expression of this construct resulted in a catalytically inactive, 40 kDa recombinant polypeptide, which required denaturing detergent for solubilisation (Fig. 2.4). Therefore, removal of 115 amino acids from the C-terminus of NEST results in the loss of enzyme activity. As NEST 2F/3R expressed well in *E. coli* and showed potent esterase activity no further effort was made to pinpoint the exact C-terminal residue at which activity was lost.

2.2.3 Solubilisation, purification and reconstitution of NEST

Expression of the NEST 2F/3R construct produced a 55 kDa catalytically active recombinant protein, hereafter simply termed NEST, which was used for all subsequent experiments.

2.2.3.1 Solubilisation of NEST

As recombinant NEST did not express as a soluble protein, the next step was to establish a suitable detergent for solubilisation. Three detergents were chosen, Triton X-100 (TX-100), CHAPS and sodium deoxycholate (DOC). These detergents have been shown to have partial success in solubilising NTE from brain tissue (Ishikawa et al., 1983; Johnson, 1971; Davis & Richardson, 1987; Pope & Padilla, 1989a).

Triton X-100 is a non-ionic detergent with uncharged hydrophilic polyoxyethylene head groups. It has a low critical micellar concentration (CMC = 0.015-0.019 %) and is therefore difficult to remove by dialysis. CHAPS is a zwitterionic detergent with a relatively high CMC (0.25-0.5%), which facilitates its removal from protein samples by dialysis. Some membrane proteins, because of their hydrophobic nature, have a tendency to interact non-specifically with other proteins when solubilised by detergents. Non-ionic detergents are not able to prevent these interactions, however ionic and zwitterionic detergents, such as CHAPS, can. Sodium deoxycholate is a bile acid salt with a CMC of

0.21%. Bile acid salts are anionic detergents, which can prevent non-specific interactions between proteins during solubilisation without denaturation. However, due to their charge they have the potential to bind to ion exchange columns.

TX-100 (0.3%), CHAPS (0.3%) and deoxycholate (0.5%) were capable of solubilising a similar proportion of NEST, as shown by western blot analysis of the supernatant, after centrifugation at $100,000 \times g$ (Fig. 2.6). When the amount of NEST in the pellet and supernatant were compared it was found 0.3% TX-100, 0.3% CHAPS and 0.5% DOC solubilised less than 30% of the NEST protein. Although, this is not very efficient solubilisation it is possible that some of the NEST is not folded correctly and is present in insoluble aggregates, known as inclusion bodies. As denaturing detergents (such as the ionic detergent sodium dodecyl sulphate) are required for extraction of proteins from inclusion bodies, none of the detergents tested would be able to extract NEST if it was present in inclusion bodies. After solubilisation of NEST in these detergents the supernatants were measured for NTE PV-hydrolase activity (Table 2.2). Addition of TX-100, CHAPS and DOC all resulted in almost complete loss of NEST catalytic activity in both the supernatant and pellet samples.

It is clear from these data that the addition of detergent results in the loss of catalytic activity of the NEST protein. This phenomenon has been observed before for other membrane proteins, such as glycerophosphate acyltransferase from rat liver mitochondria (Vancura & Haldar, 1994), the Na^+/K^+ -ATPase of electric eel (Brotherus et al., 1979) and hen brain NTE (Davis & Richardson, 1987). This profound effect upon the activity of NEST may be due to NEST being an integral membrane protein, which requires lipid to function correctly. The addition of lipid during detergent solubilisation of NTE has been shown to reduce this loss of catalytic activity (Davis & Richardson, 1987; Thomas et al., 1990). CHAPS was selected as the detergent for solubilisation as it can be removed easily by dialysis (cf. TX-100) and is electrically neutral (cf. DOC) and therefore can be used for iso-electric focusing and ion-exchange chromatography.

As >99% of catalytic activity was lost even at low concentrations of CHAPS, solubilisation of NEST was carried out with the concentration of CHAPS, which gave the best recovery. The presence of 1mM EDTA in the purification of NTE has been shown to help retain

NTE catalytic activity (Mackay et al., 1996). As nickel chromatography is the first purification step 0.5mM EDTA was used, as higher concentrations of EDTA effect the binding of His-tagged proteins to the nickel resin. The final solubilisation conditions were 50mM sodium phosphate buffer (pH 7.8), 300mM NaCl, 0.5mM EDTA and 2% CHAPS. After solubilisation at 4°C for 90min, the mixture was centrifuged at $100,000 \times g$ for 60min at 4°C to remove any insoluble material. Using these solubilisation conditions approximately 60-70% of the NEST protein could be solubilised. It is possible that a large proportion of the NEST which could not be solubilised is not folded correctly and is present in inclusion bodies.

2.2.3.2 Purification of NEST using nickel affinity and gel filtration chromatography

The pET-21b vector expresses a hexahistidine tag on the C-terminus of NEST, which allows the recombinant NEST to be purified by nickel-chelate chromatography. The supernatant, obtained after solubilisation of NEST from bacterial lysates, was incubated with the Ni-NTA resin (50% slurry) for 60min at room temperature, with continuous mixing. After 60min, the material was centrifuged to pellet the nickel resin and the resulting supernatant, which contains any unbound material, was carefully decanted off the resin. The nickel resin was washed three times in sodium phosphate buffer containing 0.3% CHAPS and 50mM imidazole. This wash step has two benefits: firstly, it enables the CHAPS concentration to be reduced from 2% down to 0.3%, as a high CHAPS concentration is only required for solubilisation and not purification. Secondly, the presence of 50mM imidazole allows the removal of endogenous proteins with histidine residues that interact with the Ni-NTA matrix.

The NEST protein was subsequently eluted in sodium phosphate buffer containing 0.3% CHAPS and 300mM imidazole. It was demonstrated that three elution steps resulted in the best recovery of the NEST protein (Fig. 2.7a). However, a proportion of the NEST always remained tightly bound to the Ni-NTA matrix, as demonstrated by boiling the resin in SDS sample buffer, running on SDS-PAGE and blotting onto nitrocellulose (Fig. 2.7b). After a single purification step NEST was found to be 65% pure (determined using Image Quant analysis) (Fig. 2.7a, lane 3).

The material eluted from the nickel resin was pooled and concentrated 30-fold using a Vivaspin 15ml concentrator (MWCO 30,000 kDa). The concentrated protein was loaded onto a gel filtration column (see Methods), which was equilibrated and run in sodium phosphate buffer containing 0.3% CHAPS and 1mM DTT. DTT was not present in the purification up to this point as it effects the ability of the Ni-NTA resin to bind proteins.

The gel filtration profile (A_{280}) showed one distinct peak (Fig. 2.8). Fractions were collected and NEST was found to elute at fractions #29-32, corresponding to the single peak. NEST-containing fractions were identified primarily by Western blot using the T7 tag monoclonal antibody and thereafter using standard Coomassie stained SDS-polyacrylamide gels. NEST ran at 55 kDa on SDS-PAGE and was greater than 95% pure (determined by Image Quant analysis) (Fig. 2.7a, lane 6).

2.2.3.3 Reconstitution of NEST into synthetic phospholipid liposomes

Membrane reconstitution has been used successfully to restore functional activity to a number of integral membrane proteins, such as the Na^+/K^+ -ATPase (Mohraz, 1999) and the Shaker K^+ channel (Santacruz-Tolozza et al., 1994). Purification of active proteins is a prerequisite for detailed structural analysis, since activity is the key indication that the structural integrity of the protein has been preserved during biochemical procedures.

Throughout the purification procedure the NEST protein was monitored by Western blots probed with the T7 tag antibody. Due to the presence of detergent throughout the solubilisation and purification procedure, purified NEST was catalytically inactive. Even at 0.3% CHAPS more than 99% of the PV-hydrolase activity was lost. After the two step purification procedure NEST was greater than 95% pure and 1-2mg of pure protein could be obtained from a 0.8 litre starting culture.

The characteristics, which NEST shows upon detergent solubilisation, i.e. loss of activity and dependence on lipid, suggest that NEST is an integral membrane protein. Therefore, to restore catalytic activity, lipid must be added back into the system and detergent must be removed. As CHAPS has a relatively high CMC, detergent can be removed by dialysis.

NEST-containing fractions from each gel filtration run were combined and the amount of protein determined by the Bradford protein assay (Bradford, 1976). The synthetic lipid L- α -phosphatidylcholine, dioleoyl (DOPC) was chosen as it has been used successfully for membrane protein reconstitution (Li et al., 1996). A stock solution of 10mg/ml DOPC was made up in sodium phosphate buffer and detergent was added until the solution cleared. The final CHAPS concentration was 9%. NEST and DOPC were combined and mixed at room temperature for 3 hours. The final CHAPS concentration in the lipid/protein mixture was approximately 0.82%. After three hours the lipid/protein/detergent mix was injected into a dialysis cassette and dialysed at room temperature against 200 volumes of sodium phosphate buffer containing 300mM NaCl, 0.5mM EDTA and 1mM DTT.

The length of dialysis proved to be critical. Initially samples were dialysed for 7 days, changing the dialysis buffer daily, to ensure that all detergent had been removed. However, later experiments demonstrated that after 2 to 3 days activity was at its greatest and therefore a 2-day dialysis was employed for all the subsequent reconstitution experiments. With the two day dialysis method, the buffer was exchanged twice daily to ensure that all of the CHAPS was removed.

Several lipid to protein ratios were tested 1:2, 1:1, 2:1, 3:1, 4:1, 6:1 and 8:1. The lipid to protein ratio, 3:1, produced the most catalytically active reconstituted NEST, with the 2:1 and 4:1 ratios producing slightly less active protein. At a ratio of 1:2 very little PV-hydrolase activity could be detected. From initial reconstitution experiments a protein concentration of 0.21mg/ml was shown to be optimal. At lower protein concentrations (0.1 mg/ml) very little active reconstitution was observed and higher protein concentrations (0.4 mg/ml) resulted in precipitation of the NEST protein.

Phenyl valerate hydrolase assays were carried out in the absence of paraoxon or mipafox. This is possible as NEST is the only protein present in the system and therefore the standard differential assay (Johnson, 1977) is no longer required. The PV-hydrolase activity of the reconstituted NEST in DOPC liposomes was found to be 2.01 ± 0.35 10^6 nmol/min/mg protein. Controls were also carried out either with protein or lipid (DOPC) only. The lipid control showed no PV-hydrolase activity, as expected. The protein control showed approximately 0.1% of reconstituted NEST PV-hydrolase activity. The

same amount of PV-hydrolase activity (0.1%) was also found in the purified NEST gel filtration samples.

A time course of the reaction of NEST in DOPC liposomes with the substrate phenyl valerate was carried out to establish that the kinetic characteristics of NEST with the substrate are the same as for native NTE. Previous work on NTE has shown that up to 20min incubation with phenyl valerate the reaction is linear. Therefore the standard differential PV-hydrolase assay designed by Johnson (1977) uses this fixed time of substrate hydrolysis. A plot of incubation time with phenyl valerate versus PV-hydrolase activity for NEST showed that the enzyme reaction is also linear up to 20min and becomes non-linear from 20-40min (Fig. 2.9).

The influence of pH on NEST PV-hydrolase activity was also investigated (Fig. 2.10). Over the pH range 6.8 to 9, PV-hydrolase activity changed very little, but at pH 6.3 activity was decreased by approximately 50%. This differs somewhat from NTE activity in hen brain microsomes which changes only slightly in the pH range 9 to 6 and declines rapidly as the pH is changed from 6 to 4 (Johnson, 1982). This subtle difference may reflect ionisation of histidine residues ($pK_a \sim 6$) in the different systems, i.e. full-length NTE in biological membranes versus NEST in DOPC liposomes. However, at pH 8, NEST can hydrolyse phenyl valerate and this reaction was found to be linear up to 20min. Therefore, under the standard PV-hydrolase assay conditions NEST behaves in a similar fashion to native NTE.

2.2.4 Comparison of NEST in bacterial membranes and DOPC liposomes with native NTE in chicken brain microsomes

NEST has been over-expressed in *E. coli* and produces a 55 kDa recombinant protein with NTE PV-hydrolase activity, which could be purified and actively reconstituted into DOPC liposomes. To demonstrate that NEST is a valid system for studying the structure and function of NTE, NEST in *E. coli* lysates and purified NEST in DOPC liposomes were compared to native NTE from chicken brain membranes with respect to their catalytic centre activity, OP reactivity and aging.

2.2.4.1 Catalytic Centre Activity of NEST and NTE

To determine an accurate turnover number for NTE and NEST it was necessary to calculate the catalytic centre activity. This value circumvents the need for an accurate determination of the concentration of NTE or NEST protein in heterogeneous preparations. The NTE PV-hydrolase activity (pmoles PV hydrolysed/min) was determined for a given volume of NEST in *E. coli* lysates, NEST in DOPC liposomes and NTE from chicken brain microsomes. The same volume of each membrane preparation was then labelled with [³H]DFP and the samples run on SDS-PAGE. The respective bands, 55 kDa for NEST and 155 kDa for NTE, were excised, gel pieces were treated with sodium hydroxide and radioactivity in the eluates was determined by scintillation counting. From the specific activity of the [³H]DFP the number of pmoles DFP bound to NEST and NTE were calculated. The catalytic centre activity was then determined using the following equation:

$$\text{Catalytic centre activity} = \frac{\text{PV hydrolysed (pmol/min)}}{\text{DFP bound (pmol)}}$$

As shown in Table 2.3, the catalytic centre activity of NEST in *E. coli* lysates and NEST in DOPC liposomes is similar to that of native NTE from chicken brain membranes. These results also agree closely with previous values found by Meredith and Johnson (1988) of $1.53 \pm 0.08 \times 10^5 \text{ min}^{-1}$ and by Williams (1983) of $1.6 \times 10^5 \text{ min}^{-1}$ for hen brain NTE. This data therefore suggests that NEST alone is sufficient to provide full catalytic activity and is capable of reacting with [³H]DFP (a neuropathic OP) in the same manner as native NTE.

2.2.4.2 Covalent inhibitors of NEST and NTE

Having established that NEST has the same catalytic centre activity as native NTE it was essential to demonstrate that NEST could react with a set of covalent NTE inhibitors with the same specificity as native NTE. Five NTE inhibitors were chosen, which included the neuropathic OPs, phenyl saligenin phosphate (PSP), diisopropylfluorophosphate (DFP) and

mipafox (MIP), and the non-neuropathic inhibitors, phenyl dipentylphosphinate (PDPP) and phenyl methylsulfonylfluoride (PMSF).

For these inhibition experiments the *E. coli* lysate preparation was used due to the large amount of material required. The previous section demonstrated that NEST in *E. coli* lysates had the same catalytic centre activity as NEST in DOPC liposomes, therefore it would be expected that both preparations of NEST react in the same way with NTE inhibitors. From the IC₅₀ values obtained it is evident that NEST reacts with the five inhibitors in a similar fashion to chicken brain NTE and the rank order of potency PSP>PDPP>DFP>MIP>PMSF is identical (Table 2.4). In general, the IC₅₀ values for NEST were slightly higher than for chicken NTE (1.5-2.5 fold). Interestingly, the IC₅₀ values of PSP, DFP, MIP and PMSF for human brain NTE (Lotti & Johnson, 1978) are similar to those found for NEST and are all 1.5-1.7 fold higher than those found for hen brain NTE. This may explain some of the differences in IC₅₀ values found between (human) NEST and NTE from chicken brain.

2.2.4.3 Aging of NEST and NTE

NTE appears to be unique among the DFP-sensitive serine hydrolases, in that it undergoes a rapid aging reaction ($T_{1/2} < 7.5$ min) in which one of the isopropyl groups in the organophosphorylated enzyme is transferred to a distinct residue, designated site Z, in the same polypeptide (Clothier & Johnson, 1979; Williams, 1983). This intramolecular rearrangement results in a negative charge at the active site of the enzyme (Johnson, 1974; Clothier & Johnson, 1980).

The tritiated isopropyl groups bound to the active site serine and site Z in [³H]DFP-labelled NTE can be liberated into solution by treatment with sodium hydroxide: the latter is readily volatile (putatively isopropanol) and the former is not (mono-isopropylphosphate). Measurement of the radioactivity with and without freeze-drying allows the percentage of volatile counts to be determined. This method has been called the “volatilisable counts assay” (Williams, 1983) and is one technique for determining whether NTE has aged. NEST and NTE both showed around 30% volatile counts (Table 2.5). Therefore, NEST appears to age in the same way as native NTE from chicken brain microsomes.

Another technique to determine whether aging of NTE has occurred is the use of reactivators, such as potassium fluoride (KF) or nucleophilic oximes (e.g. isonitrosoacetophenone). Clothier and Johnson (1979) showed that aged DFP-inhibited NTE could not be reactivated with KF. In their preliminary experiments it was found that the only inhibited NTE which could be reactivated was the phosphinylated enzyme. Although KF can be used to differentiate between DFP-inhibited ('aged') and phosphinate-inhibited ('non-aged') NTE, it is not as effective as isonitrosoacetophenone (INAP). INAP has been shown to give > 90% reactivation of phosphinate-inhibited NTE (Meredith & Johnson, 1988). Using chicken brain membranes and NEST in bacterial membranes it was shown that with DFP-inhibited enzyme no reactivation was possible with INAP, whereas with phenyl di-n-pentyl phosphinate-inhibited enzyme almost complete reactivation occurred (Table 2.6).

Along with the results for the volatilisable counts assay this demonstrates that NEST can age in the same manner as native NTE. It is worth noting that the proportion of total covalently bound tritium associated with site Z in aged, [³H]DFP-inhibited NTE or NEST fell short of the value expected (50%) if aging goes rapidly to completion. However, DFP-inhibited NTE and DFP-inhibited NEST could not be reactivated by oxime, suggesting that aging has indeed gone to completion. Therefore, it appears that under the incubation conditions used, either the transfer of the shed isopropyl group to site Z from the serine may not be totally efficient or the bond formed between the transferred isopropyl group and site Z may be rather labile.

2.2.5 Determination of residues critical to catalysis and aging of NTE

2.2.5.1 Identification of the active site serine and possible candidates for site Z

To determine which residues within NEST were labelled with [³H]DFP, NEST in DOPC liposomes were incubated with [³H]DFP and digested with endoproteinase Glu-C (V8). Fractionation of these digests on SDS-PAGE resolved twelve polypeptide bands with molecular weights between 6-40 kDa in relative amounts determined by densitometry (Fig. 2.11). The amounts of total and volatilisable radioactivity following sodium hydroxide treatment of excised polypeptide bands were determined which, together with

densitometric data allowed estimation of the relative specific activities of each polypeptide fragment (Table 2.7).

In addition, digests run on SDS-PAGE were blotted onto polyvinylidene difluoride (PVDF) so that N-terminal sequence information could be obtained for the bands of interest (Table 2.7). A combination of N-terminal sequencing of individual bands and prediction of the size of the fragments generated by endoproteinase Glu-C cleavage of NEST allowed creation of a partial peptide map (Fig. 2.12).

Band 6 had the highest specific activity and had approximately 30% volatile counts associated with it. When this 17 kDa band was sequenced it was found to start at the sequence AGVPV, which lies just upstream of the GX SXG consensus sequence. Given that Band 6 had 30% volatile counts it is likely that this peptide contains not only the active site serine but also site Z. Band 3 also had a high specific activity and contains the consensus sequence GX SXG.

Another band of interest was Band 8, which had greater than 80% volatile counts. Sequencing of this band showed that it does not contain the consensus sequence, suggesting that this band contains site Z, but not the active site serine. The low specific activity associated with this band also suggests that the catalytic serine is not present in this peptide.

Consideration of specific radioactivity and the distribution of volatilisable counts among the various polypeptide fragments led to the conclusion that both the active site serine and site Z are located between residues 955-1166 of NEST.

Band 6 of the endoproteinase Glu-C digest was subjected to repeated cycles of Edman degradation and a peak of radioactivity was found to associate with serine 966 (Fig. 2.13a). Therefore serine 966, which lies at the centre of the serine hydrolase consensus sequence, is the catalytic serine to which organophosphates bind. The highest percentage of volatilisable counts, suggestive of the presence of site Z, was associated with Band 8. Edman degradation of this polypeptide yielded a small peak of radioactivity, which was coincident with aspartate D1044 (Fig. 2.13b).

These data suggest that D1044 is a possible candidate for site Z. However, the amount of radioactivity associated with D1044 was small and therefore, it can not be ruled out that other residues within Band 8 also have radioactivity associated with them. To try and determine whether any other residues within Band 8 bound [³H]DFP, it was necessary to further digest this peptide fragment. Band 8 was treated with trypsin and the peptides generated were run on reverse-phase HPLC (RP-HPLC). Several peptides were identified, which were not present in the control trypsin sample, however, the yields were very low. Very little radioactivity was present in fractions from the RP-HPLC but two peptides were found to contain radioactivity which was above background levels. Unfortunately, the amount of peptide remaining was insufficient for N-terminal sequencing to be carried out (data not shown).

2.2.5.2 Identification of residues critical for catalysis by site-directed mutagenesis

Most serine hydrolases for which crystal structures have been solved use a catalytic triad in which a histidine is within hydrogen bond distance of both the nucleophilic serine and an acidic (aspartate or glutamate) residue (Dodson & Wlodawer, 1998). Sequence alignment of proteins homologous to NTE, from *Drosophila* (SWS), *C. elegans* (YOLA), yeast (YMF9), *Mycobacterium tuberculosis* (mtcy20B11) and *E. coli* (YCHK) shows a conserved C-terminal domain of about 200 amino acids (Fig. 2.14). Within this common C-terminal domain are several conserved residues. Noticeably the motif GX SXG around the active site serine of NTE is retained throughout this family (Lush et al., 1998).

In addition, there are several conserved histidines, aspartates and a glutamate residue (His945, His1053, Asp960, Asp1004, Asp1033, Asp1044, Asp1086, and Glu1032). Site-directed mutagenesis of these conserved residues and the active site serine was carried out on the NEST cDNA construct (Fig. 2.15) to identify the residues involved both in the catalytic triad of NTE the 'aging' reaction. Mutant cDNA constructs were sequenced to confirm the correct mutation had been made and then polypeptides were expressed in the BL21(DE3)pLysS strain. After normalising, by comparing the levels of recombinant polypeptides on Western blots (Fig. 2.16), the esterase activities and [³H]DFP binding in lysates of bacteria expressing the mutant NEST constructs were determined.

The active site serine (S966), which was confirmed by [³H]DFP labelling (Fig. 2.13a), was mutated to alanine. This substitution has been shown to minimise disturbance in protein structure (Bordo & Argos, 1991). As expected, mutation of this residue resulted in complete loss of activity (Fig. 2.17a) and [³H]DFP binding (Fig. 2.17b).

The candidate catalytic aspartate residues were mutated to asparagine. D960N and D1086N mutations reduced catalytic activity 10,000 fold (Fig. 2.17a) and also resulted in a loss of [³H]DFP binding (Fig. 2.17b). It is conceivable that mutation of D960 results in a conformational change, as this residue lies in the putative transmembrane segment TM4. D1086, however, does not lie in a putative transmembrane domain and in the primary structure lies 120 amino acids away from the catalytic serine. However, it is possible that mutation of this residue results in a change in the structure of the protein such that catalytic activity is lost.

Mutation of two other aspartates D1004 and D1033 led to a minor loss (60-90%) of activity, while mutation of D1044 or E1032 had no apparent effect. As shown in section 2.2.5.1, D1044 has been identified as a residue, within Band 8, to which [³H]DFP binds (Fig. 2.13b). This result suggested that D1044 might be site Z, the residue to which an isopropyl group is transferred upon aging of DFP-inhibited NTE. However, mutation of this residue to asparagine resulted in an enzyme with the same percentage volatile counts as wild-type NEST (27.0%, n = 2). If site Z is a single residue then we would expect mutation of D1044 to result in an enzyme, which could no longer age. This was not observed, suggesting that there may be more than one acceptor for the isopropyl group, which is transferred upon aging of the enzyme. There are several other conserved aspartate residues within NEST, including D1086 which is critical for catalysis and D1004 which, when mutated to asparagine, results in an enzyme with 40% wild-type activity (Fig. 2.17a) and only half the percentage volatile counts of wild-type ($14.8 \pm 4.5\%$; n=3).

Within the core 200-residue region, mutation of two conserved histidines to alanine, H945A and H1053A, had no apparent effect on PV-hydrolase activity (Fig. 2.17a) or [³H]DFP binding (Fig. 2.17b). Subsequently all the remaining 9 histidines in NEST were individually mutated to alanine. H860A and H885A showed substantially reduced (>300-fold) catalytic activity (Fig. 2.17a) and [³H]DFP binding (Fig. 2.17b). Although the H860A mutant of NEST showed less than 0.1% of the activity of the wild-type, it is unlikely that

this histidine is directly involved in a catalytic triad. This is because a tyrosine residue is found in the corresponding position in SWS, the *Drosophila* homologue. In addition, it has been shown that a portion of SWS, co-linear with NEST, expressed in *E. coli* has substantial NTE-like esterase activity (Glynn & Kretzschmar, unpublished). H885 is conserved in all eukaryotic homologues of NTE, but the loss of catalytic activity resulting from this mutation is substantially less (30-fold) than in the D960N or D1086N mutants.

2.3 GENERAL DISCUSSION

Cloning of human NTE (Lush et al., 1998) has provided the opportunity to over-express this integral membrane protein in an *in vitro* system. Transient transfection of D16 into COS-7 cells resulted in a 3-6 fold increase in NTE PV-hydrolase activity and the production of a 155 kDa polypeptide, demonstrating that D16 encodes full-length, catalytically active NTE.

Expression of shorter constructs of NTE in *E. coli* established the minimal protein sequence required for catalytic activity (734-1216). Of the ten constructs tested only two, NEST 2F/3R (727-1216) and NEST 4F/3R (734-1216) had catalytic activity and could be extracted from *E. coli* lysates under non-denaturing conditions. NEST 2F/3R was chosen as it expressed at a higher level than NEST 4F/3R and had more potent esterase activity.

Expression of NEST 2F/3R (NTE 727-1216) produced a 55 kDa recombinant protein, termed NEST, for NTE esterase domain. The recombinant protein was not soluble in aqueous buffers and required detergent for solubilisation. NEST was solubilised in 2% CHAPS and purified on nickel resin, using the C-terminal hexahistidine tag. After this one purification step, NEST was found to be 65% pure. A second gel filtration step was used to further purify NEST, which resulted in greater than 95% pure protein. Due to the presence of 2% CHAPS in the solubilisation and 0.3% CHAPS in the purification the purified NEST was catalytically inactive. This loss of activity in the presence of detergent suggests that NEST is an integral membrane protein, which requires lipid for its PV-hydrolase activity. This was demonstrated by the fact that reconstitution of NEST into DOPC liposomes, by detergent dialysis, resulted in catalytically active NEST (2.01×10^6 nmol/min/mg protein).

Recombinant NEST was compared to native NTE from chicken brain membranes in terms of catalytic centre activity, OP reactivity and aging. NEST in DOPC liposomes and NEST in *E. coli* lysates had similar catalytic centre turnover numbers to native NTE from chicken brain microsomes, 1.5, 1.87 and $1.56 \times 10^5 \text{ min}^{-1}$ respectively. NEST in *E. coli* lysates and native NTE also showed the same rank order to covalent inhibition by a series of five NTE inhibitors with IC₅₀ values ranging over four orders of magnitude. Following inhibition by the non-neuropathic OP, PDPP, treatment of NEST and NTE preparations with oxime allowed reactivation of most of the esterase activity (> 75%). By contrast, neither preparation could be reactivated after inhibition by the neuropathic OP, DFP, indicating that aging had occurred.

The OP-aging reaction of DFP-inhibited NTE is rapid and does not result in quantitative liberation of an isopropyl group into free solution as occurs with DFP-inhibited acetylcholinesterase (Berends et al., 1959): instead this group is transferred to a second site within NTE, dubbed site Z. The isopropyl groups attached to the active site serine and site Z in aged [³H]DFP-inhibited NTE can be distinguished because alkaline hydrolysis liberates non-volatile ([³H]mono-isopropylphosphate) and volatile ([³H]isopropanol) radioactive fractions, respectively (Clothier & Johnson, 1979; Meredith & Johnson, 1989). In this study, following aging of [³H]DFP-labelled preparations, approximately 30% of the radioactivity associated with NEST (in *E. coli* lysates and in DOPC liposomes) or native NTE was bound to site Z.

NEST therefore provides a valid system for studying the characteristics of the enzyme domain of NTE, as it has the same catalytic centre activity, OP reactivity and aging characteristics as native NTE. These results also suggest that NEST is folded in the same way as the enzyme domain of native NTE. Within NTE's esterase domain, S966, was confirmed as the catalytic serine, by mutagenesis and [³H]DFP labelling. In addition, two aspartates, D960 and D1086, appear to be essential for catalytic activity.

Most serine hydrolases use a catalytic triad of a catalytic serine, histidine and acidic (Asp or Glu) residue (Dodson & Wlodawer, 1998). The pH profile of NEST suggests a histidine residue is required for esterase activity. Mutation of two histidines in NEST to alanine, H860 and H885, resulted in significantly reduced catalytic activity. However, it seems

unlikely that H860 is directly involved in the catalytic triad because this residue is not conserved in the *Drosophila* NTE homologue, which does have esterase activity. H885 is conserved in all eukaryotic homologues of NTE, but the loss of catalytic activity resulting from this mutation is substantially less (30-fold) than in the D960N or D1086N mutants. Therefore, this raises the possibility that NTE may not have a conventional catalytic triad. Interestingly, two mammalian serine hydrolases, fatty acid amide hydrolase (FAAH) and cytosolic phospholipase A2 (cPLA2), have recently been shown to function catalytically without using a histidine residue (Patricelli et al., 1999; Dessen et al., 1999).

Intramolecular transfer of an isopropyl group from the active site serine to site Z is a feature of the aging reaction of DFP-inhibited NTE. In this study, it was found that some of the transferred [³H]isopropyl group was associated with aspartate D1044. However, when this residue was mutated to asparagine, intramolecular transfer to site Z occurred to the same extent, implying a degree of non-selectivity in the process. Attempts to identify other candidate acceptor residues for the isopropyl transfer proved unsuccessful, but the fact that D1044 could act as an acceptor suggests that other aspartates within residues 955-1166 of the NEST sequence could do the same. The severe loss of activity in the D960N and D1086N mutants suggest that one or both of these residues lie close to the catalytic serine and may act as an isopropyl acceptor. In addition, mutation of D1004 resulted in an enzyme with only half the percentage volatile counts as wild-type NEST and therefore D1004 is also a potential candidate as an isopropyl group acceptor. Therefore, there appears to be a degree of non-selectivity in the transfer process. Overall, it can be concluded that while aging of one molecule of DFP-inhibited NTE results in intramolecular transfer of one isopropyl group to one aspartate residue, within a population of DFP-inhibited NTE molecules isopropyl transfer may involve different aspartate residues.

During this study YCHK, the smallest member of this novel family of proteins, was also expressed in *E. coli* (data not shown). Although, YCHK showed no differential activity (i.e. paraoxon-resistant and mipafox-sensitive), it did show significantly more phenyl valerate hydrolase activity in TE buffer than in buffer containing paraoxon. To confirm whether this paraoxon-sensitive activity was due to YCHK, the pET vector alone was expressed in *E. coli* and assayed. The level of PV-hydrolase activity for YCHK was several orders of magnitude lower than that of NEST, which may be due to the fact that phenyl

valerate is not an appropriate substrate for this homologue. However, the PV-hydrolase activity of YCHK could be inhibited using the serine protease inhibitor, pefabloc (IC₅₀ = 310 μ M), but interestingly DFP and MIP had no apparent effect. Therefore, YCHK has a PV-hydrolase activity, which is distinct from the well-characterised activity of neuropathy target esterase. This may not be surprising as YCHK only contains the putative transmembrane segments TM3 and TM4, and not TM2, which was shown to be essential for the catalytic activity of NTE.

CELL TYPE	NTE PV-HYDROLASE ACTIVITY (nmol/10⁶ cells/min)
3T3	0.56 ± 0.16
CHO	1.52 ± 0.38
HEK293	3.65
COS-7	3.76 ± 0.77
L35	4.64

Table 2.1: Endogenous NTE phenyl valerate hydrolase activity of five cell lines. Approximately 1×10^6 cells were used for each assay tube and samples were assayed in duplicate. The standard PV-hydrolase assay was used, with 20 min preincubation at 37°C with either 40µM paraoxon or 40µM paraoxon plus 50µM mipafox, followed by 20min incubation with the substrate phenyl valerate. Data are presented as the mean of 2-3 experiments (where n=3 standard deviations are shown).

DETERGENT	PERCENTAGE CONTROL ACTIVITY (%)	
	Supernatant	Pellet
0.3% TX-100	2.5	2.7
0.3% CHAPS	0.2	0.7
0.5% DOC	0.1	0.04

Table 2.2: Effect of detergents on NEST activity in the soluble and particulate fractions of bacterial lysates. The standard differential PV-hydrolase assay was carried out on the supernatant and pellet fractions following centrifugation ($100,000 \times g$, 60min, 4°C). All samples were assayed in duplicate and activities are expressed relative to the total activity found in bacterial lysates in the absence of detergent (12690 nmol/min/mg protein).

MEMBRANE PREPARATION	CATALYTIC CENTRE ACTIVITY ($\times 10^5 \text{ min}^{-1}$)
NTE in chicken brain microsomes	1.56 ± 0.04
NEST in <i>E. coli</i> lysates	1.87 ± 0.56
NEST in DOPC liposomes	1.50 ± 0.56

Table 2.3: Catalytic centre activities for NEST in *E. coli* lysates, NEST in DOPC liposomes and NTE from chicken brain microsomes. Values shown are the mean of four separate experiments \pm standard deviation.

INHIBITOR	NTE	NEST
PSP	0.0029 ± 0.0003	0.0035 ± 0.0003
PDPP	0.15 ± 0.03	0.27 ± 0.02
DFP	0.56 ± 0.06	0.96 ± 0.1
MIP	6.1 ± 0.23	8.7 ± 0.22
PMSF	55 ± 5.5	153 ± 43

Table 2.4: IC₅₀ values (μM) for covalent inhibitors of NTE and NEST. Inhibition assays (20min: 37°C) were carried out with a range of 8 concentrations, with duplicate samples for each concentration. DFP, PDPP and PMSF stock solutions were made up in dimethylformamide (DMF) with the final DMF concentration being no greater than 1%. PSP was made up in dimethylsulfoxide (DMSO) and mipafox in Tris/Citrate pH6. The final concentration of DMSO did not exceed 1%. Values shown represent the mean ± standard deviation of 4-6 separate experiments.

MEMBRANE PREPARATION	SITE Z ASSOCIATED [³ H]ISOPROPYL (%)
NTE in chicken brain microsomes	30.7 ± 9.1
NEST in <i>E. coli</i> lysates	29.9 ± 4.8
NEST in DOPC liposomes	31.8 ± 7.2

Table 2.5: Aging of native NTE and NEST. The percentage volatile counts of NEST in *E. coli* lysates, NEST in DOPC liposomes and NTE in chicken brain microsomes were determined. Data presented are the mean of 4-6 experiments ± standard deviation.

MEMBRANE PREPARATION	REACTIVATION WITH DFP (%)	REACTIVATION WITH PDPP (%)
NTE in chicken brain microsomes	0	87.0 ± 12.4
NEST in bacterial lysates	0	75.1 ± 9.70

Table 2.6: Reactivation of NTE and NEST with the oxime isonitrosoacetophenone (INAP). NEST in bacterial lysates and NTE in chicken brain microsomes were incubated with either 5 μ M DFP or PDPP for 20min at 37°C. Reactivation was carried out by incubating inhibited samples with 22mM INAP for 60min at 37°C. Phenyl valerate hydrolase activity present after reactivation was measured. Data shown represent the mean \pm standard deviation of three experiments.

BAND #	SPECIFIC ACTIVITY	% VOLATILE COUNTS	N-TERMINAL SEQUENCE
1	251.7	10.8	n/d
2	296.8	12.6	n/d
3	597.0	14.4	GAGPT
4	161.7	17.2	n/d
5	299.1	5.9	n/d
6	614.2	28.1	AGVPV
7	50.6	27.8	n/d
8	94.5	81.3	DLWLP
9	141.5	39.5	n/d
10	2.0	51.0	GAGPT
11	10.4	44.5	DLWLP
12	466.1	9.9	AGVPV

Table 2.7: Specific radioactivity, percentage volatile counts and N-terminal sequence (not done for all 12 bands) for the twelve distinct polypeptide bands.

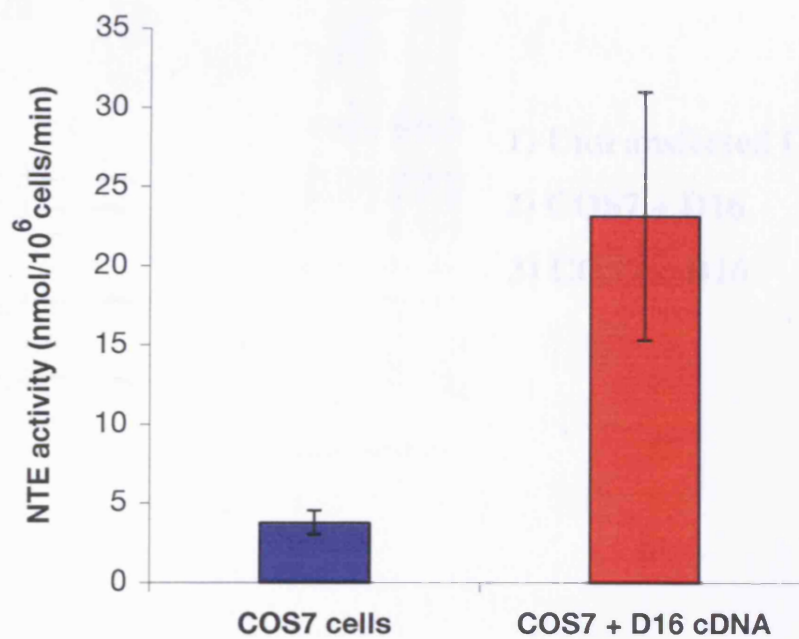


Fig. 2.1: Transient transfection of D16 cDNA in COS7 cells. NTE activities for control COS7 cells (blue) and COS7 cells transfected with D16 cDNA (red) are shown. Experiments were carried out four times and standard deviations are shown.

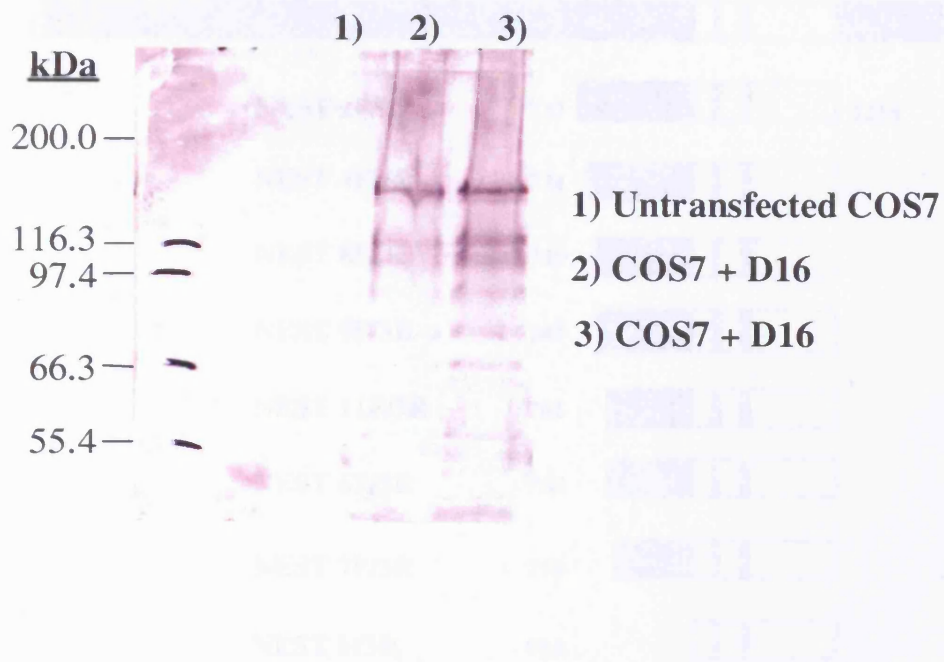


Fig. 2.2: Western blot of untransfected and D16 transfected COS7 cells. COS7 cells transfected with D16 and control untransfected cells were harvested by centrifugation and washed in Tris/EDTA pH8.0. After addition of SDS sample buffer, samples were run on 7.5% SDS-PAGE, blotted onto nitrocellulose and probed with an antibody to the C-terminus of NTE. Detection was achieved by using an alkaline phosphatase conjugated 2° antibody.

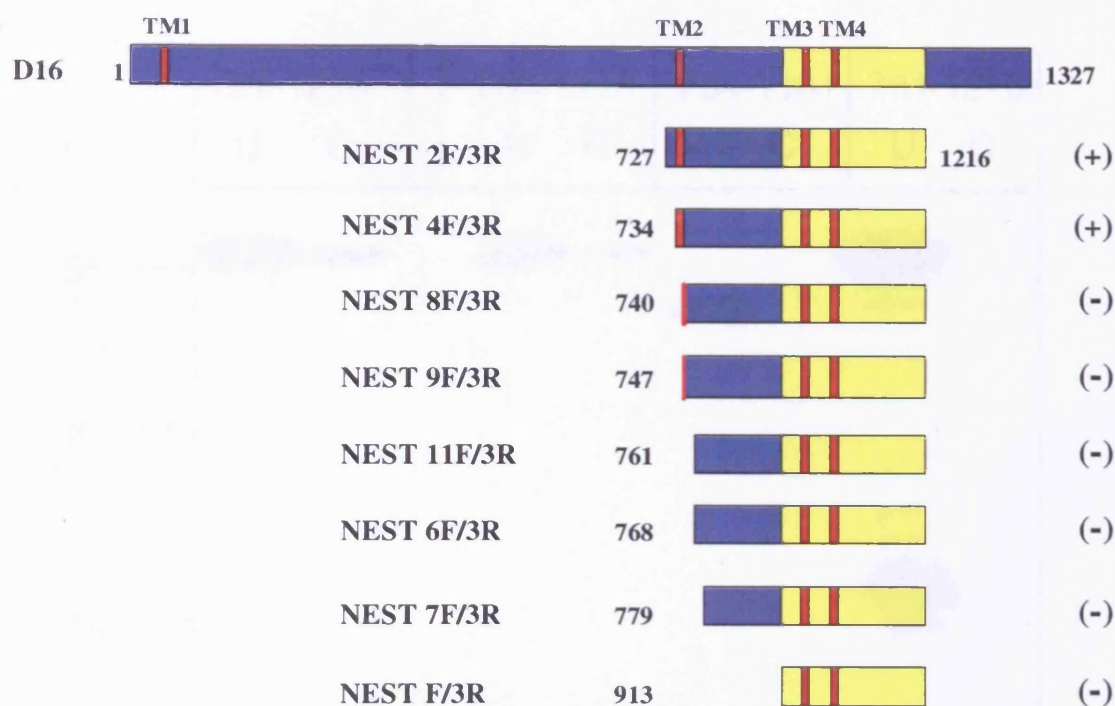


Fig. 2.3: NEST constructs expressed in the *E. coli* expression system. NEST PCR products were made by PCR using the D16 cDNA in pTarget™ as a template and forward and reverse primers (1F-11F, 3R). The diagram represents the portion of full-length NTE (D16) encoded by each of the shorter constructs. The four putative transmembrane segments (as predicted by TMpred) are shown in red (NB. NEST 8F and 9F/3R only contain a portion of TM2) and the highly conserved 200 amino acid region is shown in yellow. The catalytic activity of the expressed recombinant proteins was determined using the standard differential PV-hydrolase assay. The absence (-) or presence (+) of esterase activity is indicated in brackets.

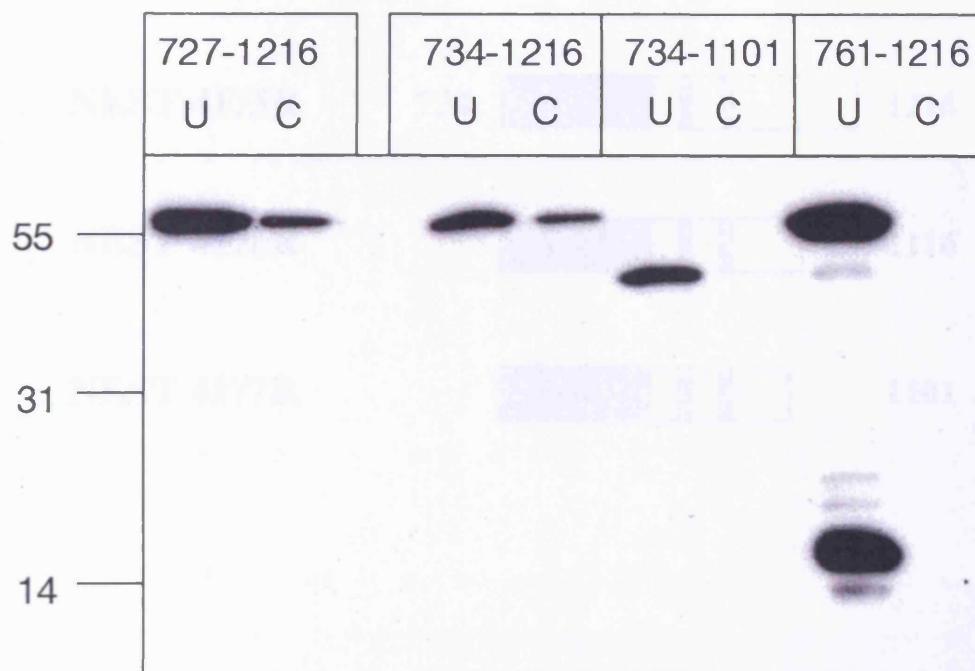


Fig. 2.4: Western blot of NEST constructs solubilised in non-denaturing and denaturing detergent. *E. coli* lysates containing recombinant polypeptides NEST 2F/3R (727-1216), NEST 4F/3R (734-1216), NEST 4F/7R (734-1101) and NEST 11F/3R (761-1216) were extracted (4°C, 30min) either with 8M urea and 1% CHAPS (U) or with 1% CHAPS only (C) and centrifuged at 100,000 × g for 45min. Extracts were run on 12.5% SDS-polyacrylamide gel, and recombinant polypeptides were detected by Western blotting with an antibody to the N-terminal T7 tag epitope. In this figure the migration of standard markers (molecular mass in kilodaltons) is shown on the left side of the blot.

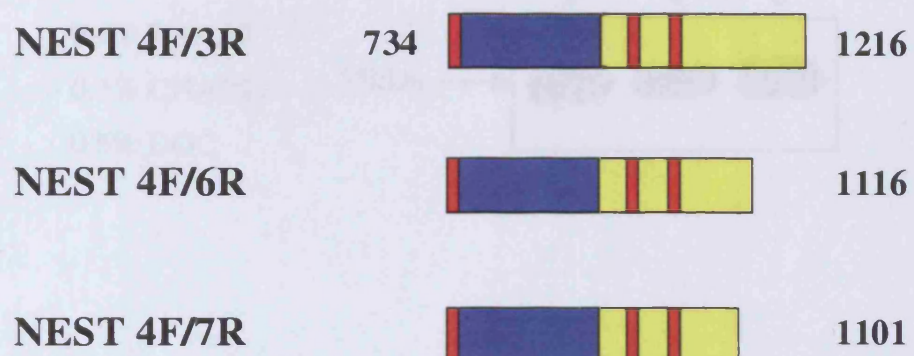


Fig. 2.5: Constructs designed to investigate the C-terminal boundary of NEST. PCR products corresponding to NEST 4F/6R and 4F/7R were generated. NEST 4F/6R and NEST 4F/7R lack 100 and 115 residues respectively, at the C-terminus of NEST 4F/3R.

Fig. 2.5: Constructs designed to investigate the C-terminal boundary of NEST. PCR products corresponding to NEST 4F/6R and 4F/7R were generated. NEST 4F/6R and NEST 4F/7R lack 100 and 115 residues respectively, at the C-terminus of NEST 4F/3R.

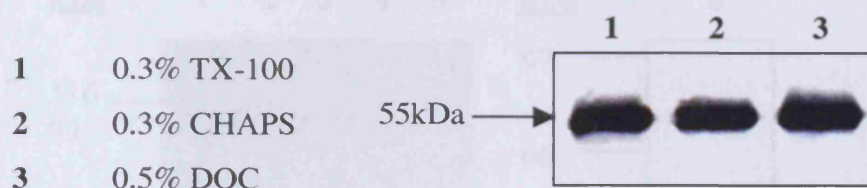
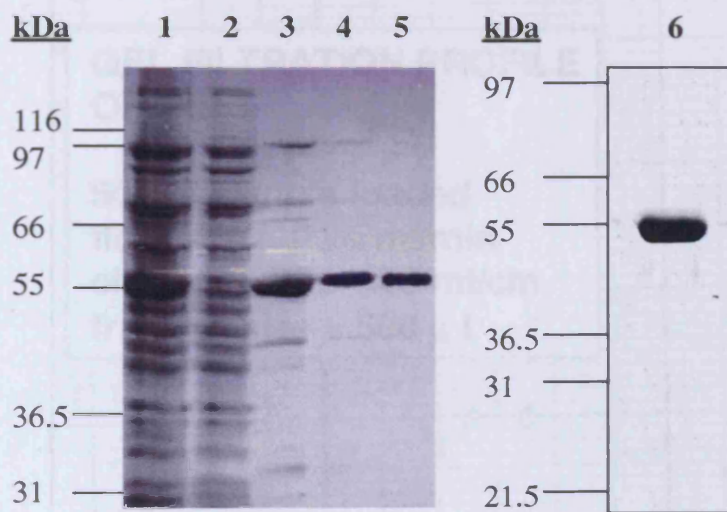
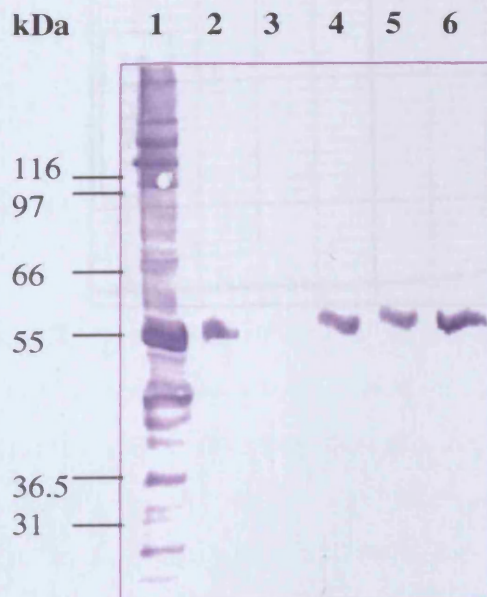


Fig. 2.6: Western blot of NEST (55 kDa) solubilised in Triton X-100, CHAPS and deoxycholate. *E. coli* lysates containing recombinant NEST were solubilised in 0.3% TX-100, 0.3% CHAPS and 0.5% DOC for 120min on ice. The solubilisation mixture was centrifuged at $100,000 \times g$ for 60min at 4°C and the resulting supernatants were run on SDS-PAGE and transferred onto nitrocellulose. The blot was probed with the T7 tag monoclonal antibody followed by a alkaline phosphatase conjugated secondary antibody.

(a)



(b)



(a)

- 1 solubilised NEST after $100,000 \times g$ spin
- 2 Unbound material
- 3 Eluate 1
- 4 Eluate 2
- 5 Eluate 3
- 6 NEST peak from gel filtration column

(b)

- 1 solubilised NEST after $100,000 \times g$ spin
- 2 Unbound material
- 3 Wash
- 4 Eluate 1
- 5 Eluate 2
- 6 NEST bound to Ni-NTA resin

Fig. 2.7: Gel filtration profile of NEST. NEST purified on Ni-NTA agarose was concentrated and loaded onto the gel filtration column and run in phosphate buffer containing 0.1% CHAPS. 600 µl fractions were collected and NEST-containing fractions

Fig. 2.7: (a) Coomassie stained gels and (b) Western blot of NEST purification.

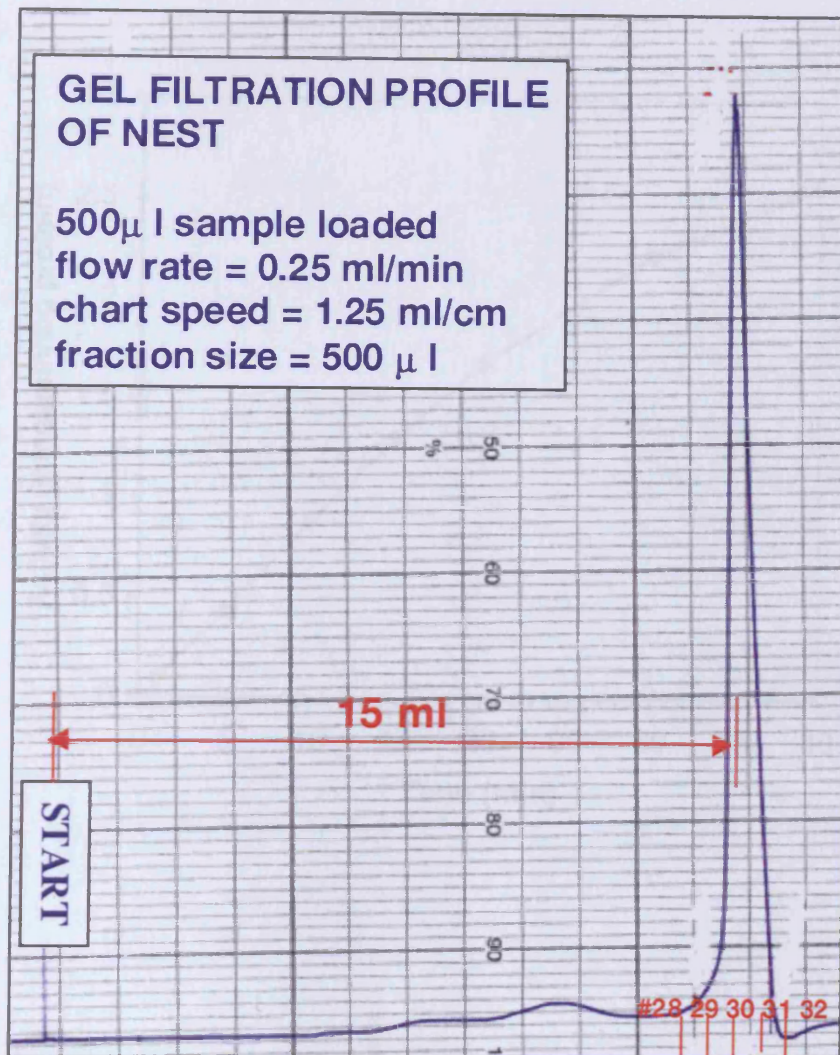


Fig. 2.8: Gel filtration profile of NEST. NEST purified on Ni-NTA agarose was concentrated and loaded onto the gel filtration column and run in phosphate buffer containing 0.3% CHAPS. 0.5ml fractions were collected and NEST-containing fractions were identified primarily by Western blots probed with the T7 tag antibody.

Fig. 2.8: Gel filtration profile of NEST. NEST purified on Ni-NTA agarose was concentrated and loaded onto the gel filtration column and run in phosphate buffer containing 0.3% CHAPS. 0.5ml fractions were collected and NEST-containing fractions were identified primarily by Western blots probed with the T7 tag antibody.

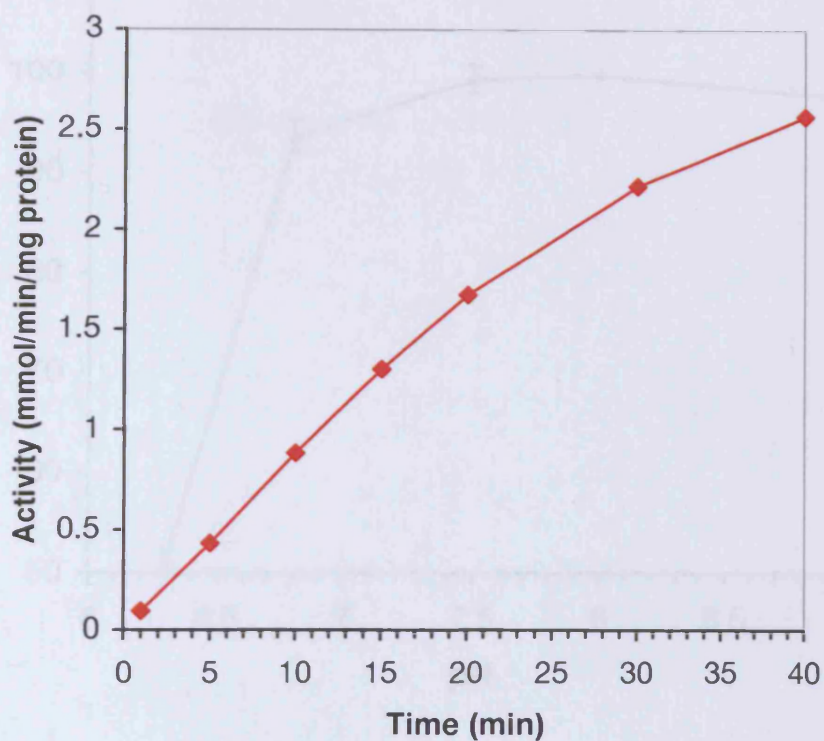


Fig. 2.9: Time course of NEST phenyl valerate hydrolase activity. NEST in DOPC liposomes was incubated with 1.4mM phenyl valerate for 1-40 min and the amount of PV-hydrolase activity was determined at each time point. Data points shown are the mean of duplicate samples and are from one representative experiment. The time course experiment was repeated a further two times with identical results.

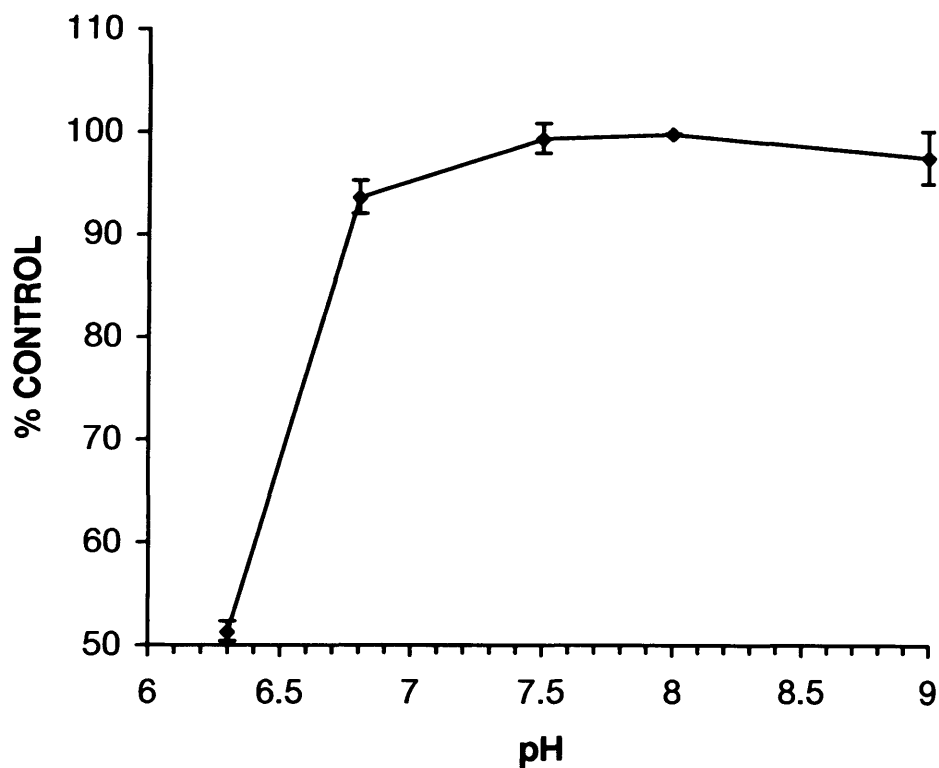


Fig. 2.10: Influence of pH on NEST phenyl valerate hydrolase activity. Activities were determined with a variety of buffers (NaP, pH 6.3; Tris/HCl, pH 6.8; NaP, pH 7.5; Tris/HCl, pH 8.0; Tris/HCl, pH 9.0) containing 1mM EDTA and were calculated as a percentage of the activity at pH 8.0. Data points are the mean of three experiments \pm standard deviation.

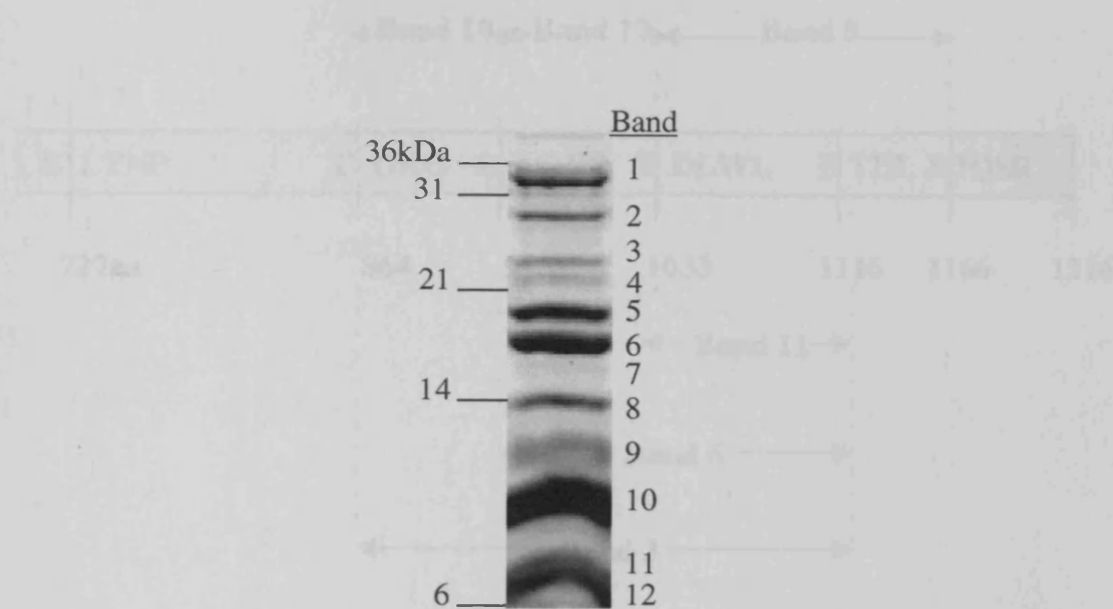


Fig. 2.11: Proteolytic digest of tritiated DFP-labelled NEST. NEST in DOPC liposomes was incubated with $4.7\mu\text{M}$ [^3H]DFP for 60min at 37°C , digested with endoproteinase Glu-C and run on a 15% Tricine gel.

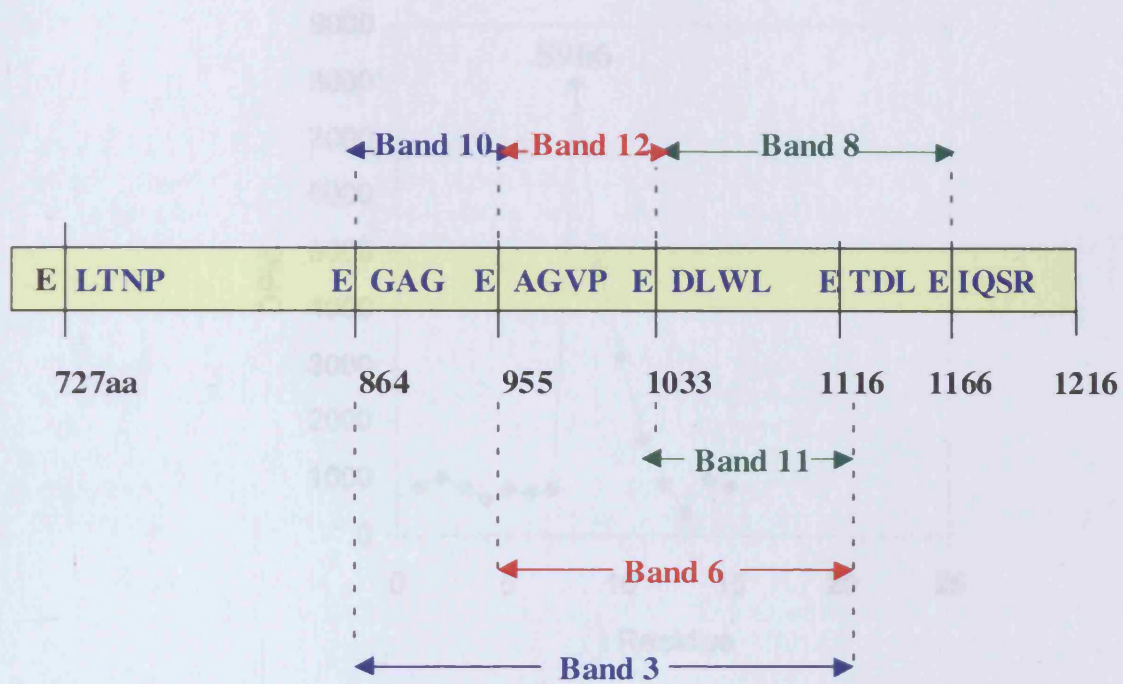
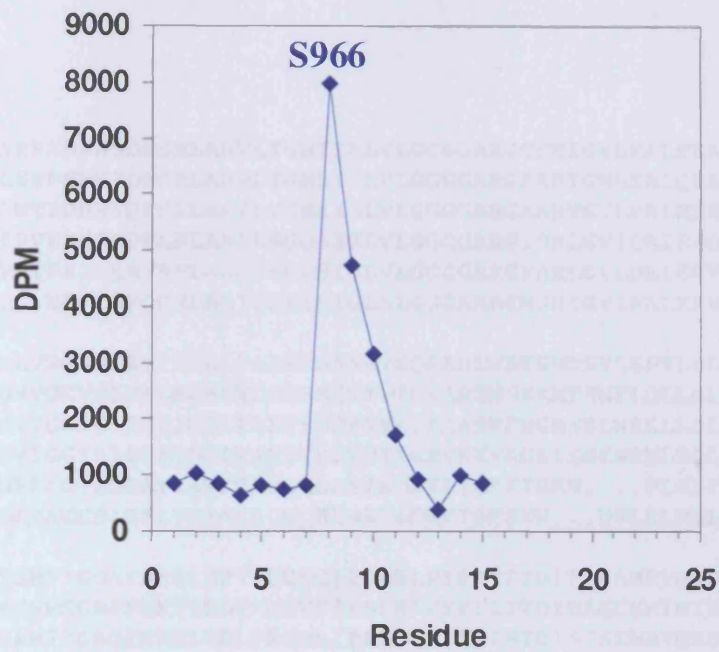


Fig.2.12: Partial peptide map of NEST. A partial peptide map was constructed using the N-terminal sequence data and size of the respective polypeptide fragments.

Fig. 2.13: Localization of [¹⁴C]DPP-derived label in NEST fragments. Bands 4 and 8, Band 6 (a) and Band 9 (b) were subjected to repeated cycles of Edman degradation and the position of release in amino acids at each Edman cycle was determined.

(a) Band 6



(b) Band 8

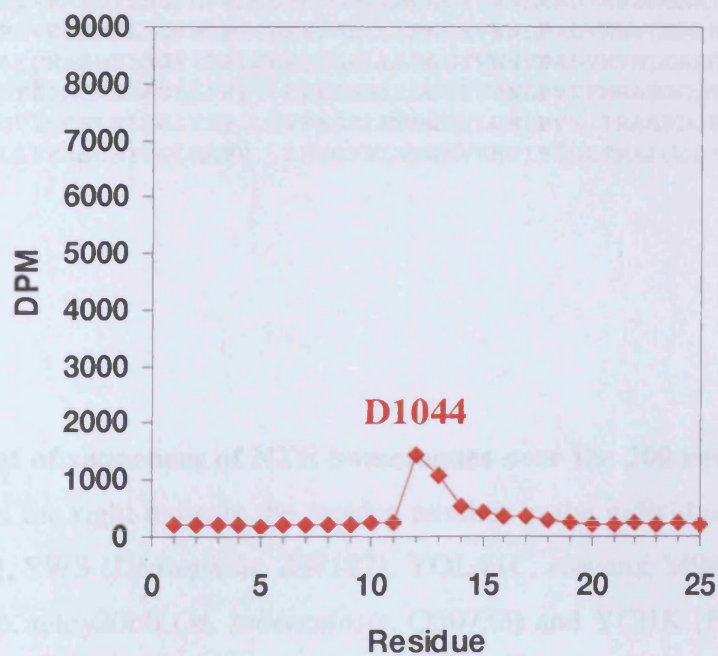
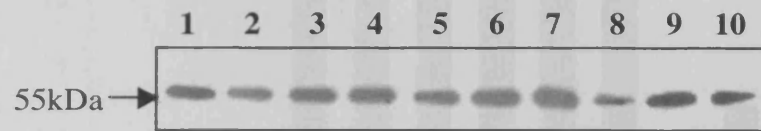


Fig. 2.13: Localisation of $[^3\text{H}]$ DFP-derived label in NEST fragments Bands 6 and 8. Band 6 (a) and Band 8 (b) were subjected to repeated cycles of Edman degradation and the amount of tritium in aliquots at each Edman cycle was determined.

NTE-human	SRRADRHSDFSRLARVLTGNTIALVLGGGGARGCSHIGVLKALEEAGVPV	959
sws-insect	LSEPNMHSDFSRLARWLTGNSIGLVLGGGGARGAAHIGMLKAIQEAGIPV	978
YOL4-caeel	FWTPDRRSDFSRLARILTGNAIGLVLGGGGARGAAHVGLRALREEGIPV	966
YMF9-yeast	TPVHRHKNDFLRLARILSGQAIGLVLGGGGARGISHLGVIQAIIEEQGIPV	1399
mtcy20b11	VHYRRILENVRPLAARIAGRSIGLVLGGGGARGFAHLGVLDELERVGVTI	816
YCHK-ecoli	...MATIAFQGNLAGIMRKIKIGLALGSGAARGWSHIGVINALKKVGIEI	47
NTE-human	DLVGGTSIGSFIGALYAEERSASRTKQARAREWAKSMTSVLEPVLDLTYPV	1009
sws-insect	DMVGGVSIGALMGALWCSESNITTVTQKAREWSKMTKWFLQLLDLTYPI	1028
YOL4-caeel	DIVGGTSIGSLIGGLYAETPDDVVVETRAASWFNGMSSLWRKLLDLTYAH	1016
YMF9-yeast	DVIGGTSIGSFIGGLYAKDYDLVPIYGRVKKFAGRISSIWRMLTDLTWPV	1449
mtcy20b11	DRFAGTSMGAVIAVFGACGMDAATADAYAYEYFIRHN...PLSDYAFPV	862
YCHK-ecoli	DIVAGCSIGSLVGAAYACD.RLSALEDWVTSFSYW...DVLRLMDLSWQR	93
NTE-human	TSMFTGSAFNRSIHRVFQDKQIEDLWLPYFNVTDDITASAMRVHKDGLSW	1059
sws-insect	TSMFSGREFNKTIHDTFGDVSIEDLWIPYFTLTTDITASCHRIHTNGSLW	1078
YOL4-caeel	SAMFTGAQFNFSIKDLFEERLIEDLWISYFCISTDISTSEMRVHRSGPLW	1066
YMF9-yeast	TSYTTGHEFNNGIWKTFGDTRIEDFWIQYYCNSTNITDSVQEIHSFGYAW	1499
mtcy20b11	RGLVRGRRTLTLLEAAGDRLVEELPKFRCVSVDLLARRPVVHRRGRLV	912
YCHK-ecoli	GGLLRGERVFNQYREIMPETEIENCSSRRFAAVATNLSTGRELWFTEGDLH	143
NTE-human	RYVRASMTLSGYLPPCLDPKDGHLMDGGYINNLPADIARSMGAKTVIAI	1109
sws-insect	RYVRSMSLSGYMPPCLDPKDGHLMDGGYVNNLPADVMMHNLGAAHIIAI	1128
YOL4-caeel	AYCRASMSLAGYLPPLCDPQDGHLLMDGGYVNNVPADVMMRNLGARCVIAC	1116
YMF9-yeast	RYIRASMSLAGLLPPL..EENGSMLLDGGYVDNLPVTEMRRARGCQTIFAV	1547
mtcy20b11	DVIGCSLRRLPGIYPP..QVYNGRLHVDGGVLDNLPVS.TRASPDGPLIAV	959
YCHK-ecoli	LAIRASCSIPGLMAPV..AHNGYWLVDGAVVNPPIPISLTRALGADIVIAV	191

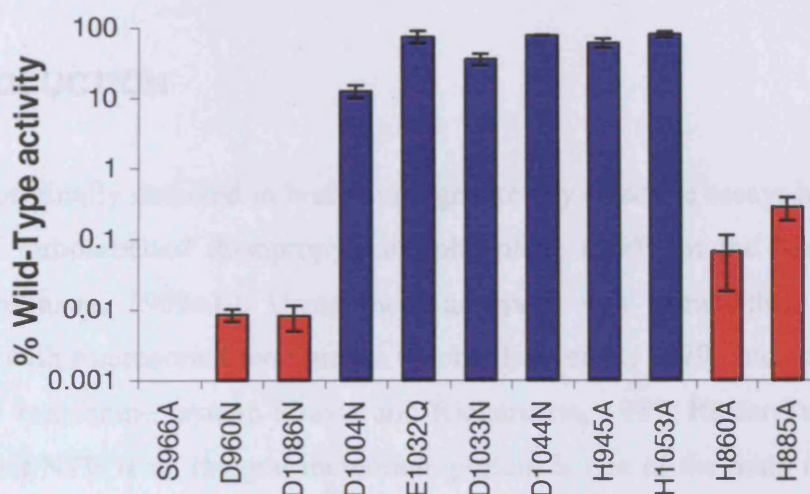
Fig.2.14: Alignment of sequences of NTE homologues over the 200 residue conserved region. Numbers on the right indicate the residue number in the individual proteins: NTE (human; AJ004832), SWS (*Drosophila*; Z97187), YOL4 (*C. elegans*, M98552), YMF9 (*S. cerevisiae*, Q04958), mtcy20b11 (*M. tuberculosis*, Q50733) and YCHK (*E. coli*, P39407). Conserved residues, which were mutated in NEST, are shown in blue and all other conserved residues are shown in bold.



1 H945A	2 D960N	3 S966A	4 D1004N	5 E1032Q
6 D1033N	7 D1044N	8 H1053A	9 D1086N	10 WT

Fig. 2.16: Western blot to demonstrate expression levels of nine NEST mutants compared to wild-type (W.T.) NEST. Recombinant proteins were detected using the T7 tag antibody.

(a)



(b)

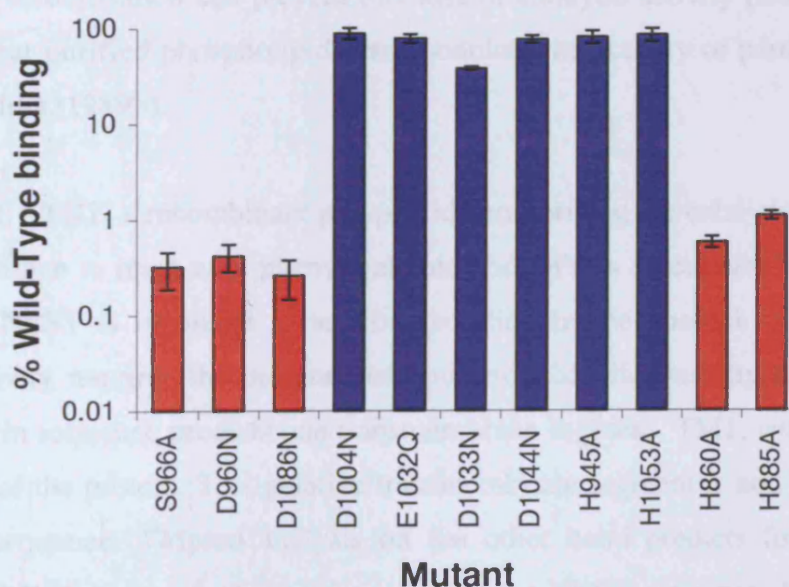


Fig. 2.17: (a) Phenyl valerate hydrolase activity and (b) [^3H]DFP binding of NEST mutants expressed as a percentage of wild-type NEST PV-hydrolase activity. After normalising the protein levels, standard differential PV-hydrolase assays and [^3H]DFP binding assays were carried out. Data shown are the mean \pm standard deviation of 3-4 separate experiments.

CHAPTER 3: INVESTIGATION OF THE MOLECULAR ORGANISATION OF NEST IN DOPC LIPOSOMES.

3.1 INTRODUCTION

NTE was originally detected in brain homogenates by selective assays involving either the binding of radiolabelled diisopropylfluorophosphate (DFP) or the hydrolysis of phenyl valerate (Johnson, 1969a,b). Using these assays it was shown that, in brain, NTE is associated with microsomal membranes (Richardson et al., 1979) and has the properties of an integral membrane protein (Davis and Richardson, 1987; Ruffer-Turner et al., 1992). The fact that NTE is an integral membrane protein is one of the main reasons why active NTE has been so difficult to isolate. Solubilisation of NTE has been shown to lead to a change in sensitivity to OP inhibitors (Johnson, 1971) or a significant loss of catalytic activity (Davis & Richardson, 1987). Furthermore, studies have shown that the presence of lipid during solubilisation can prevent this loss of catalytic activity (Davis & Richardson, 1987) and that purified phospholipids can modulate the activity of partially purified NTE (Pope & Padilla, 1989b).

In Chapter 2, NEST, a recombinant polypeptide comprising the catalytic domain of human NTE, was shown to react with phenyl valerate and OPs in a very similar fashion to NTE. Like NTE, NEST is insoluble in aqueous solution in the absence of detergent and its esterase activity requires the presence of phospholipid. Standard hydropathy analysis of NTE's protein sequence predicts one transmembrane segment, TM1, which is found at the N-terminus of the protein. This putative transmembrane segment is not, however, found in the NEST sequence. TMpred analysis on the other hand predicts four transmembrane segments, TM1-4, three of which are present in the NEST sequence. In this chapter, the membrane-associating properties of NEST were investigated.

3.2 RESULTS AND DISCUSSION

3.2.1 Membrane association of NEST

At the outset of these studies it was clear that NEST was not a soluble cytoplasmic protein. The recombinant polypeptide was firmly associated with particulate fractions of *E. coli* and required detergent for solubilisation and during purification (see Chapter 2). A commonly used method for investigating the membrane association of a protein is phase partitioning, which makes use of the unusual properties of the detergent, Triton X-114 (Bordier, 1981). Triton X-114 is soluble in aqueous buffers at 0°C, but above 20°C it separates out as a distinct detergent phase. In general, hydrophilic proteins are found in the aqueous phase and hydrophobic proteins in the detergent phase. Several integral membrane proteins including rhodopsin (Justice et al., 1995) and ATP diphosphohydrolase (Battastini et al., 1998) have been shown to partition into the detergent rich phase in TX-114 extracts.

Using the method of Bordier (1981), reconstituted NEST was subjected to TX-114 phase partitioning, and the aqueous and detergent phases analysed by SDS-PAGE (Fig. 3.1). NEST was found to partition predominantly into the detergent phase as shown in Fig. 3.1. In addition, NEST was labelled with [³H]DFP and subjected to phase partitioning; it was found that 98.1 ± 2.08 % of the radioactivity was associated with NEST in the detergent phase. Therefore, NEST appears to have the characteristics of an integral membrane protein.

During the phase partitioning experiments it was observed that inhibition of NEST by [³H]DFP caused a change in the solubility of NEST in TX-114. To further investigate this phenomenon, untreated NEST and DFP-inhibited NEST were solubilised in either 1.5% TX-114 or 1% CHAPS and centrifuged at $100,000 \times g$. The supernatants were run on SDS-PAGE (Fig. 3.2a) and the relative amounts of NEST in each gel lane were calculated using densitometry. Only 38.5 ± 1.5 % of DFP-inhibited NEST was solubilised in TX-114 compared to untreated NEST. However, when CHAPS was used for solubilisation there was no significant difference between the two samples (DFP-inhibited NEST was 95.6 ± 3.0 % of control). These results demonstrate a difference between the solubility of DFP-

inhibited NEST in the non-ionic detergent, TX-114, compared to the zwitterionic detergent, CHAPS.

To determine whether the effect observed was unique to the neuropathic organophosphate DFP, NEST was inhibited by PSP (neuropathic), PDPP (non-neuropathic) or PMSF (non-neuropathic) and solubilised in TX-114. Untreated and inhibited NEST samples were run on SDS-PAGE (Fig. 3.2b). As shown in Fig. 3.2b, DFP was the only NTE inhibitor tested, which resulted in a reduction of TX-114 solubilisation. When NEST is inhibited by DFP it undergoes a second reaction, termed aging, which results in the intramolecular transfer of an isopropyl group to site Z leaving a negative charge at the active site. In Chapter 2, it was demonstrated that the isopropyl group is transferred to an aspartate residue. Not all OPs, which undergo the aging reaction with NTE, form stable covalent adducts with site Z. For example, aging of saligenin octyl-phosphonate-inhibited NTE results in the liberation of more than 85% of the [³H]-labelled saligenin group into the incubation medium (Yoshida et al., 1995). Therefore, the failure of saligenin groups to form stable adducts with site Z might underlie the observation that reaction of NEST liposomes with DFP, but not with PSP, inhibits subsequent solubilisation of the polypeptide with a non-ionic detergent. It seems possible that formation of an isopropyl-aspartyl ester from an aspartate residue could increase, albeit slightly, the hydrophobicity of NEST.

Proteinase K treatment has been used to examine the topology of several membrane proteins, such as the gastric H⁺/K⁺-ATPase (Raussens et al., 1997) and the nicotinic acetylcholine receptor (nAChR) (Gorne-Tschelnokow et al., 1994). To try to determine the topology of NEST in the DOPC liposomes, proteinase K digestion was carried out in the absence of CHAPS and in the presence of either 1% CHAPS or 1% CHAPS plus 1% SDS (Fig. 3.3). In the absence of detergent, almost no digestion was visible after three hours at 4°C. In contrast, in the presence of 1% CHAPS, there was limited digestion with a 24 kDa resistant core apparent after 210min at 4°C. This agrees with the finding of the phase partitioning experiment that NEST is indeed an integral membrane protein. When SDS was also added to the digestion mixture, complete digestion of NEST occurred, therefore the presence of the 24 kDa core is not due to depletion of proteinase K (Fig. 3.3).

Western blot analysis was carried out using the T7 tag antibody to the N-terminus and His₆ antibody to the C-terminus (Fig. 3.4). In both cases in the absence of CHAPS there was no significant change in the proportion of 55 kDa band at '0' and '210' min time points, which suggests both N- and C- termini are still intact after proteinase K treatment. In the presence of CHAPS there were no bands detected with the His₆ antibody suggesting that the C-terminus is lost first. The T7 tag detected some of the digested fragments, but after 210min no bands could be detected, including the 24 kDa resistant fragment. The fact that both tags were unaffected by proteinase K in the absence of CHAPS would suggest that both N- and C-termini are either inside the liposome or that they are protected within a hydrophobic portion of the protein. In addition, these data suggest that NEST inserts unidirectionally into synthetic DOPC liposomes and that the 24 kDa protease-resistant fragment lacks both the N- and C-termini.

3.2.2 Does NEST form a transmembrane pore?

TMpred analysis of NTE predicts that the active site serine (S966) lies within the putative transmembrane segment TM4. Extreme caution must be taken in interpreting this sort of secondary structure prediction, as it could equally well indicate the presence of a hydrophobic section of helix buried in the centre of a folded protein. In section 3.2.1, evidence was obtained that NEST is an integral membrane protein. Therefore, there must be some form of membrane-associating or spanning segments present in NEST. If the catalytic serine is located within a membrane then this would require a particular tertiary and quaternary structure to allow for juxtapositioning of the other important catalytic residues (i.e. an aspartate and possibly a histidine) and to allow access of water to hydrolyse the acylated-enzyme intermediate. Conceivably, TM4 of NEST could line the aqueous lumen of a transmembrane pore thus allowing access of water to the active site serine.

To test the possibility that NEST might form a transmembrane pore a system was required in which electrophysiological recordings could be made of NEST in DOPC liposomes. Two approaches have been used to study the characteristics of reconstituted channels: one approach uses giant proteoliposomes and the other uses planar lipid bilayers. In proteoliposome studies there are two main advantages: high reproducibility and relatively

simple experimental procedures. However, it is rather difficult to establish a constant membrane potential or ionic gradient across the membrane. In contrast, in planar lipid bilayer studies, it is quite easy to control the membrane potential and the solution composition on both sides of the membrane. However, the disadvantage in this system is that transmembraneous reconstitution of proteins is difficult.

The giant liposome approach was chosen, as it is the simpler technique and did not require special apparatus needed for the planar lipid bilayer method. The activity of several channels has been studied using this method including the nicotinic acetylcholine receptor (nAChR) from Torpedo membranes (Riquelme et al., 1990a), the glycine receptor from rat spinal cord (Riquelme et al., 1990b), the phosphate carrier from *S. cerevisiae* mitochondria (Herick et al., 1997), and the large mechanosensitive ion channel (MscL) of *E. coli* (Hase et al., 1995).

The method for giant liposome formation was designed on the basis of the dehydration/rehydration method established by Criado and Keller (1987). Briefly NEST in DOPC liposomes were fused with an asolectin/cholesterol mix (9:1) and subjected to a dehydration/rehydration protocol. After this step giant liposomes could be seen under the light microscope. Patch clamp analysis was carried out on wild type and S966A mutant NEST-containing giant liposomes. Giant liposomes containing no NEST protein were used as a control. Dr. Philip Forshaw (Neurotoxicology section, MRC Toxicology Unit) carried out all of the electrophysiological recordings and prepared the data for Figs. 3.5-3.7 (Forshaw et al., submitted to J. Biol. Chem.).

Qualitatively, the membrane currents for patches of NEST-liposomes could be divided into two types: those displaying only a stable current (DC) type (>10s dwell time) over a minimum observation period of 10 minutes, and those displaying high frequency (<10ms dwell time) gating activity designated as "kinetic activity" superimposed on a steady-state DC level. Patches from liposomes prepared with and without NEST displayed clearly distinct distributions of DC conductance (Fig. 3.5a). Control liposomes prepared without NEST showed a uniform distribution around a conductance of approximately 60pS. This high background is presumably a reflection of the leakiness of the system, even though gigaohm seals were obtained between the micropipette tip and the asolectin-cholesterol liposomes. Frequency-conductance histograms (Fig. 3.5) for NEST excised patches

showed several maxima: the lowest of these was at 60pS, which probably reflects patches which lacked a NEST molecule; additional maxima were seen at 100-120pS, 160-180pS, 240-260pS and a small proportion showed conductances in the range 340-560pS. This distribution is consistent with a mean of 1.9 active pores per patch.

Out of 189 NEST-containing patches, 70 (37%) showed evidence of rapid gating (kinetic) activity. Kinetic activity in NEST patches was more likely to occur when the holding voltage (V_h) was maintained at greater than +80mV, indicating a moderate voltage-dependence. Kinetic activity could be resolved into distinct levels; the most frequent conductance transitions observed were 55-60pS (25%) and 100-110pS (33%), while larger conductance transitions of 150-160pS (7%) and 200-210pS (7%) were less frequent (Fig. 3.5b). Frequency analysis of both DC and kinetic modes suggests a patch containing a single pore-forming unit of NEST has a unitary conductance of 55-60pS.

A representative current recording for a NEST patch, demonstrating 100 and 55pS transitions superimposed on a DC current of 180pS, is shown in Fig. 3.6a. In contrast, current recordings from patches containing the S966A mutant form of NEST showed much less time in kinetic activity mode and displayed conductance transitions of 55 and 27pS (Fig. 3.6b). However, 40% of the total number (25) of S966A patches analysed showed some kinetic activity, which is comparable to wild-type NEST (37%). Because of the absence of kinetic activity in control patches, subsequent studies on NEST patches focused on those displaying kinetic activity.

Voltage-current relationships in excised patches containing wild-type or S966A mutant NEST were similar at membrane potentials between -120mV and +80mV (Fig. 3.6c). However, above +80mV the wild-type NEST displayed a greater total current, reflecting the additional kinetic component superimposed on the DC current. Negative voltages gave rise to smaller total current amplitudes and less frequent kinetic activity than positive voltages. This rectification suggests that incorporation of the NEST pore-forming unit into liposomes is uni-directional rather than random. This is supported by the results from the proteinase K digestion (Section 3.2.1). The asymmetric voltage-current relationship displayed by wild-type and S966A NEST indicates that the current rectifies at positive values of V_h (Fig. 3.6c). This rectification indicates that the pore becomes increasingly closed at negative membrane potentials. The open probability (P_0) of the transmembrane

pore (determined at V_h values of +80 to +100mV) was 0.72 ± 0.02 (n=25) for wild-type and 0.67 ± 0.10 (n=5) for the serine mutant.

To determine the effects of NTE covalent inhibitors on NEST patches, these reagents were added to the bath solution of an excised patch, which had shown a stable pattern of kinetic activity over the preceding minutes. Figure 3.7a shows current recordings before and 3min after addition of the neuropathic OP, diisopropylfluorophosphate (DFP). Comparison of these traces revealed that the initial conductance, which had a kinetic component with 110 and 55pS transitions superimposed on a DC conductance of 80pS, was reduced to the baseline value with no 110pS kinetic transitions and less frequent 55pS transitions. This change corresponded to a decrease in the open probability (P_0) of the pore from 0.67 to 0.42. Experiments in which P_0 of the NEST-mediated conductance was determined before and 3min after addition of covalent inhibitors of NEST catalytic activity (Chapter 2, Table 2.4) are summarised in Fig. 3.7b. Two neuropathic OPs, DFP and phenyl saligenin phosphate (PSP) caused a mean reduction in P_0 of approximately 50%, but PSP did not affect the mean P_0 of patches containing the S966A mutant, indicating that the effect was mediated by a covalent reaction with the active site serine (S966) residue. In contrast, the non-neuropathic covalent inhibitors, phenyl dipentylphosphinate (PDPP) and phenylmethylsulfonyl fluoride (PMSF) did not significantly alter the P_0 of patches containing wild-type NEST (Fig. 3.7b). Therefore, it appears that neuropathic OPs can alter the properties of the pore formed by NEST in DOPC liposomes while non-neuropathic NTE inhibitors cannot. This suggests that it is an effect of aging, which is causing this alteration in kinetic activity. It is conceivable that the formation of a negative charge at the active site serine (S966) upon aging is sufficient to cause a change in the conformation of the pore, such that the activity is reduced.

3.2.3 Are monomers of NEST catalytically active?

The results from the patch clamp experiments demonstrate that NEST is capable of forming a pore when incorporated into liposomes. According to the TMpred programme NEST contains three putative transmembrane segments, TM2-4. Clearly a monomer of NEST, containing only three α -helices, would not be sufficient to form a membrane-

spanning pore. Therefore, if the TMpred prediction is correct, NEST would have to form an oligomer in order to form a transmembrane pore.

To establish the molecular weight of NEST by gel filtration, four standard proteins were used to calibrate the column (Fig. 3.8): β -amylase (200 kDa), BSA (66 kDa), carbonic anhydrase (29 kDa) and cytochrome c (12.4 kDa). The elution volumes (V_e) of the standard proteins were determined photometrically. Using blue dextran (\approx 2000 kDa), the void volume (V_0) of the gel filtration column was also determined. From a plot of log molecular weight versus V_e/V_0 for the standard proteins and NEST it is evident that NEST runs anomalously on gel filtration (Fig. 3.9). NEST was found to run at the same position as cytochrome c, which is 12.4 kDa, rather than at 55 kDa as indicated on SDS-PAGE. To determine if this effect was due to the CHAPS concentration being too close to the CMC, the column was run in buffer containing 0.6% CHAPS. NEST was found to elute in the same fractions (data not shown), whether the buffer contained 0.3 or 0.6% CHAPS. Therefore, it is likely that the reason for this retardation on gel filtration is due to an interaction with the column matrix, suggesting that NEST is a very hydrophobic protein.

The characteristics shown by NEST on gel filtration do not compare with several studies on NTE, where NTE was shown to run on gel filtration with a molecular mass ranging from 850-1500 kDa (Pope & Padilla, 1989a; Chemnitius et al., 1984; Thomas et al., 1990). NTE runs as a 155 kDa monomer on SDS-PAGE, therefore, these results suggest that NTE exists as an oligomer. Thomas et al. (1990) demonstrated that inclusion of asolectin in the gel filtration buffer resulted in NTE eluting with an apparent molecular weight of greater than 1500 kDa, compared to 850 kDa in the absence of asolectin. Therefore, as NTE was only partially purified in these studies it is possible that lipid was still present in the sample, resulting in the aggregation of NTE and producing this high molecular weight observation.

This hypothesis seems to be correct, because when NEST liposomes are solubilised in limiting detergent (0.1% CHAPS) and run on gel filtration (0.1% CHAPS) two peaks are observed (Fig. 3.10). The first peak elutes after the void volume ($<$ 2000 kDa) and the second peak elutes at a position corresponding to an apparent molecular weight of 12.4 kDa. The first peak contains large aggregates of NEST and the second peak contains

monomers of NEST. Western blot analysis of the pooled fractions from the first and second peak showed that there was approximately four times as much protein present in the monomer peak compared to the aggregate peak. When the peaks were assayed for PV-hydrolase activity the aggregate peak had approximately five times as much activity. Therefore taking into account the protein concentrations, the aggregate peak was 20-fold more active than the monomer peak. This result would suggest that there is lipid present in the large aggregate peak, as the catalytic activity is partially preserved.

Mackay et al. (1996) showed that in the non-ionic detergent, polyoxyethylene W1, NTE eluted at approximately 200 kDa on gel filtration. Solubilisation of NTE in CHAPS, lauryldimethylamine oxide, Triton X-100 or octylglucoside, however, resulted in NTE eluting in the void volume, as demonstrated by Pope and Padilla (1989a), Chemnitius et al. (1984) and Thomas et al. (1990). Mackay et al. (1996) suggested that the polyoxyethylene W1 detergent protected NTE by providing a highly lipophilic environment. Davis and Richardson (1987) reported a similar effect by demonstrating that the inclusion of exogenous phosphatidylcholine in the purification of NTE preserved NTE catalytic activity in solution.

The results from the gel filtration chromatography experiments demonstrate that NEST exists as a catalytically inactive monomer in detergent solution. To investigate the molecular organisation of catalytically active NEST in the lipid bilayer, experiments were carried out using reconstituted NEST in DOPC liposomes.

One approach to help define the molecular organisation of proteins is the use of bifunctional cross-linking agents; this has been used with a number of membrane proteins, such as the large mechanosensitive (MscL) ion channel (Hase et al., 1997), ryanodine receptor (Shoshan-Barmatz et al., 1995) and the outer membrane phospholipase A (OMPLA) of *E. coli* (Dekker et al., 1997). The technique of chemical cross-linking of protein complexes in intact membranes and the subsequent molecular weight determinations of the cross-linked aggregates by SDS-gel electrophoresis, yield information on the size of the protein complex in its native environment. Several cross-linkers are commercially available and they vary with respect to their functional groups and the length of their spacer arms. Three cross-linkers were used to investigate whether NEST forms an oligomeric complex when incorporated into DOPC liposomes; EGS

[Ethylene glycolbis (succinimidylsuccinate)], Sulfo-EGS [Ethylene glycolbis (sulfo-succinimidylsuccinate)] and glutaraldehyde.

Sulfo-EGS and EGS are homobifunctional N-hydroxysuccinimide esters (NHS-esters), both with a spacer arm length of 16.1Å. EGS is water-insoluble and sulfo-EGS is its water-soluble analogue. Primary amines are principle targets for NHS-esters. While five amino acids have nitrogen in their side chains, only the ϵ -amine of lysine reacts significantly with NHS-esters. Glutaraldehyde is also a bifunctional cross-linking reagent, which reacts with lysine residues. The approximate distance between the glutaraldehyde reactive groups is not known, since at neutral or slightly basic pH, the predominant reactive species of glutaraldehyde are α,β -unsaturated aldehyde polymers.

NEST in DOPC liposomes cross-linked with EGS (0-10mM), sulfoEGS (0-30mM) and glutaraldehyde (0-30mM) all showed a similar pattern of cross-linking when samples were run on 7.5% SDS-PAGE (Fig. 3.11). All of these cross-linkers resulted in the disappearance of the 55 kDa NEST monomer and appearance of additional bands of higher molecular mass, including dimers, tetramers and larger multimers. A similar result was found when the ryanodine receptor (RyR) was cross-linked with glutaraldehyde and EGS (Shoshan-Barmatz et al., 1995). Cross-linking with these bifunctional reagents resulted in the disappearance of the 470 kDa RyR monomer and concomitant appearance of dimer and tetramer bands. The RyR has previously been shown to be a tetramer using electron microscopy (Radermacher et al., 1994). These results, therefore, suggest that NEST may form an oligomer (dimer or tetramer) when incorporated into DOPC liposomes.

The effect of these three cross-linkers on NEST phenyl valerate hydrolase activity, however, was different (Fig. 3.12). Glutaraldehyde caused no inhibition of PV-hydrolase activity at concentrations up to 10mM and caused about 30% inhibition at 30mM. Both EGS and sulfoEGS caused no inhibition up to 1mM, but became very inhibitory at concentrations above this with 40% and 65% inhibition, respectively, at 10mM. Because glutaraldehyde could be used across a larger range of concentrations, due to solubility, and was found to cause very little inhibition of enzyme activity, this cross-linker was used in all subsequent experiments.

An interesting phenomenon was observed for glutaraldehyde when 0.5% CHAPS was included in the phenyl valerate hydrolase assay. This concentration of CHAPS is sufficient to cause approximately 90% inhibition of NEST PV-hydrolase activity over the time course of the assay. However, with increasing concentrations of glutaraldehyde a protection of NEST activity was observed, with approximately 50% of the original NEST activity retained at 10mM glutaraldehyde (Fig. 3.13a).

One explanation for the protection observed with glutaraldehyde could simply be due to a reaction with the lysine residues. To test whether this was true, the cross-linking experiment was carried out with valeraldehyde, which will react with lysine residues but is not capable of cross-linking the protein. Using a range of valeraldehyde concentrations between 0-100mM, no protection of NEST PV-hydrolase activity was observed (Fig. 3.13b). Therefore, the protection shown in the presence of glutaraldehyde does not seem to be due to a non-specific reaction with lysine residues.

Another explanation for the protection of NEST PV-hydrolase activity is that cross-linked oligomers somehow retain an increasing amount of lipid, which results in a retention of NEST PV-hydrolase activity even in the presence of 0.5% CHAPS. This could explain why the protection increases up to a glutaraldehyde concentration of 10mM and then plateaus, since above 10mM glutaraldehyde most of the monomer has already been cross-linked into large aggregates, which are found in the stacking gel.

When samples of NEST cross-linked with 0-20 mM glutaraldehyde are run on 7.5% SDS-PAGE, there appears to be no correlation between the protection of activity and the presence of a particular oligomer. In addition, the amount of NEST PV-hydrolase activity, in the absence of CHAPS, is 90% of control for the 20mM glutaraldehyde sample even though a large majority of the monomer (83%) has been cross-linked into large aggregates (Fig. 3.14). Therefore, it seems that NEST is catalytically active even when present in aggregates of greater than 200 kDa.

To determine whether NEST monomers are capable of binding a neuropathic OP, samples were treated with [³H]DFP before and after cross-linking with glutaraldehyde. The monomer, dimer, tetramer and larger aggregate bands were excised from gels and the amount of radioactivity determined. It was found that all of the bands contained

radioactivity, whether treated with [³H]DFP before or after cross-linking. When the densitometry values were taken into account no differences in specific radioactivity were observed (data not shown). These results, therefore, demonstrate that a monomer of NEST is sufficient for binding of [³H]DFP. However, it does not rule out the possibility that NEST can also exist and function as an oligomer.

Another approach to determine the molecular organisation of a protein is radiation-inactivation analysis. This method is based on the destruction of the biological activity of the protein in situ by X-irradiation. Protein inactivation is a function of the total dose of radiation and this dose-dependency is in turn closely related to the target size, that is, the molecular volume of the fully functional protein.

Radiation-inactivation analysis has been used to determine the functional size of several enzymes, such as NTE (Carrington et al., 1985) and the calcium-independent phospholipase A2 from P388D1 macrophages (Ackermann et al., 1994). Carrington et al. (1995) estimated the target size of NTE activity to be 105 kDa, suggesting NTE functions as a monomer. To determine whether NEST also has a monomer as the functional unit, P.Glynn, L.H. Luthjens and M.R. Hom carried out radiation-inactivation studies (unpublished data). The results of four separate experiments demonstrated that the target size of NEST in DOPC liposomes is 52.8 ± 4.5 kDa. Therefore, it seems that for both native NTE and NEST a monomer is sufficient for catalytic activity.

3.3 GENERAL DISCUSSION

In Chapter 2, it was demonstrated that recombinant NEST (NTE residues 727-1216) represented the catalytic domain of human NTE. Detergent was required to maintain the solubility of NEST throughout the purification procedure suggesting that NEST is an integral membrane protein. To further characterise the membrane association of NEST, TX-114 phase partitioning was carried out. The results clearly showed that >98% of functional NEST was found in the detergent phase, a characteristic of integral membrane proteins. Proteinase K treatment was also used to investigate the association of NEST with the lipid bilayer and the orientation of NEST in DOPC liposomes. In the absence of detergent the 55 kDa NEST protein was resistant to proteolysis, but was rendered more

sensitive by the addition of 1% CHAPS. Even in the presence of CHAPS, proteolysis was limited and fragments of approximately 24 kDa appeared particularly resistant. NEST was also shown to display highly anomalous migration on gel filtration, eluting with cytochrome c (12.4 kDa) rather than as a 55 kDa polypeptide as indicated by SDS-PAGE. This suggests that NEST is markedly retarded on gel filtration due to hydrophobic interactions with the column matrix.

All the results so far clearly demonstrate that NEST, the esterase domain of human NTE, is membrane-associated. This finding does not agree with the secondary structure prediction by standard hydropathy analysis that the only transmembrane segment (TM1) is very near to the N-terminus of NTE (residues 11-32) and is not present in the NEST protein (residues 727-1216). The other secondary structure prediction, using TMpred analysis, predicts four transmembrane segments, three of which are present in the NEST protein (TM2-4).

The TMpred prediction that the active site serine (S966) is at the centre of the putative transmembrane segment TM4, led to the investigation of the pore-forming ability of NEST in DOPC liposomes. Patches containing NEST displayed membrane currents, which were qualitatively different to control patches lacking NEST protein. In addition, patches containing the S966A mutant spent less time in kinetic activity mode and displayed smaller conductance transitions than wild-type NEST. Addition of the neuropathic OPs, DFP and PSP, reduced the kinetic activity seen in NEST patches, whereas the non-neuropathic inhibitors, PDPP and PMSF, had no effect. Also PSP had no effect on the kinetic activity displayed by the S966A mutant. The fact that neuropathic and not non-neuropathic covalent inhibitors decreased the open probability of the NEST transmembrane pore suggests that it is the aging event, which is causing this effect and not merely a covalent interaction with the active site serine. Generation of a negative charge on the serine could conceivably cause a disturbance in the local hydrophobic environment, thereby disrupting the conformation of the pore.

The results of the cross-linking were inconclusive. NEST could be cross-linked, suggesting that the liposome membrane provides an environment where dimers and tetramers can exist. However, no correlation could be made between the protection of esterase activity by glutaraldehyde in the presence of detergent and the increase in concentration of a particular oligomer. [³H]DFP was shown to react with the monomer, dimer and tetramer species,

suggesting that a monomer is sufficient at least for organophosphate binding. Shoshan-Barmatz et al. (1995) demonstrated a similar pattern of cross-linking for the ryanodine receptor (RyR), which has been confirmed as a tetramer using electron microscopy (Radermacher et al., 1994). I did attempt to visualise NEST in DOPC liposomes by negative staining (uranyl acetate) and electron microscopy, but this was not successful. In order to visualise proteins using negative stain either the N- or C-terminus has to be outside the membrane or there has to be a large extracellular loop. If the N- and C-termini of NEST are indeed within the liposome (as suggested by proteinase K digestion) and a large proportion of NEST (24 kDa) is tightly associated with the membrane this may explain why very little could be detected by electron microscopy. Radiation inactivation studies carried out by P. Glynn, L.H. Luthjens and M.R. Hom (unpublished data) calculated a target size of approximately 53 kDa for NEST in DOPC liposomes, indicating that the functional unit of NEST is a monomer.

If a monomer of NEST is sufficient for catalytic activity then it is difficult to see how the TMpred prediction of three membrane-spanning segments could be correct, particularly as the catalytic serine is predicted to lie at the centre of transmembrane segment TM4. To my knowledge the minimum number of α -helices required to form a functional membrane-spanning pore is four. The CHIP28 water channel has been shown to contain four functional membrane-spanning segments (Van Hoek et al., 1991) and radiation inactivation experiments indicated that a CHIP28 monomer mediated osmotic water permeability in kidney brush border membranes (Van Hoek & Verkman, 1992). For the TMpred prediction to be correct NEST would have to form an oligomer for the active site serine to have access to water for catalysis. This is clearly not the case as a monomer of NEST is sufficient for catalytic activity. Therefore, neither standard hydropathy analysis nor TMpred analysis can adequately explain the membrane-associating characteristics displayed by the NEST protein.

Given that the TMpred prediction is incorrect, then the membrane association of NEST may instead be due to a β -sheet structure. The 27 kDa outer membrane phospholipase A (OMPLA) of *E. coli* forms a membrane-spanning beta-barrel structure with its active site serine located on the exterior of this barrel facing the outer leaflet side of the membrane (Snijder et al., 1999). Membrane-spanning proteins with beta-barrel structures are also

found in eukaryotes and include polypeptides of the outer membranes of chloroplasts (OEP 75; Hinnah et al., 1997) and mitochondria (voltage-dependent anion channel; Mannella, 1998). These pore-forming proteins consist of 16- or 18-stranded β -barrels. Standard hydropathy analysis of the VDAC and OEP75 protein sequences predicts that both these proteins contain no transmembrane or membrane-associated α -helices. However, TMpred analysis of OEP75, but not VDAC, predicts two possible transmembrane segments.

NEST is an integral membrane protein and a 24 kDa core has been shown to be resistant to proteolysis. Therefore, it may be possible that NEST also forms a β -barrel structure, but until more structural information on NEST is available it is merely speculation. However, the fact that standard hydropathy analysis predicts no transmembrane helices in NEST and the low TMpred scores for transmembrane segments, TM2-4, support the presence of β -sheet rather than α -helical structure. If the active site serine of NEST is also located on the exterior of a β -barrel structure, as found in OMPLA (Snijder et al., 1999), this would allow access of water for catalysis. In addition, the presence of the negative charge produced during aging may block the pore by a local conformational change, which would explain the effect of neuropathic OPs on patches containing NEST. Interestingly, OMPLA does not function as a transmembrane pore since the N- and C-termini and several loop structures obstruct the mouth of the pore. It is possible that the pore-forming ability of NEST does not have any physiological role, since the other two thirds of NTE not present in NEST may obstruct the mouth of the pore.

Another possibility is that a NEST monomer is sufficient for phenyl valerate hydrolase activity and [3 H]DFP binding, but that it is an oligomer or aggregate of NEST, which forms a pore in the DOPC liposomes. The 29 kDa *Pseudomonas aeruginosa* cytotoxin has been shown to form a pore upon insertion into erythrocyte membranes (Sliwinski-Korell et al., 1999). Analysis of the cytotoxin primary structure indicates predominant β -sheet and amphiphilic character, which is a characteristic of many of the bacterial pore-forming toxins. *P. aeruginosa* cytotoxin forms a pore in membranes by functional pentamerisation. In contrast, natural antimicrobial peptides with amphipathic α -helical structures have been shown to disrupt biological membranes by pore formation (Agawa et al., 1991; Cruciani et al., 1991; Matsuzaki et al., 1994). These peptides form channels by self-aggregation of peptide monomers, whereby hydrophilic residues on one side of the helix face inward and

hydrophobic residues on the opposite side of the helix interact with fatty acid side chains of the lipid bilayer. Therefore, the pore-forming ability of NEST could be due to either an oligomeric structure (β -sheet or α -helical) or a monomeric β -barrel structure.

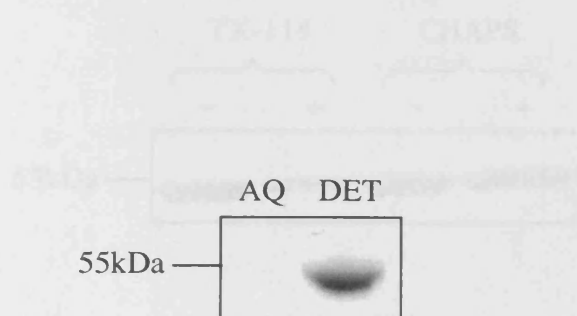
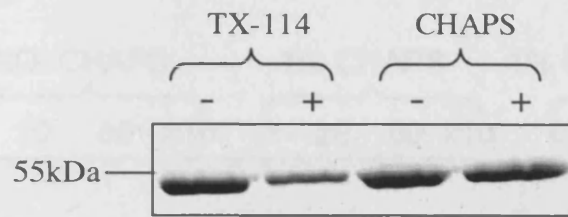


Fig. 3.1: Phase partitioning of Triton X-114-solubilised NEST. Phase partitioning using Triton X-114 was carried out according to the method of Bordier (1981). The aqueous phase (AQ) and detergent (DET) phase were diluted appropriately and run on 12% SDS-PAGE.

Fig. 3.1: SDS-PAGE of (a) Untreated (-) and PSP-inhibited (+) NEST solubilised in TX-114 or CHAPS. (a) Untreated, PSP-inhibited, DFP-inhibited, PDPP-inhibited and PMSF-inhibited NEST solubilised in TX-114. (b) Untreated were incubated with 5 μ M PSP, 5 μ M DFP, 5 μ M PDPP or 1 μ M PMSF for 30 min at 37°C. Untreated NEST was also included as a control. Samples were solubilised in either 1% TX-114 or 1% CHAPS for 45 min at 4°C and centrifuged at 100,000 \times g for 1 hour at 4°C. The resulting supernatants were run on 12% SDS-PAGE.

(a)



(b)

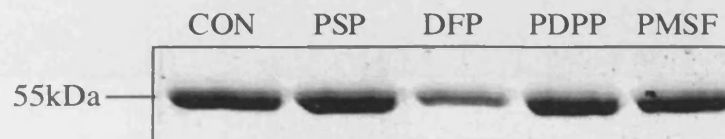


Fig. 3.2: SDS-PAGE of (a) Untreated (-) and DFP-inhibited (+) NEST solubilised in TX-114 or CHAPS. (b) Untreated, PSP-inhibited, DFP-inhibited, PDPP-inhibited and PMSF-inhibited NEST solubilised in TX-114. NEST liposomes were incubated with 5 μ M PSP, 5 μ M DFP, 5 μ M PDPP or 1mM PMSF for 60min at 37°C. Untreated NEST was also included as a control. Samples were solubilised in either 1.5% TX-114 or 1% CHAPS for 45min on ice and centrifuged at 100,000 \times g for 60min at 4°C. The resulting supernatants were run on 12% SDS-PAGE.

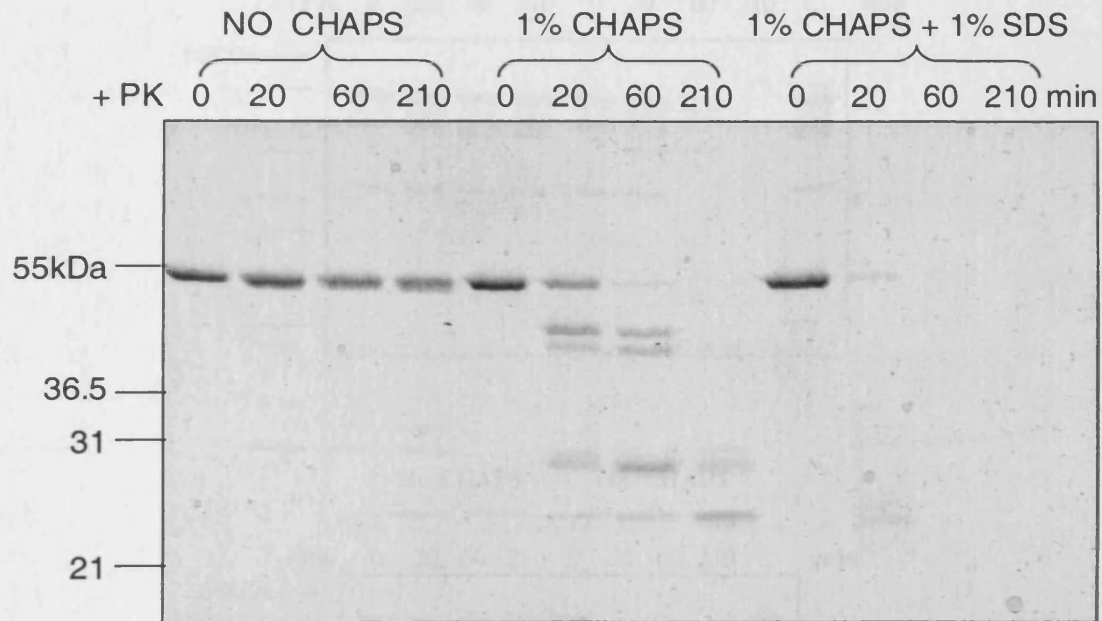


Fig. 3.3: Proteinase-K treatment of NEST-containing liposomes. NEST liposomes were incubated for 0, 20, 60 and 210min with proteinase K (PK) to give a NEST: PK (w/w) ratio of 35:1. Samples were incubated with no CHAPS, 1% CHAPS or 1% CHAPS + 1% SDS.

Fig. 3.4: T7 and N1b Nests of proteinase K digestion of NEST in BQPC liposomes. Samples of NEST bound with proteinase K (PK) for 0, 20, 60 and 210min in the presence or absence of CHAPS were run on SDS-PAGE (Fig. 3.3). Blotted onto nitrocellulose and probed with rabbit anti-T7 IgG or the primary antibody as a control (reacts to T7) and also probed with rabbit anti-N1b IgG. The results are shown in Fig. 3.4. The results show that NEST is stable in BQPC liposomes in the presence of PK and that the degradation of NEST is not dependent on the presence of CHAPS.

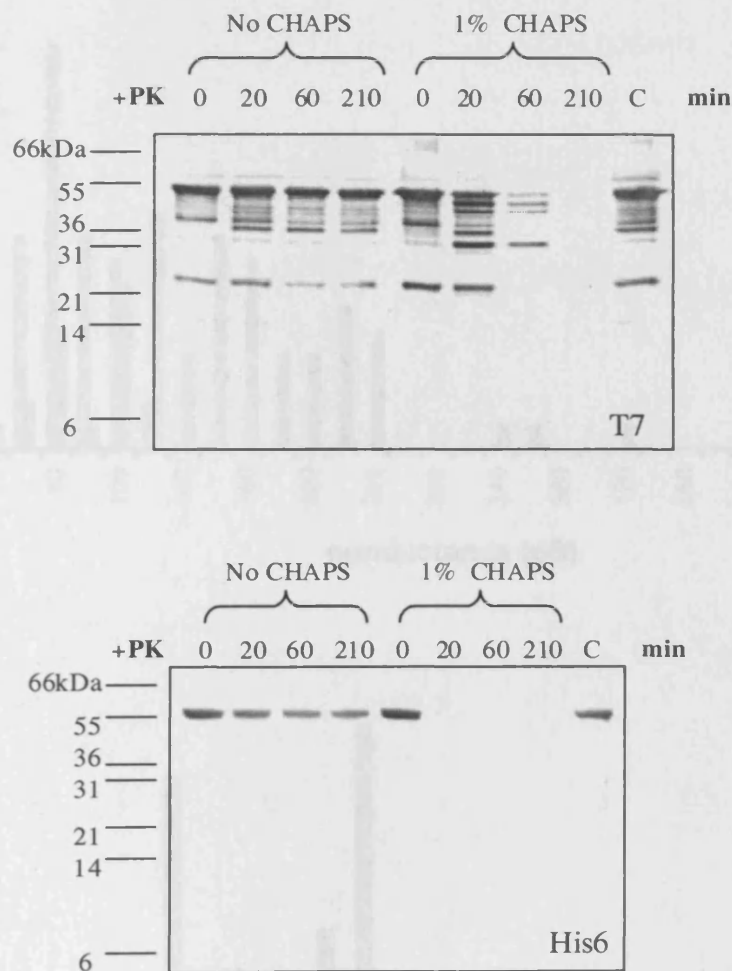
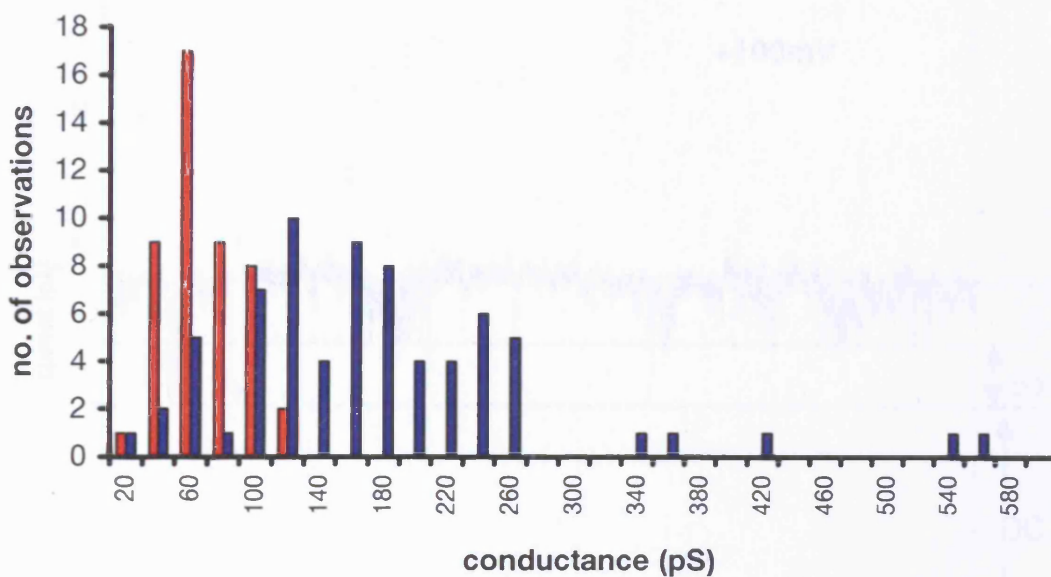


Fig. 3.4: T7 and His₆ blots of proteinase K digestion of NEST in DOPC liposomes. Samples of NEST treated with proteinase K (PK) for 0, 20, 60 and 210min in the presence or absence of CHAPS were run on SDS-PAGE (Fig. 3.3), blotted onto nitrocellulose and probed with either the T7-tag or His₆ primary antibody. A control reaction (C) was also included on each blot to demonstrate that after PMSF treatment and addition of SDS-sample buffer no digestion by PK occurs.

(a)



(b)

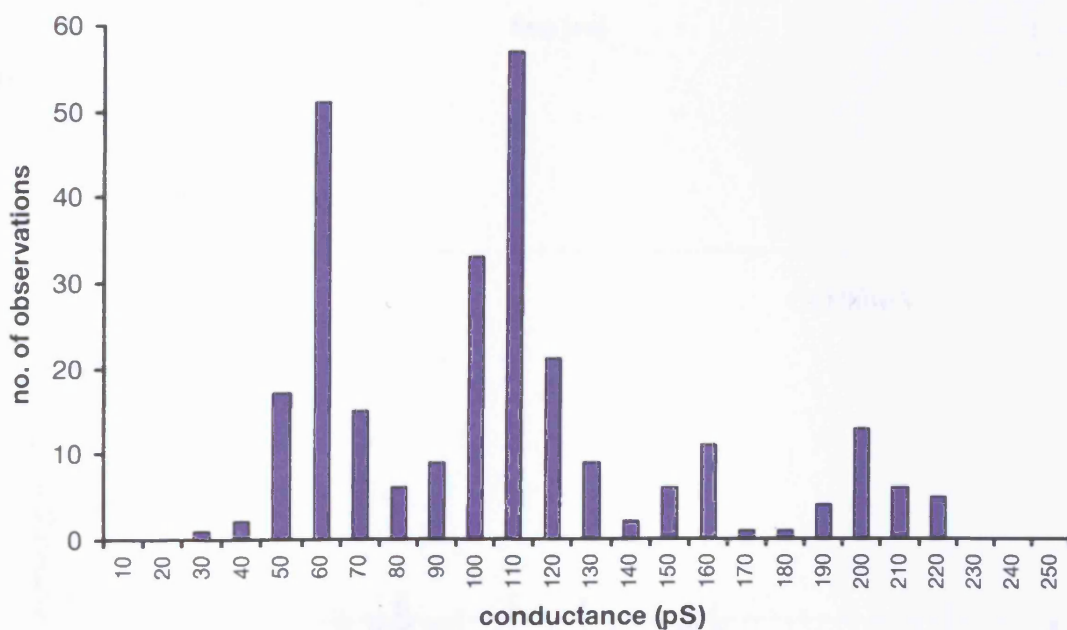
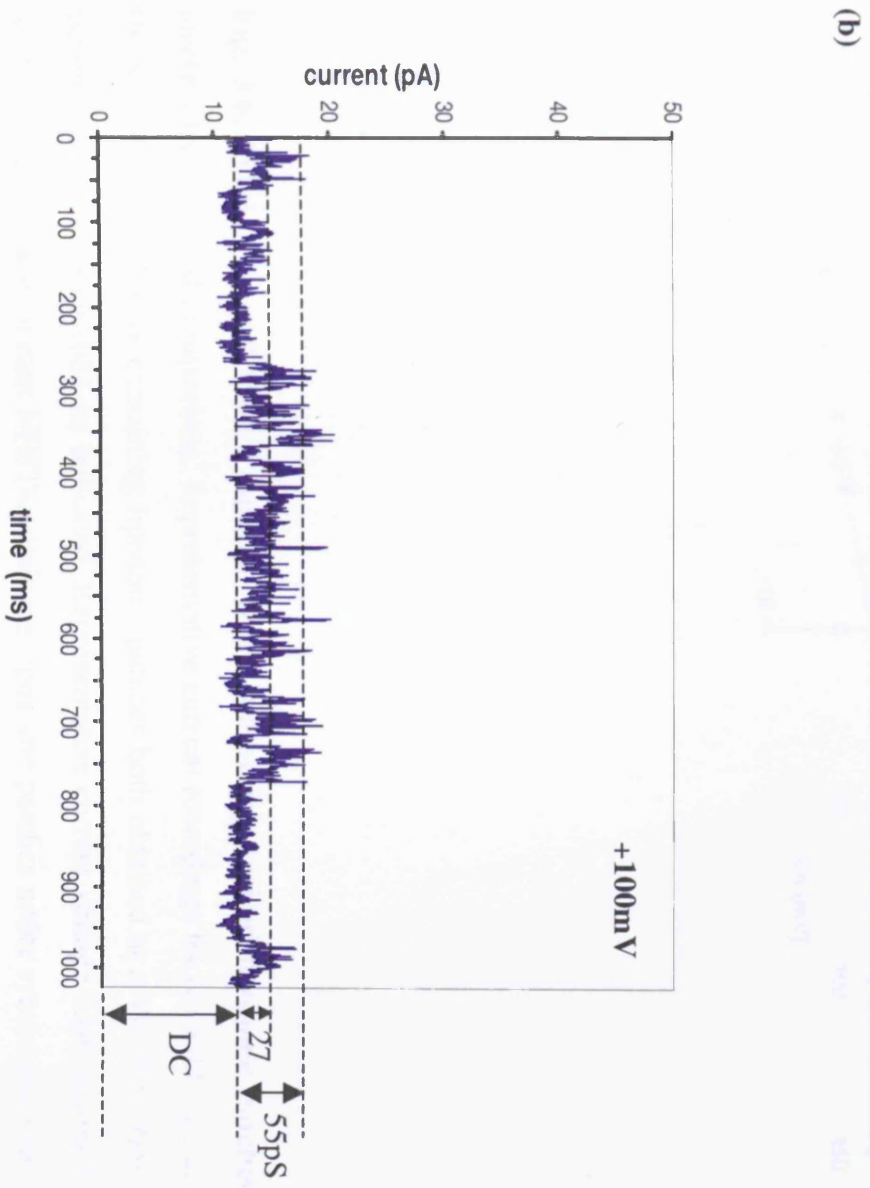
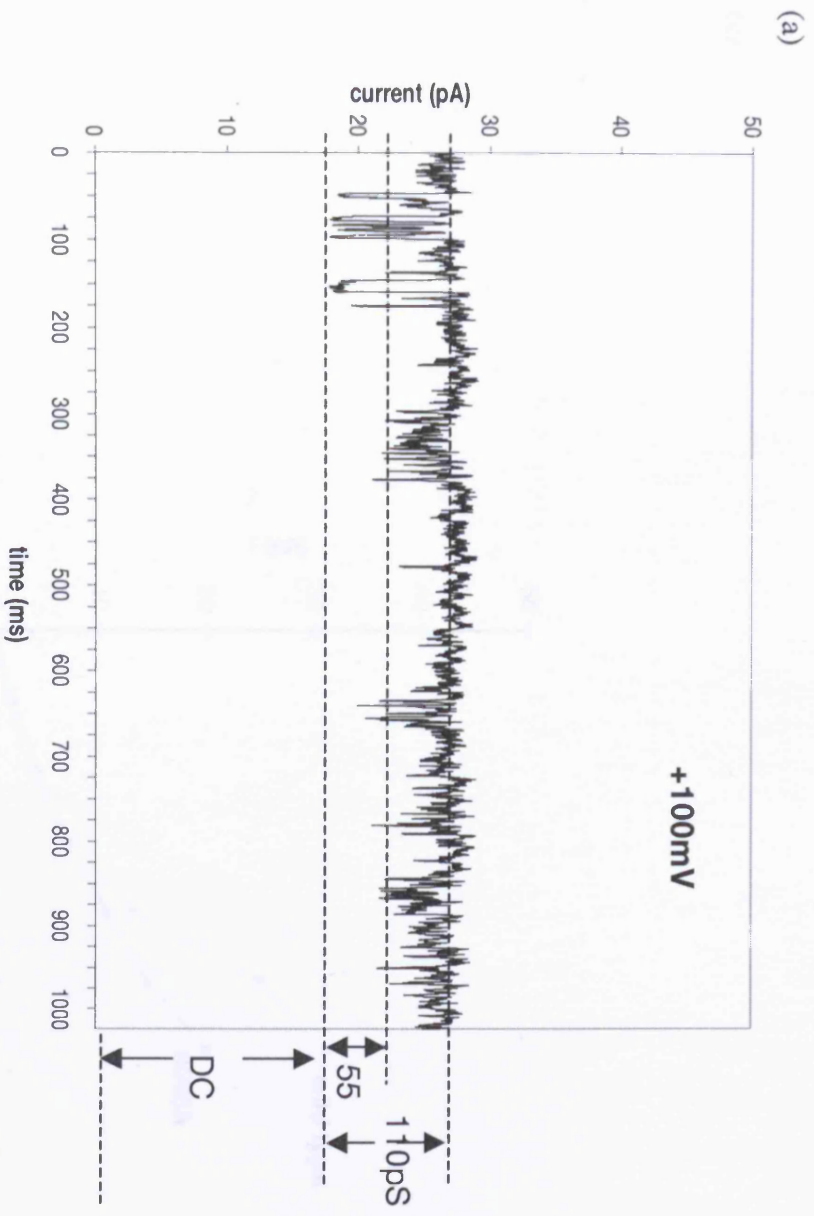


Fig. 3.5: Long and short dwell-time pores in NEST-containing excised liposome patches. (a) Absolute conductance distribution in patches with long-dwell time (DC) currents. Patches were excised from giant liposomes prepared without (red bars; $n=46$) or with NEST (blue bars; $n=71$). (b) Distribution of conductance transition amplitudes (for example see Fig. 3.6a) in 9 NEST-containing liposome patches displaying "kinetic" channel activity.



(c)

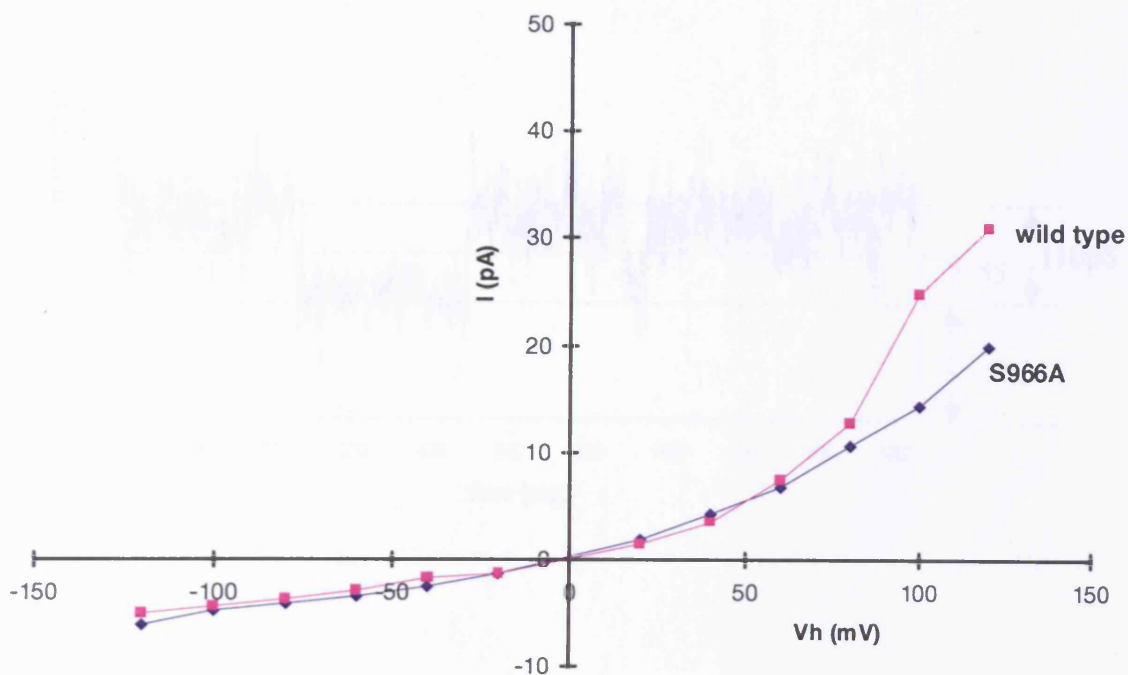
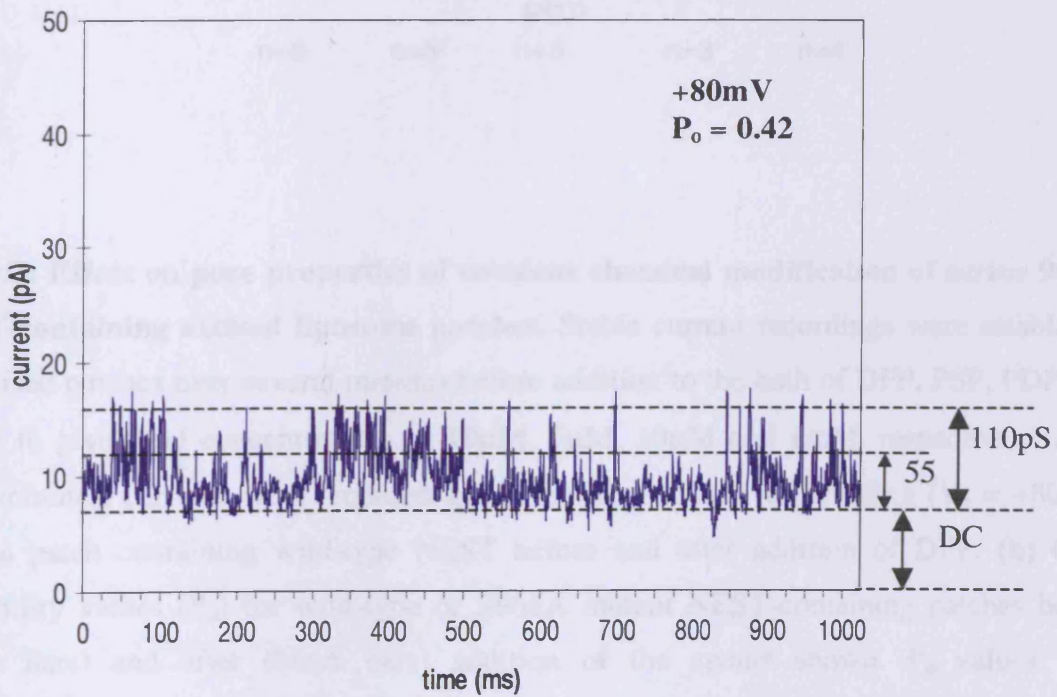
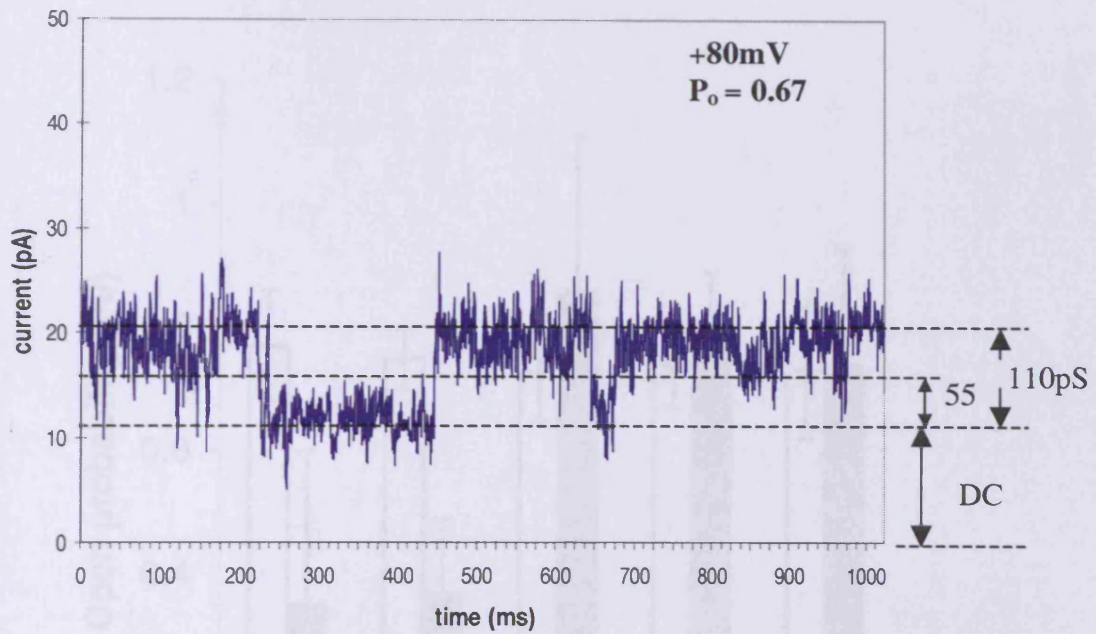


Fig. 3.6: Wild-type and S966A mutant NEST-containing excised liposome patches: electrophysiological comparison. Representative current recordings for (a) wild-type and (b) S966A mutant NEST-containing liposome patches both obtained at a V_h of +100mV; conductance transitions (pS) are indicated. Representative current-voltage relationships for wild-type and S966A mutant NEST-containing liposome patches under symmetrical ionic conditions are shown in (c).

(a)



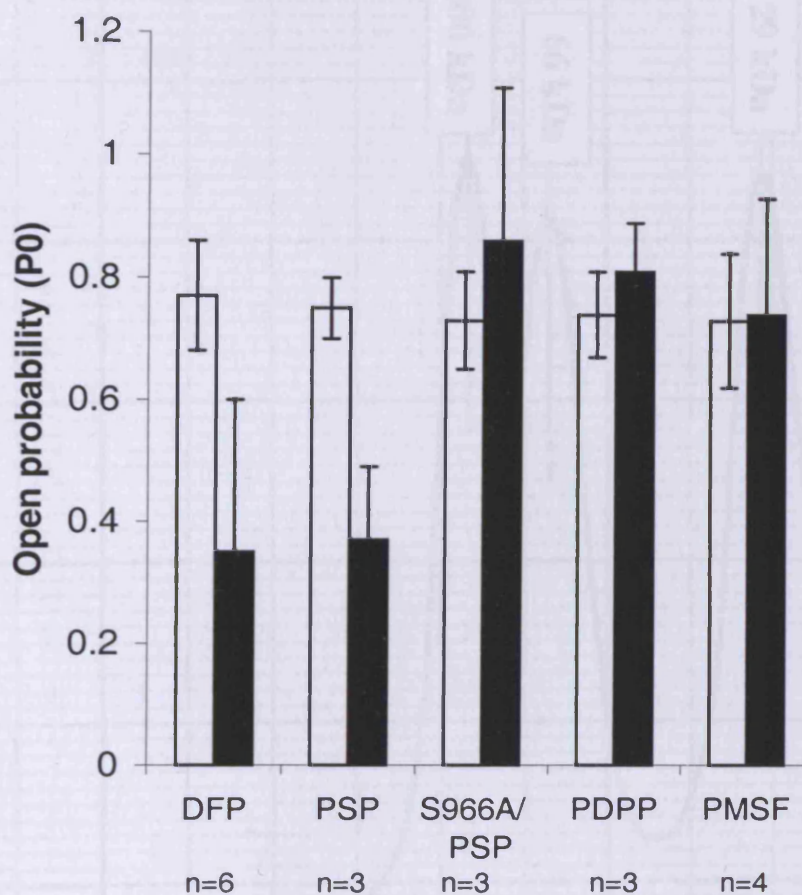


Fig. 3.7: Effect on pore properties of covalent chemical modification of serine 966 in NEST-containing excised liposome patches. Stable current recordings were established in excised patches over several minutes before addition to the bath of DFP, PSP, PDPP, or PMSF to give final concentrations of 10 μ M, 5 μ M, 10 μ M and 1mM, respectively. After three minutes, currents were recorded again. (a) Representative recording ($V_h = +80$ mV) from a patch containing wild-type NEST before and after addition of DFP. (b) Open probability values (P_o) for wild-type or S966A mutant NEST-containing patches before (white bars) and after (black bars) addition of the agents shown. P_o values were significantly different (T-test) after addition of DFP ($P = 0.017$) and PSP ($P = 0.034$).

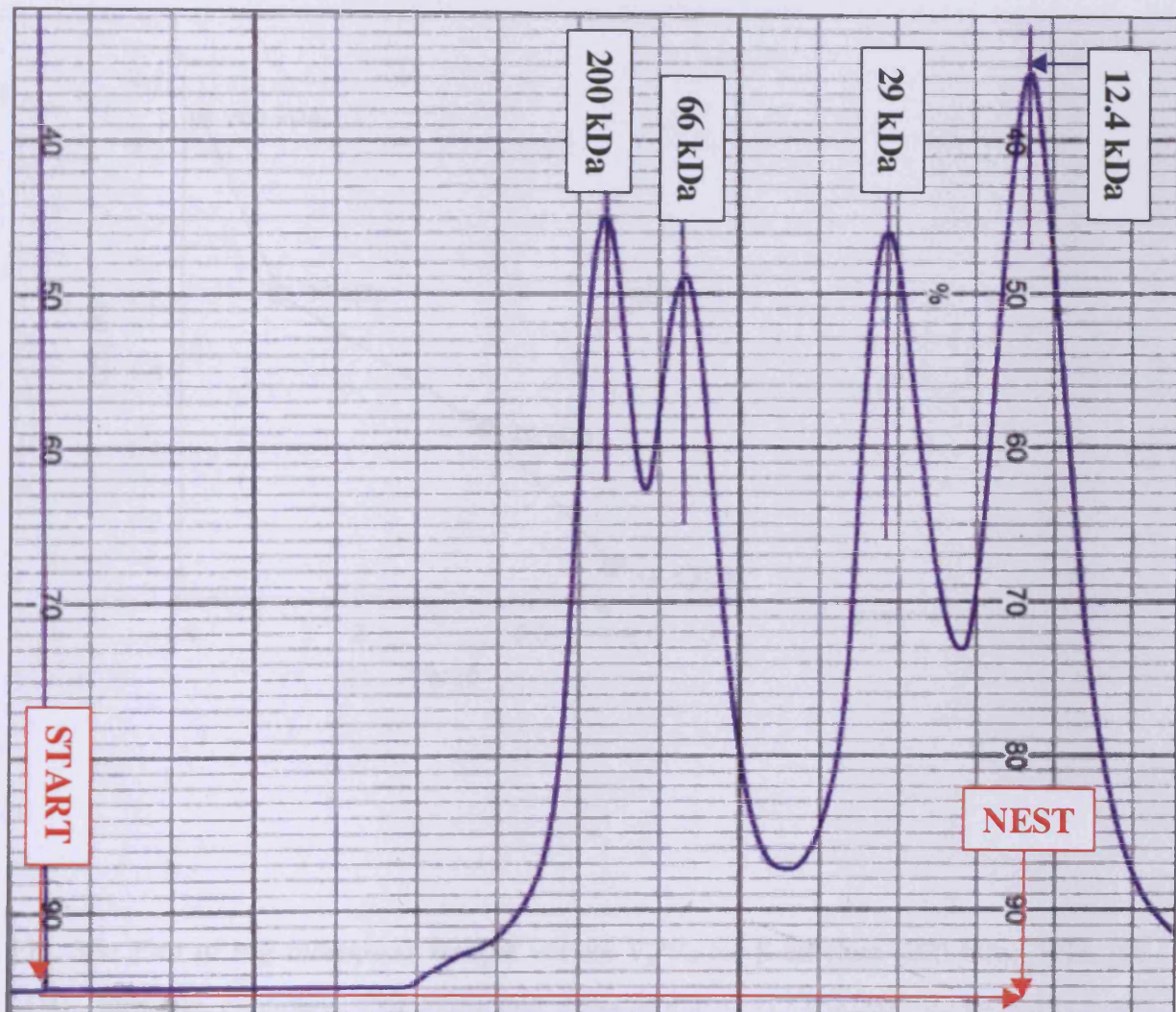


Fig. 3.8: Gel filtration profile of standard proteins. Solutions of β -amylase (200 kDa), BSA (66 kDa), carbonic anhydrase (29 kDa) and cytochrome c (12.4 kDa) were made up in the gel filtration buffer containing 0.3% CHAPS, so that they were directly comparable with NEST. From the trace the elution volumes (V_e) of the four standards were determined and used along with the known void volume (V_0) to determine the apparent molecular weight of NEST on gel filtration.

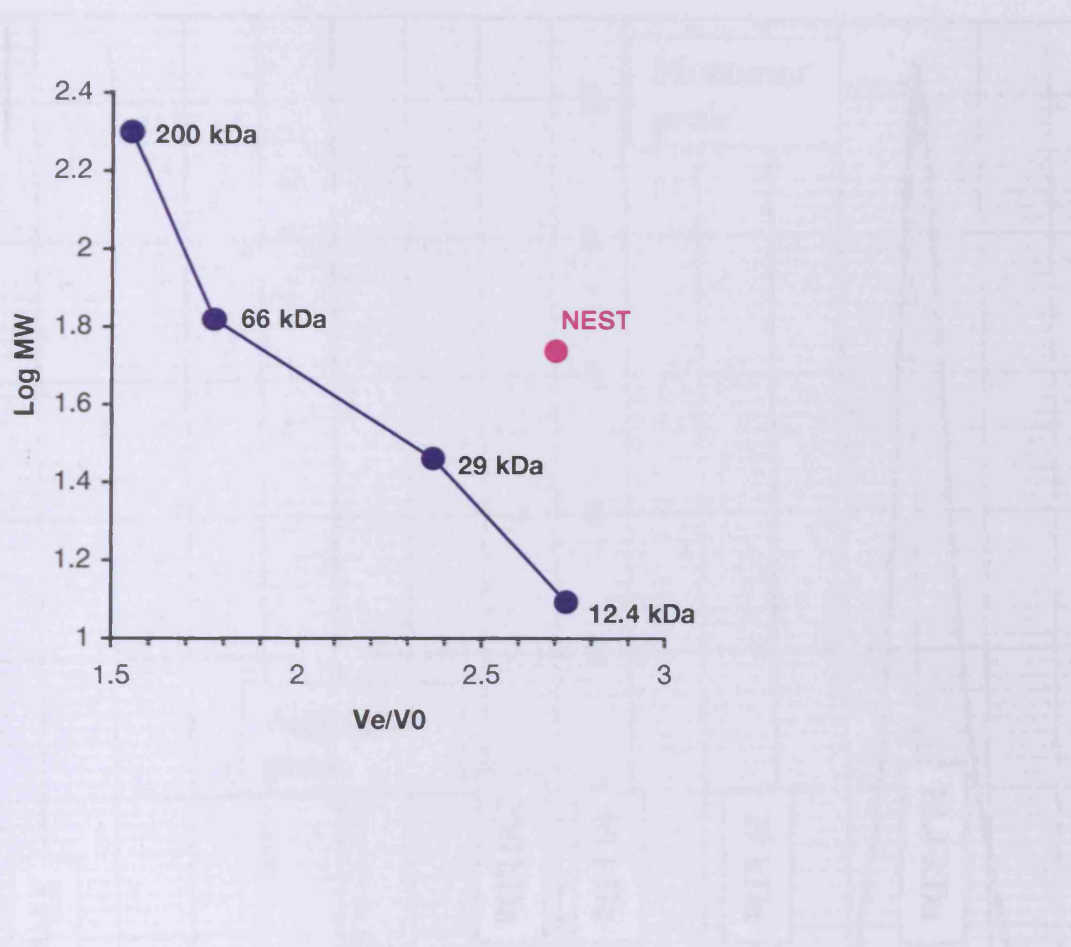


Fig. 3.9: Plot of log molecular weight versus V_e/V_0 for β -amylase (200 kDa), BSA (66 kDa), carbonic anhydrase (29 kDa) and cytochrome c (12.4 kDa). V_e/V_0 ratios were calculated for the standard proteins and NEST, where V_e is the elution volume and V_0 is the void volume.

Fig. 3.10: Gel filtration profile of NEST-crosslinked dimer in boiling reducing detergent. NEST dimer was treated with 0.1% CHAPS at room temperature for 45 min before running on gel filtration in buffer containing 0.1% CHAPS. The aggregate and monomer peaks are indicated in red and the elution positions of the four protein standards are indicated in black. In addition, the void volume (V_0), which is 2.6 ml is also shown.

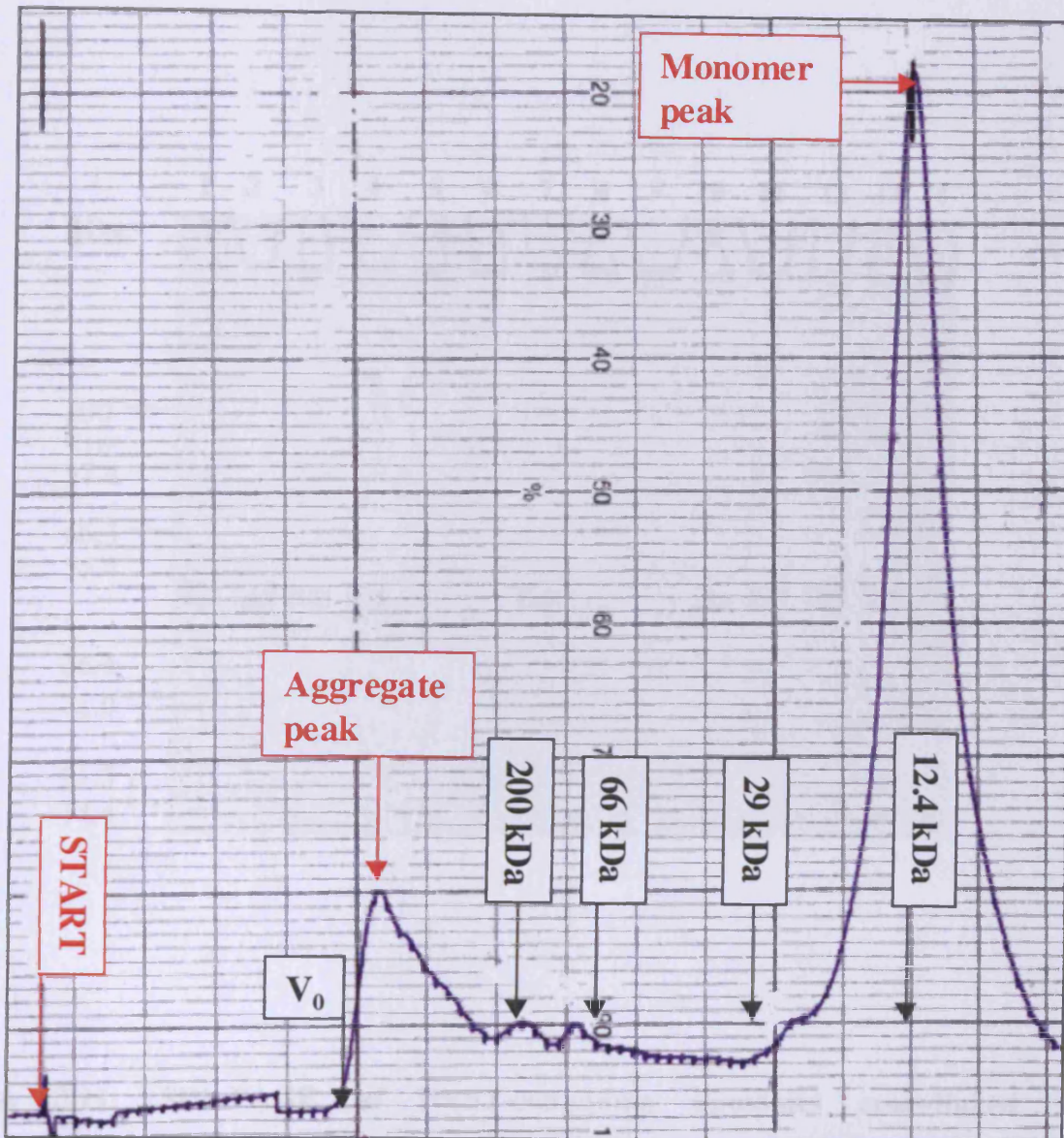


Fig. 3.10: Gel filtration profile of NEST-containing liposomes solubilised in limiting detergent. NEST liposomes were incubated with 0.1% CHAPS at room temperature for 45min before running on gel filtration in buffer containing 0.1% CHAPS. The aggregate and monomer peaks are indicated in red and the elution positions of the four protein standards are indicated in black. In addition, the void volume (V_0), which is 5.6 ml is also shown.

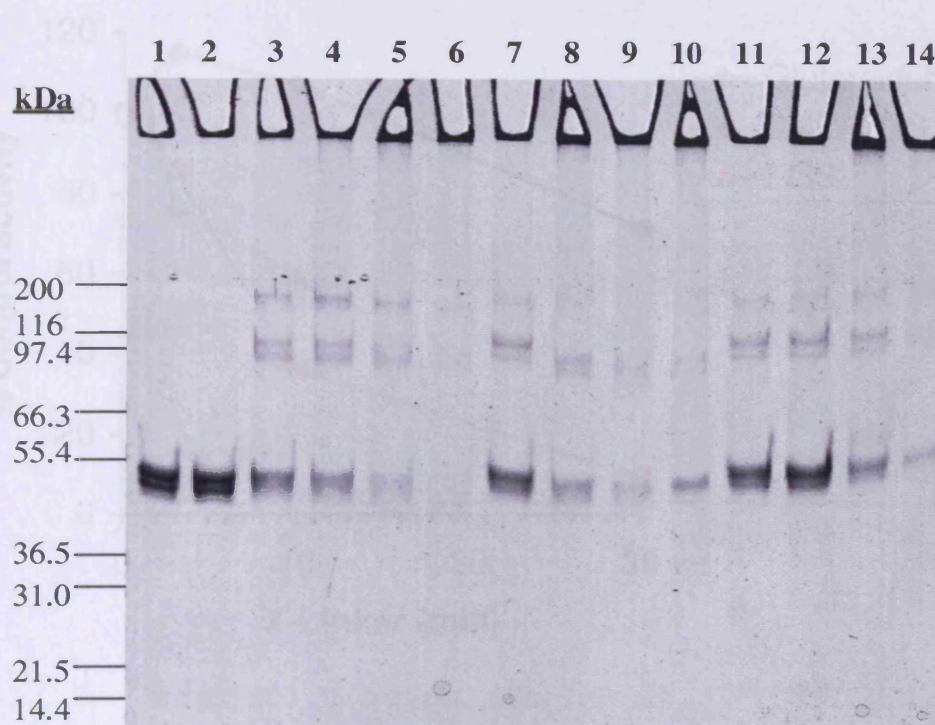


Fig. 3.11: SDS-PAGE of NEST-containing liposomes cross-linked with glutaraldehyde, Sulfo-EGS and EGS. NEST liposomes were incubated with glutaraldehyde (1, 3, 10, 30 mM) (**lanes 3-6**), Sulfo-EGS (1, 3, 10, 30mM) (**lanes 7-10**) and EGS (0.5, 1, 3, 10 mM) (**lanes 11-14**) for 120min at 4°C. A control was also included with NEST in the absence of cross-linker (**lanes 1-2**). The cross-linking reaction was quenched with 30mM Tris/HCl pH 8.0 at room temperature for 30min and SDS sample buffer added. Samples were run on 7.5% SDS-PAGE.

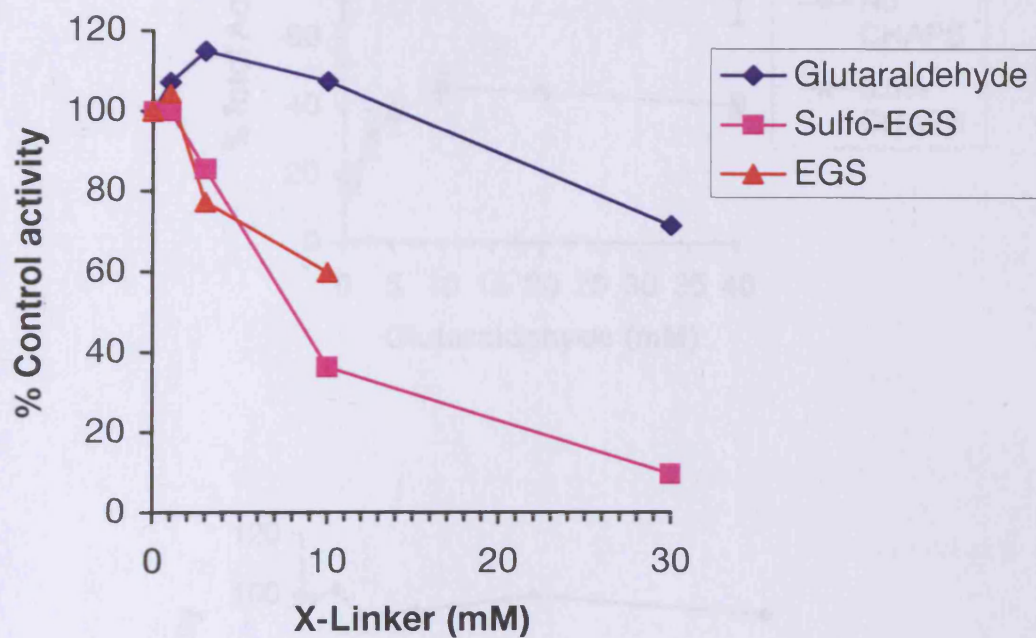
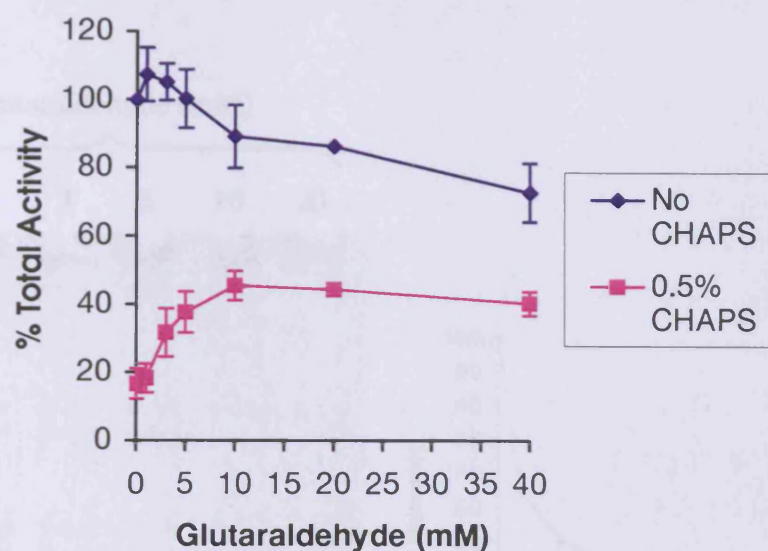


Fig. 3.12: Effects of varying cross-linker concentration on NEST phenyl valerate hydrolase activity. NEST was incubated with glutaraldehyde (0-30mM), Sulfo-EGS (0-30mM) and EGS (0-10mM) for 2 hours on ice and the reaction quenched with 25mM Tris pH 8.0. NEST phenyl valerate hydrolase activity was measured for each cross-linker concentration. Data points shown are the mean of duplicate samples.

(a)



(b)

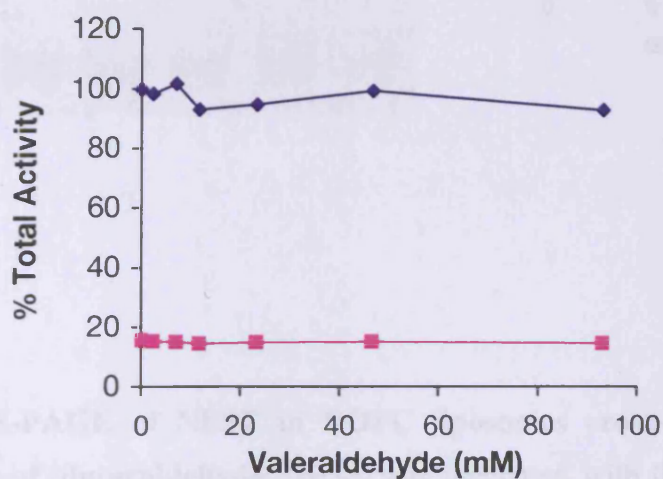


Fig. 3.13: Effect of varying the concentration of (a) glutaraldehyde and (b) valeraldehyde on NEST phenyl valerate hydrolase activity. NEST was incubated with 0, 1, 3, 5, 10, 20 and 40mM glutaraldehyde or 0, 2.3, 7, 11.6, 23, 46.5 and 93mM valeraldehyde. After 120min at 4°C, aliquots were removed from each sample and diluted in Tris/EDTA pH 8.0. PV-hydrolase assays were carried out in the presence or absence of 0.5% CHAPS. Data points shown represent the mean of 3-5 experiments \pm standard deviation for glutaraldehyde and the mean of duplicate samples in one experiment for valeraldehyde.

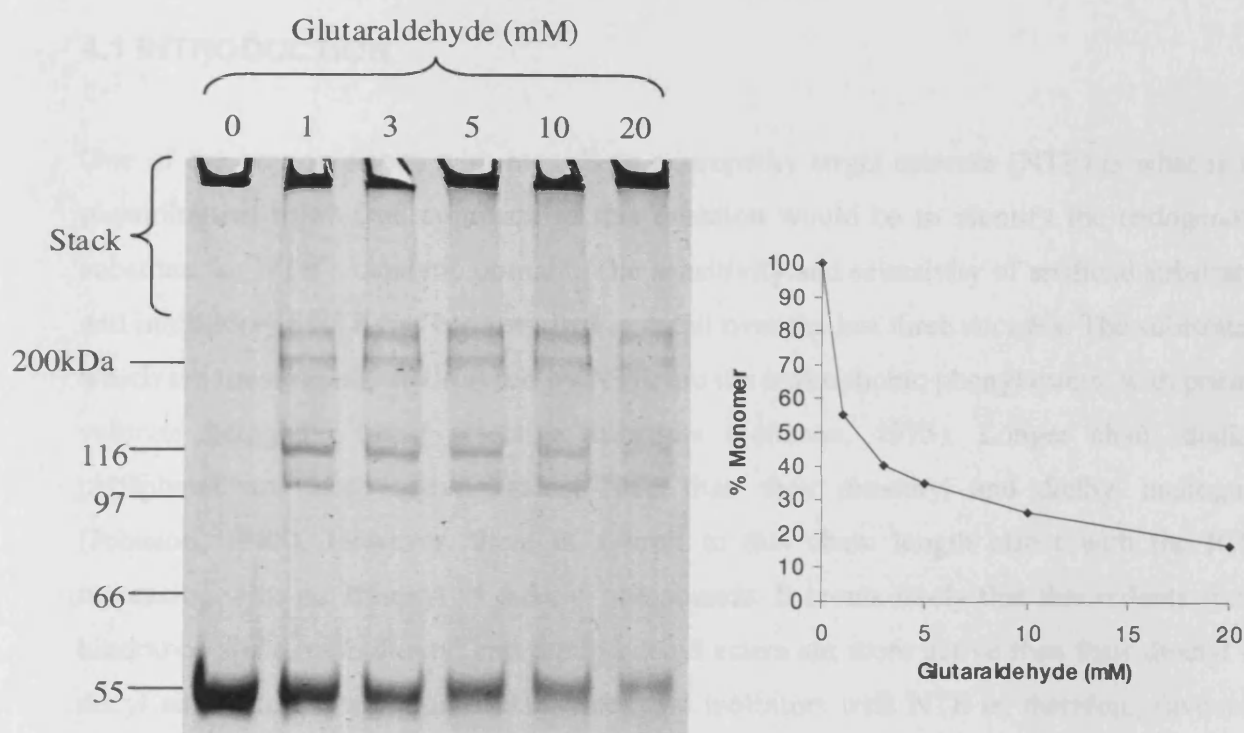


Fig. 3.14: SDS-PAGE of NEST in DOPC liposomes cross-linked with increasing concentrations of glutaraldehyde. NEST was incubated with 0, 1, 3, 5, 10 and 20mM glutaraldehyde for 120min at 4°C. Cross-linking reactions were stopped by the addition of 30mM Tris/HCl pH 8.0. SDS sample buffer was added and samples run on 7.5% SDS-PAGE. The graph shows the percentage of monomer remaining (determined by densitometry) at each glutaraldehyde concentration.

CHAPTER 4: PRELIMINARY INVESTIGATIONS INTO IDENTIFYING A POSSIBLE SUBSTRATE FOR NTE.

4.1 INTRODUCTION

One of the key questions with regards to neuropathy target esterase (NTE) is what is its physiological role? One approach to this question would be to identify the endogenous substrate for NTE's catalytic domain. The sensitivity and selectivity of artificial substrates and inhibitors of NTE has been studied in detail over the last three decades. The substrates, which are most rapidly hydrolysed by NTE, are the hydrophobic phenyl esters, with phenyl valerate being the most selective substrate (Johnson, 1975). Longer chain dialkyl phosphates are more active against NTE than their dimethyl and diethyl analogues (Johnson, 1988). However, there is a limit to this chain length effect with the IC₅₀ increasing with the dihexyl to didecyl compounds. It seems likely that this reflects steric hindrance since methyl/octyl and methyl/decyl esters are more active than their dioctyl or decyl analogues. Interaction of substrates and inhibitors with NTE is, therefore, favoured by the presence of large hydrophobic side-chains in the molecule. This pattern is similar to that of chymotrypsin, although NTE does not hydrolyse amides or peptides (Johnson, 1975).

A BLAST search for proteins homologous to NTE revealed a low homology between a calcium-independent phospholipase A₂ (iPLA₂) and NTE (Chapter 1; Fig.1.8). This area of homology contains the serine hydrolase consensus sequence GX₂SXG, which is present in the NEST protein. Phospholipase A₂ constitutes a large and diverse family of enzymes that hydrolyse the sn-2 fatty acid on phospholipids producing a free fatty acid and a lysophospholipid. These lipid products may serve as intracellular second messengers or can be further metabolised to potent inflammatory mediators, such as eicosanoids and platelet-activating factors. Since the *Drosophila* homologue of NTE has been proposed to play a role in cell signalling during neural development (Kretzschmar et al., 1997; see Chapter 1.5), NTE might similarly metabolise a lipid substrate to generate a signalling molecule.

The main objective of the studies in this chapter was to gain insight into the endogenous substrate for NTE and perhaps shed some light on its physiological role. Having validated NEST as a model system for studying the catalytic properties of NTE (Chapter 2), this part of the project now examined NEST's reactivity with various classes of natural lipids, including monoglycerides, diglycerides, lysophospholipids, phospholipids and fatty acid amides and with several inhibitors thought to be relatively selective for phospholipases A2.

4.2 RESULTS & DISCUSSION

4.2.1 Effect of phospholipids on NEST phenyl valerate hydrolase activity

Because it is relatively difficult to set up assays to determine whether various lipids are hydrolysed by NEST (see 4.2.3), my first approach was to investigate whether any lipids would affect (in particular compete with) the hydrolysis of phenyl valerate by NEST. Previous studies have shown that the phenyl valerate hydrolase activity of NTE can be modulated by the presence of phospholipids. Davis and Richardson (1987) demonstrated that the loss of NTE catalytic activity, upon solubilisation in sodium cholate, could be prevented if asolectin was included during the solubilisation step; however, addition of asolectin after solubilisation could not restore the catalytic activity of NTE. In contrast, Pope and Padilla (1989b) showed some restoration of catalytic activity when partially purified NTE, in 0.3% CHAPS, was incubated with phosphatidylcholine (PC), phosphatidylethanolamine (PE) and phosphatidylserine (PS), but not phosphatidylinositol (PI); the latter phospholipid at a concentration of 40 μ g/ml caused approximately 40% inhibition of NTE PV-hydrolase activity.

To establish whether phospholipids could modulate NEST activity in DOPC liposomes, exogenous phospholipids were added into the phenyl valerate hydrolase assay. The experiment was based on the method used by Pope and Padilla (1989b). The results of the PV-hydrolase assay (Fig. 4.1) demonstrate that PC, PE, PI and PS (0-40 μ g) do not significantly effect NEST PV-hydrolase activity in DOPC liposomes. This differs from the results of Pope and Padilla (1989b) described above. However, since NEST in DOPC liposomes has similar catalytic centre activity to native NTE (Chapter 2.2.4.1) it may not

be surprising that additional phospholipid caused no increase in activity. However, no inhibition was observed with PI as shown by Pope and Padilla (1989b).

To further investigate the possible modulatory effects of the different phospholipids, purified NEST (after gel filtration) was reconstituted into PC, PE, PI and PS liposomes. As PE alone can not form lipid bilayers, DOPC was also included in this sample to achieve reconstitution of NEST. NEST was also reconstituted into DOPC in the same experiment as a control. After detergent dialysis the specific activity of each reconstituted preparation was measured using the PV-hydrolase assay (Table 4.1). After reconstitution of NEST into PC, PS and PE + DOPC, a small decrease in specific activity ($\approx 25-30\%$) was observed compared to control DOPC liposomes. Interestingly, no decrease was observed with PI, which had previously been shown to inhibit the activity of partially purified NTE (Pope & Padilla, 1989b).

Because addition of PC, PE, PI or PS (up to $40\mu\text{g/ml}$; approximately $50\mu\text{M}$) exogenously, or direct reconstitution of NEST into these various phospholipids, did not appear to have any significant affect on the phenyl valerate hydrolase activity of NEST some other phospholipids – platelet-activating factor, lyso-platelet-activating factor, arachidonyl platelet-activating factor and lysophosphatidylcholine - were added into the PV-hydrolase assay. Platelet-activating factor (PAF) differs from phosphatidylcholine (PC) with respect to the sn-1 bond: in the case of PAF it is an ether linkage, whereas in PC it is an ester linkage.

Both PAF and lysoPAF could inhibit NEST PV-hydrolase activity with IC_{50} values of 20 and $27\mu\text{M}$ respectively (Fig. 4.2). Lyso-phosphatidylcholine (lysoPC) and arachidonyl PAF (AA-PAF), however, were much less inhibitory, causing only 40% inhibition at 1mM and 20% inhibition at $250\mu\text{M}$ respectively (Fig. 4.2). The fact that both PAF and lysoPAF were potent inhibitors compared to AA-PAF suggests that a phospholipid with long chain fatty acids at both the sn-1 and sn-2 position can not be accommodated in the active site of NEST. In addition, the presence of an ester bond in lysoPC compared to an ether bond in lysoPAF results in a 500-fold reduction in potency of the phospholipid.

To further characterise the inhibition of NEST PV-hydrolase activity by PAF, the time course of inactivation was examined. NEST was preincubated with PAF (10, 25, 50 μ M) for periods of 1-20min. A semi-logarithmic plot of the percentage control activity versus preincubation time resulted in a linear inactivation time course up to 20min, indicating first-order kinetics (Fig. 4.3). Therefore, the inhibition of NEST by PAF is progressive.

PAF is a potent lipid mediator involved in inflammatory and allergic reactions (Dentan et al., 1996). PAF has also been implicated as a messenger in long term potentiation (Kato et al., 1994). PAF acetyl hydrolase (PAF-AH), an enzyme that degrades PAF, is a phospholipase A2 (PLA2) that specifically hydrolyses phospholipids in which the sn-2 fatty acid is an acetyl group. Hydrolysis of PAF by PAF-AH results in the production of biologically inactive lysoPAF. The reported K_m of the purified enzyme is 13.7 μ M (Stafforini et al., 1987).

4.2.2 Inhibitors of serine hydrolases: effects on NEST phenyl valerate hydrolase activity

As NTE shows a sequence homology with a calcium-independent phospholipase A2, reagents known to inhibit phospholipase A2 and other serine hydrolases were tested to determine whether they could inhibit NEST phenyl valerate hydrolase activity (Table 4.2). In this section, the inhibition of NEST by these compounds is compared to other enzymes, in particular the phospholipase A2 family. IC50 values for NEST were determined under standardised conditions: that is preincubation at 37°C for 20min before addition of phenyl valerate. Each inhibitor was used at seven concentrations spanning 2 to 3 orders of magnitude. To facilitate comparison, literature IC50 values for the action of these inhibitors on other enzymes, which are cited in the following discussion, have been crudely adjusted to those expected for a 20min preincubation at 37°C.

4.2.2.1 p-Bromophenacyl bromide (BPAB)

BPAB is a hydrophobic reagent, which acts by covalent modification of a histidine residue at the active site of phospholipases A2. BPAB irreversibly inhibits PLA2s from various

sources, such as pancreatic PLA2 (Volwerk et al., 1974), the cobra venom enzyme (Roberts et al., 1977) and most other venom PLA2s (Serrano et al., 1999). BPAB also inhibits several other enzymes, such as bovine pancreatic alpha-chymotrypsin, yeast alcohol dehydrogenase, human platelet phosphatidylinositol (PI)-specific phospholipase C (Kyger & Franson, 1984) and fatty acid amide hydrolase (Maurelli et al., 1995).

BPAB inhibits the calcium-dependent PLA2 from rat retinal lysates with an IC50 of $\approx 130\mu\text{M}$ (Sastry & Hemontolor, 1998), whereas the calcium-dependent PLA2 purified from P388D1 macrophages is much less sensitive with an IC50 of $\approx 800\mu\text{M}$ (Lister et al., 1989). NEST activity was inhibited by BPAB with half maximal inactivation observed at $4.4\mu\text{M}$ (Table 4.2).

Although BPAB inhibits phospholipases it is a non-specific inhibitor and it has previously been shown that BPAB is capable of modifying residues other than histidine, such as cysteine (Kyger & Franson, 1984). However, another commonly used modifier of histidine residues, diethyl pyrocarbonate (DEPC), was also tested and this reagent also inhibited NEST phenyl valerate hydrolase activity (IC50 = 1-2mM). DEPC has also been shown to inhibit hen brain NTE with 30% inhibition at 1.5mM (Johnson MK., 1982). The inhibition of NEST by BPAB and DEPC suggests that a histidine residue is essential for catalytic activity in accord with the pH profile for NEST PV-hydrolase activity and the results of mutating histidines H860 and H885 (Chapter 2).

4.2.2.2 Bromoenol lactone (BEL)

BEL and several other lactone compounds were originally synthesised as mechanism-based inhibitors of chymotrypsin (Daniels et al., 1983). These lactones act as suicide substrates for serine proteases by acyl transfer of the lactone carbonyl to the serine hydroxyl. The halomethylketone produced remains tethered to the active site serine rendering the enzyme catalytically inactive. BEL inhibits chymotrypsin with a Ki of $17.3\mu\text{M}$ (Daniels et al., 1983), but also inhibits magnesium-dependent phosphatidate phosphohydrolase (IC50 = $12\mu\text{M}$; Balsinde & Dennis, 1996b) and fatty acid amide hydrolase (IC50 = $0.4\mu\text{M}$; Beltramo et al., 1997). BEL does not, however, inhibit purified recombinant human lysophospholipase (Wang et al., 1999).

BEL is also a potent irreversible, mechanism-based inhibitor of calcium-independent phospholipases A2. It possesses greater than 1000-fold selectivity for inhibition of the calcium-independent PLA2 (iPLA2) versus the calcium-dependent ones. BEL inhibits myocardial iPLA2 with half maximal inactivation at less than 100nM after a 5min preincubation at 20°C (Hazen et al., 1991). BEL also inhibits the intracellular iPLA2s present in P388D1 macrophages (Ackermann et al., 1995) and CHO cells (Balboa et al., 1997) with IC50 values of approximately 15 and 30nM, respectively. BEL inhibited NEST phenyl valerate hydrolase activity with an IC50 of 94nM (Table 4.2), which is clearly more typical of calcium-independent rather than calcium-dependent phospholipase A2s.

4.2.2.3 Methyl arachidonyl fluorophosphonate (MAFP)

MAFP, a relatively stable arachidonyl binding site directed phosphorylation reagent, was initially designed as the active-site directed inactivator of the calcium-sensitive and arachidonyl selective Group IV phospholipase A2 (cPLA2) (Street et al., 1993). cPLA2 is a phospholipid hydrolase, which uses the hydroxyl group of serine-228 residue as its catalytic nucleophile (Huang et al., 1996). MAFP irreversibly inhibits cPLA2 at low μM concentrations (Balsinde & Dennis, 1996a), by a direct action on the catalytic serine within the arachidonyl-binding site. MAFP also inhibits the Group VI calcium-independent phospholipase A2 (iPLA2) (Lio et al., 1996) and human lysophospholipase (Wang et al., 1999) with IC50 values of 0.125 and 0.9 μM , respectively.

When MAFP was tested as an inhibitor of NEST phenyl valerate hydrolase activity it was found to have an IC50 value of 2nM (Table 4.2). To explore the characteristics of MAFP inhibition of NEST further, the time course of inactivation was examined. NEST was preincubated with MAFP for periods of 1-60min. A semi-logarithmic plot of the percentage control activity versus preincubation time resulted in a linear inactivation time course up to 10min, indicating first-order kinetics (Fig. 4.4). A similar time-dependent inactivation by MAFP was shown for the macrophage P388D1 iPLA2 (Lio et al., 1996).

Out of the reagents tested, MAFP was found to be the most potent inhibitor of NEST PV-hydrolase activity with half maximal inhibition at 2nM (Table 4.2). This value was significantly lower than the IC50 values quoted for cPLA2 and iPLA2, but compared well

with the potency of MAFP for fatty acid amide hydrolase (FAAH) ($IC_{50} = 3.75nM$) (Deutsch et al., 1997).

4.2.2.4 Trifluoromethyl ketone analogues of arachidonic and palmitic acid (AACOCF₃ and PACOCF₃)

Trifluoromethyl ketones (TFMKs) potently inhibit a large number of serine hydrolases, by forming a reversible tetrahedral adduct with the active site serine (Gelb et al., 1985; Ashour & Hammock, 1987). Several TFMKs are very potent inhibitors of NTE. Thomas et al. (1990) investigated the potencies of a series of TFMKs against NTE. Of the aliphatic TFMKs tested, 3-octylthio-1,1,1-trifluoroketone (OTFK) was the most potent with an IC_{50} of 58.8nM. The IC_{50} values for the heptyl- and decyl- analogues were also low, 95 and 71.5nM, respectively, but below a chain length of 7 and above a chain length of 10 the potency of these compounds decreased significantly.

The trifluoromethyl ketone analogue of arachidonic acid was designed as a selective inhibitor of the Group IV calcium-dependent, cytosolic phospholipase A₂ (cPLA₂) versus the secretory phospholipase A₂ (sPLA₂) (Street et al., 1993). The macrophage calcium-independent phospholipase A₂ (iPLA₂) is also inhibited by AACOCF₃, as well as by the analogue of palmitic acid (Ackermann et al., 1995). P388D1 cell iPLA₂ is reversibly inhibited by PACOCF₃ ($IC_{50} = 6\mu M$) and CHO cell iPLA₂ is also inhibited by the same reagent with an IC_{50} of 4.5 μM (Balboa et al., 1997). AACOCF₃ inhibited P388D1 cell iPLA₂ with an IC_{50} value of 22.5 μM . Importantly, PACOCF₃ was found to be 4-fold more potent than AACOCF₃ at inhibiting macrophage iPLA₂. This is consistent with the substrate preference found previously using mixed micellar substrates, in which the rate of hydrolysis for dipalmitoylphosphatidylcholine was 4-fold faster than that for 1-palmitoyl-2-arachidonoyl-sn-glycerol-3-phosphorylcholine (Ackermann et al., 1994).

Trifluoromethyl ketones have also been shown to inhibit fatty acid amide hydrolase (FAAH) (Boger et al., 1999). Studies have shown that FAAH is inhibited by AACOCF₃ with IC_{50} values in the low micromolar range (Koutek et al., 1994; Maurelli et al., 1995; Beltramo et al., 1997). However, the most potent trifluoromethyl ketone inhibitor of FAAH

is the oleic acid derivative, which has a K_i of 82nM (Boger et al., 1999) and has been used for the purification of FAAH from rat liver membranes (Cravatt et al., 1996).

In contrast to iPLA2, AACOCF3 was the more potent TFMK inhibitor of NEST phenyl valerate hydrolase activity. AACOCF3 was about 10-fold more potent than PACOCF3 (Fig. 4.6), with IC_{50} values of 2.5 μ M and 28.5 μ M respectively (Table 4.2). However, these fatty acid analogues are 40- and 475-fold less potent than 3-octylthio-1,1,1-trifluoroketone (OTFK), which has an IC_{50} of 58nM (Thomas et al., 1990). The heptyl- and decyl- analogues also had IC_{50} values lower than AACOCF3 suggesting that the optimal alkyl chain length, which can fit into the active site of NTE, is about 10.

4.2.2.5 N-Arachidonyl-5-hydroxytryptamine (AA-5HT)

Arachidonylserotonin (AA-5HT) is a synthetic compound, which acts as a non-covalent inhibitor of FAAH. AA-5HT inhibited anandamide hydrolysis in mouse N18TG2 neuroblastoma cells with an IC_{50} value of 18 μ M (Bisogno et al., 1998), but had no inhibitory action against the Group IV cPLA2. AA-5HT was shown to inhibit NEST phenyl valerate hydrolase activity with half maximal inactivation at 50 μ M (Table 4.2). In contrast, anandamide and oleamide (FAAH substrates) did not inhibit PV-hydrolase activity significantly, with only 9.5 and 9.8% inhibition at 250 μ M, respectively.

4.2.2.6 Phenylmethanesulfonyl fluoride (PMSF)

PMSF is a non-selective sulfonylation reagent, which inhibits a variety of enzymes, such as trypsin, chymotrypsin, FAAH (Deutsch et al., 1997) and NTE (Atkins & Glynn, 2000) with IC_{50} values of >1mM, 375 μ M, 1.35 μ M and 55 μ M, respectively. NEST in bacterial membranes (Atkins & Glynn, 2000) and NEST in DOPC liposomes is also inhibited by PMSF with IC_{50} values of 153 μ M and $107 \pm 37.9\mu$ M (n=3), respectively. PMSF is two times more potent against FAAH than AACOCF3, whereas for NEST AACOCF3 is 30 times more potent than PMSF.

4.2.3 POTENTIAL ENDOGENOUS SUBSTRATES FOR NEUROPATHY TARGET ESTERASE (NTE)

Before testing any potential substrates for NEST it was necessary to run several control experiments. A lipid extract (see Methods 6.7.8) was prepared from both wild type and S966A mutant NEST in dioleoylphosphatidylcholine (DOPC) liposomes. These extracts were run on thin layer chromatography (TLC) along with DOPC, oleic acid and arachidonic acid standards which could be detected by subsequent reaction with iodine vapour (Fig. 4.6a). Both the NEST and S966A mutant extracts showed a spot at the position of DOPC and also two other unknown spots. The NEST extract also had an additional spot on the TLC plate, which coincided with oleic acid. This suggests that at some point during reconstitution (2 days dialysis) NEST is capable of cleaving oleic acid from DOPC, as there is no evidence of hydrolysis with the serine mutant. Thus, it would appear that NEST shows a small amount of either PLA1 or PLA2 activity under these reconstitution conditions.

4.2.3.1 Phospholipid substrates

In section (4.2.2) it was shown that various phospholipase A2 inhibitors are capable of inhibiting NEST phenyl valerate hydrolase activity. Therefore, to establish whether NEST shares any functional characteristics with PLA2s, several phospholipid substrates were tested. Phospholipases A2 are a very diverse family of enzymes and as such show different substrate preferences to each other. For example, the calcium-independent phospholipase A2 (iPLA2) from the brush border membrane of the small intestine shows very active phospholipase A2 and lysophospholipase activity (Pind & Kuksis, 1988; Gassama-Diagne et al., 1989; Gassame-Diagne et al., 1992). In addition, this iPLA2 has also been shown to express a glycerol ester lipase activity, hydrolysing triacylglycerol, diacylglycerol and monoacylglycerol substrates (Gassame-Diagne et al., 1992). The intracellular iPLA2s, on the other hand, show very little lysophospholipase activity (Ackermann et al., 1994; Hazen et al., 1990). In general, phospholipase A2s hydrolyse the sn-2 ester bond of phospholipids, releasing a free fatty acid and a lysophospholipid.

As radioactive substrates are very expensive this investigation into a potential substrate for NEST was carried out using unlabelled substrates (except for 1-stearoyl-[2-

^{14}C]arachidonyl-phosphatidylinositol; [^{14}C]-PI), containing either oleoyl or arachidonyl at the sn-2 position. As both of these fatty acids contain unsaturated carbon bonds these could be detected on thin layer chromatography (TLC) using iodine. To directly compare NEST activity with phospholipase A2 activity, bee venom phospholipase A2 (14 kDa secretory phospholipase) was used as a positive control. All substrate assays, for NEST and bee venom sPLA2, were carried out using standard conditions unless otherwise stated: 50mM Tris/HCl buffer pH8, 1mM Ca^{2+} , 0.03% Tx-100 and 100 μM substrate with incubation at 37°C for 30min. In the case of [^{14}C]-PI, the substrate was a mixture of 5 μM [^{14}C]arachidonyl-PI + 100 μM unlabelled PI. In addition, sPLA2 was used at a concentration of 0.038 mg/ml compared to 0.15 mg/ml for NEST, as the molecular weights of these two proteins vary by approximately 4-fold.

1-stearoyl-2-arachidonyl-phosphatidylcholine (-PC) and 1-stearoyl-[2- ^{14}C] arachidonyl-phosphatidylinositol (-PI) were tested as substrates for NEST and bee venom sPLA2. After incubation of the enzyme and substrate at 37°C for 30min, the lipids were extracted and samples were run on TLC. In the case of 1-stearoyl-[2- ^{14}C]arachidonyl-PI the spot containing arachidonic acid was scraped off and the amount of free [^{14}C]arachidonic acid determined by scintillation counting (Table 4.3). As expected both of these phospholipid substrates were hydrolysed by bee venom sPLA2, releasing free arachidonic acid. In contrast, NEST was unable to cleave either 1-stearoyl-2-arachidonyl-PC (Fig. 4.6b) or 1-stearoyl-[2- ^{14}C]arachidonyl-PI (Table 4.3).

In addition, having demonstrated a low level of hydrolysis of DOPC by NEST over two days of dialysis, exogenous DOPC was added as a substrate. After 30min incubation at 37°C there was no evidence of any additional hydrolysis of DOPC (Fig. 4.6c). Therefore, it appears that NEST has no or very little PLA2 activity on phospholipids compared to bee venom sPLA2.

Phospholipases A2 can hydrolyse diacyl phospholipids with various fatty acids at the sn-2 position. The release of arachidonic acid from the sn-2 position is of particular importance for the generation of eicosanoids. PLA2 also provides precursors for platelet-activating factor formation when the sn-1 position of the phospholipid contains an alkyl ether linkage. Purified cytosolic calcium-independent PLA2 (iPLA2) from P388D1 cells hydrolyses

dipalmitoyl-PC roughly 4-fold faster than 1-palmitoyl-2-arachidonoyl-PC, 15-fold faster than 1-*O*-hexadecyl-2-arachidonoyl-PC (arachidonoyl PAF) and 20-fold faster than palmitoyl-lyso-PC (Ackermann et al., 1994) and displays a preference for palmitoyl > arachidonoyl. In contrast, the well-characterised plasmalogen-specific canine myocardial iPLA2 (Hazen et al., 1990) has a substrate preference for plasmalogen (alkylenyl phospholipid) > sn-1 alkyl-ether PC > diacyl PC and displays a preference for arachidonoyl > palmitoyl. The iPLA2 from CHO cells can also hydrolyse arachidonoyl PAF, but in addition, hydrolyses the acetyl group at the sn-2 position of PAF (Tang et al., 1997). This indicates a unique flexibility at the active site in being able to accommodate not only long but short chain fatty acids. In contrast, the cPLA2 and sPLA2 enzymes do not display any PAF acetylhydrolase activity (Tang et al., 1997).

To determine whether NEST is capable of hydrolysing sn-1 alkyl-ether phospholipids, the substrate 1-*O*-hexadecyl-2-arachidonoyl-PC (arachidonoyl PAF) was used; bee venom sPLA2 was used as a positive control. Bee venom sPLA2 was capable of hydrolysing 100µM arachidonoyl-PAF (PAF) and free arachidonic acid was detected on TLC (Fig. 4.6d). NEST, however, was not able to hydrolyse this substrate and no free arachidonic acid was detected (Fig. 4.6d). From the phospholipid substrates and the assay conditions tested it seems unlikely that NEST functions as a phospholipase A2.

In section 4.2.1 it was demonstrated that PAF and lysoPAF inhibited NEST PV-hydrolase activity, whereas lysoPC did not. Since lysoPAF was as effective as PAF at inhibiting NEST PV-hydrolase activity it seems unlikely that either of these could act as a substrate for NTE, as lysoPAF does not contain a hydrolysable ester bond. Therefore an explanation for the lack of potency of lysoPC as an inhibitor of NEST PV-hydrolase activity may in fact be due to the hydrolysis of lysoPC by NEST. To test whether lysophospholipids are hydrolysed by NEST, lysophosphatidylcholine (oleoyl-lysoPC) and lysophosphatidic acid (oleoyl-lysoPA) were tested as possible substrates. LysoPC was used at 1mM instead of 100µM, as detection of this substrate on TLC was very poor. This is because lysoPC does not run very far on TLC and the resolution near the point of application of the sample is very poor. However, taking into account the relative amounts of oleic acid present in NEST only samples and NEST with lysoPC allowed a reasonable assessment of whether hydrolysis had occurred. Neither NEST nor the secretory phospholipase A2 from bee venom could hydrolyse lysoPC (Fig. 4.7a) or lysoPA (Fig. 4.7b), suggesting that they do

not possess any lysophospholipase activity. However, given the limitations of the TLC system used and the lack of radiolabelled substrate, the possibility that NEST does have some lysophospholipase activity can not be ruled out. Several other phospholipase A2s do show lysophospholipase activity, such as, the iPLA2 from brush border membranes of the small intestine (Gassame-Diagne et al., 1992), and the Group IV calcium-dependent cytosolic phospholipase A2s (Reynolds et al., 1993; Leslie, 1991).

4.2.3.2 Phosphatidic acid, tri-, di- and mono-acyl glycerols

The production of diacylglycerol in cells is achieved through a variety of catalytic processes (Fig. 4.8). Magnesium-dependent phosphatidate phosphohydrolase (PAP-1) converts PA to DAG. Also the degradation of phosphatidylinositol (PI) to DAG is catalysed by a PI-specific phospholipase C (Chau & Tai, 1982). DAG has two potential signalling roles: Firstly, arachidonic acid can be cleaved from the sn-2 position of DAG (1-stearoyl-2-arachidonylglycerol), which can act as a messenger itself or can be used in the production of eicosanoids. Secondly, it activates a serine/threonine protein kinase (PKC) that phosphorylates selected proteins in the cell. Metabolism of DAG to arachidonate (AA) requires the sequential action of two enzymes, a diglyceride lipase and monoglyceride lipase (Chau & Tai, 1981; Balsinde et al., 1991). The first enzyme catalyses specifically the deacylation of the sn-1 fatty acyl residue of a diacylglycerol, whereas the second enzyme catalyses the hydrolysis of the resulting 2-arachidonyl monoacylglycerol to arachidonate and glycerol. DAG is also converted to triacylglycerol (TAG) by a diglyceride acyltransferase. TAG is the most common lipid-based energy reserve in nature.

To determine whether NEST may be involved in the metabolism of DAG, TAG or PA, 1-stearoyl-2-arachidonyl-glycerol (DAG), triarachidonin (TAG), 2-arachidonyl glycerol (MAG) and 1-stearoyl-2-arachidonyl-phosphatidic acid (PA) were tested as substrates (substrate concentration 100 μ M). Bee venom phospholipase was also tested against the same substrates. NEST showed no detectable activity with DAG, TAG or PA substrates, as determined by detection of free arachidonic acid on TLC. Bee venom PLA2 showed a small amount of hydrolysis of 2-arachidonyl-PA (Fig. 4.9a), but had no detectable activity against the DAG or TAG substrates.

NEST was found to hydrolyse 100 μ M 2-arachidonyl glycerol, producing free arachidonic acid whereas sPLA2 did not (Fig. 4.9b). NEST was able to completely hydrolyse 50 μ M 2-AG leaving no detectable substrate on the TLC plate, but when 10 μ M 2-AG was tested, the presence of the substrate or free arachidonic acid could no longer be detected (Fig. 4.9c). Previous studies have found the K_m for 2-AG hydrolysis in N18TG2 and RBL-2H3 cells to be 91 and 29 μ M respectively (Di Marzo et al., 1998). Therefore the activity of NEST on 2-AG compares quite well with other reported 2-AG hydrolytic activities.

Having established that 2-AG was hydrolysed by NEST, a synthetic FAAH substrate, arachidonyl ethylene glycol (AEG), was also tested. NEST was shown to hydrolyse 100 μ M AEG, releasing free arachidonic acid (Fig. 4.9c), but bee venom PLA2 could not hydrolyse this substrate. Out of all of the physiological substrates tested, 2-arachidonyl glycerol was the only one hydrolysed by NEST. Therefore, NEST has a monoacylglycerol lipase activity.

4.2.3.3 Fatty acid amides

It has already been demonstrated that the FAAH inhibitors, MAFP and AA-5HT (Section 4.2.2) inhibit NEST phenyl valerate hydrolase activity and that NEST can hydrolyse 2-arachidonyl glycerol (2-AG). FAAH is an integral membrane enzyme that can hydrolyse 2-AG and the fatty acid family of endogenous signalling lipids (Cravatt et al., 1996; Maurelli et al., 1995; Goparaju et al., 1998). Representative fatty acid amides include the endocannabinoid anandamide (AE) and the sleep-inducing lipid oleamide (OE). As NEST was capable of hydrolysing 2-AG, anandamide and oleamide were tested as potential substrates for NEST, using the previous assay conditions (except for anandamide where Tris/HCl pH9.0 was used instead). Bee venom PLA2 was also assayed with the substrates for comparison with NEST under identical assay conditions. Anandamide (100 μ M) and oleamide could not be hydrolysed by either NEST or bee venom sPLA2 (Fig. 4.10a,b). Therefore neither NEST nor bee venom sPLA2 possess any fatty acid amide hydrolase activity.

4.3 GENERAL DISCUSSION

The homology between NTE and a calcium-independent phospholipase A2 provided a starting point for seeking the endogenous substrate for NTE and hence providing some insight into its physiological role. The five phospholipase inhibitors tested all caused inhibition of NEST phenyl valerate hydrolase activity, the most potent being MAFP; however, it is clear from the literature that all of these inhibitors are not selective for one particular enzyme. AACOCF3 and PACOCF3 showed IC50 values in the same range as the calcium independent iPLA2s. The 10-fold difference in potency between these two compounds revealed a preference of NEST for arachidonyl over palmitoyl. Both the canine myocardial iPLA2 (Hazen et al., 1990) and cytosolic cPLA2 (Dennis EA., 1994) show a preference for substrates containing arachidonic acid at the sn-2 position, whereas the P388D1 macrophage iPLA2 has a preference for palmitoyl over arachidonyl (Ackermann et al., 1994).

The combination of MAFP and BEL inhibition is usually used to distinguish between calcium-independent and calcium-dependent phospholipase A2. In the case of NEST, the IC50 of BEL is similar to that of iPLA2, but MAFP is 60-fold more potent against NEST than iPLA2. The inhibition of NEST by MAFP in the low nanomolar range shows a similarity between FAAH and NEST. NEST is also inhibited by arachidonylserotonin, a compound which has been used as a FAAH inhibitor. By contrast, PMSF is 170-fold more potent against FAAH than NEST.

Of particular interest is the inhibition of NEST by both PAF and lysoPAF, but not by AA-PAF or lysoPC. These results suggest that the structures of lysoPAF and PAF can be accommodated in the active site of NEST, but that of AA-PAF can not. AA-PAF differs from PAF in that the sn-2 group is arachidonyl rather than acetyl. Clearly in the presence of a hexadecyl group at the sn-1 position, an arachidonyl group at the sn-2 position can not fit into the active site, presumably due to steric hindrance. The difference between lysoPC and lysoPAF is subtler in that the sn-1 bond in PAF is an ether bond rather than an ester bond. A previous study by Yu et al. (1990) investigated the effect of several phospholipid analogues on phospholipase A2 activity. They demonstrated that increasing the hydrophobicity of the sn-1 functional group significantly enhanced the inhibitory potency of these amide phospholipid analogues. Therefore, as an ether bond at the sn-1 position of

lysoPAF is more hydrophobic than the ester bond found in lysoPC this may explain part of the difference seen in the inhibitory potencies of these two phospholipids on NEST PV-hydrolase activity. Another explanation is that NEST can hydrolyse the sn-1 ester bond in lysoPC, but not the sn-1 ether bond in lysoPAF. However, using TLC no hydrolysis could be detected when lysoPC was tested as a potential substrate.

The use of inhibitors is clearly limited, since in general, they are not highly selective for one enzyme. NEST does, however, show some similarities with both calcium-independent phospholipase A2 and fatty acid amide hydrolase. These findings provided a basis for choosing potential endogenous substrates. Several phospholipase A2 and FAAH substrates were tested, along with several other common lipid molecules. There was no evidence of PLA2 activity by NEST, using either phospholipids (AA-PC, AA-PI, DOPC) or a sn-1 alkyl ether phospholipid (AA-PAF). Likewise, NEST showed no evidence of hydrolytic activity against triacylglycerol, diacylglycerol or phosphatidic acid nor against the FAAH substrates anandamide and oleamide. The only hydrolytic activity observed was with 2-AG, indicating that NEST shows a monoacylglycerol lipase activity.

2-AG is an endogenous ligand for the cannabinoid receptors CB1 and CB2 (Devane et al., 1992). Recently, it was demonstrated that FAAH could hydrolyse 2-AG as efficiently as anandamide (Di Marzo et al., 1998; Goparaju et al., 1998). Monoacylglycerols, including 2-AG, are also hydrolysed by other enzymes, such as lipases and esterases (Tornqvist et al., 1976; Mentlein et al., 1984; Mentlein et al., 1985; Somma-Delpéro et al., 1995). A recent study by Goparaju et al. (1999) investigated the enzymes of porcine brain, which hydrolyse 2-AG. They identified an enzyme distinct from FAAH, which was principally responsible for the hydrolysis of 2-AG in porcine brain. This enzyme was present in both cytosolic and particulate fractions and could be inhibited by MAFP at very low nanomolar concentrations.

Di Marzo et al. (1998) also identified a 2-AG hydrolysing activity distinct from FAAH in neuronal- (N18TG2 cells) and basophil-like cells (RBL-2H3). This activity was found at highest levels in membrane fractions of (73.2 and 78.2% of total activity respectively). 2-AG and 1(3)-AG, which is derived from 2-AG following acyl migration, were hydrolysed by both cell types. In addition, 1mM Zn²⁺ and 1mM Cu²⁺ resulted in 75 and 80% inhibition of the 2-AG hydrolytic activity, respectively, whereas neither Mg²⁺ nor EDTA had any

effect. Earlier work on hen brain NTE by M.K. Johnson (1982) showed that 0.4mM Zn^{2+} and 0.22mM Cu^{2+} resulted in 80 and 65% inhibition of NTE PV-hydrolase activity, respectively, but again Mg^{2+} and EDTA had no effect. Although part of the 2-AG hydrolytic activity in N18TG2 and RBL-2H3 cells could be ascribed to FAAH, the remainder did not coincide with FAAH activity.

From the investigation into an endogenous substrate it can be concluded that NEST shows some monoacylglycerol lipase activity, when assayed with 2-AG as the substrate. It is therefore possible that NTE may catalyse the hydrolysis of 2-AG *in vivo*. However, whether this is indeed the true substrate for NTE is as yet unknown. There are certainly numerous enzymes, which are also capable of hydrolysing 2-AG, including FAAH and other monoacylglycerol lipases, which would suggest that if this is the physiological function of NTE then it is not an essential enzyme. These results do, however, provide a basis for investigating the physiological role of NTE in the future. Expression of full-length NTE in mammalian cells will provide a system for studying the role of NTE in lipid metabolism particularly in the context of cellular signalling.

PHOSPHOLIPID	SPECIFIC ACTIVITY (10⁶nmol/mg/min)	% DOPC ACTIVITY
DOPC	2.27 ± 0.001	100
PC	1.70 ± 0.015	75
PE + DOPC (1:3; w/w)	1.74 ± 0.025	76
PI	2.36 ± 0.041	104
PS	1.61 ± 0.028	71

Table 4.1: Phenyl valerate hydrolase activity of NEST reconstituted into DOPC, PC, PE + DOPC, PI and PS liposomes. Specific activities for each reconstituted sample and the percentage of activity relative to DOPC control are shown. Values are the mean of three experiments ± standard deviation. (PC from bovine brain (Sigma P6638); PE from bovine brain (Sigma P9137); PI from bovine liver (Sigma P2517) and PS from bovine brain (Sigma P6641)).

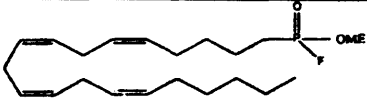
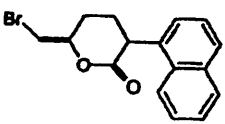
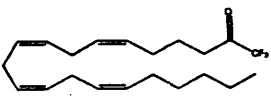
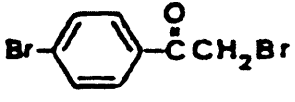
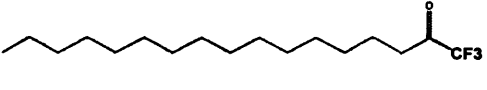
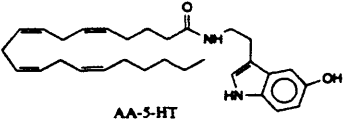
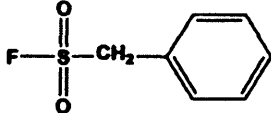
INHIBITOR	IC50 (μM)		
	NEST PV-ase	iPLA2	FAAH
 Methyl arachidonyl fluorophosphonate (MAFP)	0.002 ± 0.0009 (3)	0.125 ⁽³⁾	0.004 ⁽⁴⁾
 BEL	0.094 ± 0.02 (5)	0.03 ⁽¹⁾	0.4 ⁽⁶⁾
 Arachidonyl trifluoromethyl ketone (Arach-CF ₃)	2.5 (2)	22.5 ⁽²⁾	2.7 ⁽⁴⁾
 BPAB	4.43 ± 0.6 (3)	-----	-----
 PACOCF ₃	28 (2)	6 ⁽²⁾	-----
 AA-5HT	50 (1)	-----	18 ⁽⁵⁾
 PMSF	107 ± 38 (3)	-----	1.35 (4)

Table 4.2: IC₅₀ values (μM) for the action of inhibitors on NEST phenyl valerate hydrolase activity. Literature IC₅₀ values are also shown for comparison. Inhibition assays were carried out using duplicate samples for each concentration. Values shown are the mean ± standard deviation and the number of experiments is indicated in brackets. References: ⁽¹⁾ Balboa et al., 1997; ⁽²⁾ Ackermann et al., 1995; ⁽³⁾ Lio et al., 1996; ⁽⁴⁾ Deutsch et al., 1997; ⁽⁵⁾ Bisogno et al., 1998; ⁽⁶⁾ Beltramo et al., 1997. FAAH is fatty acid amide hydrolase and iPLA2 is calcium-independent phospholipase A2.

SAMPLE	[¹⁴ C]AA (%)
sPLA2	100
NEST	0.26 ± 0.1
CONTROL	0.45 ± 0.1

Table 4.3: Hydrolysis of 1-stearoyl-[2-¹⁴C]arachidonyl-phosphatidylinositol. Values were calculated using the amount of free [¹⁴C]arachidonic acid released by bee venom phospholipase A2 as 100%. Control samples omitted enzyme. Data shown are an average of three separate experiments ± standard deviation.

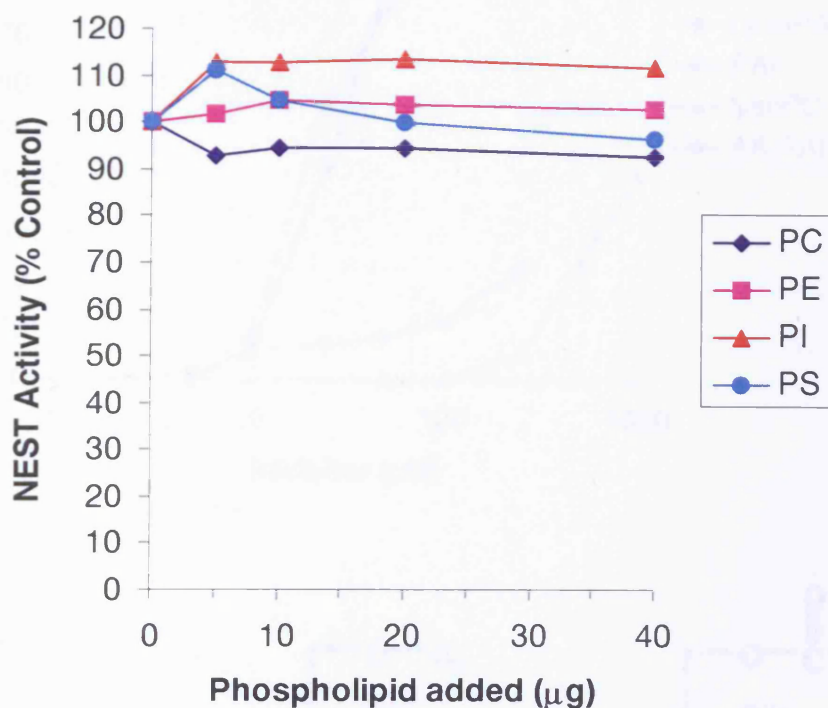


Fig. 4.1: Effect of phosphatidylcholine (PC), phosphatidylethanolamine (PE), phosphatidylinositol (PI) and phosphatidylserine (PS) on NEST PV-hydrolase activity. NEST liposomes were preincubated in 1.0ml with PC, PE, PI or PS (0-40µg) for 20min at 37°C before addition of the substrate phenyl valerate. After a further 20min incubation at 37°C, the amount of enzyme activity remaining was determined. Phospholipid stock solutions made up in Tris/EDTA buffer pH 8, were sonicated before adding to the assay. Data points shown are the mean of duplicate samples.

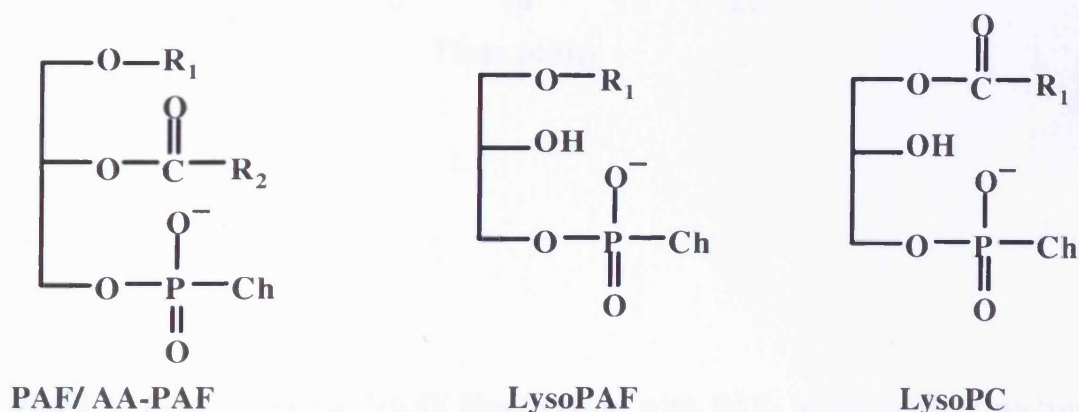
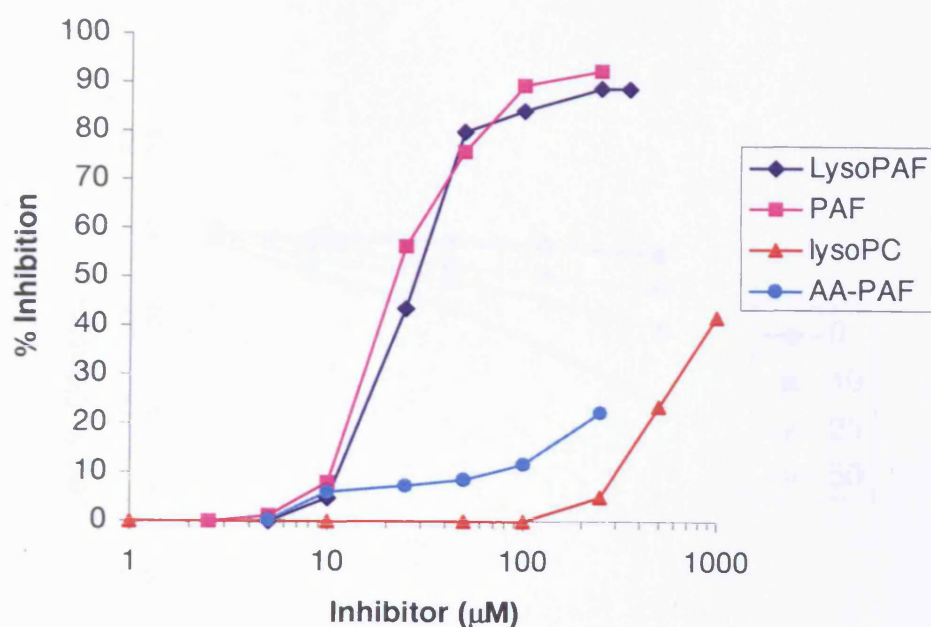


Fig. 4.2: Inhibition of NEST PV-hydrolase activity by PAF, lysoPAF, AA-PAF and lysoPC. NEST was preincubated with PAF in DMSO (0-250μM), lysoPAF in water (0-500μM), AA-PAF in DMSO (0-250μM), and lysoPC in water (0-1000μM) for 20min at 37°C. The substrate, phenyl valerate, was added to the reaction (final concentration = 1.4mM) and PV-hydrolase activity was measured after a further 20min at 37°C. The enzyme activity is plotted as the percentage of the control enzyme assayed in the absence of inhibitor. Data points are an average of duplicates. Structures are shown for PAF/ AA-PAF, lysoPAF and lysoPC, where R₁ = hexadecyl (C16:0), R₂ = acetyl for PAF; R₁ = hexadecyl, R₂ = arachidonyl (C20:4) for AA-PAF; R₁ = hexadecyl for lysoPAF; R₁ = oleoyl (C18:1) for lysoPC and Ch = choline.

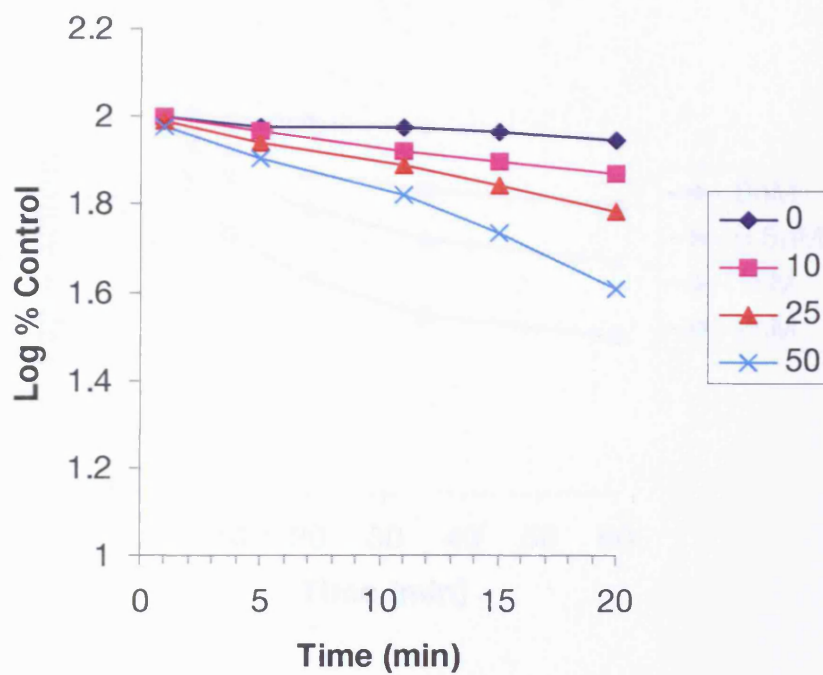


Fig. 4.3: Time-course of NEST inactivation with PAF. NEST was preincubated with 0, 10, 25, 50 μM MAFP for 1-20 min. Remaining NEST activity was measured after 20min incubation with phenyl valerate in 0.03% Triton X-100. Data points shown are an average of duplicate samples.

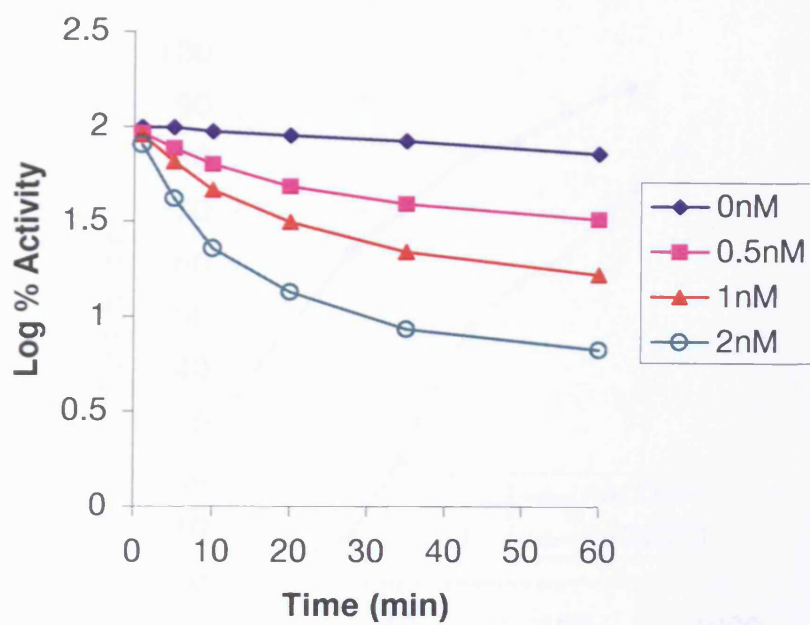


Fig. 4.4: Time-course of NEST inactivation with MAFP. NEST was preincubated with 0, 0.5, 1, 2nM MAFP for 1-60 min. Remaining NEST activity was measured after 20min incubation with phenyl valerate in 0.03% Triton X-100. Data points shown are an average of duplicate samples.

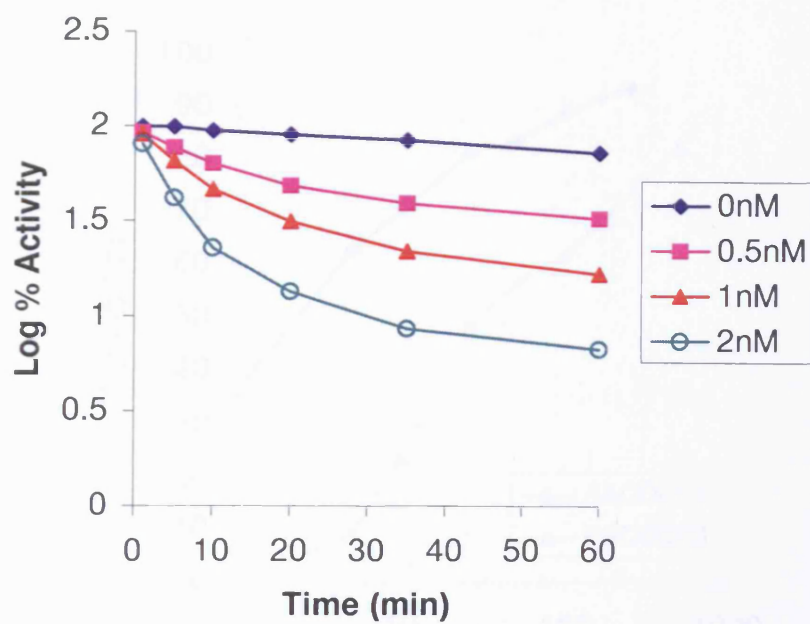


Fig. 4.4: Time-course of NEST inactivation with MAFP. NEST was preincubated with 0, 0.5, 1, 2nM MAFP for 1-60 min. Remaining NEST activity was measured after 20min incubation with phenyl valerate in 0.03% Triton X-100. Data points shown are an average of duplicate samples.

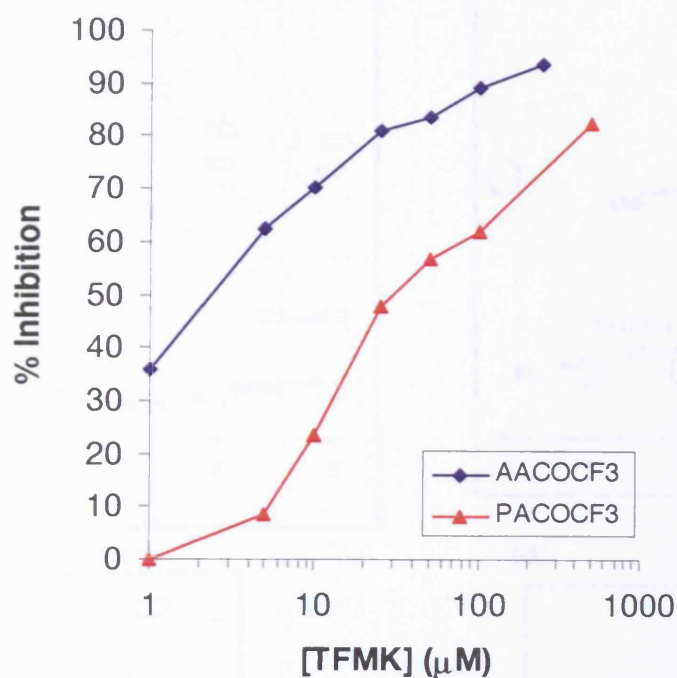


Fig. 4.5: Inhibition of NEST PV-hydrolase activity by the trifluoromethyl ketone analogues of arachidonic and palmitic acid. The enzyme activity is plotted as the percentage of the control enzyme assayed in the absence of inhibitor. Data points represent the average of duplicates.

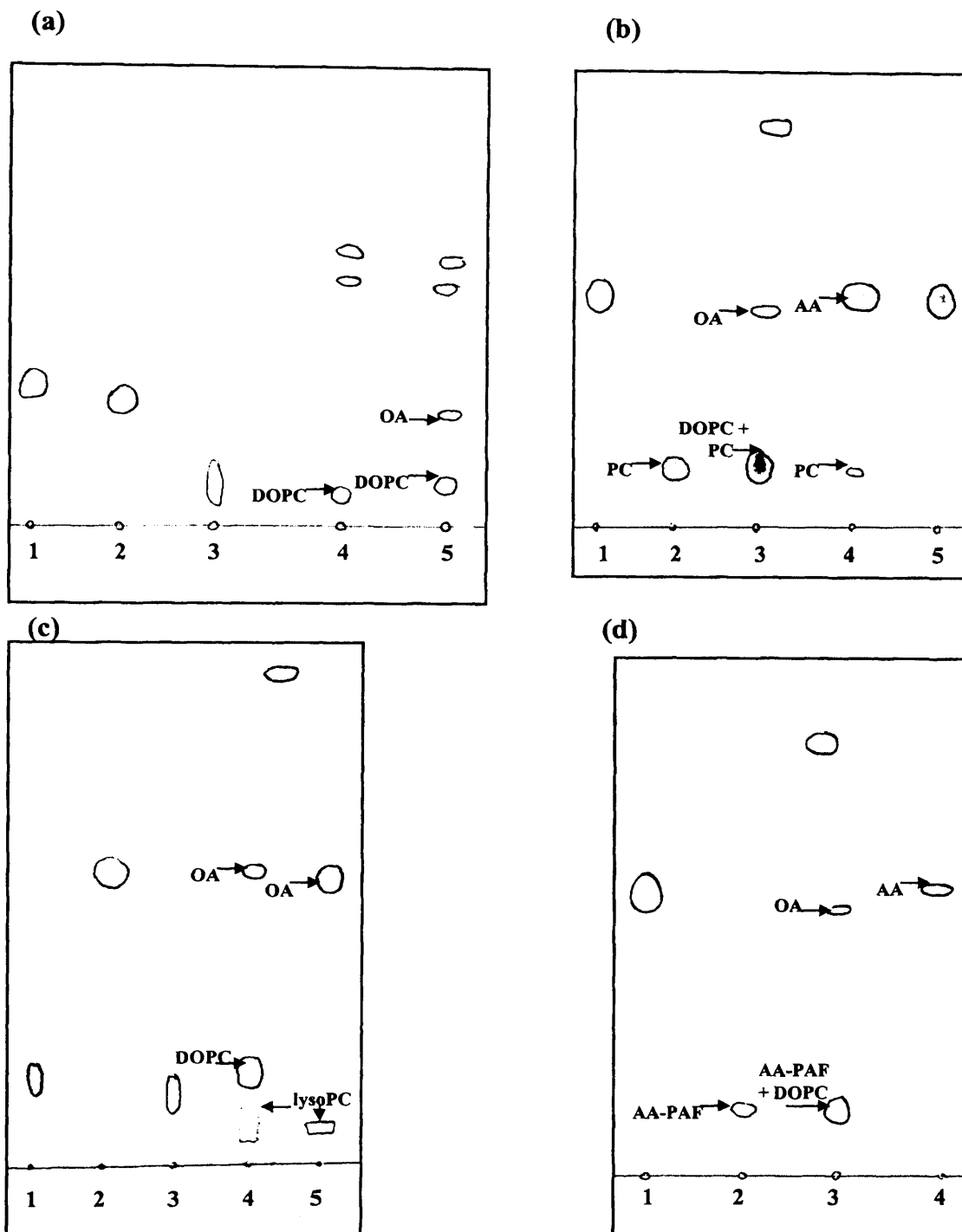


Fig. 4.6: TLC plates showing: (a) 10µg arachidonic acid (AA) (1), 10µg oleic acid (OA) (2), 10µg dioleoylphosphatidylcholine (DOPC) (3), serine mutant (S966A) lipid extract (4) and wild-type NEST lipid extract (5). (b) 10µg AA (1, 5), 100µM β -arachidonyl-phosphatidylcholine (AA-PC) (2), 100µM AA-PC + NEST (3), 100µM AA-PC + sPLA2 (4). (c) 10µg DOPC (1), 10µg OA (2), 100µM DOPC (3), 100µM DOPC + NEST (4) and 100µM DOPC + sPLA2 (5). (d) 10µg AA (1), 100µM arachidonyl platelet-activating factor (AA-PAF) (2), 100µg AA-PAF + NEST (3) and 100µg AA-PAF + sPLA2 (4). TLC plates were run in chloroform:methanol:ammonium hydroxide (80:20:2) and subsequently exposed to iodine vapours and the lipid spots circled.

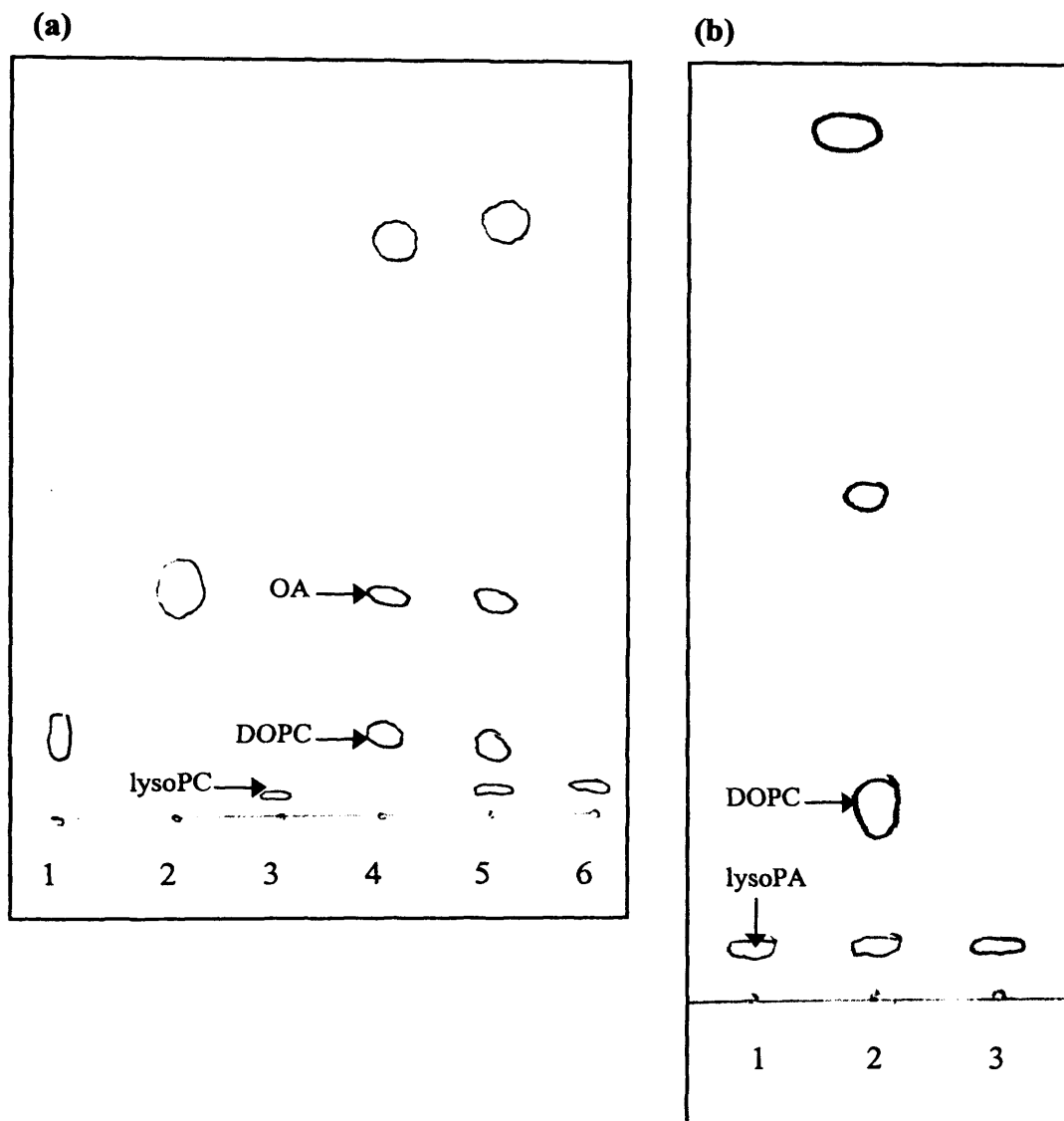


Fig. 4.7: TLC plates showing:

(a) 10 μ g DOPC (1), 10 μ g OA (2), 1mM lysoPC (3), NEST (4), 1mM lysoPC + NEST (5) and 1mM lysoPC + sPLA2 (6).

(b) 100 μ M lysoPA (1), 100 μ M lysoPA + NEST (2) and 100 μ M lysoPA + sPLA2 (3).

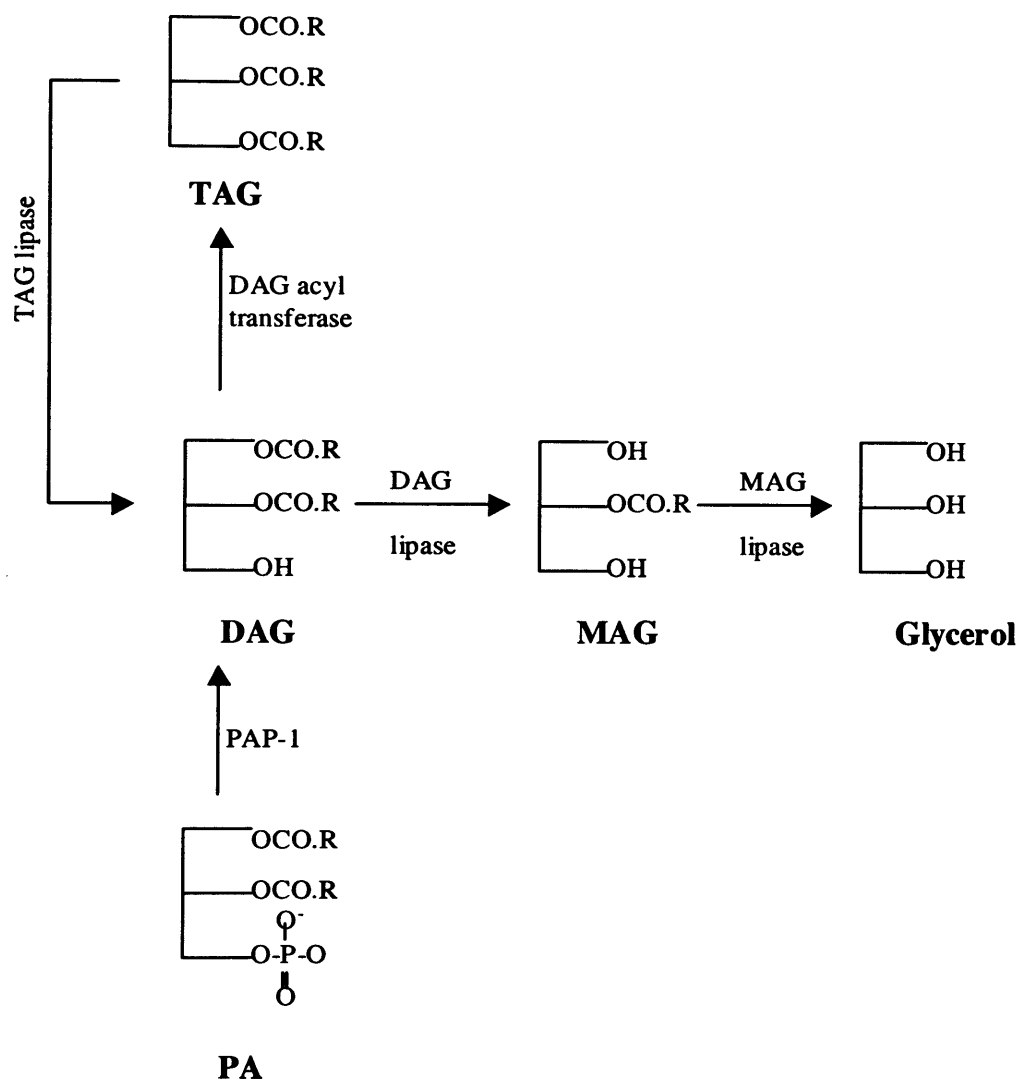


Fig. 4.8: Metabolism of diacylglycerol (DAG). Abbreviations used: triacylglycerol (TAG), monoacylglycerol (MAG), phosphatidic acid (PA) and phosphatidic acid phosphohydrolase (PAP-1).

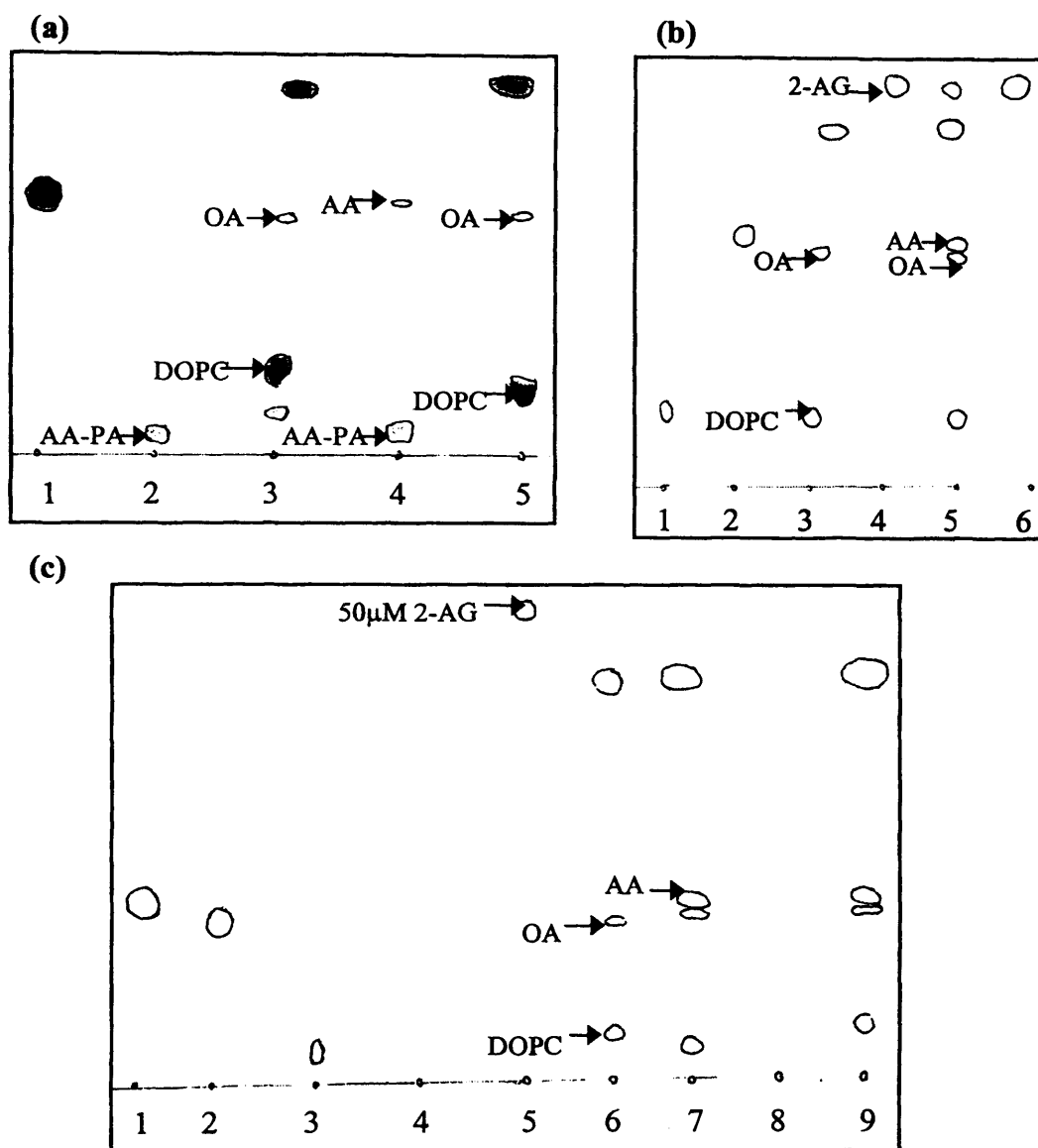


Fig. 4.9: TLC plates showing: (a) 10 μg AA (1), 100 μM arachidonyl phosphatidic acid (AA-PA) (2), 100 μM AA-PA + NEST (3), 100 μM AA-PA + sPLA2 (4) and NEST only (5). (b) 10 μg DOPC (1), 10 μg AA (2), NEST (3), 100 μM 2-AG (4), 100 μM 2-AG + NEST (5) and 100 μM 2-AG + sPLA2 (6). (c) 10 μg AA (1), 10 μg OA (2), 10 μg DOPC (3), 10 μM 2-AG (4), 50 μM 2-AG (5), 10 μM 2-AG + NEST (6), 50 μM 2-AG + NEST (7), 100 μM AEG (8) and 100 μM AEG + NEST (9).

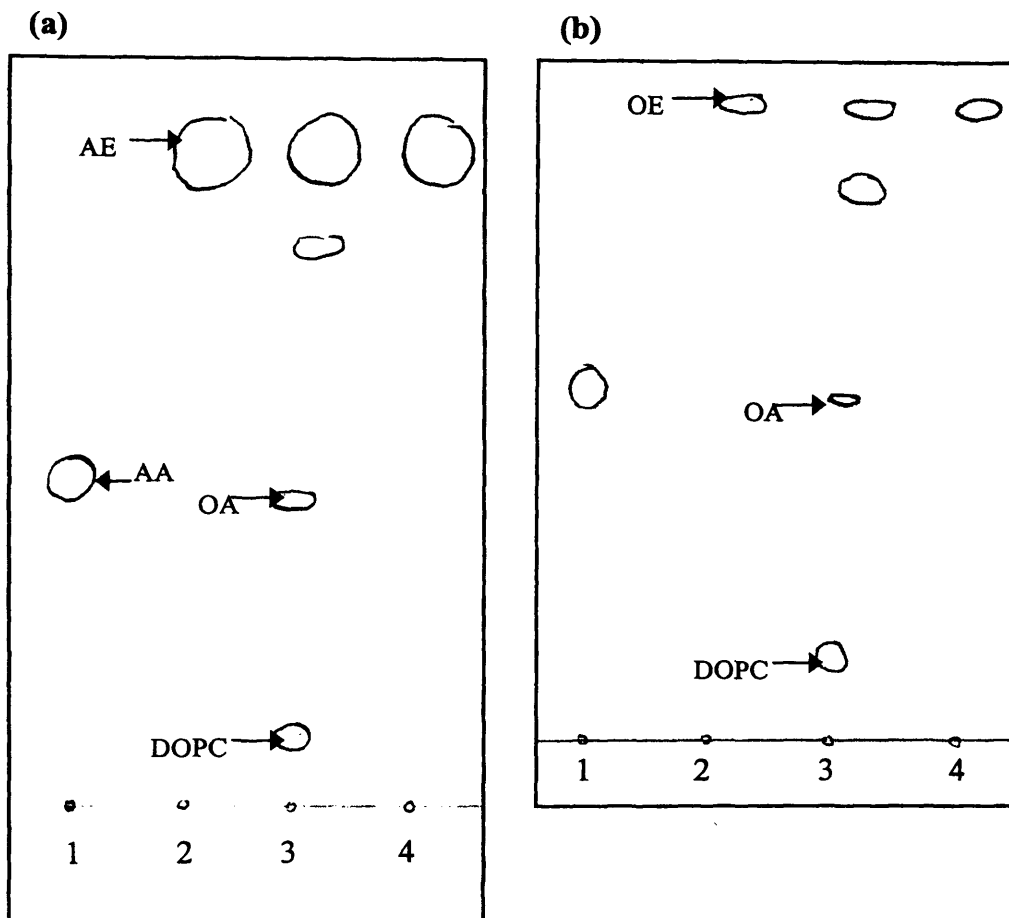


Fig. 4.10: TLC plates showing:

(a) 10 μ g arachidonic acid (1), 1 mM anandamide (AE) (2), 1 mM AE + NEST (3) and 1 mM AE + sPLA2 (4).

(b) 10 μ g oleic acid (1), 100 μ M oleamide (OE) (2), 100 μ M OE + NEST (3) and 100 μ M OE + sPLA2 (4).

CHAPTER 5: DISCUSSION

Neuropathy target esterase (NTE) has been extensively studied over the past thirty years and yet very little progress has been made towards understanding how inhibition and aging of NTE result in organophosphate-induced delayed neuropathy (OPIDN) or determining the physiological role of NTE in healthy neurones. One reason for the slow progress in this field was due to difficulties in isolating sufficient purified enzyme for characterisation studies. This is a problem encountered by many groups working on membrane-bound proteins, particularly those proteins which are found in very low abundance in native tissues.

5.1 DELINEATION OF THE RECOMBINANT NTE ESTERASE DOMAIN (NEST) AND COMPARISON WITH NATIVE NTE

The cloning of NTE was a major breakthrough, demonstrating that NTE belonged to a novel family of putative serine hydrolases. In addition, the ability to over-express NTE in various expression systems was now possible, allowing the production of large quantities of protein vital for any detailed biochemical and structural studies. Expression of the D16 cDNA clone in a mammalian expression system produced a 155 kDa recombinant protein with NTE-like catalytic activity, thus confirming that D16 encoded full-length NTE.

Using the *E. coli* expression system various constructs were expressed and the catalytic domain of human NTE, called NEST, was identified as residues 727-1216. NEST reacted covalently with the neuropathic organophosphate, diisopropylfluorophosphate (DFP) and hydrolysed the non-physiological substrate phenyl valerate in a similar fashion to native NTE. In addition, DFP-inhibited NEST was shown to undergo the aging reaction, which is essential for the initiation of OPIDN. NEST therefore provided a valid model for studying the physiological role of NTE and its role in the initiation of OPIDN.

5.2 RESIDUES INVOLVED IN CATALYSIS AND THE REACTION OF NTE WITH ORGANOPHOSPHATES

Using [³H]DFP labelling and site-directed mutagenesis several residues involved in catalysis and aging were identified. S966 was confirmed as the active site serine and aspartates, D960 and D1086, were shown to be critical for the esterase activity of NTE's catalytic domain. In chymotrypsin the active site serine is positioned 93 residues from the catalytic aspartate, whereas in OMPLA S144 is only 12 residues away from the catalytic asparagine. It is possible that due to the close proximity of D960 to S966, mutation of this residue results in a conformational change, which directly effects the orientation of S966. However, the possibility that D960 is involved in the catalytic triad can not be ruled out.

Mutagenesis also identified two histidines within NEST, H860 and H885, which, when mutated to alanine, significantly reduced the catalytic activity to below 1% of wild-type NEST. These findings accord with the observation that both diethylpyrocarbonate and bromophenacyl bromide inhibited NEST PV-hydrolase activity, and that at pH 6.0 PV-hydrolase activity was significantly reduced thus indicating that a histidine residue is essential for catalysis. One way to investigate which histidine is involved in the catalytic triad is to label NEST-containing liposomes with [¹⁴C]-*p*-bromophenacyl bromide (BPAB), digest with endoproteinase Glu-C and carry out Edman degradation. [¹⁴C]BPAB was used to successfully identify the histidine residue at the active site of pancreatic phospholipase A2 (Volwerk et al., 1974). H885 seems to be the more likely candidate for the catalytic triad since it is conserved in all of the members of this novel family of serine hydrolases. However, the loss of catalytic activity in the H885A mutant was significantly less (30-fold) than in the D960N and D1086N mutants, which suggested that catalytic triad of NTE might not contain a histidine residue. This has been found for two other serine hydrolases, fatty acid amide hydrolase and cytosolic phospholipase A2. However, as with the aspartate residues, a crystal structure for NEST will be required to determine which amino acids actually interact with S966 in the catalytic triad or dyad. The ability to purify large amounts of NEST and reconstitute catalytic activity provides the basis for starting crystallisation studies.

Aspartate, D1044, was identified as a residue to which an isopropyl group is transferred upon aging of DFP-inhibited NTE, and was therefore predicted to be site Z. However,

mutation of this residue resulted in an enzyme with the same aging characteristics as wild-type NEST. The results of the endoproteinase Glu-C digestion of [³H]DFP-labelled NEST suggested that both the active site serine and site Z were located between residues 955-1166. There are another 10 aspartate residues within this region, which could potentially act as an acceptor for the isopropyl group. Edman degradation of Band 6 demonstrated that no tritium was associated with D960. Therefore, this residue is not involved in aging of NTE. Mutation of D1004, however, resulted in an enzyme with only half the number of volatile counts as wild-type NEST, suggesting a role for this residue in the aging reaction. Whether D1086 plays a role in the aging reaction was not confirmed, as digestion of band 8 with trypsin did not yield any further information. However, the evidence obtained suggests that site Z is not a specific residue, but that several aspartates may be able to act as an acceptor for the isopropyl group transferred upon aging of DFP-inhibited NTE.

5.3 MEMBRANE-ASSOCIATION OF THE CATALYTIC DOMAIN OF HUMAN NTE

NTE is a 155 kDa integral membrane protein. Standard hydropathy analysis of the NTE protein sequence predicts only one transmembrane segment (TM1) at the N-terminus of the protein. TM1 is not present in the NEST protein and therefore NEST should be a soluble protein, according to this secondary structure prediction. TMPred analysis, however, predicts four transmembrane segments, TM1-4, within NTE, three of which are present in NEST.

Recombinant NEST was shown to be firmly associated with bacterial membranes and required detergent for solubilisation and during purification, which suggested NEST was an integral membrane protein. This was confirmed by using phase partitioning and proteinase K digestion experiments. NEST solubilised in Triton X-114 was shown to partition into the detergent-rich phase, which is a characteristic of an integral membrane protein. Proteinase K treatment demonstrated that a 24 kDa core of NEST was resistant to proteolysis even in the presence of detergent. In the absence of detergent no proteolysis could be detected, suggesting that there are no large loops exposed on the outside of the liposome. Using the T7 tag and His₆ tag antibodies, it was demonstrated that NEST inserts uni-directionally into DOPC liposomes, and that the N- and C-termini are either both

inside the liposome or folded within a hydrophobic portion of the protein. The fact that NEST in DOPC liposomes could not be visualised under the electron microscope supports the proteinase K data, as it also implies that neither the N- and C-termini nor any large polypeptide loops are exposed on the surface of the liposome.

The integral membrane properties of the NTE catalytic domain differ from many of the known eukaryotic serine hydrolases. An exception may be fatty acid amide hydrolase (FAAH); a serine hydrolase whose substrates include several neuromodulatory fatty acid amides and that has structural similarity to NTE. Analysis of the 579 amino acid sequence of FAAH predicts a type II membrane protein with a single transmembrane segment between residues 9-29 and a large cytoplasmic domain (Giang & Cravatt, 1997). However, a 30-579 mutant form of FAAH expressed in COS-7 cells showed the same membrane-associating properties as the wild-type protein with the N-terminal transmembrane segment (Patricelli et al., 1998). Therefore, residues 30-579 of FAAH contain regions that favour membrane association.

Having established that NEST was an integral membrane protein, various approaches were taken to determine the molecular organisation of NEST within the liposomes. Cross-linking studies were carried out using three different cross-linkers, but unfortunately these proved to be inconclusive. Treatment with glutaraldehyde led to a protection of catalytic activity against inactivation by detergent, but this protection could not be correlated to the formation of a specific oligomer. However, it was demonstrated that a monomer of NEST could bind [³H]DFP. Radiation inactivation experiments also supported the latter result, as the target size for NEST was found to be approximately 53 kDa. Therefore a monomer of NEST is sufficient for both hydrolysis of phenyl valerate and binding of [³H]DFP.

The fact that a monomer of NEST was catalytically active had implications for the structural predictions made using standard hydropathy analysis and the TMpred programme. In Chapter 3, it was demonstrated that NEST molecules could form a pore when incorporated into DOPC liposomes. If the TMpred prediction was correct and NEST contained only three transmembrane segments, with S966 located at the centre of TM4, then the only way NEST could conceivably form a transmembrane pore is by oligomerisation. No evidence was obtained to suggest oligomer formation is essential for

NEST's catalytic activity, therefore it seems unlikely that the TMpred programme can adequately explain the membrane-associating properties of NEST.

One explanation for the results obtained is that NEST forms a β -barrel structure within the membrane, as seen for the mitochondrial voltage-dependent anion channel (VDAC) and chloroplast outer envelope protein (OEP75). These pore-forming proteins consist of 16- or 18-stranded β -barrels. Outer membrane phospholipase A (OMPLA) of *E. coli*, a 27 kDa serine hydrolase, also forms a β -barrel structure with 12 antiparallel β -strands. Although, the β -barrel forms a transmembrane pore the N- and C-termini and three extracellular loops obstruct the pore function of this protein. The active site of OMPLA, which contains Ser144, His142 and Asn156, is located on the exterior of the β -barrel.

The 24 kDa resistant core present in NEST after proteinase K digestion could conceivably form a tightly packed β -barrel structure, which might explain the anomalous behaviour of NEST on gel filtration. Clearly, any structural predictions are only speculation and await the crystal structure of NEST. Fourier-transform infrared spectroscopy could be used to determine the α -helical and β -sheet content, but this would not yield any information on the tertiary structure of NEST.

5.4 WHAT IS THE PHYSIOLOGICAL ROLE OF NTE?

Research to date has focused on the toxicological significance of NTE, but the physiological role of NTE is still unknown. One clue as to the role of NTE came from studies of the *Drosophila* homolog, Swiss cheese (SWS). Flies containing a mutation in the *sws* gene display an age-dependent neurodegeneration, which is characterised by glial hyperwrapping of the neurones. Therefore, it may be possible that NTE also plays a role in signalling between neurones and glia.

Another possibility is that NTE plays a role in lipid metabolism. Changes in lipid metabolism have been implicated in the pathogenesis of OPIDN. Several studies carried out in the 1950's and 1960's investigated the effects of administration of organophosphates (TOCP, MIP, DFP) on the major classes of phospholipids in brain and sciatic nerve (Berry

& Cevallos, 1966; Joel et al., 1967; Sheltawy & Dawson, 1969). The results of these studies were very conflicting. Sheltawy and Dawson (1969) found no change in the lipid composition after TOCP treatment, whereas Berry and Cevallos (1966) maintained that the concentration of cholesterol esters was significantly increased in hen sciatic nerve after administration of TOCP. Interestingly, the level of palmitoyl (C16:0) monoglyceride was significantly reduced in degenerating chicken sciatic nerve, whereas the levels of the other monoglycerides and diglycerides measured were unaltered (Berry & Cevallos, 1966). Although many studies were carried out no specific alteration in lipid metabolism was ever correlated to OPIDN. The association of NTE and lipid metabolism arose again when a database search for proteins homologous to NTE revealed a low homology to a calcium independent phospholipase A2. NTE has been shown to prefer artificial substrates with large hydrophobic side chains (Johnson, 1975b), therefore, lipids are likely candidates as endogenous substrates for NTE.

Inhibitor studies with purified NEST in DOPC liposomes revealed certain similarities between NEST and two serine hydrolases, calcium independent phospholipase A2 and fatty acid amide hydrolase. However, the profile of inhibition by these inhibitors was different for all three serine hydrolases. Most of the inhibitors tested are not very specific and therefore it is difficult to draw any conclusions from these studies. However, the potent inhibition of NEST by MAFP and arachidonyl TFMK indicated a preference of arachidonyl over palmitoyl.

Preliminary investigations into identifying a possible endogenous substrate for NTE centred on substrates for phospholipases and fatty acid amide hydrolase. Of the substrates tested only 2-arachidonyl glycerol was hydrolysed by NEST, demonstrating that the catalytic domain of NTE has a monoacylglycerol lipase activity. Lysophosphatidylcholine was also tested as a substrate, but due to the limitations of the TLC method used in this study no hydrolysis could be observed. However, the fact that lyso-platelet-activating factor inhibited NEST PV-hydrolase activity and lysophosphatidylcholine did not, suggests that lysoPC is being hydrolysed by NEST. The only difference between lysoPC and lysoPAF is the bond at the sn-1 position, and although an ether bond is more hydrophobic than an ester bond, it is unlikely that this would account for the 500-fold difference seen in IC50 values. To confirm that lysoPC is a substrate for NTE it would be necessary to use a radiolabelled substrate, so that hydrolysis could be easily quantified.

In this study it has been shown that the catalytic domain of human NTE has monoacylglycerol lipase activity. In addition, NEST showed a preference for arachidonyl over palmitoyl and was potently inhibited by the arachidonyl binding site directed phosphorylation reagent, MAFP. Several other enzymes exist with monoacylglycerol lipase activity, including FAAH. Although it is possible that NTE may hydrolyse 2-AG *in vivo*, it may not be the true endogenous substrate for NTE. However, if 2-AG is the true substrate then it would suggest that NTE is not an essential enzyme, as several other enzymes could carry out its function. This is not the case, as preliminary results on the NTE knock-out mouse show that homozygotes died at embryonic day 9-12, suggesting a fundamental role for NTE during development (Moser & Buttner, unpublished).

Further work needs to be carried out to investigate the role of NTE in lipid metabolism. Expression of full length NTE in mammalian cells could be used to dissect out the pathways in which NTE is involved in the cell. A similar approach has been used successfully to determine the roles of various members of the phospholipase A2 superfamily in lipid metabolism.

Another avenue for further investigation is whether full-length NTE forms a transmembrane pore *in vivo*, and if this has any physiological significance. The observations in this study may have important implications for the long-sought mechanism of initiation of organophosphate induced delayed neuropathy (OPIDN). Covalent inhibition of NTE's esterase activity by itself is not sufficient to initiate neuropathy: A second reaction, termed aging, is also required. Therefore, modification of a property of NTE distinct from its esterase activity is the critical initiating event. The findings of the patch clamp studies have revealed a novel *in vitro* parameter (the open probability of a transmembrane pore formed by the catalytic domain of NTE), which is modified differentially by neuropathic and non-neuropathic covalent inhibitors of NTE. More speculatively, it is possible that alteration of transmembrane conductance in neuronal membranes containing organophosphate-modified NTE could provide a trigger for the subsequent pathological events.

Much more research must be carried out to elucidate the role of NTE in development and in the adult (if any). No NTE-like catalytic activity was detected in flies containing mutations in the *sws* gene (P. Glynn & D. Kretzschmar, unpublished), indicating that the

catalytic activity is crucial during development. Mutation of glycine 937 in NEST to aspartate also resulted in a loss of catalytic activity (data not shown). This single amino acid change is found in the *sws4* mutant in *Drosophila*, which results in the glial hyperwrapping phenotype. Clearly, NTE is crucial during the initial development of the mouse and a detailed histological study of NTE knock-out mouse embryos may provide clues to a function for NTE. Whether NTE has a role in the adult animal is unknown, but previous studies have shown that inhibition of NTE in the adult chicken for prolonged periods has no obvious effects *in vivo*.

Research on NEST has provided a tool to investigate the biochemistry of the catalytic domain and investigate potential substrates *in vitro*. Future work must now focus on the full-length protein to establish what role the N-terminal (regulatory) domain plays in modulating the enzyme activity of NTE. The N-terminal domain contains a region, which is homologous to the regulatory subunit of cAMP-dependent protein kinase A (PKA), therefore cyclic nucleotides may bind to this domain and regulate the catalytic activity. Interestingly, PKA has been implicated in glia-neurone interactions in vertebrates. Flies containing a mutation in the *sws* gene, show glial hyperwrapping of neurones, suggesting an involvement of the *sws* protein in signalling between neurones and glia. Clearly, if NTE also shares this function it might explain the severe effect of an NTE knock-out early on in development.

Finally it is interesting to look at the other members of this novel family of proteins, which all share a common C-terminal domain of 200 amino acids. All of the members, except YCHK, also show some homology to NTE upstream of this domain and would therefore be expected to have catalytic activity. Portions of the SWS, YOL4, YMF9 and *mtcy20B11* proteins, colinear with NEST, were expressed in *E. coli* (P. Glynn & Y. Li, unpublished). Both the SWS and YOL4 proteins showed some PV-hydrolase activity; however, neither YMF9 nor *mtcy20B11* had any catalytic activity. YCHK was also expressed in *E. coli* and showed no NTE-like PV-hydrolase activity. However, YCHK was shown to hydrolyse phenyl valerate and this activity was not sensitive to organophosphates. Therefore, although this family shares a significant homology within the C-terminal domain, it is possible that the substrate preferences for these homologs are different to that of human NTE. The study of the SWS protein from *Drosophila* and YMF9 protein from yeast may provide further clues as to the endogenous substrate and physiological role of this family of

proteins. Work has already started in this lab on the yeast homolog, YMF9. Hopefully together with the preliminary observations in this study, the yeast project and continuing research on NTE will help answer the most important question with regards to NTE: “What is the physiological role of NTE?” A greater understanding of the role of NTE in healthy neurones may also enable us to understand how inhibition and aging of NTE, which occurs within minutes, leads to the degeneration of the distal ends of large diameter axons in the peripheral nerve and spinal cord some 1-3 weeks after exposure to organophosphates.

CHAPTER 6: MATERIALS AND METHODS

6.1 MATERIALS

6.1.1 General chemicals and materials

All chemicals and reagents were purchased from Fisher or Sigma, unless otherwise specified. 1kb DNA molecular weight markers and X-Gal were supplied by Gibco-BRL and IPTG was obtained from Melford laboratories Ltd. (U.K.). Novex (R & D Systems Europe Ltd, Abingdon) supplied protein molecular weight markers, used for SDS-PAGE. Oligodeoxynucleotide primers used in PCR reactions and sequencing were made by the Protein and Nucleic Acid Chemistry laboratory (PNACL), University of Leicester and all sequencing services were provided by PNACL.

6.1.2 Organophosphates

Phenyl saligenin phosphate (PSP) and mipafox (MIP) were purchased from Oryza labs and all other organophosphates (OPs) were obtained from in-house stocks.

6.1.3 Radiochemicals

Tritiated di-isopropylfluorophosphate ([1,3-³H]DFP; 111 GBq/mmol) and 1-stearoyl-[2-¹⁴C]arachidonyl-phosphatidylinositol (740 MBq/mmol) were purchased from New England Nuclear (NEN).

6.1.4 Antibodies

The T7-Tag antibody was purchased from Novagen. The His₆ antibody and anti-mouse IgG (whole molecule) alkaline phosphatase conjugate were obtained from SIGMA.

6.1.5 Kits

The pTarget™ mammalian expression vector system was from Promega. QIAprep spin miniprep, QIAquick PCR purification, QIAquick gel extraction and plasmid midi-prep kits

were purchased from QIAGEN Ltd. (Surrey, UK). The PRISM™ Ready Reaction Cycle Sequencing kit was from the Perkin-Elmer Corporation. The QuikChange™ site-directed mutagenesis kit was obtained from Stratagene (U.K.).

6.1.6 Plasmids

The following plasmids were used during this PhD project: pBluescript plasmid pSKII(+/-) was purchased from Stratagene. pTarget™ vector and pET-21b(+) vector were purchased from Promega and Novagen, respectively.

6.1.7 Bacterial strains and growth media

The following *Escherichia coli* strains were used: XL10-Gold from Stratagene and BL21(DE3)pLysS from Cambridge Bioscience. XL10-Gold cells were used as a host for the pBluescript, pET and pTarget™ vectors. BL21(DE3)pLysS was used for the expression of the pET vector constructs. All bacterial stocks were stored at -20°C in the form of glycerol stocks, made by adding 0.6 ml overnight culture to 0.4 ml sterilised 75% glycerol. The following bacterial growth media were used: L-Broth. LB agar and NZY were obtained from core stocks. Supplements were added to the sterilised media, such as 100 µg/ml ampicillin, 20µl of 10% X-gal (w/v) and 20µl of 100mM IPTG.

6.1.8 Eukaryotic cells

All cells were obtained as frozen ampoules from liquid nitrogen storage. The eukaryotic cells, which have been cultured, are listed below.

CELL LINE	CELL TYPE
3T3 Swiss Albino	Mouse embryo fibroblast
CHO	Chinese hamster ovary
COS-7	Monkey kidney, SV40 transformed
HEK293	Hamster embryonic kidney
L35	Pig lymphocyte

6.1.9 Cell culture media and supplements

For eukaryotic cells α MEM, DMEM, RPMI 1640, 100mM sodium pyruvate and 50mM 2-mercaptoethanol were purchased from GIBCO BRL (Paisley, UK). PBS, FCS, penstrep, GLUTAMAX I and trypsin/EDTA were obtained from core stocks in-house.

All media and solutions used for tissue culture were prepared and handled under sterile conditions.

CELL LINES	MEDIUM	SUPPLEMENTS
CHO, HEK293 & COS-7	MEM Alpha with L-glutamine & 1000mg/ml D-glucose	10% FCS 1:50 Penstrep (optional)
L35	RPMI 1640 without L-Glutamine.	10% FCS 1mM Sodium pyruvate 50 μ M 2-Mercaptoethanol 2mM GLUTAMAX I
3T3	DMEM with L-Glutamine, 1000mg/ml D-Glucose, & sodium pyruvate	10% FCS 1:50 Penstrep

6.1.10 Serine hydrolase inhibitors

Arachidonyltrifluoromethyl ketone was purchased from BIOMOL research laboratories (Affiniti Research Products Ltd., U.K.). Methyl arachidonyl fluorophosphonate (MAFP) and arachidonylserotonin were purchased from Calbiochem[®] (U.K.). All other inhibitors were purchased from SIGMA.

6.1.11 Potential endogenous substrates

Lyso-Platelet activating factor (LysoPAF), platelet activating factor (PAF), arachidonylethanolamide (anandamide), N-oleoyl ethanolamine (oleamide), 2-arachidonyl glycerol (2-AG) and arachidonylethylene glycol (AEG) were purchased from Calbiochem[®]

(U.K.). 1-Stearoyl-2-arachidonyl-sn-glycerol (DAG) and 2-arachidonyl PAF were obtained from BIOMOL research laboratories. All other substrates were purchased from SIGMA.

6.2 GROWTH AND MAINTENANCE OF CELL CULTURE

6.2.1 Resuscitation of cells from frozen storage

Frozen cells were left at room temperature for 1min and immediately transferred to a 37°C water bath for 1-2 minutes until fully thawed. The ampoule was washed with 70% ethanol before slowly resuspending its contents in 10ml prewarmed media. The cells were pelleted by centrifugation at $200 \times g$ for 3 minutes, resuspended in 5-10ml media, transferred to a 25cm² culture flask and incubated at 37°C with 5% CO₂.

6.2.2 Subculturing of cell lines

Once the cells had reached confluence they were passaged. For adherent cell lines the media was removed and the cells washed with PBS. The monolayer was detached by adding Trypsin/EDTA (1x) and incubating at 37°C for 5-10 minutes. Cells were washed off using pre-warmed media and centrifuged at $200 \times g$ for 5min. The pellet was resuspended in pre-warmed media and the cells transferred to the required number of culture flasks. For suspension cell lines the media was removed (any cells adhered to the flask were detached by using a sterile cell scraper) and centrifuged at $200 \times g$ for 5min. Again the pellet was resuspended in prewarmed media and divided between culture flasks. Usually cells were split between 1:4 and 1:5 (NB. 3T3 cells were usually split 1:10).

6.2.3 Storage of cells

Confluent cells from a 75cm² flask were trypsinised and pelleted (for adherent cell lines) or just centrifuged (for suspension cell lines). The pellet was resuspended in 4ml freezing medium (10% DMSO in FCS), divided between 4 \times 1ml freezing vials and frozen in dry ice. Vials were placed in a -80°C freezer overnight and then transferred to a liquid nitrogen tank.

6.3 PROTEIN-RELATED METHODS

6.3.1 Protein concentration determination (Bradford method)

The Bio-Rad assay used for determination of protein concentration is a colorimetric assay based on the method of Bradford (1976). To obtain a standard linear plot 0, 2.5, 5, 7.5, 10, 12.5 and 15 μg BSA were pipetted into tubes in a final volume of 50 μl . Protein samples were made up in sterile water at various dilutions (1 \times , 2 \times , 5 \times , 10 \times) in a final volume of 50 μl . The dye concentrate reagent was diluted 6 \times with water, 1 ml was added to each tube and vortexed briefly. After 5 min at room temperature the absorbance at A_{595} was measured relative to the 0 μg protein standard. Using a plot of BSA absorbance values versus concentration of BSA, the concentrations of the protein samples were calculated.

6.3.2 One-dimensional SDS-polyacrylamide gel electrophoresis (SDS-PAGE)

6.3.2.1 SDS-PAGE (Laemlli)

Gel Solutions

Solution A	-	30% stock solution (w/v) acrylamide and bis-acrylamide (Scotlab)	
Solution B	-	1.5M Tris-HCl, pH 8.8	
Solution C	-	0.5M Tris-HCl, pH 6.8	
Solution D	-	10% SDS	
Solution E	-	10% APS	- prepared fresh
Solution F	-	TEMED	

Gel preparation

The choice of acrylamide concentration depends upon the molecular weight range of the proteins being studied. For example, NEST bacterial membranes or purified NEST (55 kDa) were examined on 12.5% SDS-PAGE, whereas native NTE (155 kDa) in chicken brain microsomes was examined on 7.5% SDS-PAGE. The following volumes (ml) of solutions A-F were mixed to give the percentage gel required.

SOLUTION	% ACRYLAMIDE		
	7.5	12.5	4 (STACK)
A	6.25	10.25	1.3
B	6.25	6.25	-----
C	-----	-----	2.5
D	0.25	0.25	0.1
E	0.125	0.125	0.05
F	0.013	0.013	0.01
H₂O	12.2	8.15	6.1

Solutions A, B, D and water were mixed and polymerisation was initiated by addition of APS (solution E) and TEMED (solution F). The resolving gel (7.5 or 12.5%) was poured into the gel cassette using a 10ml pipette until the level reached approximately 2cm from the top of the smaller plate. A small amount of butan-2-ol was layered over the top to exclude air and ensure the surface of the gel was level. After the resolving gel was set, the butan-2-ol was washed off with distilled water and excess water was absorbed with some filter paper (Whatman). The stacking gel was prepared by mixing solutions C, D and water, and polymerisation was initiated by addition of APS and TEMED. The gel was poured onto the resolving gel and a lane-forming comb was inserted.

Sample Preparation

One volume of 10% SDS-PAGE sample buffer (300mM Tris-HCl, pH6.8; 10% SDS, 10% glycerol, 10% DTT, 0.01% bromophenol blue) was added to 4 volumes of sample to give a final concentration of 2% sample buffer. Samples were boiled for 5min before loading onto the gel.

Gel Running Conditions

The gel was clamped into the Bio-Rad gel apparatus, the upper reservoir filled with SDS running buffer (25mM Tris, 190mM glycine, 0.1% SDS) and the lower reservoir was filled with sufficient buffer to cover the bottom of the gel. Samples were loaded into the wells using round gel tips. The gel was run at a constant voltage of 200V until the bromophenol blue dye front had just run out the end of the gel. The gel was then either stained using 0.25% Coomassie brilliant blue-R or transferred onto nitro-cellulose membrane (6.3.3.2)

6.3.2.1 Tricine-SDS-PAGE

Gel Solutions

Solution G	-	40% stock solution (w/v) acrylamide and bis-acrylamide (Scotlab)	
Solution H	-	3M Tris-HCl, pH 8.5; 0.3% SDS	
Solution I	-	glycerol	
Solution J	-	10% APS	- prepared fresh
Solution K	-	TEMED	

Gel preparation

To resolve polypeptide fragments produced by endoproteinase Glu-C digestion (6.8.5), 15% tricine gels were used. The following volumes (ml) of solutions G-K were mixed to give the stacking, spacer and resolving gels.

SOLUTION	STACKING GEL	SPACER GEL	RESOLVING GEL
G	1.2	1.8	6.1
H	3.1	2.5	5
I	-----	-----	1.6
J	0.1	0.025	0.05
K	0.01	0.0025	0.005
H₂O	8.2	3.2	2.3

The resolving gel was poured into the gel cassette until the level reached approximately 3cm from the top of the small plate. Butan-2-ol was layered on top and the resolving gel allowed to polymerise. The butan-2-ol was washed off and the spacer gel poured onto the resolving gel until the level reached 2cm from the top of the small plate. Again butan-2-ol was layered over the gel and the spacer gel was allowed to set. Finally the stacking gel was poured onto the spacer gel and a comb inserted.

Gel running conditions

Sample preparation was the same as for SDS-PAGE Laemlli. The tricine gel was run at a constant voltage of 100V for approximately 3 hours in running buffer containing 100mM Tris, 100mM tricine and 0.1% SDS. The gel was then either stained with 0.25% coomassie blue or transferred by Western blotting (6.3.3).

6.3.3 Western blot analysis

6.3.3.1 Solutions

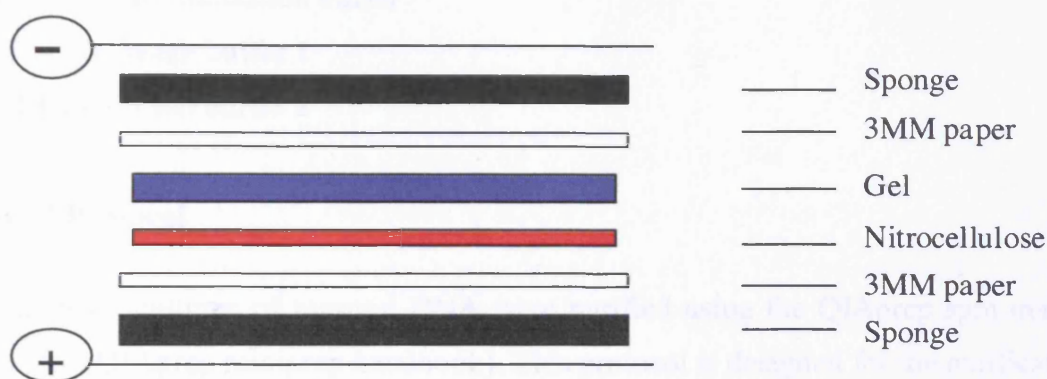
Transfer Buffer: 20% methanol, 25mM Tris, 190mM glycine.

TBST buffer: 10mM Tris, pH 8.0, 150mM NaCl, 0.1% Tween-20.

Alkaline phosphatase buffer: 0.1M Tris-HCl, pH9.5, 0.1M NaCl, 5mM MgCl₂

6.3.3.2 Transfer of SDS-PAGE gel onto nitro-cellulose or Immobilon membranes

Transfer onto nitro-cellulose was carried out according to the method of Towbin et al. (1979). Prior to blotting one sheet of nitro-cellulose, 2 sheets of Whatman 3MM chromatography paper and 2 sponges were soaked in transfer buffer. The Bio-Rad blotting apparatus was set up, as shown in the diagram below, and run at 100V for 60min. Transfer onto Immobilon membrane was identical except that the Immobilon membrane was soaked in methanol rather than transfer buffer. Once the transfer was complete the membrane was stained with 0.25% coomassie blue for 1-2 min, destained (in 50% methanol, 10% acetic acid) and dried between Whatman filter paper. The membrane was then given to PNACL to carry out N-terminal sequencing on individual polypeptide fragments.



6.3.3.3 Visualisation of proteins using an alkaline phosphatase conjugate

After transfer was complete the nitro-cellulose membrane was stained for 5min using 0.25% Ponceau S in 1% acetic acid and then rinsed with distilled water so that the molecular weight markers could be marked. The blot was incubated for 45min in 3% marvel in TBST in order to reduce any non-specific binding.

Primary antibodies were diluted, as required, in TBST and incubated with the blot (in a heat-sealed bag) for 2 hours at room temperature or overnight at 4°C. After washing (3 × TBST, 5min) the blot was further incubated with the secondary, alkaline phosphatase conjugated antibody (1:1000 dilution in TBST) for 1-2 hours. Washing was carried out as above and the blot developed using 50µl BCIP (16.5mg/ml in 100% DMF) and 50µl NBT (33mg/ml in 70% DMF) in 5ml alkaline phosphatase buffer.

6.4 ISOLATION AND PURIFICATION OF NUCLEIC ACIDS

6.4.1 Small scale preparation of plasmid DNA

6.4.1.1 Buffers supplied with QIAprep spin miniprep kit

Buffer P1: Resuspension buffer

Buffer P2: Lysis buffer

Buffer N3: Neutralisation buffer

Buffer PB: Wash buffer 1

Buffer PE: Wash buffer 2

6.4.1.2 Protocol

Small scale cultures of plasmid DNA were purified using the QIAprep spin miniprep kit protocol (QIAprep miniprep handbook). This protocol is designed for the purification of up to 20µg high-copy plasmid DNA from 1-5ml overnight cultures of *E. coli* grown in LB (Luria-Berani) medium, using a vacuum manifold. The overnight culture was centrifuged at 1,000 × g to pellet the cells, the pellet was resuspended in 250µl buffer P1 and transferred to a 1.5ml Eppendorf tube. An equal volume (250µl) of buffer P2 was added and the tube was inverted 4-6 times until the solution became viscous and slightly clear. Buffer N3 (350µl) was added and again the tube was inverted 4-6 times. The samples were then centrifuged at 10,000 × g for 10min at room temperature (microcentrifuge) before loading into the QIAprep spin miniprep columns, which were placed onto the vacuum manifold. The vacuum source was attached to the manifold and switched on to draw the solution through the column. The column was then washed with 0.5ml of buffer PB, followed by 0.75ml of buffer PE. To remove any excess wash buffer each column was transferred to a 1.5ml Eppendorf and centrifuged at 10,000 × g for 1min. The columns were transferred to fresh Eppendorfs, 50µl sterile water was added to each column and the DNA was eluted by centrifugation at 10,000 × g for 1min.

6.4.2 Medium scale preparation of plasmid DNA

6.4.2.1 Composition of buffers required for QIAGEN midiprep kit

Buffer P1: 100µg/ml RNase A; 50mM Tris-HCl, pH 8.0; 10mM EDTA. Stored at 4°C.

Buffer P2: 200mM NaOH; 1% SDS.

Buffer P3: 3.0M potassium acetate, pH 5.5.

Buffer QBT: 750mM NaCl; 50mM MOPS, pH 7.0; 15% ethanol; 0.15% Triton X-100.

Buffer QC: 1.0M NaCl; 50mM MOPS, pH 7.0; 15% ethanol.

Buffer QF: 1.25M NaCl; 50mM Tris-HCl, pH 8.5; 15% ethanol.

6.4.2.2 Protocol

Medium scale plasmid DNA preps were obtained using the QIAGEN midiprep protocol (QIAGEN plasmid handbook). This protocol is used for the purification of up to 100µg of double stranded DNA. To ensure high yields of pure DNA, 50ml overnight cultures were used. The cells were pelleted and resuspended in 4ml buffer P1. An equal volume (4ml) of buffer P2 was added to lyse the cells. After 5min at room temperature, 4ml of buffer P3 was added, the sample was mixed and incubated on ice for 15min. The sample was centrifuged at $20,000 \times g$ for 15min at 4°C and the supernatant removed immediately. The supernatant was applied to a QIAGEN-tip 100, which had been pre-equilibrated with 4ml buffer QBT. The tip was then washed with 2×10 ml buffer QC and the DNA eluted in 5ml buffer QF. The DNA was precipitated by the addition of 3.5ml isopropanol and the sample was centrifuged at $15,000 \times g$ for 30min at 4°C. The supernatant was removed, washed with 2ml 70% ethanol and recentrifuged. The pellet was allowed to air-dry for 5min and was resuspended in 200-300µl sterile water.

6.4.3 QIAquick PCR purification kit

6.4.3.1 Buffers provided with QIAquick kit

Buffer PB: Wash buffer 1

Buffer PE: Wash buffer 2

6.4.3.2 Protocol

This protocol (QIAquick spin handbook) is designed to purify single- or double-stranded PCR products (ranging from 100bp to 10kb) from primers, nucleotides, polymerases and salts using QIAquick spin columns in a microcentrifuge. Five volumes of buffer PB (250µl) was added to 1 volume of the PCR reaction (50µl). To bind the DNA the sample was applied to the QIAquick column and centrifuged at $10,000 \times g$ for 1min. The column was washed with 0.75ml buffer PE and recentrifuged. The column was placed in a fresh

Eppendorf and the DNA eluted by addition of 50 μ l sterile water and centrifugation for 1min.

6.4.4 QIAquick gel extraction kit

6.4.4.1 Buffers

Buffer QX1: Dissolves agarose gel pieces.

Buffer PE: Wash buffer

6.4.4.2 Protocol

This protocol (QIAquick spin handbook) is designed to extract and purify DNA of 100bp to 10kb from standard agarose gels in TBE buffer. The band of interested was excised from the agarose gel, weighed and dissolved in 3 volumes of buffer QX1 (100mg gel slice = 300 μ l QX1) for 10min at 50°C. Once the slice had dissolved completely 1 gel volume (100mg = 100 μ l) of isopropanol was added to the sample and mixed. The sample was applied to a QIAquick column and centrifuged at 10,000 \times g for 1min. The column was washed with 0.75ml buffer PE and the DNA eluted in 50 μ l sterile water.

6.4.5 Precipitation of oligodeoxynucleotide primers

Oligodeoxynucleotide primers used in PCR reactions and sequencing were made by the Protein and Nucleic Acid Chemistry Laboratory, University of Leicester and supplied in ammonia solution. Two volumes of 100% ethanol (800 μ l) and 1/10th volume of 2M potassium acetate (40 μ l) were added to 1 volume of the primer stock solution (400 μ l). The mixture was placed at -20°C for 30min and centrifuged at 10,000 \times g for 15min. The supernatant was aspirated off and the pellet was washed with 400 μ l cold 70% ethanol. The pellet was dried at 37°C for 15min and resuspended in 100 μ l sterile water.

6.4.6 Quantification of nucleic acid concentration by spectrophotometry

6.4.6.1 Double-stranded DNA

The concentration of DNA in aqueous solution was determined by measuring the absorbance of a dilution of the DNA solution in a quartz cuvette at 260nm. An aliquot of the DNA solution was diluted using sterile water (usually 100-fold, i.e. 5 μ l was added to 495 μ l water). The spectrophotometer was zeroed at 260nm using sterile water and the absorbance (A) of the diluted DNA solution was measured. The concentration of DNA was then calculated using the following equation:-

$$\text{dsDNA concentration } (\mu\text{g/ml}) = A_{260} \times \text{dilution} \times 50$$

Comparison of absorbance values at 260 and 280nm of a DNA solution provides an estimate of the purity of the preparation. A 260/280 ratio of approximately 1.8 for DNA indicates a protein free preparation, ratios significantly lower than these indicate protein contamination (Sambrook et al., 1989).

6.4.6.2 Oligodeoxynucleotide primers

The concentration of primers was determined using the following equation (Sambrook et al., 1989):-

$$\text{Primer concentration (pmol}/\mu\text{l}) = A_{260} \times \text{dilution} \times \frac{100}{1.5 N_A + 0.71 N_C + 1.2 N_G + 0.84 N_T}$$

where N is the number of residues of base A, G, C or T.

6.5 ENZYMIC MANIPULATION OF DNA

6.5.1 Restriction enzyme digestion

Restriction enzymes and their 10 \times reaction buffer were obtained from Stratagene. Digests were carried out according to the manufacturer's instructions. A typical digest contained

5 μ l DNA (\approx 0.5 μ g), 1.5 μ l 10 \times reaction buffer, 2 μ l restriction enzyme (\approx 20 Units) and 6.5 μ l sterile water in a final volume of 15 μ l. Reactions were incubated at 37 $^{\circ}$ C for periods ranging from 1 hour to overnight.

6.5.2 Polymerase chain reaction (PCR)

Cloned *pfu* polymerase, a proof-reading DNA polymerase, was used for all PCR reactions, as it exhibits a 6-fold lower error rate (1 in 767,000 nucleotides) than conventional thermostable enzymes (such as *Taq* polymerase). In addition, *Taq* polymerase can become denatured at 95 $^{\circ}$ C, whereas *Pfu* polymerase is very stable at this temperature. PCR amplification was carried out using a Perkin Elmer Thermal Cycler 480.

PCR reactions were carried out in a volume of 50 μ l containing 250 μ M of each dNTP, 1 μ M of forward and reverse primers, 50-100ng of template DNA, 5 μ l of 10 \times *pfu* buffer (200mM Tris-HCl, pH8.8, 20mM MgSO₄, 100mM KCl, 100mM (NH₄)₂SO₄, 1% Triton X-100, 1mg/ml nuclease free BSA) and 2.5U cloned *pfu* polymerase. PCR reactions were overlaid with 25 μ l mineral oil and cycled 30 times (denaturation at 94 $^{\circ}$ C for 40s, annealing at 58 $^{\circ}$ C for 1min30s, and primer extension at 72 $^{\circ}$ C for 1min30s). PCR amplification products were then analysed on a 1% agarose gel.

6.5.3 Dephosphorylation of linearised plasmid DNA

Calf intestinal alkaline phosphatase (CIAP, GIBCO) is a phosphomonoesterase purified from calf intestinal mucosa that hydrolyses 5'-phosphate groups from DNA, RNA and nucleotides. The linearised plasmid DNA (after restriction digest) was purified and eluted in 50 μ l sterile water (6.4.4). The dephosphorylation reaction was carried out by adding 5 μ l 10 \times CIAP buffer (500mM Tris-HCl, pH 8.5; 1mM EDTA) and 1 μ l CIAP (1 Unit) to 44 μ l of purified digested DNA. The reaction was incubated at 37 $^{\circ}$ C for 60min and the DNA purified using the QIAquick PCR purification kit (6.4.3).

6.5.4 Ligation protocol

T4 DNA ligase joins DNA fragments together by catalysing the formation of new bonds between phosphate residues located at the 5' termini of double-stranded DNA and adjacent 3'-hydroxyl moieties. When both strands of the plasmid vector carry 5'-phosphate residues, four new phosphodiester bonds are generated. However, when the plasmid DNA has been dephosphorylated, only two new phosphodiester bonds can be formed. In this case, the resulting hybrid molecules contain two single-stranded nicks that are repaired after the hybrids are introduced into competent bacteria (Sambrook et al., 1989).

A typical ligation reaction contained 50-100ng of vector DNA, 25-50ng insert DNA, 1µl 10 × ligase buffer, 1µl T4 DNA ligase (1 Unit) in a total volume of 10µl. Ligation reactions were incubated overnight at 4°C.

6.5.5 Transformation protocol

Supercompetent cells were thawed on ice for 5min and gently mixed. Next 40µl aliquots were placed into pre-chilled 15ml polypropylene tubes. Cells were incubated on ice for 10min before adding 3µl of ligation mix to the transformation reaction. The transformation reaction was mixed gently and incubated for a further 30min on ice.

For optimal transformation efficiency the transformation reactions were heat pulsed for 45s at 42°C (except for XL-10 Gold cells, which were heat-shocked for 30s) and returned immediately to ice for 2min. 0.36ml of prewarmed SOC was added to each reaction and incubated at 37°C for 1hr (shaking at 225-250 rpm).

Using a sterile spreader 80µl of each transformation reaction was spread onto separate LB-ampicillin agar plates (+/- IPTG/X-Gal). Plates were incubated overnight at 37°C and transformants picked. For selection of colonies containing pTarget + D16 blue-white colour screening was used. Approximately 60min before plating the transformations 20µl of 10% X-gal (w/v) and 20µl of 100mM IPTG were spread onto the LB-ampicillin plates. Colonies containing the correct insert are white due to the disruption of the lacZ gene,

whereas those without inserts are blue. DNA sequences were verified by carrying out sequencing reactions, which were submitted to PNACL.

6.5.6 Sequencing reactions

Sequence reactions were set up in thin-walled PCR tubes and were prepared according to the ABI PRISM™ terminator cycle sequence ready reaction kit protocol (Perkin-Elmer). For each reaction the following reagents were combined:-

Terminator ready reaction mix	8µl
Template (double-stranded DNA)	200-500ng
Primer	3.2pmol
Deionised water	
Total volume	20µl

The reaction was mixed well and centrifuged at $10,000 \times g$ (microcentrifuge) for 1min at room temperature. The mixture was overlaid with 40µl mineral oil and subjected to the following cycle sequencing protocol:-

Segment	Cycles	Temperature	Time
1	1	95°C	5min
2	2-26	95°C	30s
		50°C	15s
		60°C	4min
3	SOAK	4°C	-----

After temperature cycling the reactions were centrifuged to spin down the contents of the tube. Each sequencing reaction was carefully removed from below the mineral oil overlay and transferred to a clean 1.5ml Eppendorf tube containing 2.0µl 3M sodium acetate, pH

4.6 and 50µl of 95% ethanol. The tubes were vortexed, placed on ice for 10min to precipitate the extension products and centrifuged at $10,000 \times g$ for 30min. The supernatant was carefully aspirated off and the pellet was rinsed with 250µl of 70% ethanol. The samples were recentrifuged for 5min and the supernatant carefully aspirated off the pellet. The pellet was dried in a vacuum centrifuge (Savant DNA speed-vac 110) for 2min and the samples submitted to PNACL for sequencing.

6.5.7 Mutagenesis of NEST

Site-directed mutagenesis of NEST was performed using the QuikChange™ site-directed mutagenesis kit (Stratagene). Eighteen residues within the NEST construct were mutated: H757, H801, H860, H883, H885, H902, H916, H945, D960, S966, D1004, E1032Q, D1033, D1044, H1023, H1053, H1082 and D1086. All 11 histidines within NEST and the proposed active site serine (S966) were mutated to alanine. The five aspartates were mutated to asparagine and the glutamate to glutamine.

The QuikChange™ site-directed mutagenesis kit utilises a novel mechanism that only makes copies of the original template molecules, which means that each clone is a result of only one *in vitro* DNA replication cycle. The basic procedure uses double-stranded DNA and two synthetic oligonucleotide primers, each containing the desired mutation. The primers, each complementary to opposite strands of the vector, are extended during temperature cycling by the action of *pfu* polymerase. Temperature cycling generates copies of the plasmid by linear amplification, incorporating the mutation of interest. Next treatment with DpnI endonuclease is used to digest the parental DNA, resulting in selection of the synthesised DNA containing the desired mutation. The DNA isolated from almost all *E. coli* strains (including BL21(DE3)pLysS) is *dam* methylated and therefore susceptible to digestion by DpnI, but the DNA synthesised by *Pfu* polymerase is resistant to DpnI.

6.5.7.1 Mutagenesis primers**H757A**

(CAC)

F TG GAG CTG CAG GCC GCC CTG CAG GC
R GC CTG CAG GGC GGC CTG CAG CTC CA

H801A

(CAC)

F AG GAG GAT GCA GCC CGT ATC GTA CT
R AG TAC GAT ACG GGC TGC ATC CTC CT

H860A

(CAC)

F TA GTC CTG CTC GCC CGA GAG GAG GG
R CC CTC CTC TCG GGC GAG CAG GAC TA

H883A

(CAC)

F GG TGC TCG GGG GCC CTG CAC CTG CG
R CG CAG GTG CAG GGC CCC CGA GCA CC

H885A

(CAC)

F CG GGG CAC CTG GCC CTG CGC TGT CC
R GG ACA GCG CAG GGC CAG GTG CCC CG

H902A

(CAT)

F CT GCC AAG CTG GCT GAG CTC TAC GA
R TC GTA GAG CTC AGC CAG CTT GGC AG

H916A

(CAC)

F GC GCG GAC CGG GCC AGC GAC TTC TC
 R GA GAA GTC GCT GGC CCG GTC CGC GC

H945A

(CAC)

F GG GGC TGC TCG GCC ATC GGA GTA CT
 R AG TAC TCC GAT GGC CGA GCA GCC CC

D960N

(GAC)

F GGG GTC CCC GTG AAC CTG GTG GGC G
 R C GCC CAC CAG GTT CAC GGG GAC CCC

S966A

(TCC)

F GTG GGC GGC ACG GCC ATT GGC TCT T
 R A AGA GCC AAT GGC CGT GCC GCC CAC

D1004N

(GAC)

F GAA CCT GTG TTG AAC CTC ACG TAC C
 R G GTA CGT GAG GTT CAA CAC AGG TTC

H1023A

(CAT)

F AC CGC AGC ATC GCT CGG GTC TTC CA
 R TG GAA GAC CCG AGC GAT GCT GCG GT

E1032Q

(GAG)

F GAT AAG CAG ATT CAG GAC CTG TGG C
 R G CCA CAG GTC CTG AAT CTG CTT ATC

D1033N

(GAC)

F AAG CAG ATT GAG AAC CTG TGG CTG C
 R G CAG CCA CAG GTT CTC AAT CTG CTT

D1044N

(GAT)

F AAC GTG ACC ACA AAT ATC ACC GCC T
 R A GGC GGT GAT ATT TGT GGT CAC GTT

H1053A

(CAC)

F CC ATG CGA GTC GCC AAA GAT GGC TC
 R GA GCC ATC TTT GGC GAC TCG CAT GG

H1082A

(CAC)

F CC AAG GAC GGG GCC CTA CTC ATG GA
 R TC CAT GAG TAG GGC CCC GTC CTT GG

D1086N

(GAT)

F CAC CTA CTC ATG AAT GGC GGC TAC A
 R T GTA GCC GCC ATT CAT GAG TAG GTG

6.5.7.2 Mutagenesis reactions

Control and sample reactions were set up as shown below:-

<u>Control</u>	<u>Sample</u>
5 μ l 10 \times reaction buffer	5 μ l 10 \times reaction buffer
2 μ l control plasmid	1 μ l NEST pET construct (\approx 50ng)
1.25 μ l control primer #1	1.25 μ l forward primer (100ng/ μ l)
1.25 μ l control primer #2	1.25 μ l reverse primer (100ng/ μ l)
1 μ l dNTP mix	1 μ l dNTP mix
38.5 μ l H ₂ O	39.5 μ l H ₂ O
<u>1μl <i>pfu</i> Turbo</u>	<u>1μl <i>pfu</i> Turbo</u>
50 μ l	50 μ l

Each reaction was overlaid with 30 μ l of mineral oil and subjected to temperature cycling using the following cycling parameters:-

Segment	Cycles	Temperature	Time
1	1	95°C	30s
2	12-18	95°C	30s
		55°C	1min
		68°C	14min
3	SOAK	37°C	-----

After temperature cycling, 1 μ l DpnI restriction enzyme was added directly to each amplification reaction below the mineral oil overlay. Each reaction was mixed thoroughly by pipetting the solution up and down several times. The reaction mixtures were centrifuged at 10,000 \times g (microcentrifuge) for 1min and immediately incubated at 37°C for 60min to digest the parental (that is non-mutated) double-stranded DNA. The reactions were then transformed into Epicurian Coli XL1-Blue supercompetent cells using the transformation protocol described in section 6.5.5. The entire volume of each sample

transformation reaction was plated onto LB-ampicillin plates and incubated at 37°C for >16 hours. Only half of the control transformation reaction was plated onto a LB-ampicillin plate containing X-gal (20µl of 10%) and IPTG (20µl of 100mM IPTG).

The control reaction is used to demonstrate the effectiveness of the QuikChange site-directed mutagenesis kit. The pWhitescript™ 4.5 kb control plasmid contains a stop codon (TAA) at the position where a glutamine codon (CAA) would normally appear in the β-galactosidase gene. XL1-Blue supercompetent cells transformed with this control plasmid appear white on LB-ampicillin plates containing IPTG and X-gal, because the β-galactosidase (β-gal) activity has been obliterated. The oligonucleotide control primers create a point mutation that reverts the threonine residue of the stop codon back to a cysteine residue to produce a glutamine codon. Following transformation colonies containing the mutation will have the β-gal (blue) phenotype. The number of blue and white colonies on the control plate are counted and the mutagenesis efficiency (M.E.) is determined using the following equation:-

$$\text{M.E. (\%)} = \frac{\text{Number of blue colonies (cfu)}}{\text{Total number of colonies (cfu)}} \times 100$$

The mutagenesis efficiency was found to be approximately 90% for all mutagenesis experiments carried out. Colonies were picked from the transformation plates and minipreps were carried out to obtain DNA for sequencing. Each clone was sequenced to check for the correct mutation and positive transformants were subsequently transformed into the *E. coli* expression strain BL21(DE3)pLysS.

6.6 *ESCHERICHIA COLI* EXPRESSION

6.6.1 *E. coli* expression constructs

The following NTE constructs were generated using PCR, digested with BamHI and Sall and ligated into the pET-21b vector (Novagen). The pET vectors, initially developed by Studier and Moffatt (1986), allow expression of cloned genes under the transcriptional

control of a bacteriophage T7 promoter. Expression is initiated when a chromosomal copy of the T7 RNA Polymerase gene is induced, such as is present in the bacterial strain BL21(DE3)pLysS.

The BL21(DE3)pLysS strain contains a plasmid that expresses low levels of T7 lysozyme, a natural inhibitor of T7 RNA polymerase. The amount of T7 lysozyme produced by pLysS is sufficient to prevent transcription from the T7 promoter in the uninduced state, but too low to have a significant effect on transcription once T7 RNA polymerase expression is induced by IPTG. Thus toxic inserts are easier to establish in the BL21(DE3)pLysS host, but are still expressed at high levels.

The pET-21b vector contains unique BamHI and EcoRI cloning sites. These sites are preceded by a region, which encodes an eleven amino acid sequence derived from the amino terminus of the T7 gene-10 protein. Expression of sequences cloned into this site will produce a fusion protein, which initiates at the amino terminal methionine of the gene-10 peptide. A monoclonal antibody to the T7-tag allows detection of recombinant proteins using Western Blot analysis. The pET-21b vector also encodes a hexahistidine (His₆) tag, which is fused to the C-terminus of the recombinant protein, allowing both immunochemical detection using a His₆ monoclonal antibody and purification of recombinant proteins using nickel chelate chromatography.

All NEST constructs were transformed firstly into XL-10 Gold cells. Transformants were picked and checked for the correct insert by sequencing. Having identified positive transformants, plasmid DNA was isolated and transformed into the BL21(DE3)pLysS expression strain.

6.6.2 Oligonucleotide design

Oligonucleotide primers were designed to generate the various NEST constructs (see Fig. 2.3). Each forward primer consisted of 2 BamHI restriction sites, an extra nucleotide (G) and 21 nucleotides (7 amino acids) of the NTE cDNA sequence. The extra nucleotide was required to facilitate in frame cloning. Each reverse primer consisted of 2 SalI restriction sites and 21 nucleotides (7 amino acids) from the NTE cDNA sequence.

6.6.2.1 NEST forward primers**NEST-F**

Extra

BamHI BamHI nt A D R H S D F
 GGA TCC GGA TCC |G| GCG GAC CGG CAC AGC GAC TTC

NEST-2F

BamHI BamHI L T N P A S N
 GGA TCC GGA TCC |G| CTC ACC AAC CCA GCC AGC AAC

NEST-3F

BamHI BamHI Q M D F A I D
 GGA TCC GGA TCC |G| CAG ATG GAC TTC GCC ATC GAC

NEST-4F

BamHI BamHI L A T V A I L
 GGA TCC GGA TCC |G| CTG GCA ACT GTG GCA ATC CTG

NEST-6F

BamHI BamHI L N S D I I R
 GGA TCC GGA TCC |G| CTT AAC AGT GAC ATC ATC CGG

NEST-7F

BamHI BamHI A S A L D S I
 GGA TCC GGA TCC |G| GCC TCC GCA CTG GAT AGC ATC

NEST-8F

BamHI BamHI L P V C A E V
 GGA TCC GGA TCC |G| CTG CCT GTG TGT GCT GAG GTC

NEST-9F

BamHI BamHI P M V A F T L
 GGA TCC GGA TCC |G| CCC ATG GTG GCC TTC ACG CTG

NEST-11F

BamHI BamHI A I G P T L L
 GGA TCC GGA TCC |G| GCC ATC GGT CCG ACG CTA CTC

6.6.2.2 NEST reverse primers**NEST-3R**

Sall Sall (S-R-G-N-V-I-E)
 GTC GAC GTC GAC CTC AAT GAC GTT GCC ACG GCT

NEST-6R

Sall Sall (D-V-G-S-Q-D-E)
 GTC GAC GTC GAC CTC ATC CTG GCT CCC CAC GTC

NEST-7R

Sall Sall (A-D-I-A-R-S-M)
 GTC GAC GTC GAC CAT GCT GCG GGC GAT GTC CGC

6.6.3 Protein expression and purification

All constructs were expressed in the *E. coli* strain BL21(DE3)pLysS. All recombinant polypeptides had an N-terminal T7 tag for immunochemical detection and a C-terminal His₆ tag for affinity purification. Due to cloning problems NEST 4F/6R (encoding NTE 734-1116) could not be expressed.

6.6.3.1 Small-scale expression cultures

Glycerol stocks of the nine NEST constructs in BL21(DE3)pLysS were added to 10ml of L-broth containing 100µg/ml ampicillin and grown overnight at 37°C, shaking at 225rpm.

The overnight culture (2ml) was used to inoculate 18ml of L-broth (with antibiotic) and grown for approximately 45min or until the A_{600} was 0.5-0.7.

Expression was induced by the addition of 2mM IPTG and cultures were grown for a further 4-5 hours, after which the cells were harvested by centrifugation ($1,000 \times g$ for 20min at 4°C) and washed once with phosphate-buffered saline (PBS). Cell pellets were freeze-thawed and resuspended in 10ml TE pH 8.0. Cell lysates were then extracted for 30min at 4°C with either 8M urea plus 1% CHAPS or 1% CHAPS. To determine the solubility of the NEST constructs the extracts were centrifuged at $100,000 \times g$ for 60min at 4°C and the supernatants run on SDS-PAGE. Recombinant polypeptides were detected by Western blotting using the T7 tag antibody. Cell lysates were also tested for their NTE-like esterase activity using the phenyl valerate hydrolase assay (see Section 6.8.1).

6.6.3.2 Large-scale expression cultures

Cells transformed with the construct containing amino acids 727-1216, called NEST (for NTE-esterase domain), were cultured on a large scale for protein purification. The method was similar to that of 6.6.3.1 except a larger overnight culture ($2 \times 40\text{ml}$) was set up and used to inoculate $2 \times 400\text{ml}$ L-Broth containing $100\mu\text{g/ml}$ ampicillin. Again the expression culture was grown until the OD^{600} was 0.5-0.7 ($\approx 45\text{min}$) and induced using 2mM IPTG. Cultures were grown for a further 4-5 hours, cells were harvested by centrifugation at $1,000 \times g$ for 20min at 4°C and washed once with 100ml PBS. Pellets were stored overnight at -20°C prior to solubilisation and purification.

6.6.3.3 Solubilisation of NEST constructs

Preliminary investigations were carried out to determine the most suitable detergent for extraction of catalytically active NEST (NEST 2F/3R). NEST was incubated with 0.3% Triton X-100 (TX-100), 0.3% CHAPS and 0.5% sodium deoxycholate (DOC) for 120min at 4°C and centrifuged at $100,000 \times g$ for 60min at 4°C . The supernatants and pellets were run on SDS-PAGE followed by blotting onto nitrocellulose, and recombinant NEST was detected using the T7 tag monoclonal antibody. Using densitometry the percentage of NEST solubilised was determined. In addition, the supernatants and pellets were assayed

for their NTE-like esterase activity (Phenyl valerate hydrolase assay; 6.8.1) to determine the loss of activity, if any, upon solubilisation.

A large-scale expression culture (800ml) was used for purification of the NEST construct. Freeze-thawed cell pellets were extracted in 90ml Buffer A (50mM sodium phosphate buffer pH7.8, 0.5mM EDTA, 300mM NaCl) containing 2% CHAPS, for 90min at 4°C. The mixture was centrifuged at $100,000 \times g$ for 60min at 4°C in order to remove any insoluble material.

6.6.3.4 Purification on nickel resin

The resulting supernatant was adsorbed onto 4.5ml of nickel-nitrilotriacetic acid-agarose (Ni-NTA, QIAGEN) for 60min at room temperature. Ni-NTA agarose (QIAGEN) is composed of Nickel-nitriloacetic acid coupled to Sepharose[®], which offers high binding capacity and minimal non-specific binding. The NTA ligand can bind approximately 5-10mg of protein per ml of resin.

After centrifugation at $1,000 \times g$ for 10min at 4°C, the unbound material was removed and the resin washed three times with 15ml Buffer A containing 0.3 % CHAPS and 20mM imidazole. The low concentration of imidazole helps to reduce non-specific binding of proteins, which weakly interact with the resin. In order to elute the recombinant His₆ tagged protein the imidazole concentration was increased to 300mM. The protein was eluted by the addition of 3 x 10ml of Buffer A containing 0.3 % CHAPS and 300mM imidazole and the eluates were pooled.

6.6.3.5 Gel filtration chromatography

Gel filtration was performed with a 8mm × 30cm 300SW column (Nihon Waters Ltd.) using a HPLC system. The column was equilibrated for 60min at 0.25ml/min and run at 0.25ml/min in Buffer A containing 0.3% CHAPS and 1mM dithiothreitol (DTT). The column's void volume (≈ 5.6 ml) was determined using dextran blue (2000 kDa) and standardised using known molecular weight standards; β -amylase (200 kDa), bovine serum albumin (BSA, 66 kDa), carbonic anhydrase (29 kDa) and cytochrome c (Cyt c, 12.4 kDa).

Before loading the sample onto the gel filtration column the elution fractions were concentrated ($2 \times 15\text{ml}$) to approximately $0.5\text{-}0.75\text{ml}$ using a Vivaspin (Viva Science Ltd, Lincoln, UK) concentrator with a 30 kDa molecular weight cut-off (MWCO). The concentrated sample ($0.5\text{-}0.75\text{ml}$) was removed from the concentrator and centrifuged at $10,000 \times g$ for 5min to remove any precipitated protein. The samples were injected onto the column and 0.5ml fractions collected. Initially NEST-containing fractions were detected by Western blot analysis using the T7-tag monoclonal antibody and subsequently by Coomassie stained 12.5% SDS-polyacrylamide gels. The NEST-containing fractions were pooled and the amount of protein present was determined using the Bradford protein assay (6.3.1).

6.6.3.6 Functional reconstitution of recombinant NEST

As NEST activity was lost during solubilisation and purification it was necessary to reconstitute NEST back into lipid. Dioleoylphosphatidylcholine (DOPC), a synthetic phospholipid, was tested as it has been successful in previous studies. 0.2ml of DOPC stock solution (20mg/ml in chloroform) was placed in a glass vial, dried under a stream of nitrogen gas and resuspended in 0.3ml 50mM sodium phosphate buffer $\text{pH}7.8$ forming an opaque suspension. Solid CHAPS was added to this mixture until it became transparent (0.036g added \therefore 9% CHAPS final) and the volume was made up to 0.4ml with NaP buffer to give a 10mg/ml stock of DOPC.

Initially several lipid to protein ratios were tested ($1:2$, $1:1$, $2:1$, $3:1$, $4:1$, $6:1$ and $8:1$) to determine the most effective ratio for active reconstitution. Two controls were also carried out to ensure that neither protein alone nor DOPC alone had any effect upon phenyl valerate hydrolase activity (6.8.1). The samples were placed in Eppendorfs and mixed at room temperature for 3 hours .

After preincubation of the lipid/detergent and protein/detergent, the mixture was injected into a slide-a-lyzer dialysis cassette (Pierce) and dialysed against 1 litre of Buffer A with 1mM DTT. The buffer was changed daily for one week, after which samples were removed from the cassettes and assayed for their PV-hydrolase activity (6.8.1). These preliminary experiments established that a lipid to protein ratio of $3:1$ was the most effective. In addition, the number of days the samples needed to be dialysed was

investigated, by removal of aliquots from the cassette at 1, 2, 3 and 7 days. After 2 days dialysis the NTE-like catalytic activity was at its greatest, therefore a protocol of 2 days was used and the dialysis buffer was exchanged twice daily.

Purified NEST (at 0.21mg/ml) in 0.3% CHAPS and DOPC in 9% CHAPS were mixed at a lipid to protein ratio of 3 to 1 (w/w). The final CHAPS concentration was approximately 0.82%. After 3 hours the protein/detergent/lipid mixture was injected into dialysis cassettes (1-3ml capacity; 10,000 MWCO) and dialysed against 200 times the volume of Buffer A plus 1mM DTT.

6.7 MAMMALIAN EXPRESSION

6.7.1 Mammalian expression constructs

For mammalian expression the pTarget™ expression vector was used, which has several advantages, one being that it allows blue/white selection of transformants. The pTarget vector carries the human cytomegalovirus (CMV) immediate-early enhancer/promoter region to promote constitutive expression of cloned DNA inserts in mammalian cells and can therefore be used for transient or stable expression. The pTarget Vector also contains the simian virus 40 (SV40) enhancer and early promoter region upstream of the neomycin phosphotransferase gene. The SV40 early promoter contains the SV40 origin of replication, which will induce transient, episomal replication of the pTarget vector in cells expressing the SV40 large T antigen, such as COS-7 cells, as used in this study.

Because there are no ATG sequences in either the multiple cloning region or between the transcriptional start site and the multiple cloning region, an ATG for the initiation of translation ~~an ATG~~ had to be present in the inserted DNA. Full length D16 (4.5kb clone containing ATG start site) was subcloned into pTarget using NotI and XhoI restriction sites. Positive clones were identified using the blue/white selection and checked by sequencing (6.5.6).

6.7.2 Large scale transfections using Perfect™ lipids (Invitrogen)

Before starting the protocol plasmid DNA was required at a concentration of 1µg/ml in sterile water. (For a transfection using a 90mm dish, 29µg of DNA was required). Plasmid DNA was prepared using the QIAGEN midiprep kit (6.4.2).

Firstly COS-7 cells were seeded to obtain approximately 60% confluence by the following day (0.75×10^6 / 90mm dish). On day two lipid and DNA solutions were prepared at a lipid: DNA ratio of 6:1 (w/w). The appropriate amount of DNA and lipid were each mixed with 0.5ml serum-free medium and then combined to make 1ml of transfection mixture.

COS-7 cells were washed once with sterile PBS (14.5ml/90mm dish) and 1ml transfection mixture added to the cells along with the relevant volume of serum-free medium (13.5ml/90mm dish). After four hours incubation at 37°C, 5% CO₂ the transfection mixture was aspirated and replaced with the appropriate volume of complete medium (14.5ml/90mm dish). Cells were returned to the incubator for a further 48 hours and then assayed for expression of recombinant protein by Western blotting (6.3.3) and PV-hydrolase assay (6.8.1).

6.8 ENZYME-RELATED METHODS

6.8.1 Phenyl valerate hydrolase assay (Johnson, 1977)

NTE-like esterase activity was assayed as the paraoxon resistant (40µM) and mipafox sensitive (50µM) hydrolysis of phenyl valerate to phenol analysed colorimetrically (Johnson, 1977). All measurements were made in duplicate, therefore, 4 tubes were required for each test condition. To the first 2 tubes, 0.25ml of 160µM paraoxon (PXN) and 0.25ml of TE (50mM Tris-HCl/1mM EDTA, pH 8) (B Value) were added. To the second 2 tubes, 0.25ml of 160µM PXN and 0.25ml of 200µM mipafox (MIP) (C Value) were added. In the following stages tubes were vortexed well after each addition.

To all tubes 0.5ml of diluted enzyme-containing solution was added at 15sec intervals, transferring each tube to a 37°C water-bath. After 20min incubation 1.0ml of substrate (0.5mg/ml phenyl valerate in 0.03% Triton X-100) was added to each tube and incubated for a further 20min at 37°C. Finally 1ml of SDS/AAP and 0.5ml of potassium ferricyanide were added to all of the tubes. The colour was read at A_{486} after approximately 10min. For the non-enzymatic hydrolysis blank, the above procedure was followed except the addition of tissue was omitted. The tissue was added after SDS/AAP and before potassium ferricyanide. The A_{486} for the amount of colour due to NTE activity was calculated by subtracting the C value from the B value. To determine the rate of hydrolysis of phenyl valerate by NTE the following equation was used:-

$$\text{Rate of hydrolysis} = (A_{486}/E_m \times V/(v \times c \times t)) \times 10^6 \text{ nanomoles/ mg (or } 10^6 \text{ cells)/ min}$$

Where:- A_{486} = absorbance (B-C) due to NTE, E_m = Molar extinction coefficient (16,470 $M^{-1} \text{ cm}^{-1}$), V = assay volume (ml), v = volume of tissue added (ml), c = mg protein (or density of cells ($n \times 10^6$ cells/ ml)), t = time with substrate (min).

The standard PV-hydrolase assay (Johnson, 1977) was used to determine the NTE-like activity in transfected COS-7 cells and bacterial lysates of the various NEST constructs. However, for PV-hydrolase assays with paraoxon-treated NEST bacterial membranes and chicken brain microsomes (CBM), the B value was obtained by addition of 0.5ml TE buffer, pH8.0 to 0.5ml diluted tissue and the C value was obtained by addition of 0.5ml 100 μ M mipafox to 0.5ml diluted tissue. For PV-hydrolase assays with purified NEST in DOPC liposomes the differential assay, using paraoxon and mipafox, was not required. Therefore, only two tubes were required, which contained 0.5ml diluted tissue and either 0.5ml TE or 0.5ml inhibitor (2 \times required concentration). For all PV-hydrolase assays the tissue was diluted to give an A_{486} of approximately one. In general, bacterial lysates, CBM and NEST liposomes were diluted 250-500 fold, 25-50 fold and 10,000-fold, respectively.

6.8.2 Inhibition of NEST and NTE phenyl valerate hydrolase activity

6.8.2.1 Preparation of NEST-containing bacterial particulate fraction

An overnight culture containing 15ml L-Broth with 100 µg/ml ampicillin and 60 µl NEST glycerol stock was incubated overnight at 37°C. The following day 10ml of overnight culture was used to inoculate 50ml L-Broth + AMP and expression of recombinant NEST was induced with 2mM isopropyl-β-D-thiogalactopyranoside (IPTG). After 150min the cells were harvested by centrifugation at 1,000 × g for 10min at 4°C and the pellet resuspended in 10ml Tris/EDTA pH 8.0. The suspension was frozen at -80°C for approximately 60-90min and thawed at room temperature. Paraoxon (PXN) was added to give a final concentration of 160µM and the mixture was incubated at 37°C for 30min. The reaction was stopped by dilution with Tris/EDTA pH 8.0 and immediate centrifugation at 100,000 × g for 45min at 4°C (Beckman 70Ti rotor). The pellet was resuspended in 20ml of TE pH 8.0, using the Ultra Turrax T25 (small probe), and stored as 1ml aliquots at -80°C.

6.8.2.2 Chicken brain microsomes (CBM)

Six chicken brains (≈ 15g) were homogenised in 10 volumes of Tris/EDTA pH 8.0 (150ml), using an Ultra Turrax T25 homogeniser (large probe), and centrifuged at 9,000 × g for 10min at 4°C (Beckman JA17 rotor). The supernatant was carefully decanted before centrifuging at 100,000 × g for 45min at 4°C (Beckman 70Ti rotor). The pellet was resuspended in 5 volumes (75ml) TE pH 8.0, and incubated with 160µM paraoxon for 30min at 37°C. The reaction was stopped by dilution with TE pH 8.0 and immediate centrifugation at 100,000 × g for 45min at 4°C. The pellet was resuspended in 1.5 volumes TE pH 8.0 (22.5ml) and 1ml aliquots were stored at -80°C until further use.

6.8.2.3 Reaction with covalent inhibitors of NTE

Aliquots of NEST bacterial membranes and chicken brain membranes were incubated at 37°C for 20min, in the absence or presence of 50µM mipafox, with a range of concentrations of five covalent inhibitors of NTE. Subsequently, phenyl valerate (PV) was

added, and the samples were incubated for a further 20min at 37°C, after which the NTE-like esterase activity was determined from colorimetric assay of the phenol formed (Johnson, 1977). The five compounds tested were phenyl saligenin phosphate (PSP, 0-100nM), phenyl dipentylphosphinate (PDPP, 0-1µM), diisopropylfluorophosphate (DFP, 0-5µM), mipafox (MIP, 0-50µM) and phenylmethylsulfonyl fluoride (PMSF, 0-1mM). DFP, PDPP and PMSF stock solutions were made using dry dimethylformamide (DMF) as the solvent. PSP was made up in dimethylsulfoxide (DMSO) and MIP was made up in Tris/Citrate pH 6.0. Inhibitors were added in a volume of no greater than 10µl and the concentration of solvent present never exceeded 1%.

Phenyl valerate hydrolase assays carried out in the presence of increasing concentrations of DMF and DMSO revealed that enzyme activity is not significantly affected by DMSO (10% inhibition at 10% DMSO) but with concentrations of DMF greater than 1% activity was markedly reduced (70% inhibition at 10% DMF) (Fig. 6.1). The percentage inhibition was calculated by the following equation:-

$$\text{Inhibition (\%)} = \frac{[(A_{486} \text{ of control} - A_{486} \text{ of experimental}) \times 100]}{A_{486} \text{ of control}}$$

The values of percentage inhibition versus log of inhibitor concentration were plotted and the value for 50% inhibition (IC₅₀) was determined by inspection of the graph.

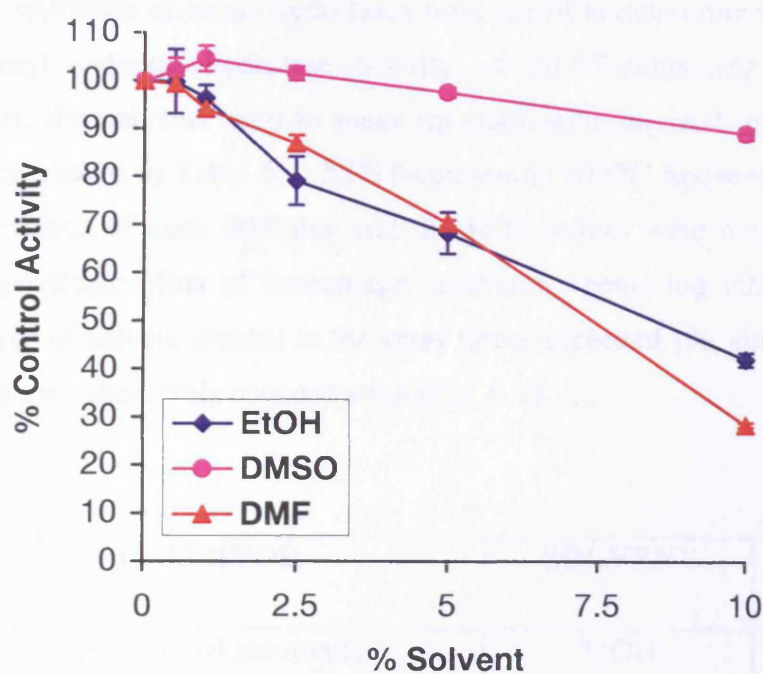


Fig. 6.1: Effects of solvents on NEST PV-hydrolase activity. NEST-containing liposomes were incubated for 20min at 37°C with various concentrations (0, 0.5, 1, 2.5, 5, 10%) of ethanol (EtOH), dimethylsulfoxide (DMSO) and dimethylformamide (DMF). Phenyl valerate was then added and the samples incubated for a further 20min at 37°C. The rate of phenyl valerate hydrolysis was determined according to the equation in section 6.8.1, and the percentage inhibition calculated relative to control (0% solvent).

6.8.2.4 Reaction of NEST-containing DOPC liposomes with serine hydrolase inhibitors

Several inhibitors of serine hydrolases were tested to determine whether they could inhibit the phenyl valerate hydrolase activity of NEST-containing DOPC liposomes. The inhibitors, the solvents used to make up stock solutions and the range of concentrations tested are shown in Table 6.1. NEST-containing DOPC liposomes were incubated with 8 concentrations of each inhibitor and the IC₅₀ values were determined by inspection of semi-logarithmic plots of percentage inhibition versus log inhibitor concentration. The percentage of solvent present in the assay never exceeded 1%, since both ethanol and DMF are inhibitory above this concentration (Fig. 6.1).

INHIBITOR	SOLVENT	RANGE
Arachidonyl serotonin (AA-5HT)	EtOH	0-100 μ M
Arachidonyl trifluoromethylketone (AACOCF ₃)	DMSO	1-250 μ M
Bromo-enol lactone (BEL)	DMSO	5-1000 nM
Bromophenacyl bromide (BPAB)	DMF	0.1-100 μ M
Diethylpyrocarbonate (DEPC)	DMF	0.01-5 mM
Methylarachidonyl fluorophosphonate (MAFP)	DMSO	0.5-50 nM
Phenylmethylsulfonyl fluoride (PMSF)	DMF	0.01-1mM
Palmitoyl trifluoromethylketone (PACOCF ₃)	DMSO	1-500 μ M

Table 6.1: Serine hydrolase inhibitors. A list of the compounds tested, the solvent used and the concentration range used are shown in the above table. Inhibitors were incubated with NEST liposomes for 20min at 37°C. Phenyl valerate was added and reactions were incubated for a further 20min at 37°C.

6.8.2.5 Reaction of NEST-containing DOPC liposomes with phospholipids

NEST-containing liposomes were incubated with various phospholipids (PC, PE, PI and PS) according to the method of Pope and Padilla (1989b). 100 μ l of phospholipid (10mg/ml stock solution in chloroform) was placed in a glass vial and the chloroform evaporated under a stream of nitrogen gas. The dried lipid was then resuspended in 10ml Tris/EDTA, pH 8.0 and sonicated with a small probe (10 \times 1s bursts). The phospholipids were tested at concentrations between 0-40 μ g/ml (\equiv 0-50 μ M).

Several other lipids were also tested to determine whether they could inhibit NEST PV-hydrolase activity. These included platelet activating factor (PAF), lyso-platelet activating factor (lysoPAF), arachidonyl-platelet activating factor (AA-PAF), lyso-phosphatidylcholine (lysoPC), anandamide (AE), and oleamide (OE). PAF, AA-PAF and AE were made up in dry DMSO. OE was made up in dry DMF, lysoPC was made up in ethanol and lysoPAF in water. NEST liposomes were incubated with PAF (0-250 μ M), lysoPAF (0-500 μ M), AA-PAF (0-250 μ M), lysoPC (0-1000 μ M), anandamide (0-250 μ M) and oleamide (0-250 μ M). LysoPC was not soluble in DMSO or DMF and therefore ethanol was used as a solvent. At the higher concentrations of lysoPC (500, 1000 μ M) the ethanol concentration was greater than 2.5% and therefore any inhibition seen at these concentrations was due to the effect of ethanol on NEST PV-hydrolase activity and not lysoPC. Solubility was a key problem when trying to test lipids as inhibitors. Most lipids are not soluble in DMF or DMSO and require either ethanol or detergent for solubilisation. Therefore the number of lipids tested as inhibitors was limited.

6.8.2.6 Radiation inactivation experiments

P. Glynn, L. Luthjens and M. Hom carried out all of the radiation inactivation experiments (n=4). NEST-containing DOPC liposomes were diluted in TE pH 8.0, containing 10% glycerol and 10mM DTT, to a concentration of approximately 20pmol NEST/ml. Glucose-6-phosphate dehydrogenase (G6PDH; *Leuconostoc mesenteroides*; Sigma) was included in the mixture at 25 units/ml as an internal standard. Aliquots (0.4ml) of the mixture were frozen in glass ampoules which were heat-sealed and subsequently subjected to varying doses of radiation at -135 $^{\circ}$ C as described previously (Schoonderwoerd et al., 1996). On opening, the air in the ampoules was purged with nitrogen, after which the samples were

thawed and assayed for NEST (phenyl valerate hydrolase) esterase activity (6.8.1) and G6PDH activity using a Sigma kit.

6.8.3 Oxime reactivation

Oxime reactivation experiments followed a previously described procedure (Meredith & Johnson, 1988). Paraoxon treated samples of NEST bacterial membranes and chicken brain microsomes were incubated for 20min with either 5 μ M DFP (20.5 μ l of 200 μ M), 5 μ M PDPP (20.5 μ l of 200 μ M) or solvent (20.5 μ l DMF) in a final volume of 800 μ l. At these concentrations of DFP and PDPP, approximately 90% of NTE-like activity was inhibited. The samples were diluted with TE pH 8.0 (3.0ml) to stop the reaction and centrifuged at 100,000 \times g for 60min at 4 $^{\circ}$ C (Optima TLA 100.4 rotor). The pellets were resuspended in 800 μ l TE pH 8.0, and 350 μ l was incubated with either 22mM potassium chloride (KCl, 2.5ml of 25mM) or 22mM 2-isonitrosoacetophenone (INAP, 2.5ml of 25mM) for 60min at 37 $^{\circ}$ C. After 60min the samples were placed on ice and 900 μ l cold TE pH 8.0 was added. Samples were centrifuged at 150,000 \times g for 30min at 4 $^{\circ}$ C and the pellets resuspended in 3ml TE pH8.0. Samples were diluted further in TE pH 8.0, if required, and assayed for NTE-like esterase activity, as described in section 6.8.1. The percentage reactivation in the presence of PDPP or DFP was determined using the following equation:-

$$\text{Percentage reactivation (\%)} = \frac{(A_{486} \text{ OP} + \text{INAP})}{(A_{486} \text{ of control})} \times 100$$

6.8.4 [3 H]DFP-labelling experiments

To determine the percentage volatile counts and catalytic centre activity of NEST and native NTE, CBM, NEST bacterial membranes and NEST-containing DOPC liposomes were incubated with 4.6 μ M [1,3- 3 H]diisopropylfluorophosphate at 37 $^{\circ}$ C for 60min. Preliminary experiments revealed that, under these conditions, reaction with [3 H]DFP was

complete by 20-40min, by which time phenyl valerate hydrolase activity was >95% inhibited. The reaction was stopped by addition of SDS sample buffer and boiling for 5min. Samples were run on 7.5% (for native NTE) and 12.5% (for NEST) SDS-polyacrylamide gels and the gels stained with Coomassie blue. Pieces of gel containing the 155 kDa and 55 kDa polypeptides (NTE and NEST respectively) were excised and agitated in 1.0ml 0.5M sodium hydroxide (NaOH) overnight at room temperature to liberate protein-bound tritium.

6.8.4.1 Volatilisable counts assay (Williams, 1983)

To determine the amount of [³H]isopropyl group adducted with site Z, equal aliquots of the NaOH eluate were counted, either directly (total) or after overnight freeze-drying to remove [³H]isopropyl alcohol (volatilisable). Each 1ml sample was divided into 2 × 400μl aliquots and 400μl glacial acetic acid added to each. One of the two samples was counted directly, after addition of 15ml scintillant (Packard Ultima Gold). The other sample was frozen at -80°C and freeze-dried overnight. This treatment results in the loss of the volatile counts from site Z. The freeze-dried sample was resuspended in 800μl water, 15ml scintillant added and the sample subjected to scintillation counting (Wallac 1410 liquid scintillation counter). The percentage of volatile counts was calculated by:-

$$\text{Volatile counts (\%)} = \frac{\text{Direct counts (DPM)} - \text{Freeze-dried counts (DPM)}}{\text{Direct counts (DPM)}} \times 100$$

6.8.4.2 Catalytic centre activity

An equal volume of acetic acid (1ml) was added to the NaOH eluate (1ml) and the amount of total radioactivity present in the sample was determined by liquid scintillation counting. The NTE-like PV-hydrolase activity was also determined for the same volume of CBM, NEST bacterial membranes and NEST liposomes used for the [³H]DFP-labelling experiment. For purified NEST-containing liposomes, the differential paraoxon and mipafox assay was not necessary, and activity was determined simply as phenyl valerate

hydrolysed in 20min at 37°C. The catalytic centre activity was determined using the following equation:-

$$\text{Catalytic centre activity (min}^{-1}\text{)} = \frac{\text{Phenyl valerate hydrolysed (pmoles/min)}}{[\text{}^3\text{H}]\text{DFP bound (pmoles)}}$$

6.8.5 Endoproteinase Glu-C digestion

To determine the locations of the active site serine and site Z, 500µl of NEST-containing liposomes was incubated with 4.6µM [³H]DFP for 60min at 37°C and centrifuged at 100,000 × g to remove excess DFP. The liposomes were resuspended in 60µl Tris/EDTA buffer pH 8.0, 0.1% SDS, and 2mM DTT and boiled for 5min. Endoproteinase Glu-C (10µl of 1mg/ml stock) was added at a NEST/Glu-C ratio of 10:1 (w:w) and incubated for 120min at 37°C. SDS-sample buffer (15µl) was added and the digest boiled before fractionating on a 15% tricine gel. Total and volatile counts were determined for individual polypeptide fragments in excised gel pieces as described in section 6.8.4.1. The N-terminal sequences of individual fragments were determined by Edman degradation after blotting the tricine gel onto an Immobilon membrane. To determine the individual residues labelled with tritium, aliquots from each cycle of Edman degradation were subjected to scintillation counting.

A trypsin digest was carried out in order to investigate residues within Band 8, which were labelled with tritium. The method used was essentially the same as described by Fernandez et al. (1992). Band 8 was excised from a PVDF blot (Immobilon) and washed twice with 0.5ml of 20% acetonitrile. The band was then incubated with 0.5ml polyvinylpyrrolidone (PVP40; 0.2% in methanol (w/v)) for 30min at room temperature and then washed thoroughly with distilled water (3 × 0.5ml) to remove any unbound PVP40. The membrane was cut into 1 × 1mm squares and incubated with 50µl digestion buffer (1% reduced TX-100; 10% acetonitrile; 100mM Tris-HCl, pH 8.0) and 5µl trypsin (100ng/µl) at 37°C for 24 hours. After 24 hours the digest was sonicated for 5min and the 50µl removed from above the membrane pieces. The membrane was washed once with digestion buffer (50µl) and

twice with 0.1% trifluoroacetic acid (50 μ l TFA). The extracts were pooled and freeze-dried overnight. A control reaction was also carried out in which 50 μ l digestion buffer was incubated with 5 μ l trypsin for 24 hours and subsequent treatments were the same as for the membrane digest. Both samples were given to PNACL and the digest and control trypsin sample were separated on reverse phase high performance liquid chromatography (RP-HPLC). Fractions collected from individual peaks on HPLC (Band 8) were divided into two and half the fraction was measured to determine whether any radioactivity was associated with the polypeptide fragment. Two fractions, which contained radioactivity above background, were given to PNACL for sequencing. However, the concentration of polypeptide present was insufficient to obtain any sequence information.

6.8.6 Proteinase K treatment

Proteinase K (PK) is a serine hydrolase, which has been used to study the membrane topology of several membrane-bound proteins (Raussens et al., 1997; Gorne-Tschelnokow et al., 1994). PK is a fairly non-specific protease but favours peptide bonds to the C-terminal side of aliphatic, aromatic and other hydrophobic residues.

NEST-containing DOPC liposomes (200 μ l) were diluted 4-fold in buffer A (50mM NaP, pH 7.8; 0.5mM EDTA; 300mM NaCl), buffer A containing 1% CHAPS, or buffer A containing 1% CHAPS and 1% SDS. At '0' time point 100 μ l from each reaction was transferred to a separate 1.5ml Eppendorf, 2 μ l 100mM PMSF and 25 μ l 10% SDS-sample buffer were added and the samples were immediately boiled for 5min. Proteinase K (PK) was then added to the reactions (20 μ l of 100 μ g/ml) to give a NEST:PK ratio of 35:1 (w/w). After 20, 60 and 210min, 100 μ l from each reaction was transferred to a 1.5ml Eppendorf and 2 μ l 100mM PMSF added to stop further digestion by PK. SDS-sample buffer (25 μ l) was added and the samples were immediately boiled for 5min. A control reaction was also set up in which 100 μ l of NEST-containing liposomes (diluted 4-fold) was added to 2 μ l 100mM PMSF and 25 μ l 10% SDS-sample buffer, followed by addition of 3.3 μ l PK. The sample was then boiled for 5min and run on 12.5% SDS-PAGE along with the 0, 20, 60 and 210min samples. Samples were also analysed by Coomassie blue

staining of 12.5% polyacrylamide gels and by Western blotting. Recombinant NEST was detected by probing the blots with either the T7 tag or the His₆ primary antibody.

6.8.7 Phase partitioning

Phase partitioning was carried out essentially as described by Bordier (1981). An equal volume of 2% Triton X-114 (in 20mM Tris-HCl, pH 8.0) was added to NEST-containing DOPC liposomes (200 μ l). The sample was incubated for 30min at 4°C, before centrifuging at 100,000 \times g for 45min at 4°C. The resulting supernatant (400 μ l) was layered onto buffered 6% sucrose (in 10mM Tris-HCl, pH 8.0; 150mM NaCl; 0.06% TX-114), warmed to 30°C for 5min and then centrifuged at 100 \times g for 5min. The aqueous layer was removed and received 0.5% fresh TX-114. The mixture was overlaid onto the sucrose cushion used previously, incubated at 30°C, and centrifuged. At the end of this separation, the aqueous layer and detergent layer were removed and transferred to separate Eppendorf tubes. TX-114 (2%) was added to the aqueous layer and the mixture was centrifuged at 100 \times g for 5min, to remove any residual detergent. The aqueous and detergent layers were diluted to give equal volumes and similar salt and detergent levels. SDS-sample buffer was added and samples were run on a 12.5% polyacrylamide gel.

6.8.8 Potential substrates

To investigate potential endogenous substrates for NTE, NEST-containing liposomes were incubated with various lipid substrates shown in Table 6.2. Due to the expense of radiolabelled substrates this preliminary investigation of potential substrates was carried out using unlabelled substrates (except for 1-stearoyl-[2-¹⁴C]arachidonyl-phosphatidylinositol). All of the substrates tested contained arachidonyl or oleoyl at the sn-1 or sn-2 position, to allow detection of the free fatty acid on thin layer chromatography (TLC) using iodine vapour. Iodine was used as it can detect fatty acids, which contain unsaturated carbon bonds.

Bee venom phospholipase A2 (sPLA2), a 14 kDa secretory phospholipase, was also incubated with the various substrates for comparison with NEST. A typical substrate reaction (100 μ l) contained 50 μ l NEST (0.15mg/ml) or 50 μ l bee venom sPLA2

(0.0375mg/ml), 5µl 1M Tris-HCl pH 8.0 (pH 9.0 for AE), 1µl 1M CaCl₂, 3µl 1% Triton X-100, 1 or 10µl substrate (10mM stock in EtOH) and sterile water (40 or 31µl). For control substrate reactions no NEST or sPLA2 protein was included to ensure that no non-specific hydrolysis was occurring during incubation. In addition a NEST protein control (no substrate) was included to determine the pattern of lipid spots present before substrate addition.

All reactions were incubated at 37°C for 30min, then 0.35ml ether/methanol/1M citric acid (30:4:1 by volume) was added to extract the lipids. The tubes were vortexed and centrifuged briefly in a microcentrifuge to separate the ether layer from the remaining mixture. The ether layer was then carefully removed from the surface and transferred to a fresh Eppendorf tube. The ether was evaporated under a stream of nitrogen gas and the lipids resuspended in 20µl ethanol.

A silica gel TLC plate (20 × 20cm; ALUGRAM[®] SIL G/UV₂₅₄ from Macherey-Nagel) was prepared by marking a line in soft pencil 2cm from the base of the plate. Individual circles were drawn on the line for each sample and the circles were positioned approximately 1.5cm apart. Standards of arachidonic acid, oleic acid and dioleoylphosphatidylcholine were made up in ethanol at a concentration of 10mg/ml. Standards (1µl) and samples (20µl) were applied to the plate by pipetting onto the individual circles and drying immediately with a hair dryer. For the samples, only 5µl was applied at a time, otherwise the spot became too diffuse and the lipids were not concentrated in a small, defined area.

Once all the samples had been applied the plate was lowered into a large TLC tank containing a mobile phase of chloroform/methanol/25% ammonium hydroxide (80:20:2 by volume). The plate was run for approximately 1 hour or until the solvent front was 2cm from the top of the TLC plate. The plate was removed, dried with a hair dryer and exposed to iodine vapours. After 30-60s the plate was removed and the lipid spots which were stained with iodine were circled in pencil. This is necessary as the iodine fades after several hours. Once the iodine had faded completely (1-2 days) the plates were scanned into Paint Shop Pro 6 and the images were stored as JPEG files.

COMMON NAME	ABBREVIATION
1-stearoyl-2-arachidonyl-phosphatidylcholine	AA-PC
1-stearoyl-[2- ¹⁴ C]arachidonyl-phosphatidylinositol	[¹⁴ C]AA-PI
dioleoylphosphatidylcholine	DOPC
1- <i>O</i> -hexadecy-2-arachidonyl-phosphatidylcholine	AA-PAF
lysophosphatidic acid, oleoyl	lysoPA
lysophosphatidylcholine, oleoyl	lysoPC
1-stearoyl-2-arachidonyl glycerol	DAG
triarachidonin	TAG
2-arachidonyl glycerol	2-AG
arachidonylethylene glycol	AEG
2-arachidonyl phosphatidic acid	AA-PA
arachidonylethanolamide (anandamide)	AE
N-oleoyl ethanolamine (oleamide)	OE

Table 6.2: Lipid molecules tested as substrates for NEST. A list of the physiological substrates tested and their abbreviations are shown. Stock solutions of all substrates were made up in ethanol.

6.9 ELECTROPHYSIOLOGY

6.9.1 Preparation of DOPC liposomes containing NEST and of giant liposomes

Wild-type and S966A mutant forms of NEST were expressed in *E. coli*, extracted, purified and incorporated into dioleoylphosphatidylcholine (DOPC) liposomes as described previously (6.6.3.6). The concentration of catalytically-active NEST in NEST-DOPC liposome preparations was determined by reaction with [³H]diisopropylfluorophosphate (DFP), SDS-PAGE, alkaline hydrolysis of the tritiated NEST adduct and scintillation counting as described previously (6.8.4). The amount of S966A mutant NEST in DOPC-liposome preparations was determined by comparison with wild-type NEST on Coomassie-stained SDS-PAGE.

The protocol used for the preparation of giant liposomes was essentially as described for analogous studies of the mechanosensitive channel of *E. coli* (Hase et al., 1995; Delcour et al., 1989). All aqueous solutions were sterile-filtered before use. An aliquot (approx. 5-15 μ l) of NEST liposomes containing 5 - 15 pmol of wild-type NEST (or an equivalent amount of S966A mutant NEST) was mixed with 1.0 ml of a suspension of 4.5 mg asolectin (Sigma P3644) and 0.5 mg cholesterol (Sigma C8667) in 5mM Hepes buffer, pH 7.4 with 2mM dithiothreitol (DTT). The mixture was frozen at -80°C , then thawed at room temperature to promote fusion of the liposomes. Aliquots (20 μ l) of the mixture were then dried on glass slides in a dessicator for 4-5 h at 4°C and subsequently rehydrated for 18 h at 4°C by addition of 20 μ l of Krebs buffer (100mM NaCl; 50mM KCl; 0.87 mM CaCl₂; 1mM EGTA; 5mM Hepes, pH 7.4). The giant multi-lamellar liposomes formed by this dehydration-rehydration cycle were harvested from the glass slide by pipetting, partially separated from small liposomes by low-speed centrifugation (600xg; 10min) and resuspended in Krebs buffer equivalent to half the volume of mixture originally pipetted onto the slide.

6.9.2 Patch-clamp recording experiments

Giant liposomes were prepared and given to P. Forshaw, who carried out all of the electrophysiological recordings. All patch-clamp experiments were carried out at room

temperature (20-25°C). A 20 μ l aliquot of giant liposome suspension was placed in the centre of a 60mm petri dish and diluted to a final volume of 2.5ml Krebs buffer. The dish of giant liposomes was mounted on the stage of an inverted microscope and the liposomes viewed using Hoffman modulation contrast optics. At this point an aliquot of MgCl₂ (1M) solution was added to give a dish concentration of 15 - 20mM; this manipulation resulted, within a few minutes, in the formation of unilamellar blebs on the surface of the giant liposome (Delcour et al., 1989) which readily formed gigaohm seals (10-50G Ω) when lightly touched with the tip of a micropipette. These pipettes were constructed from borosilicate glass (Drummond Scientific Co.) using a Kopf micropipette puller and had tip diameters of approximately 1 μ m; they were not fire-polished and had tip resistances of 10-15M Ω when filled with the same buffered solution as the bath. An Ag/AgCl electrode inside the patch pipette connected to the input of an Axopatch-1D patch-clamp amplifier; the circuit was completed by grounding the bath with a Ag/AgCl 'Driflo' reference electrode (Clarke Electromedical). Membrane voltages refer to the pipette side of the inside-out patch.

Currents from the patch-clamp amplifier were filtered by a 1kHz low pass filter then digitized (Digidata 1200, Axon Instruments) at 4kHz and stored on PC disc. Analysis of patch currents for fast gating (kinetic activity) and steady state current levels (DC only) and the construction of amplitude histograms were carried out using the PCLAMP 6 programmes (Axon Instruments). Patch holding potential (V_h) was set manually; most of the data were obtained using V_h set at +80 or +100mV, maintained at the set level for the duration of an experiment in order to minimise channel rundown. The V_h chosen for each patch was the minimum voltage that gave maximum conductance. By normal convention an upward deflection in the current response to a voltage step is regarded as an outward current.

Covalent inhibitors of NEST were dissolved in dry dimethylformamide (DMF) and an aliquot of the stock solution mixed externally with 0.5ml of patch-clamp solution; this solution was then added directly to the dish of liposomes using a fine hypodermic needle. The final concentration of DMF did not exceed 0.1% (v/v) which did not in itself change patch conductance or channel activity.

6.10 ELECTRON MICROSCOPY

NEST-containing DOPC liposomes were diluted in sodium phosphate buffer and 5 μ l was placed on a carbon-coated copper grid. The grids were glow-discharged immediately before sample application to ensure interaction of the protein molecules with the surface of the grid. The sample was left on the grid for approximately 1-2min and the grid was washed 4-5 times with sterile water and was finally placed on a droplet of 2% uranyl acetate for 1min. The grid was dried carefully with Whatman filter paper and placed in a grid box. The grids were then examined under a Philips electron microscope equipped with a lose-dose kit. Images were recorded on film (SO163; Eastman Kodak Co.).

REFERENCES

- Abou-Donia M.B. and Lapadula D.M. (1990) Mechanisms of organophosphorus ester-induced delayed neurotoxicity: type I and type II. *Ann. Rev. Pharmacol. Toxicol.* **30**, 405-440.
- Ackermann E.J., Conde-Frieboes K. and Dennis E.A. (1995) Inhibition of macrophage Ca^{2+} -independent phospholipase A_2 by bromoenol lactone and trifluoromethyl ketones. *J. Biol. Chem.* **270**, 445-450.
- Ackermann E.J., Kempner E.S. and Dennis E.A. (1994) Ca^{2+} -independent cytosolic phospholipase A_2 from macrophage-like P388D₁ cells. *J. Biol. Chem.* **269**, 9227-9233.
- Agawa Y., Lee S., Ono S., Aoyagi H., Ohno M., Taniguchi T., Anzai K. and Kirino Y. (1991) Interaction with phospholipid bilayers, ion channel formation, and antimicrobial activity of basic amphipathic alpha-helical model peptides of various chain length. *J. Biol. Chem.* **266**, 20218-20222.
- Aldridge W.N. (1995) Defining thresholds in occupational and environmental toxicology. *Toxicol. Lett.* **77(1-3)**, 109-118.
- Aldridge W.N. and Reiner E. (1972) Enzyme inhibitors as substrates, North-Holland Publishing Co., Amsterdam.
- Ashour M-B. and Hammock B.D. (1987) Substituted trifluoroketones as potent, selective inhibitors of mammalian carboxylesterases. *Biochem. Pharmacol.* **36**, 1869-1879.
- Atkins J. and Glynn P. (2000) The catalytic domain of human neuropathy target esterase: membrane association and critical residues. *J. Biol. Chem.* **275**, 24477-24483.
- Axelsen P.H., Harel M., Silman I. and Sussman J.L. (1994) Structure and dynamics of the active site gorge of acetylcholinesterase: Synergistic use of molecular dynamics simulation and X-ray crystallography. *Protein Sci.* **3**, 188-197.

Balboa M.A., Balsinde J., Jones S.S. and Dennis E.A. (1997) Identity between the Ca^{2+} -independent phospholipase A_2 enzymes from P388D₁ macrophages and Chinese hamster ovary cells. *J. Biol. Chem.* **272**, 8576-8580.

Balsinde J. and Dennis E.A. (1996a) Distinct roles in signal transduction for each of the phospholipase A_2 enzymes present in P388D₁ macrophages. *J. Biol. Chem.* **271**, 6758-6765.

Balsinde J. and Dennis E.A. (1996b) Bromoenol lactone inhibits magnesium-dependent phosphatidate phosphohydrolase and blocks triacylglycerol biosynthesis in mouse P388D₁ macrophages. *J. Biol. Chem.* **271**, 31937-31941.

Balsinde J., Diez E. and Mollinedo F. (1991) Arachidonic acid release from diacylglycerol in human neutrophils. Translocation of diacylglycerol-deacylating enzyme activities from an intracellular pool to plasma membrane upon cell activation. *J. Biol. Chem.* **266**, 15638-15643.

Battastini A.M.O., Emanuelli T., Koester L., Wink M.R., Benan C.D., Dias R.D. and Sarkis J.J.F. (1998) Studies of the anchorage of ATP diphosphohydrolase in synaptic plasma membranes from rat brain. *Intl. J. Biochem. & Cell Biol.* **30(6)**, 669-678.

Beltramo M., di Tomaso E. and Piomelli D. (1997) Inhibition of anandamide hydrolysis in rat brain tissue by (E)-6-(bromomethylene) tetrahydro-3-(1-naphthalenyl)-2H-pyran-2-one. *FEBS Lett.* **403**, 263-267.

Berends F., Posthumus C.H., Sluys I.V.D. and Deierkauf F.A. (1959) The chemical basis of the "ageing process" of DFP-inhibited pseudocholesterase. *Biochim. Biophys. Acta* **34**, 576-578.

Berry J.F. and Cevallos W.H. (1966) Lipid class and fatty acid composition of peripheral nerve from normal and organophosphorus-poisoned chickens. *J. Neurochem.* **13**, 117-124.

Bidstrup P.L., Bonnell J.A. and Beckett A.G. (1953) Paralysis following poisoning by a new organic phosphorus insecticide (mipafox). *Br. Med. J.* **1**, 1068-1069.

Bisogno T., Melck D., De Petrocellis L., Bobrov M.Y., Gretskaya N.M., Bezuglov V.V., Sitachitta N., Gerwick W.H. and Di Marzo V. (1998) Arachidonylserotonin and other novel inhibitors of fatty acid amide hydrolase. *Biochem. Biophys. Res. Commun.* **248**, 515-522.

Blow D.M. (1990) More of the catalytic triad. *Nature* **343**, 694-695.

Blow D.M. (1996) The tortuous story of Asp...His...Ser: structural analysis of α -chymotrypsin. *Trends Biochem. Sci.* **22**, 405-408.

Boger D.L., Sato H., Lerner A.E., Austin B.J., Patterson J.E., Patricelli M.P. and Cravatt B.F. (1999) Trifluoromethyl ketone inhibitors of fatty acid amide hydrolase: A probe of structural and conformational features contributing to inhibition. *Bioorg. & Med. Chem. Lett.* **9**, 265-270.

Bordier C. (1981) Phase separation of integral membrane proteins in Triton X-114 solution. *J. Biol. Chem.* **256**, 1604-1607.

Bordo D. and Argos P. (1991) Suggestions for "safe" residue substitutions in site-directed mutagenesis. *J. Mol. Biol.* **217**, 721-729.

Bouldin T.W. and Cavanagh J.B. (1979a) Organophosphorus neuropathy: I. A teased-fibre study of the spatio-temporal spread of axonal degeneration. *Amer. J. Pathol.* **94**, 241-252.

Bouldin T.W. and Cavanagh J.B. (1979b) Organophosphorus neuropathy: II. A fine-structural study of the early stages of axonal degeneration. *Amer. J. Pathol.* **94**, 253-270.

Bradford M.M. (1976) A rapid and sensitive method for the quantification of microgram quantities of protein utilising the principle of protein dye binding. *Anal. Biochem.* **72**, 248-254.

Brotherus J.R., Jost P.C., Griffith O.H. and Hokin L.E. (1979) Detergent inactivation of sodium- and potassium-activated adenosinetriphosphatase of the electric eel. *Biochemistry* **18**, 5043-5050.

Bugg T. (1997) An introduction to enzyme and coenzyme chemistry, Blackwell Science.
Carrington C.D. and Abou-Donia M.B. (1985) Characterization of [³H]di-isopropyl phosphorofluoridate-binding proteins in hen brain. *Biochem. J.* **228**, 537-544.

Carrington C.D., Fluke D.J. and Abou-Donia M.B. (1985) Target size of neurotoxic esterase and acetylcholinesterase as determined by radiation inactivation. *Biochem. J.* **231**, 789-702.

Chang F-C.T., Foster R.E., Beers E.T., Rickett D.L. and Filbert M.G. (1990) Neurophysiological concomitants of soman-induced respiratory depression in awake, behaving guinea pigs. *Toxicol. Appl. Pharmacol.* **102**, 233-250.

Chau L-Y. and Tai H-H. (1981) Release of arachidonate from diglyceride in human platelets requires the sequential action of a diglyceride lipase and a monoglyceride lipase. *Biochem. Biophys. Res. Comm.* **100(4)**, 1688-1695.

Chau L-Y. and Tai H-H. (1982) Resolution into two different forms and study of the properties of phosphatidylinositol-specific phospholipase C from human platelet cytosol. *Biochim. Biophys. Acta* **713**, 344-351.

Chemnitius J.M., Haselmeyer K.H. and Zech R. (1984) Neurotoxic esterase: Gel filtration and isoelectric focusing of carboxylesterases solubilized from hen brain. *Life Sci.* **34**, 1119-1125.

Clothier B. and Johnson M.K. (1979) Rapid aging of neurotoxic esterase after inhibition by di-isopropyl phosphorofluoridate. *Biochem. J.* **177**, 549-558.

Clothier B. and Johnson M.K. (1980) Reactivation and aging of neurotoxic esterase inhibited by a variety of organophosphorus esters. *Biochem. J.* **185**, 739-747.

Cravatt B.F., Giang D.K., Mayfield S.P., Boger D.L., Lerner R.A. and Gilula N.B. (1996) Molecular characterization of an enzyme that degrades neuromodulatory fatty-acid amides. *Nature* **384**, 83-87.

Creighton T.E. (1984) *Proteins: Structures and molecular properties*, W.H. Freeman and company, New York.

Criado M. and Keller B.U. (1987) A membrane fusion strategy for single-channel recordings of membranes usually non-accessible to patch-clamp pipette electrodes. *FEBS Lett.* **224**, 172-176.

Cruciani R.A., Barker J.L., Zasloff M., Chen H.C. and Colamonici O. (1991) Antibiotic magainins exert cytolytic activity against transformed cell lines through channel formation. *Proc. Natl. Acad. U.S.A.* **88**, 3792-3796.

Cygler M., Schrag J.D., Sussman J.L., Harel M., Silman I., Gentry M.K. and Doctor B.P. (1993) Relationship between sequence conservation and three-dimensional structure in a large family of esterases, lipases, and related proteins. *Protein Sci.* **2**, 366-382.

Daniels S.B., Cooney E., Sofia M.J., Chakravarty P.K. & Katzenellenbogen J.A. (1983) Haloenol lactones. *J. Biol. Chem.* **258**, 15046-15053.

Davis C.S. and Richardson R.J. (1987) Neurotoxic esterase: Characterization of the solubilized enzyme and the conditions for its solubilization from chicken brain microsomal membranes with ionic, zwitterionic, or nonionic detergents. *Biochem. Pharmacol.* **36**, 1393-1399.

De Geus P., van Die I., Bergmans H., Tommassen J. and de Haas G. (1983) Molecular cloning of *pldA*, the structural gene for outer membrane phospholipase of *E. coli* K12. *Mol. Gen. Genet.* **190**, 150-155.

Dekker N., Tommassen J., Lustig A., Rosenbusch J.P. and Verheij H.M. (1997) Dimerization regulates the enzymatic activity of *Escherichia coli* outer membrane phospholipase A. *J. Biol. Chem.* **272**, 3179-3184.

- Delcour A.H., Martinic B., Adler J. and Kung C. (1989) Modified reconstitution method used in patch-clamp studies of *Escherichia coli* ion channels. *Biophysical Journal*. **56**(3), 631-636.
- Dennis E.A. (1994) Diversity of group types, regulation, and function of phospholipase A₂. *J. Biol. Chem.* **269**, 13057-13060.
- Dennis E.A. (1997) The growing phospholipase A₂ superfamily of signal transduction enzymes. *TIBS* **22**, 1-2.
- Dentan C., Tselepis A.D., Chapman M.J. and Ninio E. (1996) Pefabloc, 4-[2-aminoethyl]benzenesulfonyl fluoride, is a new, potent nontoxic and irreversible inhibitor of PAF-degrading acetylhydrolase. *Biochim. Biophys. Acta* **1299**, 353-357.
- Dessen A., Tang J., Schmidt H., Stahl M., Clark J.D., Seehra J. and Somers W.S. (1999) Crystal structure of human cytosolic phospholipase A₂ reveals a novel topology and catalytic mechanism. *Cell* **97**, 349-360.
- Deutsch D.G., Omeir R., Arreaza G., Salehani D., Prestwich G.D., Huang Z. and Howlett A. (1997) Methyl arachidonyl fluorophosphonate: A potent irreversible inhibitor of anandamide amidase. *Biochem. Pharmacol.* **53**, 255-260.
- Devane W.A., Hanus L., Breuer A., Pertwee R.G., Stevenson L.A., Griffin G., Gibson D., Mandelbaum A., Etinger A. and Mechoulam R. (1992) Isolation and structure of a brain constituent that binds to the cannabinoid receptor. *Science* **258**, 1946-1949.
- Di Marzo V., Bisogno T., Sugiura T., Melck D. & De Petrocellis L. (1998) The novel endogenous cannabinoid 2-arachidonyl glycerol is inactivated by neuronal- and basophil-like cells: Connections with anandamide. *Biochem. J.* **331**, 15-19.
- Dodson G. and Wlodawer A. (1998) Catalytic triads and their relatives. *TIBS* **23**, 347-352.
- Dudek B.R. and Richardson R.J. (1982) Evidence for the existence of neurotoxic esterase in neural and lymphatic tissue of the adult hen. *Biochem. Pharmacol.* **31**(6), 1117-1121.

Fernandez J., DeMott M., Atherton D. and Mische S.M. (1992) Internal protein sequence analysis: Enzymatic digestion for less than 10µg of protein bound to polyvinylidene difluoride or nitrocellulose membranes. *Anal. Biochem.* **201**, 255-264.

Forshaw P.J., Atkins J., Luthjens L.H., Hom M.L., Ray D.E. and Glynn P. An organophosphate-sensitive transmembrane pore formed in vitro by the catalytic domain of a human serine hydrolase. Submitted to *J. Biol. Chem.* August 2000.

Garrett R.H. and Grisham C.M. (1995) *Biochemistry*. Second Edition, Saunders College Publishing.

Gassama-Diagne A., Fauvel J. and Chap H. (1989) Purification of a new, calcium-independent, high molecular weight phospholipase A₂/lysophospholipase (phospholipase B) from guinea pig intestinal brush-border membrane. *J. Biol. Chem.* **264**, 9470-9475.

Gassama-Diagne A., Rogalle P., Fauvel J., Wilson M., Klæbe A. and Chap H. (1992) Substrate specificity of phospholipase B from guinea pig intestine. A glycerol ester lipase with broad specificity. *J. Biol. Chem.* **267**, 13418-13424.

Gelb M.H., Svaren J.P. and Abeles R.H. (1985) Fluoro ketone inhibitors of hydrolytic enzymes. *Biochemistry* **24**, 1813-1817.

Giang D.K. and Cravatt B.F. (1997) Molecular characterization of human and mouse fatty acid amide hydrolases. *Proc. Natl. Acad. Sci. U.S.A.* **94**, 2238-2242.

Glynn P., Holton J.L., Nolan C.C., Read D.J., Brown L., Hubbard A. and Cavanagh J.B. (1998) Neuropathy target esterase: Immunolocalization to neuronal cell bodies and axons. *Neuroscience* **83**(1), 295-302.

Glynn P., Read D.J., Guo R., Wylie S and Johnson M.K. (1994) Synthesis and characterisation of a biotinylated organophosphorus ester for detection and affinity purification of a brain serine esterase: neuropathy target esterase. *Biochem. J.* **301**, 551-556.

Gnatt A., Loewenstein Y., Yaron A., Schwarz M. and Soreq H. (1994) Site-directed mutagenesis of active site residues reveals the plasticity of human butyrylcholinesterase in substrate and inhibitor interactions. *J. Neurochem.* **62**(2), 749-755.

Goparaju S.K., Ueda N., Taniguchi K. and Yamamoto S. (1999) Enzymes of porcine brain hydrolyzing 2-arachidonylglycerol, an endogenous ligand of cannabinoid receptors. *Biochem. Pharmacol.* **57**, 417-423.

Goparaju S.K., Ueda N., Yamaguchi H. and Yamamoto S. (1998) Anandamide amidohydrolase reacting with 2-arachidonylglycerol, another cannabinoid receptor ligand. *FEBS Lett.* **422**, 69-73.

Gorne-Tschelnokow U., Strecker A., Kaduk C., Naumann D. and Hucho F. (1994) The transmembrane domains of the nicotinic acetylcholine receptor contain alpha-helical and beta structure. *EMBO J.* **13**(2), 338-341.

Hase C.C., Le Dain A.C. and Martinac B. (1995) Purification and functional reconstitution of the recombinant large mechanosensitive ion channel (MscL) of *Escherichia coli*. *J. Biol. Chem.* **270**, 18329-18334.

Hase C.C., Minchin R.F., Kloda A. and Martinac B. (1997) Cross-linking studies and membrane localization and assembly of radiolabelled large mechanosensitive ion channel (MscL) of *Escherichia coli*. *Biochem. Biophys. Res Commun.* **232**, 777-782.

Hazen S.L., Stuppy R.J. and Gross R.W. (1990) Purification and characterization of canine myocardial cytosolic phospholipase A2. *J. Biol. Chem.* **265**, 10622-10630.

Hazen S.L., Zupan L.A., Weiss R.H., Getman D.P. and Gross R.W. (1991) Suicide inhibition of canine myocardial cytosolic calcium-independent phospholipase A2. Mechanism-based discrimination between calcium-dependent and -independent phospholipases A2. *J. Biol. Chem.* **266**, 7227-7232.

Herick K., Kramer R. and Lühring H. (1997) Patch clamp investigation into the phosphate carrier from *Saccharomyces cerevisiae* mitochondria. *Biochim. Biophys. Acta.* **1321**, 207-220.

Hierons R. and Johnson M.K. (1978) Clinical and toxicological investigations of a case of delayed neuropathy in man after acute poisoning by an organophosphorus pesticide. *Arch. Toxicol.* **40**, 279-284.

Hinnah S.C., Hill K., Wagner R., Schlicher T. and Soll J. (1997) Reconstitution of a chloroplast protein import channel. *EMBO J.* **16(24)**, 7351-7360.

Ho Y.S., Swenson L., Derewenda U., Serre L., Wei Y., Dauter Z., Hattori M., Adachi T., Aoki J., Arai H., Inoue K. and Derewenda Z.S. (1997) Brain acetylhydrolase that inactivates platelet-activating factor is a G-protein-like trimer. *Nature* **385**, 89-93.

Hofmann K. and Stofel W. (1993) TMbase – A database of membrane spanning protein segments. *Biol. Chem. Hoppe-Seyler* **34**, 166.

Huang Z., Payette P., Abdullah K., Cromlish W.A. and Kennedy B.P. (1996) Functional identification of the active-site nucleophile of the human 85-kDa cytosolic phospholipase A2. *Biochemistry* **35**, 3712-3721.

Ishikawa Y., Chow E., McNamee M., McChesney M. and Wilson B.W. (1983) Separation of paraoxon and mipafox sensitive esterases by sucrose density gradient sedimentation. *Toxicol. Lett.* **17**, 315-320.

Joel C.D., Moser H.W., Najno G. and Karnovsky M.L. (1967) Effects of bis-(monoisopropylamino)-fluoro-phosphine oxide (mipafox) and of starvation on the lipids in the nervous system of the hen. *J. Neurochem.* **14**, 479-488.

Johnson M.K. (1969a) A phosphorylation site in brain and the delayed neurotoxic effect of some organophosphorus compounds. *Biochem. J.* **111**, 487-495.

Johnson M.K. (1969b) The delayed neurotoxic effect of some organophosphorus compounds: identification of the phosphorylation site as an esterase. *Biochem. J.* **114**, 711-717.

Johnson M.K. (1970) Organophosphorus and other inhibitors of brain "neurotoxic esterase" and the development of delayed neurotoxicity in hens. *Biochem. J.* **120**, 523-531.

Johnson M.K. (1971) Solubilisation procedures cause changes in the response of brain neurotoxic esterase to inhibitors. *Biochem. J.* **122**, 51p-52p.

Johnson M.K. (1974) The primary biochemical lesion leading to the delayed neurotoxic effects of some organophosphorus esters. *J. Neurochem.* **23**, 785-789.

Johnson M.K. (1975a) The delayed neuropathy caused by some organophosphorus esters: mechanism and challenge. *Crit. Rev. Toxicol.* **3**, 289-316.

Johnson M.K. (1975b) Structure-activity relationships for substrates and inhibitors of hen brain neurotoxic esterase. *Biochem. Pharmacol.* **24**, 797-805.

Johnson M.K. (1977) Improved assay of neurotoxic esterase for screening organophosphates for delayed neurotoxicity potential. *Arch. Toxicol.* **37**, 113-115.

Johnson M.K. (1980) Neurotoxicity: Mechanisms explored and exploited. *Nature* **287**, 105-106.

Johnson M.K. (1982) The target for initiation of delayed neurotoxicity by organophosphorus esters: Biochemical studies and toxicological applications. *Rev. Biochem. Toxicol.* **4**, 141-212.

Johnson M.K. (1988) Sensitivity and selectivity of compounds interacting with neuropathy target esterase. Further structure-activity studies. *Biochem. Pharmacol.* **37**, 4095-4104.

Johnson M.K. (1992) Molecular events in delayed neuropathy: experimental aspects of neuropathy target esterase. In: B. Ballantyne and T.C. Marrs (Eds.), *Clinical and Experimental Toxicology of Organophosphates and Carbamates*, Butterworth Heinemann, Oxford, pp. 90-113.

Johnson M.K. and Lauwerys R. (1969) Protection by some carbamates against the delayed neurotoxic effects of di-isopropyl phosphorofluoridate. *Nature* **222**, 1066-1067.

Johnson M.K. and Read D.J. (1987) The influence of chirality on the delayed neuropathic potential of some organophosphorus esters: Neuropathic and prophylactic effects of stereoisomeric esters of ethyl phenylphosphonic acid (EPN Oxon and EPN) correlate with quantities of aged and unaged neuropathy target esterase in vivo. *Toxicol. & Appl. Pharmacol.* **90**, 103-115.

Johnson M.K., Bird I. and Meredith C. (1988) Phenyl di-n-pentylphosphinate: a convenient reactivable inhibitor for studies on neuropathy target esterase (NTE) and protection against organophosphate-induced delayed polyneuropathy. *Toxicol. Lett.* **40**, 133-140.

Justice J.M., Murtagh Jr. J.J., Moss J. and Vaughan M. (1995) Hydrophobicity and subunit interactions of rod outer segment proteins investigated using Triton X-114 phase partitioning. *J. Biol. Chem.* **270**, 17970-17976.

Kato K., Clark G.D., Bazan N.G. and Zorumski C.F. (1994) Platelet-activating factor as a potential retrograde messenger in CA1 hippocampal long-term potentiation. *Nature* **367**, 175-179.

Kossiakoff A.A. and Spencer S.A. (1981) Direct determination of the protonation states of aspartic acid-102 and histidine-57 in the tetrahedral intermediate of the serine proteases: Neutron structure of trypsin. *Biochemistry* **20**, 6462-6474.

Koutek B., Prestwich G.D., Howlett A.C., Chin S.A., Salehani D., Akhavan N. and Deutsch D.G. (1994) Inhibitors of arachidonoyl ethanolamide hydrolysis. *J. Biol. Chem.* **269**, 22937-22940.

Krejci E., Duval N., Chatonnet A., Vincens P. and Massoulié J. (1991) Cholinesterase-like domains in enzymes and structural proteins: Functional and evolutionary relationships and identification of a catalytically essential aspartic acid. *Proc. Natl. Acad. U.S.A.* **88**, 6647-6651.

Kretzschmar D., Hasan G., Sharma S., Heisenberg M. and Benzer S. (1997) The *Swiss cheese* mutant causes glial hyperwrapping and brain degeneration in *Drosophila*. *J. Neurosci.* **17**(19), 7425-7432.

Kyger E.M. and Franson R.C. (1984) Nonspecific inhibition of enzymes by p-bromophenacyl bromide. Inhibition of human platelet phospholipase C and modification of sulfhydryl groups. *Biochim Biophys. Acta* **794**(1), 96-103.

Leslie C.C. (1991) Kinetic properties of a high molecular mass arachidonyl-hydrolyzing phospholipase A2 that exhibits lysophospholipase activity. *J. Biol. Chem.* **266**, 11366-11371.

Li S., Song K.S. and Lisanti M.P. (1996) Expression and characterization of recombinant caveolin. *J. Biol. Chem.* **271**, 568-573.

Li W. and Casida J.E. (1998) Organophosphorus neuropathy target esterase inhibitors selectively block outgrowth of neurite-like and cell processes in cultured cells. *Toxicol. Lett.* **98**, 139-146.

Lienhard G.E. (1973) Enzymatic catalysis and transition-state theory. *Science* **180**, 149-154.

Lio Y.C., Reynolds L.J., Balsinde J. and Dennis E.A. (1996) Irreversible inhibition of Ca(2+)-independent phospholipase A2 by methyl arachidonyl fluorophosphonate. *Biochim. Biophys. Acta* **1302**, 55-60.

Lister M.D., Glaser K.B., Ulevitch R.J. and Dennis E.A. (1989) Inhibition studies on the membrane-associated phospholipase A2 in vitro and prostaglandin E2 production in vivo of the macrophage-like P388D1 cell. Effects of manoilide, 7,7-dimethyl-5,8-eicosadienoic acid, and p-bromophenacyl bromide. *J. Biol. Chem.* **264**, 8520-8528.

Lotti M. and Johnson M.K. (1978) Neurotoxicity of organophosphorus pesticides: Predictions can be based on *in vitro* studies with hen and human enzymes. *Arch. Toxicol.* **41**, 215-221.

Lotti M. and Johnson M.K. (1980) Neurotoxic esterase in human nervous tissue. *J. Neurochem.* **34(3)**, 747-749.

Lotti M., Becker C.E. and Aminoff M.J. (1984) Organophosphate polyneuropathy: Pathogenesis and prevention. *Neurology* **34(5)**, 658-662.

Luirink J., van der Sande C., Tommassen J., Velkamp E., de Graaf F.K. and Oudega B. (1986) Effects of divalent cations and of phospholipase A activity on excretion of cloacin DF13 and lysis of host cells. *J. Gen. Microbiol.* **132**, 825-834.

Lush M.J., Li Y., Read D.J., Willis A.C. and Glynn P. (1998) Neuropathy target esterase and a homologous *Drosophila* neurodegeneration-associated mutant protein contain a novel domain conserved from bacteria to man. *Biochem. J.* **332**, 1-4.

Mackay C.E., Hammock B.D. and Wilson B.W. (1996) Identification and isolation of a 155-kDa protein with neuropathy target esterase activity. *Fundamental Appl. Toxicol.* **30**, 23-30.

Mannella C.A. (1998) Conformational changes in the mitochondrial channel protein, VDAC, and their functional implications. *J. Struct. Biol.* **121**, 207-218.

Marcel V., Estrada-Mondaca S., Magne F., Stojan J., Klæbe A. and Fornier D. (2000) Exploration of the *Drosophila* acetylcholinesterase substrate activation site using a reversible inhibitor (Triton X-100) and mutated enzymes. *J. Biol. Chem.* **275**, 11603-11609.

- Marrs T.C. (1993) Organophosphate poisoning. *Pharmac. Therp.* **58**, 51-66.
- Mason H.J., Waine E., Stevenson A. and Wilson H.K. (1993) Aging and spontaneous reactivation of human plasma cholinesterase activity after inhibition by organophosphorus pesticides. *Hum. Exp. Toxicol.* **12**, 497-503.
- Matsuzaki K., Murase O., Tokuda H., Funakoshi S., Fujii N. and Miyajima K. (1994) Orientational and aggregational states of magainin 2 in phospholipid bilayers. *Biochemistry* **33**, 3342-3349.
- Matthews B.W., Sigler P.B., Henderson R. and Blow D.M. (1967) Three-dimensional structure of tosyl- α -chymotrypsin. *Nature* **214**, 652-656.
- Maurelli S., Bisogno T., De Petrocellis L., Di Luccia A., Marino G. and Di Marzo V. (1995) Two novel classes of neuroactive fatty acid amides are substrates for mouse neuroblastoma 'anandamide amidohydrolase'. *FEBS Lett.* **377**, 82-86.
- Mentlein R., Berge R.K. and Heymann E. (1985) Identity of purified monoacylglycerol lipase, palmitoyl-CoA hydrolase and aspirin-metabolizing carboxylesterase from rat liver microsomal fractions. *Biochem. J.* **232**, 479-483.
- Mentlein R., Suttorp M. and Heymann E. (1984) Specificity of purified monoacylglycerol lipase, palmitoyl-CoA hydrolase, palmitoyl-carnitine hydrolase, and nonspecific carboxylesterase from rat liver microsomes. *Arch. Biochem. Biophys.* **228**, 230-246.
- Meredith C. and Johnson M.K. (1988) Neuropathy target esterase: Rates of turnover in vivo following covalent inhibition with phenyl di-*n*-pentylphosphinate. *J. Neurochem.* **51**(4), 1097-1110.
- Mohraz M. (1999) Reconstitution of detergent-solubilized Na⁺,K⁺-ATPase and formation of two-dimensional crystals. *J. Struct. Biol.* **125**(1), 76-85.

Moretto A. and Lotti M. (1988) Organ distribution of neuropathy target esterase in man. *Biochem. Pharmacol.* **37**(15), 3041-3043.

Nostrandt A.C. and Ehrich M. (1992) Development of a model cell culture system in which to study early effects of neuropathy-inducing organophosphorus esters. *Toxicol. Lett.* **60**, 107-114.

Ollis D.L., Cheah E., Cygler M., Dijkstra B, Frolow F., Franken S.M., Harel M., Remington J.S., Silman I., Schrag J., Sussman J.L., Verschueren K.H.G. and Goldman A. (1992) The α/β hydrolase fold. *Protein Eng.* **5**, 197-211.

Patricelli M.P. and Cravatt B.F. (1999) Fatty acid amide hydrolase competitively degrades bioactive amides and esters through a nonconventional catalytic mechanism. *Biochemistry* **38**, 14125-14130.

Patricelli M.P., Lashuel H.A., Giang D.K., Kelly J.W. and Cravatt B.F. (1998) Comparative characterization of a wild type and transmembrane domain-deleted fatty acid amide hydrolase: Identification of the transmembrane domain as a site for oligomerization. *Biochemistry* **37**, 15177-15187.

Patricelli M.P., Lovato M.A. and Cravatt B.F. (1999) Chemical and mutagenic investigations of fatty acid amide hydrolase: Evidence for a family of serine hydrolases with distinct catalytic properties. *Biochemistry* **38**, 9804-9812.

Pickard R.T., Chiou G., Strifler B.A., DeFelippis M.R., Hyslop P.A., Tebbe A.L., Yee Y.K., Reynolds L.J., Dennis E.A., Kramer R.M. and Sharp J.D. (1996) Identification of essential residues for the catalytic function of 85-kDa cytosolic phospholipase A₂. *J. Biol. Chem.* **271**, 19225-19231.

Pind S. and Kuksis A. (1988) Solubilization and assay of phospholipase A₂ activity from rat jejunal brush-border membranes. *Biochim. Biophys. Acta* **938**, 211-221.

Pope C.N. and Padilla S.S. (1989a) Chromatographic characterization of neurotoxic esterase. *Biochem. Pharmacol.* **38**, 181-188.

Pope C.N. and Padilla S.S. (1989b) Modulation of neurotoxic esterase activity in vitro by phospholipids. *Toxicol. and Appl. Pharmacol.* **97**, 272-278.

Powers J.C. and Harper J.W. (1986) in Proteinase inhibitors (Barrett A.G. Eds.) pp. 55-151, Elsevier Science Publishers BV, Amsterdam.

Radermacher M., Rao V., Grassucci R., Frank J., Timmerman A.P., Fleischer S. and Wagenknecht T. (1994) Cryo-electron microscopy and three-dimensional reconstruction of the calcium release channel/ryanodine receptor from skeletal muscle. *J. Cell Biol.* **127**, 411-423.

Raussens V., Ruyschaert J-M. and Goormaghtigh E. (1997) Fourier transform infrared spectroscopy study of the secondary structure of the gastric H⁺,K⁺-ATPase and its membrane-associated proteolytic polypeptides. *J. Biol. Chem.* **272**, 262-270.

Reynolds L.J., Hughes L.L., Louis A.I., Kramer R.M. and Dennis E.A. (1993) Metal ion and salt effects on the phospholipase A₂, lysophospholipase, and transacylase activities of human cytosolic phospholipase A₂. *Biochim. Biophys. Acta* **1167**, 272-280.

Richards P., Johnson M., Ray D. and Walker C. (1999) Novel protein targets for organophosphorus compounds. *Chem.-Biol. Interact.* **119-120**, 503-511.

Richardson R.J., Davis C.S. and Johnson M.K. (1979) Subcellular distribution of marker enzymes and of neurotoxic esterase in adult hen brain. *J. Neurochem.* **32**, 607-615.

Riquelme G., Lopez E., Garcia-Segura L.M., Ferragut J.A. and Gonzalez-Ros J.M. (1990a) Giant liposomes: A model system in which to obtain patch-clamp recordings of ionic channels. *Biochemistry* **29(51)**, 11215-11222.

Riquelme G., Morato E., Lopez E., Ruiz-Gomez A., Ferragut J.A., Gonzalez-Ros J.M. and Mayor Jr F. (1990b) Agonist binding to purified glycine receptor reconstituted into giant liposomes elicits two types of chloride currents. *FEBS Lett.* **276**, 54-58.

Roberts M.F., Deems R.A., Mincey T.C. and Dennis E.A. (1977) Chemical modification of the histidine residue in phospholipase A2 (*Naja naja naja*): A case of half-site reactivity. *J. Biol. Chem.* **252**, 2405-2411.

Rüffer-Turner M.E., Read D.J. and Johnson M.K. (1992) Purification of neuropathy target esterase from avian brain after prelabelling with [³H]-di-isopropyl phosphorofluoridate. *J. Neurochem.* **58**, 135-141.

Sambrook J., Fritsch E.F. and Maniatis T. (1989) *Molecular Cloning: A laboratory manual*. Second Edition, Cold Spring Harbour Press.

Santacruz-Toloza L., Perozo E. and Papazian DM. (1994) Purification and reconstitution of functional Shaker K⁺ channels assayed with a light-driven voltage-control system. *Biochemistry* **33**(6), 1295-1299.

Sastry B.V.R. and Hemontolor M.E. (1998) Influence of nicotine and cotinine on retinal phospholipase A2 and its significance to macular function. *J. Ocu. Pharmacol. & Therapeut.* **14**(5), 447-458.

Schoonderwoerd K., Hom M.L., Luthjens L.H., Vieira van Bruggen D. and Jansen H. (1996) Functional molecular mass of rat hepatic lipase in liver, adrenal gland and ovary is different. *Biochem. J.* **318**, 463-467.

Senanayake N. and Karalliede I. (1987) Neurotoxic effect of organophosphorus insecticides: An intermediate syndrome. *N. Engl. J. Med.* **316**, 761-763.

Serrano S.M.T., Reichl A.P., Mentele R., Auerswald E.A., Santoro M.L., Sampaio C.A.M., Camargo A.C.M. and Assakura M.T. (1999) A novel phospholipase A2, BJ-PLA2, from the venom of the snake *Bothrops jararaca*: Purification, primary structure analysis, and its characterization as a platelet-aggregation-inhibiting factor. *Arch. Biochem. Biophys.* **367(1)**, 26-32.

Sheltawy A. and Dawson R.M.C. (1969) The metabolism of polyphosphoinositides in hen brain and sciatic nerve. *Biochem. J.* **111**, 157-165.

Shoshan-Barmatz V., Hadad-Halfon N. and Ostersetzer O. (1995) Cross-linking of the ryanodine receptor/ Ca^{2+} release channel from skeletal muscle. *Biochim. Biophys. Acta* **1237**, 151-161.

Sliwinski-Korell A., Engelhardt H., Kampka M. and Lutz F. (1999) Oligomerization and structural changes of the pore-forming *Pseudomonas aeruginosa* cytotoxin. *Eur. J. Biochem.* **265**, 221-230.

Smith M.I., Elvove E. and Frazier W.H. (1930) The pharmacological action of certain phenol esters with special reference to the etiology of so-called ginger paralysis. *Public Health Reports* **45(42)**, 2509-2524.

Smith M.I. and Lillie R.D. (1931) The histopathology of tri-ortho-cresyl phosphate poisoning. *Arch. Neurol. Psychiatr.* **26**, 976-981.

Snijder H.J., Ubarretxena-Belandia I., Blauuw M., Kalk K.H., Verheij H.M., Egmond M.R., Dekker N. and Dijkstra B.W. (1999) Structural evidence for dimerization-regulated activation of an integral membrane phospholipase. *Nature* **401**, 717-721.

Sogorb MA., Vilanova E., Quintanar JL. and Viniestra S. (1996) Bovine chromaffin cells in culture show carboxylesterase activities sensitive to organophosphorus compounds. *Int. J. Biochem. Cell Biol.* **28(9)**, 983-989.

Somma-Delpero C., Valette A., Lepetit-Thevenin J., Nobili O., Boyer J. and Verine A. (1995) Purification and properties of a monoacylglycerol lipase in human erythrocytes. *Biochem. J.* **312**, 519-525.

Sondek J., Bohm A., Lambright D.G., Hamm H.E. and Sigler P.B. (1996) Crystal structure of a G_A protein $\beta\gamma$ dimer at 2.1-Å resolution. *Nature* **379**, 369-374.

Stafforini D.M., McIntyre T.M., Zimmerman G.A. and Prescott S.M. (1997) Platelet-activating factor acetylhydrolases. *J. Biol. Chem.* **272**, 17895-17898.

Stafforini D.M., Prescott S.M. and McIntyre T.M. (1987) Human platelet-activating factor acetylhydrolase. Purification and properties. *J. Biol. Chem.* **262**, 4223-4230.

Street I.P., Lin H-K., Laliberté F., Ghomaschi F., Wang Z., Perrier H., Tremblay N.M., Huang Z., Weech P.K. and Gelb M.H. (1993) Slow- and tight-binding inhibitors of the 85-kDa human phospholipase A₂. *Biochemistry* **32**, 5935-5940.

Stroud R.M., Kay L.M. and Dickerson R.E. (1971) The crystal and molecular structure of DIP-inhibited trypsin at 2.7Å resolution. *Cold Spring Harbour Symp. Quant. Biol.* **36**, 125-140.

Studier F.W. and Moffatt B.A. (1986) Use of the bacteriophage T7 RNA polymerase to direct highly selective high-level expression of cloned genes. *J. Mol. Biol.* **189**, 113-130.

Sue T., Naini A. and Miller C. (1994) High level expression and functional reconstitution of Shaker K⁺ channels. *Biochemistry* **33**, 9992-9999.

Sussman J.L., Harel M., Frolov F., Oefner C., Goldman A., Toker L. and Silman I. (1991) Atomic structure of acetylcholinesterase from *Torpedo californica*: A prototypic acetylcholine-binding protein. *Science* **253**, 872-879.

Tang J., Kriz R.W., Wolfman N., Shaffer M., Seehra J. and Jones S.S. (1997) A novel cytosolic calcium-independent phospholipase A₂ contains eight ankyrin motifs. *J. Biol. Chem.* **272**, 8567-8575.

Thomas T.C., Ishikawa Y., McNamee M.G. and Wilson B.W. (1989) Correlation of neuropathy target esterase activity with specific tritiated di-isopropyl phosphorofluoridate-labelled proteins. *Biochem. J.* **257**, 109-116.

Thomas T.C., Szekacs A., Hammock B.D., Wilson B.W. and McNamee M.G. (1993) Affinity chromatography of neuropathy target esterase. *Chem. -Biol. Interactions* **87**, 347-360.

Thomas T.C., Szekacs A., Rojas S., Hammock B.D., Wilson B.W. and McNamee M.G. (1990) Characterization of neuropathy target esterase using trifluoromethylketones. *Biochem. Pharmacol.* **40**(12), 2587-2596.

Tjoelker L.W., Eberhardt C., Unger J., Le Trong H., Zimmerman G.A., McIntyre T.M., Stafforini D.M., Prescott S.M. and Gray P.W. (1995) Plasma platelet-activating factor acetylhydrolase is a secreted phospholipase A₂ with a catalytic triad. *J. Biol. Chem.* **270**, 25481-25487.

Tormo N., Gimeno J.R., Sogorb M.A., Diaz-Alejo N. and Vilanova E. (1993) Soluble and particulate organophosphate neuropathy target esterase in brain and sciatic nerve of the hen, cat, rat and chick. *J. Neurochem.* **61**, 2164-2168.

Tornqvist H. and Belfrage P. (1976) Purification and some properties of a monoacylglycerol-hydrolyzing enzyme of rat adipose tissue. *J. Biol. Chem.* **251**, 813-819.

Towbin H., Staehelin T. and Gordon J. (1979) Electrophoretic transfer of proteins from polyacrylamide gels to nitrocellulose sheets: Procedure and some applications. *Proc. Natl. Acad. Sci. U.S.A.* **76**, 4350-4354.

Van Hoek A.N. and Verkmann A.S. (1992) Functional reconstitution of the isolated erythrocyte water channel CHIP28. *J. Biol. Chem.* **267**, 18267-18269.

Van Hoek A.N., Hom M.L., Luthjens L.H., de Jong M.D., Dempster J.A. and van Os C.H. (1991) Functional unit of 30 kDa for proximal tubule water channels as revealed by radiation inactivation. *J. Biol. Chem.* **266**, 16633-16635.

Vancura A. and Haldar D. (1994) Purification and characterization of glycerophosphate acyltransferase from rat liver mitochondria. *J. Biol. Chem.* **269**, 27209-27215.

Volwerk J.J., Pieterse W.A. and de Haas G.H. (1974) Histidine at the active site of phospholipase A₂. *Biochemistry* **13**, 1446-1454.

Wang A. and Dennis E.A. (1999) Mammalian lysophospholipases. *Biochim. Biophys. Acta* **1439**, 1-16.

Wang A., Hsiu-Chiung Y., Friedman P., Johnson CA. and Dennis EA. (1999) A specific human lysophospholipase: cDNA cloning, tissue distribution and kinetic characterization. *Biochim. Biophys. Acta* **1437**, 157-169.

Watson H., Shotton D.M., Cox J.M. and Muirhead H. (1970) Three-dimensional fourier synthesis of tosyl-elastase at 3.5Å resolution. *Nature* **225**, 806-811.

Wecker L., Laskowski M.B. and Dettbarn W.D. (1978) Neuromuscular dysfunction induced by acetylcholinesterase inhibition. *Fed. Proc.* **37**, 2818-2824.

Williams D.G. (1983) Intramolecular group transfer is a characteristic of neurotoxic esterase and is independent of the tissue source of the enzyme. *Biochem. J.* **209**, 817-829.

Williams D.G. and Johnson M.K. (1981) Gel-electrophoretic identification of hen brain neurotoxic esterase, labelled with tritiated di-isopropyl phosphorofluoridate. *Biochem. J.* **199**, 323-333.

Yoshida M., Tomizawa M., Wu S-Y., Quistad G.B. and Casida J.E. (1995) Neuropathy target esterase of hen brain: Active site reactions with 2-[octyl-³H]octyl-4H-1,3,2-benzodioxaphosphorin 2-oxide and 2-octyl-4H-1,3,2-[aryl-³H]benzodioxaphosphorin 2-oxide. *J. Neurochem.* **64(4)**, 1680-1687.

Yu L., Deems R.A., Hajdu J. and Dennis E.A. (1990) The interaction of phospholipase A2 with phospholipid analogues and inhibitors. *J. Biol. Chem.* **265**, 2657-2664.